Landscape Transformation of Cyprus from 1970 through 2070

by

Elizabeth Ridder

A Dissertation Presented in Partial Fulfillment
of the Requirements for the Degree
Doctor of Philosophy

Approved April 2013 by the
Graduate Supervisory Committee:

Patricia Fall, Chair
Soe Myint
Paul Hirt

ARIZONA STATE UNIVERSITY

May 2013

ABSTRACT

This dissertation investigates spatial and temporal changes in land cover and plant species distributions on Cyprus in the past, present and future (1973-2070). Landsat image analysis supports inference of land cover changes following the political division of the island of Cyprus in 1974. Urban growth in Nicosia, Larnaka and Limasol, as well as increased development along the southern coastline, is clearly evident between 1973 and 2011. Forests of the Troodos and Kyrenia Ranges remain relatively stable, with transitions occurring most frequently between agricultural land covers and shrub/herbaceous land covers. Vegetation models were constructed for twenty-two plant species of Cyprus using Maxent to predict potentially suitable areas of occurrence. Modern vegetation models were constructed from presence-only data collected by field surveys conducted between 2008 and 2011. These models provide a baseline for the assessment of potential species distributions under two climate change scenarios (A1b and A2) for the years 2030, 2050, and 2070. Climate change in Cyprus is likely to influence habitat availability, particularly for high elevation species as the relatively low elevation mountain ranges and small latitudinal range prevent species from shifting to areas of suitable environmental conditions. The loss of suitable habitat for some species may allow the introduction of non-native plant species or the expansion of generalists currently excluded from these areas. Results from future projections indicate the loss of suitable areas for most species by the year 2030 under both climate regimes and all four endemic species (*Cedrus brevifolia, Helianthemum obtusifolium, Pterocephalus multiflorus,* and *Quercus alnifolia*) are predicted to lose all suitable environments as soon as 2030. As striking exceptions *Prunus dulcis* (almond)*, Ficus carica* (fig), *Punica*

granatum (pomegranate) and *Olea europaea* (olive), which occur as both wild varieties and orchard cultigens, will expand under both scenarios. Land cover and species distribution maps are evaluated in concert to create a more detailed interpretation of the Cypriot landscape and to discuss the potential implications of climate change for land cover and plant species distributions.

ACKNOWLEDGMENTS

I would like to thank my advisor, Dr. Patricia Fall, for her guidance, patience and most importantly, support, through the years. I do not have to all the words to express my gratitude to Dr. Fall for her willingness to take me as a student when I was at a crossroads, her patience while I muddled through ideas and her assistance in shaping the final research project. Her mentorship and friendship pulled me through many ruts and I will always cherish the many afternoons of discussion and coffee while driving around the Cypriot countryside. I would also like to thank my other committee members, Dr. Soe Myint and Dr. Paul Hirt. Dr. Myint's expertise and guidance are invaluable and I will always appreciate his willingness to field my many, many technical and random questions, always with a smile. Dr. Hirt's knowledge of environmental history has opened my mind to new ideas regarding the manipulation and shaping of environments and to different approaches and thoughts on conservation efforts around the world.

I would like to thank the various sources of funding throughout my graduate career. This project was initially funded for a summer of field research through the School of Geographical Sciences and Urban Planning's Melvin G. Marcus and Matthew G. Bailey scholarship as well as through NSF Grant #1031527, awarded to Steven Falconer & Patricia Fall. The opportunity afforded by the IIE Fulbright and the Cyprus Fulbright Commission was truly a wonderful experience to spend nine months studying in Cyprus greatly improved the data and ideas behind this project. And to the people at and organization of CAARI, thank you for providing a letter of support for my Fulbright application, allowing access to your library, providing many directions and instructions and for your friendship.

Many, many, many thanks to the “field crew”: Patricia Fall, Mariela Soto-Berelov, Tracy Schirmang, JoAnna Klinge, Chris Galletti and Thomael Joannides. Without your assistance and wonderful senses of humor, this project would not have happened. Thank you for keeping me sane in the field and providing me with a lifetime of memories.

To the Ridders, thank you for believing I’ll make it through and for understanding my need to live far away to pursue my education. Mom, thank you for visiting me while I was in Cyprus and letting me drag you around the forest. I hope that you enjoyed your visit as much as I did. To the Kellers, I am thankful for the many wonderful meals, time on the patio and laughs. You always provided a place where I could relax and enjoy the moment with friends and family. I am unable to describe all the amazing things the Cabral/Rohr household has provided and I hope that you still let me use laundry as an excuse to spend evenings in your home. Your friendship has kept me afloat through my rough patches; thank you for adopting me into your family.

And finally, to my amazing friends Andrew Keller, Tonya Cabral-Rohr, Tracy Schirmang, Tanya Musgrave-Kelley, Scott Kelley, Mariela Soto-Berelov, Danielle Ladd, Cara Walker, Bret Waldron, Jannel Waldron, JoAnna Klinge, and Matt Pace, who swapped ideas, made me get out of the house and shared laughs, I am forever grateful.

TABLE OF CONTENTS

Page

CHAPTER Page

CHAPTER Page

LIST OF TABLES

Table Page

Table Page

LIST OF FIGURES

Figure Page

Figure Page

Figure Page

Figure Page

Figure Page

Figure Page

Figure Page

Chapter 1

INTRODUCTION

Research objectives and organization

This dissertation analyzes the spatial and temporal variations of the natural and human-created landscapes of Cyprus. One of the early questions guiding this work pertained to determining whether the political division of Cyprus in 1974 caused changes in land use and how these changes might be sensed and assessed. This major political event shifted populations on the island dramatically as the Republic of Cyprus, in particular, moved from largely agricultural lifeways to an increasingly urbanized society. Field work and conversations with archaeological, botanical, and historical scholars piqued interest in the historical, modern, and future distributions to plant species. These two ideas guided the development of the research objectives addressed in this dissertation:

1. Inference of how the landscapes of Cyprus have changed since 1974 through the use of satellite imagery and on-the-ground field observations of plant distributions;
2. Construction of modern potential vegetation models of plant species distributions based on the field observations;
3. Predict changes to the vegetation distribution under multiple climate scenarios; and,
4. Link changes of land cover and vegetation to enable detailed interpretation of changes in landscape configuration over time.

Following an introduction tying this study to preliminary work and describing the study area, this dissertation is broken into four main areas of research. Chapters 3 through 5 address objectives 1 through 3, and although can be thought of as stand-alone products, they work toward the common goal of constructing a more comprehensive assessment of how human and natural landscapes are impacted by major political and social disjunctions like the 1974 partition of Cyprus and land-use and climate changes scenarios (Chapter 6).

Landscape change

Land-use and land-cover change (LUCC) is affected by many factors, including population growth, climate change, natural resource utilization, food production, and nature-society interactions (Turner et al., 1990; Bicik et al., 2001). Land use is generally defined as the human activity occurring at a particular place; e.g. fishing, timber harvesting, or playing baseball. Land cover incorporates the combined physical and biotic characteristics of a place (Meyer and Turner, 1992). Examples of land cover include agriculture, housing development, or forest, all of which can encompass many different types of land use. Following Geist and Lambin (2002), these factors are categorized as proximate causes or underlying driving forces. Proximate causes relate to human-caused changes at the local level, while underlying driving forces are the social processes at the local, regional, national, or global levels that lead to proximate causes (Geist and Lambin, 2002). Nelson et al. (2006) further delineates the driving forces into direct and indirect drivers of LULC change. Direct drivers are "natural processes," such as climate change, land conversion, and disease. Indirect drivers are related to human societies, and include economic, socio-political, cultural and religious, and technological factors (Nelson et al.,

2006). Research within LUCC Science focuses on interactions within the human-environment system, looking to establish the causal factors for trajectories, of LUCC (Kasperson et al., 1995).

For example, Bicik et al. (2001) determined that land-use change in the Czech Republic was based on the specific influences of historical social driving forces. They found that changes in political and economic regimes led to distinctive differences in land-use trajectories, specifically in agricultural intensification or decline on rural landscapes. Similarly, Kuemmerle et al. (2006) demonstrated that land-cover change may vary significantly under different political systems, even over an environmentally homogenous region. Their study of the border area of Poland, Slovakia, and Ukraine distinguished contrasting patterns of land cover that reflected different economic histories. These results reveal the influences of divergent political trajectories from the collapse of the Austro-Hungarian Empire nearly a century ago to the recent establishment of these three independent countries following the collapse of the Soviet Union.

Remote sensing

The development of photography in the early 17th century transformed the art of capturing landscapes through painting and drawing to a scientific venture allowing for the cataloging, description, and quantification of features within a photograph. Landscapes, cities, and people were now captured "as is" and not left to the creative devices of artistic license. The camera is still considered one of the most reliable and useful remote sensing[1]

[1] Remote sensing was formally defined by the American Society for Photogrammetry and Remote Sensing as "the measurement or acquisition of information of some property of an object or phenomenon, by a recording device that is not in physical or intimate contact with the object or phenomenon under study" (Colwell 1983). This definition only implies that the image is captured at some distance from the object or

instruments for capturing photographic images that provide historical records of unique places at specific times. Acquiring multiple images of the same place allows for the comparison between capture dates to evaluate potential changes in the spatial and temporal distribution of objects or phenomena of interest that can further understanding of the underlying man-made and natural processes at work in the area (Jensen, 2000, p. 121).

General advantages and limitations apply to all types of remotely sensed images. The most significant advantage is the (virtually) permanent, long-term record created through the acquisition of imagery. Remote sensing is usually considered a "passive" sampling technique that does not disturb the objects or phenomena of interest. Many types of imagery, regardless of capture technique, contain data from a broader spectral range than the human eye can sense (color perception generally in the range of 0.4 – 0.7 μm). These long-term records, in concert with on-the-ground observations, digital elevation models (DEMs) and other mapping products enable observation and assessment of landscape transitions over time and space.

Remote sensing has been utilized to map patterns of tropical deforestation (e.g. Geist and Lambin, 2001; Arima et al., 2008), successional stages of forests (e.g. Bergen et al., 2008), ecological responses to environmental change (e.g. Walther et al., 2002; Pettorelli et al., 2005; Laba et al., 2008), and to monitor changes in biodiversity (e.g. Nagendra, 2001; Kerr and Ostrovsky, 2003; Turner et al., 2003). Remote sensing allows the mapping of land use and land cover; however, the causes (proximate causes vs. direct

---

phenomenon; however, distance is undefined, thus landscape (ground-based) photographs are included within this definition of remote sensing.

and indirect drivers) are often difficult to determine directly from imagery. To determine the causes of LUCC, many studies have focused on individual to local decision-making (households to communities), limiting the spatial extent of analysis (e.g. Turner, 1999; Vicente-Serrano et al., 2004; Lasanta-Martinez et al., 2005; Dalle et al., 2006). However, broad-scale changes in political and socio-economic driving forces are thought to override individual or local decisions regarding land use and policy (Lambin et al., 2001) but experimental manipulation of the landscape is not possible at regional or national extents (Kuemmerle et al., 2006). Thus, examination of "naturally-occurring" regime shifts, such as changes to political borders or national policies on land use, provides opportunities to examine broad-scale causes and their potential effects on land use and land cover (Kuemmerle et al., 2006).

Species distribution modeling

Species distribution models (SDMs) predict the distribution of species under various environmental predictors and time frames. Species distribution models link the fields of geography, biology, ecology, statistics, information technologies and climate sciences to inform questions regarding resource availability, fire regimes (e.g. Lawson et al., 2010), potential for invasion by non-native species (e.g. Gritti et al., 2006), impacts from climate change (e.g. Thomas et al., 2004; Gritti et al., 2006; McKenney et al., 2007; Hu et al., 2010; Butler et al., 2012), prior distributions (e.g. Soto-Berelov, 2011) and many other conservation, management, and legislative issues (Franklin, 2009). SDMs are increasingly popular in scientific literature due to the interest in the above issues, improvements in data availability (Graham et al., 2004), continuous refinement of statistical approaches and advances in computing (including climate modeling and remote

sensing) (Franklin, 2009). With regard to vegetation, SDMs are potentially useful for predicting how species will shift in distribution over time in response to changes in environmental predictors. Vegetation SDMs tie into analyses of land-use and land-cover change since vegetative cover is one of the main indicators of these phenomena, especially in remote sensing applications. Models of vertebrate and invertebrate species are also influenced by changes to the landscape, as many of these species rely on particular land covers, vegetative communities or specific plant hosts. Thus the use of predictors to indicate shifts to vegetation or land-use and land-cover should be carefully considered when constructing SDMs.

Mediterranean ecosystems, land-use change, and diversity

Mediterranean ecosystems comprise only a small amount of the earth's ecosystems (1.2 percent) (di Castri, 1981), but include approximately 48,000 plant species, including 20 percent of vascular plants (Heywood and Watson, 1995; Cowling et al., 1996; Groombridge and Jenkins, 2002). These ecosystems are defined geographically as lying between 31 and 40 degrees latitude in both the northern and southern hemispheres. Mediterranean ecosystems are characterized by wet winters, hot dry summers and woody shrubs with sclerophyllous leaves (Vogiatzakis et al., 2006). The Mediterranean Basin lies along the intersection of two major landmasses, extending from Portugal to Jordan (west to east) and Italy to Morocco (north to south). Its geological history and geomorphology have encouraged highly variable flora, fauna, habitats and landscapes (Blondel and Aronson, 1999; Quezel and Medail, 2003; Blondel, 2006). The landscapes of the Mediterranean Basin cannot be understood without taking into account the history of human-related change (Grove and Rackham, 1993; Blondel,

2006). The land-use systems that have supported Mediterranean civilizations profoundly affected the distribution and dynamics of biotic species, communities and landscapes. This basin, a center of human civilization for thousands of years, has been characterized by relatively high population densities and repeated manipulation of its landscapes (Gritti et al., 2006). Evidence indicates landscapes were intentionally managed and maintained through traditional land-use practices (fire, silviculture, pastoralism, agriculture) for many millennia (Blondel, 2008).

The long history of human manipulation of Mediterranean landscapes has led to intricate land use systems, which support high biological and cultural diversity (Zaharis, 1977; Rackham, 1990). However, recent socio-economic factors have encouraged many people to abandon traditional land use (Kinzig and Grove, 2000). In many countries this has led to a shift from agricultural lifeways to an economy dominated by service, manufacturing and technology often impacting land use and land cover (Pares-Ramos et al., 2008). In Ecuador, Rudel et al. (2002) reported increases in forest cover due to rural-to-urban shifts in populations, leading to rapid urban growth and agricultural abandonment. On Crete, city growth, agricultural intensification and promotion of tourism threaten biological and landscape diversity, as forests and grasslands are converted to crop lands and urban land use (Ispikoudis et al., 1993). In this case land cover types have shifted to range from highly productive agricultural plots to unfertile and abandoned farm lands (Grove and Rackham, 1993). Di Pasquale et al. (2004) describe increases in forest and shrub cover in recent years, particularly in former agricultural lands, reducing overall landscape heterogeneity. Further, a growing literature argues that human landscape transformations often alter ecosystem function and

interactions (e.g., Vitousek et al., 1997). A common inference holds that human-caused land-cover change leads to diminished biological diversity in ecosystems (Wilson, 1992; Vitousek et al., 1997). Thus, the consideration of the socio-economic, historical and political contexts of LUCC and the relationship of these changes to ecological patterns and processes merits increased attention (Wu and Hobbs, 2002).

In spite of the tendency to emphasize anthropogenic landscape degradation, Butzer and Harris (2007) argue against viewing Mediterranean landscapes, and Cyprus in particular, as degraded. Instead they conclude that throughout history, Cyprus experienced minimal localized human impacts, and that its biota tend to be resilient in response to human transformations (Klinge and Fall, 2010; Klinge, 2013). Butzer (2005) emphasizes the difference between human-related transformation vs. degradation. He argues that landscape changes in the Mediterranean Basin are cyclical, rather than linear, unless the disequilibrium thresholds of a particular area are surpassed. Butzer and Harris (2007) reason that although landscapes can deteriorate, in particular after agricultural abandonment, they can also regenerate. Currently, it is unclear whether the dramatic relocation of agrarian populations since 1974 has led to an overall regeneration of shrub and forested lands or whether many of these areas are now subjected to intensified agricultural practices. Thus, it seems more insightful to consider changing land use on Cyprus in terms of shifts between land-cover heterogeneity and homogeneity. These concepts can accommodate any number of trends, ranging from the conversion of forests and grasslands to large agricultural tracts to the abandonment of croplands by their agrarian owners (e.g., di Pasquale et al., 2004) without assuming reduced biodiversity. This approach emerges as particularly valuable in light of Butzer's argument against

assuming that modern land-use change on Cyprus necessarily entails landscape degradation. The concepts of heterogeneity/homogeneity will be applied to the Cypriot landscape by analyzing the land cover maps (Chapter 3) and the combined predicted vegetation and land cover maps (Chapter 6) through the use of landscape metrics (e.g. number and distribution of landscape patches).

Summary

This dissertation consists of seven chapters. Following this introduction, Chapter 2 will describe the study area in terms of the physical, botanical, and political events that underpin the subsequent chapters.

Chapter 3 addresses Objective 1 and examines how the landscape of Cyprus has changed since 1974. Using Landsat imagery, land cover will be derived for the years 1973, 1984, 2001 and 2011. Land cover change analyses will indicate the types of land cover transitions, where they occur and if changes related to politically-inspired population movements are discernible. In addition, landscape metrics will be utilized to assess if changes to landscape homogeneity/heterogeneity have occurred over this time period and the possible implications for maintaining "traditional" landscapes.

Chapter 4 addresses Objective 2 and utilizes species distribution modeling to predict the present-day suitable areas of occurrence for a set of 22 species. These models will be further employed in Chapter 5 to address Objective 3, where they are used as the baseline to predict future potential suitable areas of occurrence. To evaluate potential changes to suitable areas of occurrence, two climate change scenarios were selected over three time periods (2030, 2050 and 2070).

Chapter 6 addresses Objective 4 and links the land cover maps (Chapter 3) and the species distribution maps (Chapters 4 and 5) to create a detailed interpretation of changes to the Cypriot landscape and the possible implications of these changes for specific species and land cover types.

Chapter 7 summarizes the major findings of this dissertation.

Chapter 2

STUDY AREA

Introduction

Cyprus is located in the eastern Mediterranean Sea and is the third largest island (9,251 km^2) within the Mediterranean Basin (Figure 1). Cyprus was formed during the Tertiary period and lies along the boundary between the African and Eurasian plates. As an island, Cyprus constitutes a bounded ecological study area. Its varied topography and microclimates result in a large range of flora consisting of approximately 2000 taxa, which include 144 endemics. Although extremely rich in native flora, humans introduced most mammalian fauna, and the island has few indigenous mammal, reptile and amphibian species. The island is divided into three geomorphological zones, the Kyrenia Mountains (Pentadaktylos) including the Karpas Peninsula, the Troodos Range and foothills, and the alluvial plains (Mesaoria Plain) that extend between the two mountain ranges (Tsintides et al., 2002). Meikle (1977) adds a coastal belt to this description in which most coastal areas are low-lying (sea cliffs are rare).

The island of Cyprus provides an optimal setting in which to examine how land-cover transitions are influenced by, and also influence, political, environmental, economic, and population changes, in light of this island's rich political and cultural history and distinctive, biologically diverse landscapes. Archaeological records indicate human presence on Cyprus for approximately 10,500 years and the in-migration of farming populations during the Aceramic Neolithic (*c.* 8200-5500 BC). This settlement event brought with it many of the plant and animal domesticates associated with the coastal Levant and Anatolia, establishing the initial farming communities of Cyprus

(Steel, 2004). Due to the island's strategic geographic location in the Mediterranean, it has experienced a particularly dynamic history of political and cultural influences, being periodically articulated with or dislodged from the Phoenician, Greek, Roman, Venetian, Ottoman, and most recently, British, empires. Each of these episodes provided a distinct contribution to current species assemblages and the creation of the modern Cypriot landscape.

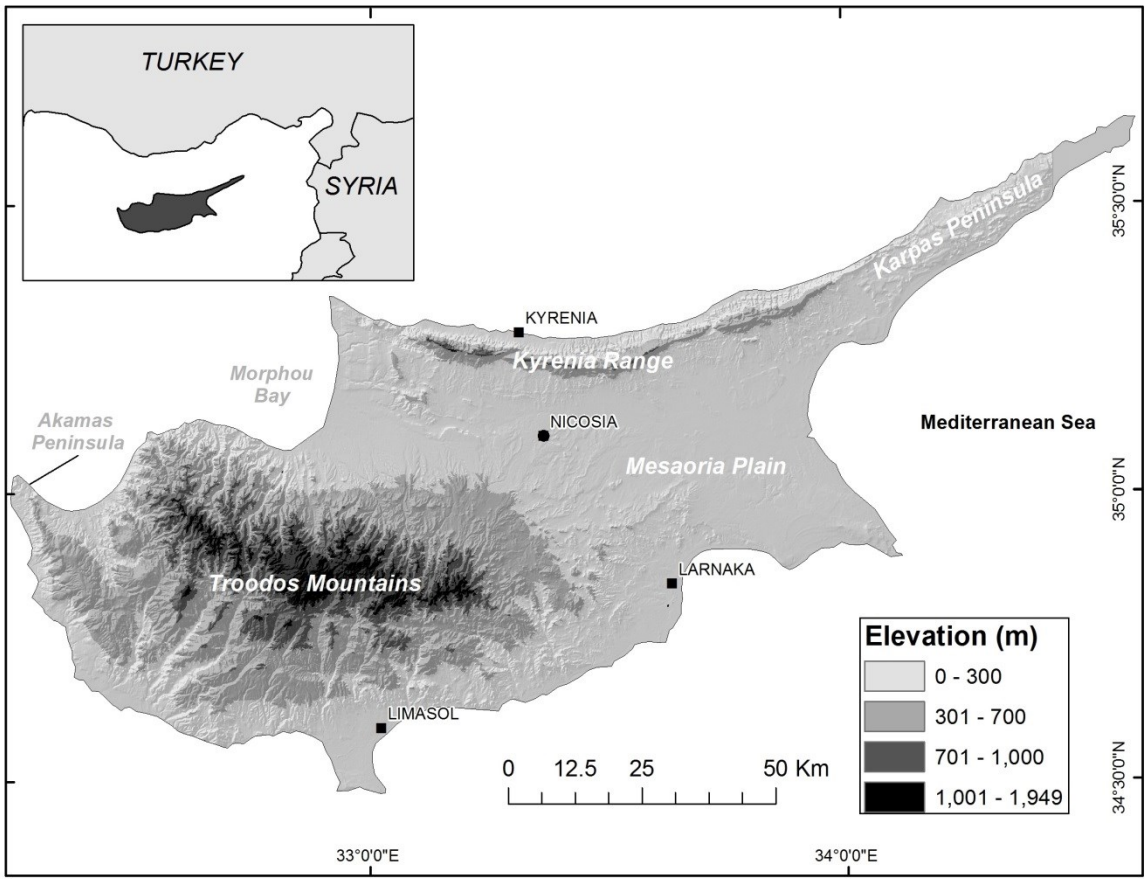

Figure 1. Cyprus is located at the eastern end of the Mediterranean Basin. The island's climate is defined by the topography and the Mediterranean Sea with temperatures decreasing with elevation and proximity to the coast. The island features two major mountain ranges the Troodos and Kyrenia Ranges, which are separated by the Mesaoria Plain.

As a result of the most recent change in imperial power, the British Crown granted the Cypriot people sovereignty over most of the island in 1960. The ensuing struggle for political power between Greek and Turkish Cypriots led to the partition of the island in 1974. Today, the southern Greek-speaking Republic of Cyprus is a member of the European Union (admitted in 2004), while the northern Turkish-speaking Turkish Republic of Northern Cyprus (TRNC) is formally recognized only by Turkey. The 1974 partition involved the relocation of thousands of Turkish Cypriots to the north and Greek Cypriots to the south. This relocation translated into a period of acute urbanization, especially as Greek-speaking populations left the farming villages and smaller towns of the north for the larger cities of the south. This relocation has shifted the economy of the Republic of Cyprus from agro-pastoralism to light manufacturing and services. Services are mainly related to tourism and finance, which account for approximately 78 percent of the Republic's gross domestic product (GDP). Due to its geographic location and modern infrastructure, Cyprus has developed into an important hub for companies and governments with interests in the Middle East, Eastern Europe, North Africa, the former Soviet Union, and the European Union. In contrast, the per-capita GDP of northern Cyprus is approximately 40 percent that of the south. Agriculture and services employ more than one-half of the working population of the TRNC, which is highly reliant on aid from the government of Turkey. Tourism in Northern Cyprus has increased since a 2004 relaxation of travel restrictions between the two parts of the island.

Climate

The climate of Cyprus is generally Mediterranean, with a long, hot summer (mid-May to mid-September) and short, mild and rainy winters (November to mid-March).

Summer weather conditions are highly influenced by low-pressure systems centered over Asia at this time, leading to high temperatures and very little precipitation. During the winter, small low-pressure systems tracking across the Mediterranean Sea bring most of the island's annual rainfall, up to 60% of the yearly total. Topography and the sea influence climate conditions, with large seasonal and daily temperature ranges between the coast and interior of the island. In addition, rainfall and temperature patterns are governed by island topography, with increases in rainfall (up to 1100 mm) at the highest elevations (annual average is approximately 480 mm) and a temperature difference of approximately 7°C between the lowlands and upper elevations regardless of season.

Botanical Divisions

To describe the distribution of vegetation, Meikle (1977; 1985) divided Cyprus into 8 botanical regions, representing the phytogeographic areas of the island (Figure 2). Boundaries between these regions are roads or rivers, following the Survey of Cyprus Administration Map (1950, revised 1958). Meikle (1977) provides a description of each of these regions (boundaries, general topographical characteristics, plants of special interest, cultural impacts), allowing for the determination of botanical regions for use in modern vegetation surveys.

Vegetation types

Conifer forests

Indigenous to Cyprus, *Pinus brutia* is distributed across the island except within the Mesaoria Plain. *Pinus brutia* is found from sea level to approximately 1400 m and commonly occurs on calcareous, or acidic sedimentary and igneous formations (Meikle, 1977, 1985). Extensive forests of *Pinus brutia* occur in the Troodos and Kyrenia Ranges.

In the Troodos *Pinus brutia* is commonly found in association with *Pistacia terebinthus, Arbutus andrachne, Ceratonia siliqua, Crataegus azarolus, Pterocephalus multiflorus, Rhamnus oleoides* and *Cistus* spp. (Fall, 2012). Within the Kyrenia Range, the association is generally composed of *Cupressus sempervirens, Olea europaea, Pistacia lentiscus, Pistacia terebinthus, Arbutus andrachne,* and *Sarcopoterium spinosum* (Fall, 2012).

Also indigenous, *Pinus nigra* occurs at the highest elevations of Cyprus, between 1100 and 1950 m in the Troodos' igneous formations (Meikle, 1977, 1985). *Pinus nigra* forms extensive forests on Mt. Olympus (Khionistra), the island's highest peak and also occurs in small patches on the peaks of Madari, Kyperounta and Spilia (Tsintides et al., 2002). *Pinus nigra* forest is sometimes composed of *Pinus brutia, Juniperus foetidissima, Rosa canina canina, Cistus creticus, Pterocephalus multiflorus and Sorbus aria*. (Fall, 2012).

Cedrus brevifolia is endemic to Cyprus and only occurs within the Cedar Valley (Tripylos) of the Pafos Forest between 900 and 1400 m (Tsintides et al., 2002). *Cedrus brevifolia* also occurs near the Kykko Monastery, Tsakkistra village and elsewhere in the Troodos and Kyrenia Ranges where it is planted.

Juniperus foetidissima is an indigenous small tree occurring at high elevations, from 1000 to 1950 m, on Mt. Olympus of the Troodos. *Juniperus foetidissima* often occurs within *Pinus nigra* forest, on rocky mountain slopes and on igneous formations (Meikle, 1977, 1985). *Juniperus phoenicea* tends to occur in *Pinus brutia* forest of the Akamas Peninsula, on dry and rocky soils and sometimes on sandy soils near the sea

(Meikle, 1977, 1985). *Juniperus phoenicea* occurs from sea level to approximately 500 m.

Figure 2. Meikle's botanical divisions of Cyprus (1977). These botanical divisions represent the major phytogeographic regions of Cyprus and were used to help delineate areas of occurrence for modern vegetation during on-the-ground surveys.

Oak forests

Quercus alnifolia is endemic to Cyprus, restricted to the Troodos Range at elevations of 300 to 1700 m (Tsintides et al., 2002). Restricted to igneous substrates, *Quercus alnifolia* often occurs with *Pinus brutia* as understory or can form extensive maquis (Meikle, 1977, 1985; Tsintides et al., 2002). *Quercus coccifera* is found in the Troodos and Kyrenia Ranges, as well as along the Akamas and Karpas Peninsulas. *Quercus coccifera* is found at elevations of 100 to 1300 m within maquis or garigue, on dry hillsides and sometimes within *Pinus brutia* forest (Meikle, 1977, 1985).

Maquis, Garigue and Batha

Meikle (1977, 1985) divides the shrub and scrublands of Cyprus into three categories based on species composition and structure. This classification assumes a degradation of the forest into one of these three types (Meikle, 1977, 1985). Maquis is uncommon and consists of shrubs 4 to 6 m in height. The species comprising maquis include *Arbutus andrachne, Pistacia terebinthus, Olea europaea, Styrax officinalis* and *Quercus coccifera*. Garigue is untilled, grazed land with shrubs less than 3 m in height. Common garigue species include *Cistus* spp., *Genista sphacelata, Calycotome villosa, Lithospermum hispidulum, Phagnalon rupestre* and occasionally *Pistacia lentiscus*. Excessive grazing reduces the landscape to batha, primarily composed of *Sarcopoterium spinosum, Fumana* spp., *Micromeria* spp., *Thymus capitatus* and other small herbs (Meikle, 1977, 1985).

Other descriptions of maquis and garigue are dependent upon rainfall and elevation. For example, Tsintides (1998) describes maquis as occurring in areas with annual rainfall of 450 to 1000 mm. Along the lower elevations, common species include *Juniperus phoenicea, Pistacia lentiscus, Ceratonia siliqua, Olea europaea, Salvia fruiticosa, Cistus* spp. and random *Pinus brutia*. At the higher elevations, maquis transitions into oak forest and is generally composed of *Arbutus andrachne, Quercus alnifolia, Pistacia terebinthus, Quercus coccifera* and *Crataegus azarolus* (Tsintides, 1998; Fall, 2012). Garigue occurs from sea level into the foothills of the Troodos and Kyrenia Ranges. Common shrubs that occur into the Troodos include *Genista spaeceolata, Calycotome villosa, Cistus* spp., *Lithodora hispidula, Pterocephalus mutliflorus, Thymus capitatus* and *Lavendula stoachas*. *Pistacia* spp., *Ceratonia siliqua* and *Pinus brutia* are dispersed throughout the island (Tsintides, 1998; Fall, 2012). Along

the southern foothills of the Kyrenia Range and drier slopes of the Mesaoria Plain, garigue is characterized by *Crataegus azarolus, Ziziphus lotus, Noaea mucronata, Phagnalon rupestre, Thymus capitatus, Sarcopoterium spinosum, Asparagus stipularis, Helianthemum obtusifolium* and *Asperula cypria* (Tsintides, 1998; Fall, 2012).

Orchards

Citrus spp. are most common along the coastal belt and are concentrated near Morphou and from Limasol to Pafos. *Olea europaea* (olive), *Punica granatum* (pomegranate) and *Ficus carica* (fig) orchards are usually found from low- to mid-elevations. *Prunus dulcis* (almond) and other *Prunus* spp. orchards are most common along mid-elevation mountain slopes (Fall, 2012).

Summary

This chapter introduces the environmental setting of Cyprus, including an overview of the topography, climate and major vegetation groups of relevance to this dissertation. The long-term land-use history of the island has created a mosaic-like landscape with many indigenous and endemic species. The recent (1974) political events that led to large-scale population shifts provide a 'natural' experimental setting in which to examine the effects of this major change on land-cover transitions and species distributions.

Chapter 3

LAND COVER TRANSITIONS 1973-2011

Introduction

Human impacts on the Earth are well documented and range from land cover transformations to changes in global biogeochemistry to alterations in the Earth's biological diversity (Marsh, 1864; Turner et al., 1990; Turner and Meyer, 1991; Vitousek et al., 1997). Sanderson et al. (2002) estimated that approximately 83 percent of the Earth's land surfaces are connected with human activities, while McKibben (1989) proposed that human activities affect all landscapes, regardless of their perceived isolation. A dichotomy has long existed in the sciences, separating "natural" from "human" or "cultural" systems, leading to the supposition that human activities degrade natural systems. As an alternative, Rappaport (1968) advocates the incorporation of ecological systems theory into anthropological work (see Stoddart, 1965 for a geographical perspective). This perspective views organisms (and thus, humans) as part of, and interacting with, the abiotic and biotic components of their environments, leading away from the assumption that human activities entail inherently negative impacts on the landscape.

One line for investigating the relationship of human activity and landscape change has relied on the use of remote sensing technologies. Traditional remote sensing methods of land-use and land-cover change (LUCC) analysis involve the use of per-pixel classification techniques (Dean and Smith, 2003), in which each pixel is assigned a single value (class) based upon the spectral properties of the objects within that particular pixel. Pixel-based approaches have been utilized to document vegetative cover (e.g. Carlson

and Sanchez-Azofeifa, 1999), determine the extent, causes, and effects of deforestation (e.g. Brokensha and Riley, 1978, Allen and Barnes, 1985; Arima et al., 2008; Mena, 2008), examine changes to land cover across political borders (e.g. Kuemmerle et al., 2006), and evaluate the impacts to land cover based on changes to political regimes (Bicik et al., 2001). Within the Mediterranean Basin, LUCC research has focused on physical transformations to the environment, demographic shifts, and regeneration of shrub lands or forests. A majority of this work has focused on the detailed collection of on-the-ground data, often at the scale of the individual or village. Much of this research has not looked at the Mediterranean Basin as a coupled human-environmental system and often cites population change as causing environmental degradation.

In general, Mediterranean ecosystems support high species, landscape, and cultural diversity. However, traditional heterogeneous Mediterranean landscapes are changing dramatically in the face of agricultural abandonment, urbanization, economic development and political dynamics. Modern land-use change in Cyprus has been particularly abrupt in comparison with other islands in the Mediterranean. The political crisis of 1974 led to the partition of Cyprus into the Greek-speaking Republic of Cyprus (a member of the European Union) and the Turkish-speaking Turkish Republic of Northern Cyprus (TRNC). Although population movements began prior to 1974, the forced resettlement of thousands of Greek Cypriots in the southern Republic and Turkish Cypriots in the north accelerated the processes of agricultural abandonment and urbanization, especially as Greek-speaking Cypriots left the farming villages of the north for the larger cities of the south.

Other episodes of landscape change in the Mediterranean have been conditioned by post-colonial politics and intensive economic development. However, the other large islands in the Western Mediterranean, Sicily, Sardinia and Corsica, were united with Italy or France by the 18th or 19th centuries. The only other large island in the Mediterranean, Crete, experienced a 20th century episode of resettlement similar to Cyprus'. In 1923 Greece and Turkey exchanged ethnic inhabitants, with Christian inhabitants from Turkey settling in Crete, and expanding its population greatly. Although the partition of Cyprus in 1974 is reminiscent of this massive resettlement, the difference in timing is particularly significant for the study proposed here. Whereas the resettlement on Crete took place 87 years ago, the large-scale land-use transformation on Cyprus has unfolded over the past 40 years, an era well-documented by modern remote sensing technology. Thus, Cyprus provides a case study of rapidly changing socio-economic factors and their effects on land use/land cover over a historically manageable time frame and leads to the following questions and predictions:

How has the Cypriot landscape changed over approximately the last 50 years (island-wide)?

1. Due to population movements and a change in the economic base of Cyprus, urban areas are expected to expand, while outlying villages are expected to decline in extent. Development along the coast is expected to increase in response to a larger tourism sector. In addition, it is expected that agricultural plots shift from small, multi-crop plots to larger, single-species plots.

Are there differences between the northern and southern portions of the island? If so, how do they differ in terms of land cover composition and change over time?

2. Differences are expected across the island with coasts developing more quickly and extensively in the southern portion of the island. Along this same line of reasoning, urban expansion is expected to be greater in the southern areas of the island. It is also expected that agricultural plots remained similar in size and configuration in the northern area due to limited trade and economic development after 1974.
3. In terms of landscape configuration, less heterogeneity is predicted in the south as urban areas and size of agricultural plots increase.

Land cover maps and the transitions between land covers for different time periods will be combined with species distribution modeling results (Chapters 4 and 5) to discuss the expected impacts of changing land covers on species distributions over time (Chapter 6).

Methods

Data acquisition

Assessments of land-cover change often are accomplished through the use of remote sensing or aerial photography. For the purposes of this case study, Landsat images provide the most economical and easily accessible data source while maintaining a spatial resolution appropriate to the scale of the processes of interest. Landsat imagery is provided at no cost and most data are available for immediate download from the USGS Earth Resources Observation and Science Center website[2]. The Landsat imagery utilized in this case study spans multiple years, sensor types, and spatial resolutions (Table 1) due to differences in flight paths and sensors between 1973 and 2011. Although

[2] http://glovis.usgs.gov/

it is not ideal to use data of differing resolutions from multiple sensor types, this is currently one of the best ways to examine LULC patterns over this time span. Cloud-free images (0-10% cloud coverage) were selected to correspond as closely as possible to 10-year anniversary dates between images. Cloud-free imagery was not available for the tip of the Karpas Peninsula in 1984 nor for the majority of the island in 1982 or 1985, so analysis was conducted without a portion of the Karpas. The 1973 Landsat 1 MSS and 1984 Landsat 5 MSS images were resampled to 30 m resolution, the same spatial resolution as the 2011 Landsat images. This resampling does not improve data quality or resolution; it just creates a grid (pixels) of the same extent as other images, which is a necessary step for maintaining the information available in the higher-resolution imagery. The inclusion of data across differing spatial and spectral properties permits the use of Landsat 1 MSS images (Table 1), which provide a snapshot of the landscape of Cyprus prior to the rapid urbanization and resettlement of the island's population triggered by the partition in 1974. Land cover *after* the partition of Cyprus will be documented through the analysis of subsequent Landsat images taken between 1984 until 2011.

Table 1. Characteristics of each Landsat image as downloaded from the United States Geological Survey (http://glovis.usgs.gov/). Landsat imagery were utilized to determine the land cover categories and their transitions between 1973 and 2011 across the entire island of Cyprus. Landsat MSS data were resampled to 30m pixel size to match other data used for analyses.

Image Type	Sensor	Image Date	Pixel size (m)	Data Type (USGS)	Sun Azimuth	Sun Elevation	Path/Row
Landsat1	MSS	3-Jan-73	79	L1T	150.7260087	25.20692169	189/35
Landsat1	MSS	3-Jan-73	79	L1T	150.0661437	26.31382248	189/36
Landsat1	MSS	4-Jan-73	79	L1T	150.5719299	25.23685933	190/36
Landsat1	MSS	4-Jan-73	79	L1T	149.910059	26.34121105	190/35
Landsat5	MSS	2-Jul-84	79	L1T	108.6011198	61.15808765	176/35
Landsat5	MSS	2-Jul-84	79	L1T	105.7882573	61.33619238	176/36
Landsat5	TM	4-Aug-90	30	L1T	112.63	57	176/36
Landsat5	TM	4-Aug-90	30	L1T	114.4973965	55.68462538	176/35
Landsat5	TM	29-Aug-90	30	L1T	125.4173837	51.07878476	175/35
Landsat7	ETM+	22-May-01	30	L1T	118.9826065	65.2556642	176/36
Landsat7	ETM	22-May-01	30	L1T	122.0773288	64.74520348	176/35
Landsat7	ETM	31-May-01	30	L1T	118.9690199	65.56355972	175/35
Landsat5	TM	29-Jul-11	30	L1T	120.9881413	61.8290057	176/35
Landsat5	TM	29-Jul-11	30	L1T	118.2264626	62.3140039	176/36
Landsat5	TM	7-Aug-11	30	L1T	124.6010025	60.300179	175/35

Accuracy assessment data

Remotely sensed data from a 2008 Landsat image were analyzed to characterize a variety of land-cover classes prior to the collection of preliminary field data in May and June 2008. The sampling area (Figure 3) was designed to provide continuous sampling from the northern coast at Kyrenia to the Akrotiri Peninsula and the adjacent city of Limasol on the south coast. This Landsat sample area totals approximately 1,485 km^2 and represents 16% of the island's area. Land-cover classes for vegetation in this area were derived using an unsupervised Iterative Self-Organizing Data Analysis (ISODATA) classification technique to create clusters based on spectral signatures within the image (Figure 4).

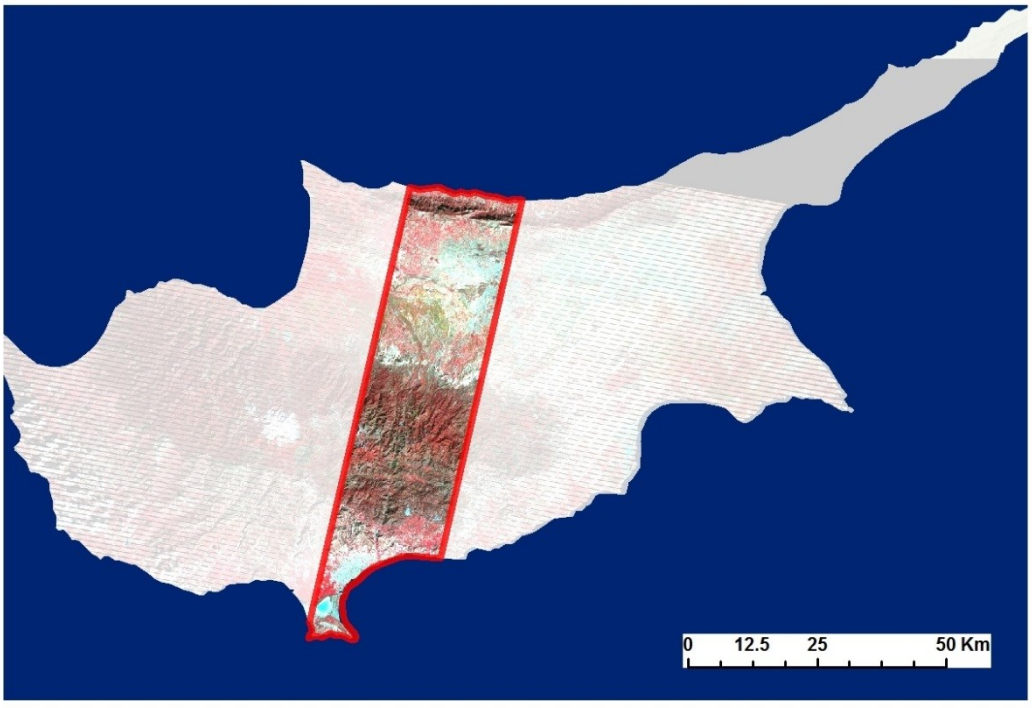

Figure 3. Image illustrating the 2008 sampling area as selected from a Landsat image of the same year. The sampling area covers a coast-to-coast transect and covers the entire elevational gradient of the island.

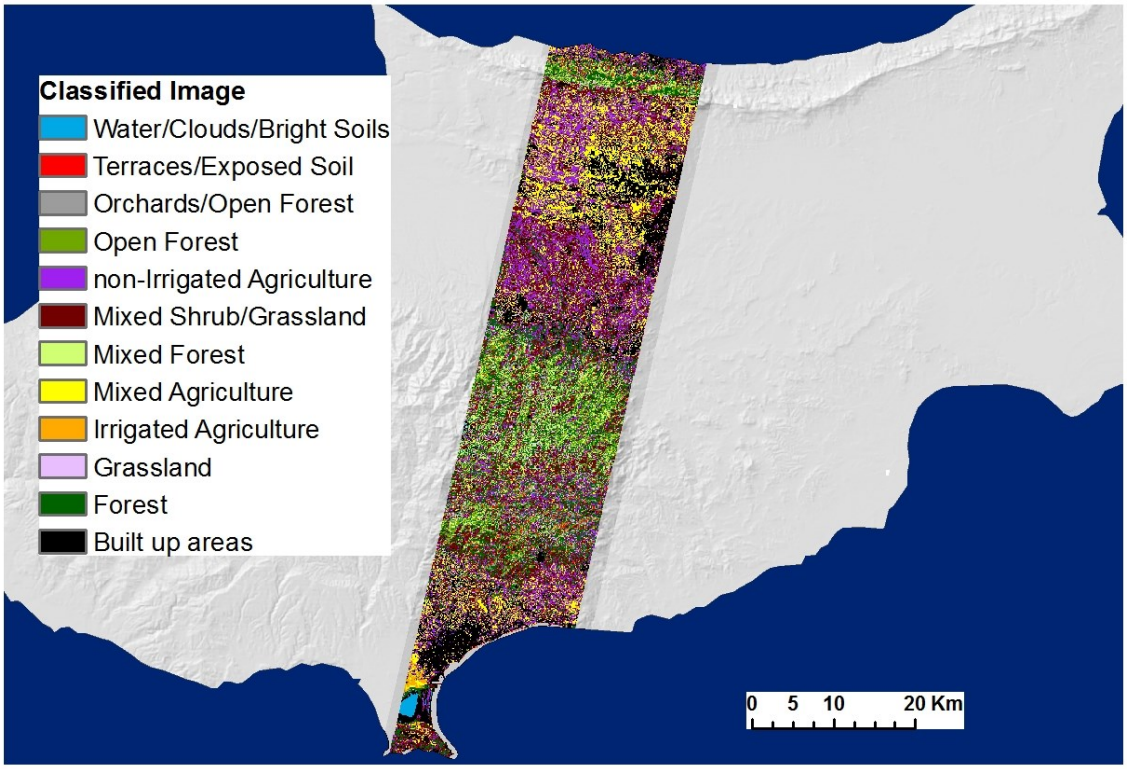

Figure 4. Land cover classification scheme and the results of the initial 2008 study area. The image was classified using ISODATA analysis and the results of the land cover classification were used to create a stratified random sample of land cover classes for on-the-ground point sampling of vegetation cover.

Seven hundred forty-eight locations across Cyprus were selected utilizing a stratified random sampling scheme based on land-cover types derived from classification of the 2008 image. During the summer 2008 field season, qualitative observations of vegetation composition and cover were collected at 131 random locations (17.5% of the random locations selected from the 2008 Landsat image). After the 2008 field season, additional vegetation data were collected at 390 non-random and 25 random sample points designated in 2009 – 2011, which were supplemented with data from 114 historical points (Figure 5). Only the field observations (n = 546; data from historical

points excluded) will be utilized in accuracy assessment of the remote sensing classifications.

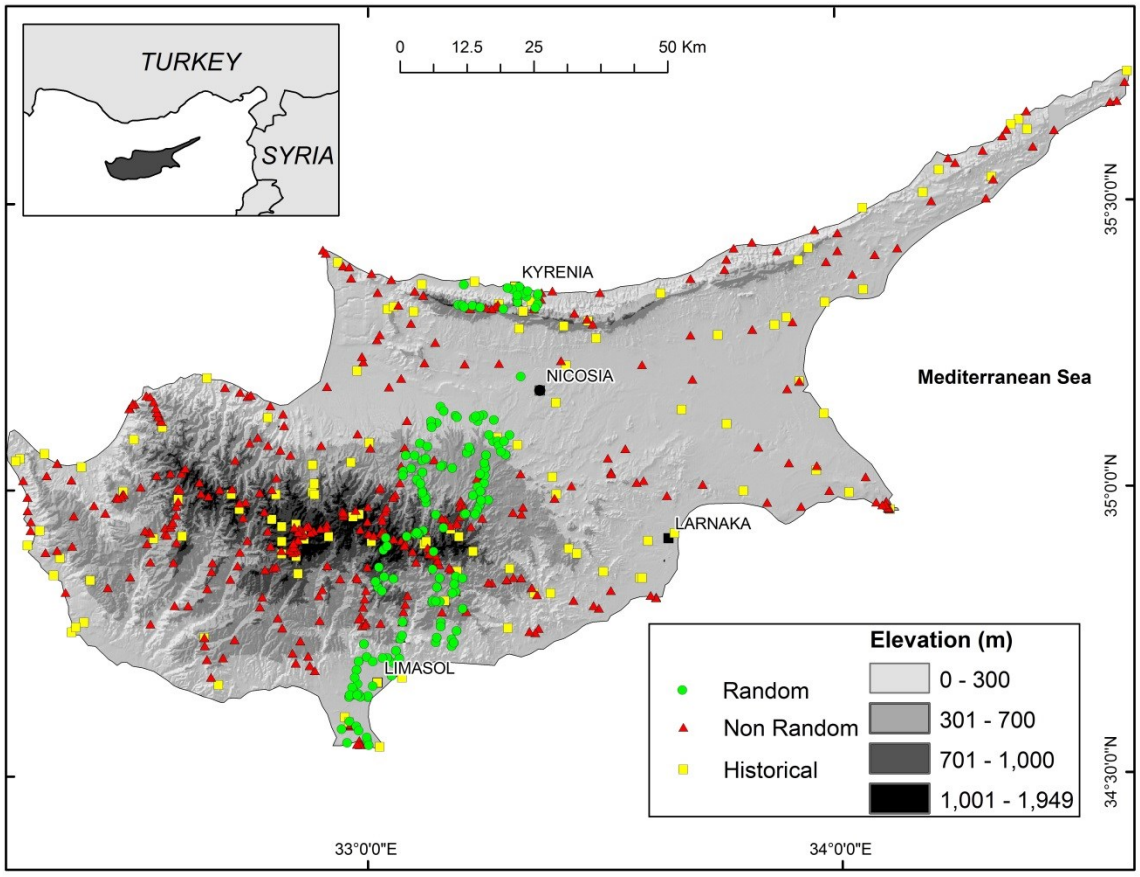

Figure 5. Distribution of vegetation sampling points across Cyprus. Sampling points were collected between 2008 and 2001 and represent a full complement of the elevational gradient of the island. Each point's geographical coordinates (latitude/longitude) were recorded, along with the species present, an estimate of the vegetative cover and the land cover category. Each point represents approximately 100 m in diameter.

At each observation point, the locational data (latitude, longitude and elevation) were determined using a hand-held global positioning system receiver (GPS). Perennial plant species for both the random and non-random points were recorded over sample areas of about 100 m diameter. In addition, aspect, substrate, plant species present and estimated vegetation cover were collected at each point. Topographic variables

(elevation, slope and aspect) were derived for all the sample points from ASTER digital elevation models (DEMs). Nomenclature follows *Trees and Shrubs in Cyprus* (Tsintides et al., 2002), *Flora of Cyprus* (Miekle, 1985), and *An Illustrated Flora of North Cyprus* (Viney, 1994).

Image pre-processing

Atmospheric correction

Electromagnetic radiation signals are distorted through absorption and scattering by aerosols and gases as they pass through the atmosphere, impacting the measurement of surface radiance by satellite systems. This radiometric distortion results in the reporting of altered reflectance values (Hodgson and Shelley, 1994) and may cause inaccurate interpretations of land cover (Holben and Justice, 1981; Colby and Keating, 1998). The type of image analysis and availability of atmospheric data dictate the necessity and ability to apply one of the available atmospheric corrections.

Several kinds of atmospheric corrections have been developed to correct for scattering and absorption due to aerosols due to their unpredictability in time and space (Chavez, 1988, 1996; Hall et al., 1991; Kaufman, 1993; Jensen et al., 1995; Lillesand et al., 2004; Mahiny and Turner, 2007). Atmospheric correction is utilized to minimize distortion by converting the digital number (DN, sometimes referred to as brightness values) to reflectance values, which provides a correction for comparisons across multiple dates and sensor types. Within IDRISI Selva[3] (v. 17.0 –17.02), four atmospheric correction models are available:

[3] http://clarklabs.org/

1. Dark object subtraction model (see Chavez, 1988). As implemented in IDRISI, an estimate of the DN of haze (using a dark object from the image as the estimate), sun elevation, central wavelength of the band, date and time of the image, and Lmin/Lmax (minimum and maximum values of radiance for the band) are required (Eastman, 2012).
2. Cos(t) model (see Chavez, 1996). This model incorporates the parameters used in the dark object subtraction model, but includes a calculation that estimates the effects of scattering and absorption. There are no additional data requirements beyond those of the dark object subtraction model (Eastman, 2012).
3. Full correction model (see Turner and Spencer, 1972; Forester, 1984). This model requires the parameters from the dark object correction model, plus an estimate of the optical thickness of the atmosphere and the spectral diffuse sky irradiance (Eastman, 2012).
4. Apparent reflectance model. This model only requires the sun elevation as a model parameter (Eastman, 2012), but does not correct for atmospheric scattering and absorption (Chavez, 1996).

The Cos(t) model was selected for use in this study, since it works well in semi-arid to arid environments (Chavez, 1996). This model first converts to normalized at-sensor reflectance, and then to proportional surface reflectance with values ranging from 0.0 to 1.0. Correction factors, including the DN for dark objects as selected using the near-infrared band (NIR) for each band and image combination, are summarized in Table 2.

Table 2. Data in this table were used to atmospherically correct each band of each Landsat image. The numbers in the header row refer to the band number for each specific path/row and satellite sensor combination. Bold numbers in the table are the wavelength of the band center (μm). Other numbers are Lmin and Lmax, or the radiance at Digital Number (DN) 0 and DN 255. The Lmin and Lmax are measured in $Wm^{-2}sr^{-1}mm^{-1}$ (Watts per square meter per steradian per micron).

		B1	B2	B3	B4	B5	B6	B7	DN haze NIR band
1973					**0.55**	**0.65**	**0.75**	**0.95**	
	189/35				0.000/201.000	9.100/171.300	-8.400/161.600	0.000/159.000	7
	189/36				0.000/201.000	9.100/171.300	-8.400/161.600	0.000/159.000	7
	190/36				0.000/201.000	9.100/171.300	-8.400/161.600	0.000/159.000	7
	190/35				0.000/201.000	9.100/171.300	-8.400/161.600	0.000/159.000	7
1984		**0.55**	**0.65**	**0.75**	**0.95**				
	176/35	2.500/220.800	2.700/163.600	3.800/150.700	2.900/117.500				4
	176/36	2.500/220.800	2.700/163.600	3.800/150.700	2.900/117.500				8
1990		**0.485**	**0.56**	**0.66**	**0.83**	**1.65**		**2.215**	
	176/36	-1.520/169.00	-2.840/333.00	-1.170/264.000	-1.510/221.000	-0.370/30.200		-0.150/16.500	8
	176/35	-1.520/169.00	-2.840/333.00	-1.170/264.000	-1.510/221.000	-0.370/30.200		-0.150/16.500	10
	175/35	-1.520/169.00	-2.840/333.00	-1.170/264.000	-1.510/221.000	-0.370/30.200		-0.150/16.500	8
2001		**0.485**	**0.56**	**0.66**	**0.835**	**1.65**		**2.22**	
	176/36	-6.200/293.700	-6.400/300.900	-5.000/234.400	-5.100/241.100	-1.000/47.570		-0.350/16.540	17
	176/35	-6.200/191.600	-6.400/196.500	-5.000/152.900	-5.100/241.100	-1.000/31.060		-0.350/10.800	18
	175/35	-6.200/191.600	-6.400/196.500	-5.000/152.900	-5.100/241.100	-1.000/31.060		-0.350/10.800	12
2011		**0.485**	**0.56**	**0.66**	**0.83**	**1.65**		**2.215**	
	176/35	-1.520/193.000	-2.840/365.000	-1.170/264.000	-1.510/221.000	-0.370/30.200		-0.150/16.500	19
	176/36	-1.520/193.000	-2.840/365.000	-1.170/264.000	-1.510/221.000	-0.370/30.200		-0.150/16.500	10
	175/35	-1.520/193.000	-2.840/365.000	-1.170/264.000	-1.510/221.000	-0.370/30.200		-0.150/16.500	15

Mosaicing

Evaluation of land cover conditions across Cyprus required use of multiple tiles from Landsat (see Table 1; a tile is indicated by the path/row combination). The combining or mosaicing of tiles increases the difficulty of processing the imagery. One issue in this regard is that even after atmospheric correction, atmospheric conditions may vary enough between images (especially across multiple paths) that the reflectance values will not match in scale. To avoid this issue, images were classified or analyzed prior to creating a mosaic of images.

Image classification and analysis

Image ratios, change images, NDVI, and Tasseled Cap

One type of spectral enhancement technique that helps to inform land-cover classification is the creation of ratio images. These "new" ratio images utilize combinations of bands to highlight differences between the spectral reflectances of materials without the effects of topography and insolation. They are utilized often in assessing the presence and condition of green vegetation (Lillesand et al., 2004). The Simple Ratio (or Ratio Vegetation Index) is expressed as: NIR/red, where NIR is the near infrared band and red is the red band. This index indicates the presence of green vegetation and also helps distinguish between bare soil and vegetation. As the density of vegetation increases within a pixel, the value increases from 1 (bare soil). A disadvantage of this index is that pixel values are not bounded (Birth and McVey, 1968). Change images are simple methods that utilize mathematical operations to evaluate change without classification of an image. Image differencing simply involves the subtraction of

one band in an image from the same band in another image (usually most recent image – older image). Percent change (recent-old/old) and standardized difference images also can be produced easily. These types of analysis can highlight areas that have changed spectrally between time periods; the threshold of change versus non-change is determined by the analyst and is commonly set at one standard deviation (Warner and Campagna, 2009). The normalized difference vegetation index (NDVI) is calculated as: (NIR-red)/(NIR+red). The brightness values in the NDVI image range from -1 to 1, where areas of high chlorophyll density, and thus, high vegetation density, have higher values than areas with low vegetation densities. An index to assess the physical characteristics of agricultural fields was developed for Landsat-1 and -2 MSS bands by Kauth and Thomas (1976). The Tasseled Cap or Kauth-Thomas Transformation allows the analyst to view vegetation brightness, greenness, and yellowness in separate bands, or as a false color composite. This transformation distinguishes agricultural fields from bare soil and other features nearly year-round. Crist and Cicone (1984) modified the Tasseled Cap Transformation for use with Landsat-4 through -7 TM, ETM, and ETM+ sensors. This version of the Tasseled Cap Transformation features brightness, greenness, and wetness as separate bands for image feature differentiation. After ratio images and spectral transformations are conducted, all of the images are qualitatively assessed for tonal differences between and among images to determine image features and to distinguish differences in vegetative cover (e.g. forest from agriculture).

Image classification

Land-cover classes for the sample points were derived using a hybrid classification technique, as this method is more robust than supervised or unsupervised techniques alone (Wulder et al. 2004), particularly in areas where training or ground truth data (e.g. site visits or aerial photographs) are not available (Bauer et al., 1994; Lark, 1995). Image classification began with the 2011 image and the classification system derived from the 2011 image is then applied to the remaining images (Table 3). Unsupervised Iterative Self-Organizing Data Analysis and Clustering (Isoclust, a variation of ISODATA) was used for image classification. An image layer consisting of all of the bands chosen for analysis (see Table 1, no derived data were used as classification layers) was analyzed by creating a set of arbitrary clusters, with pixels then assigned to the nearest cluster location using a maximum likelihood procedure (Eastman, 2012). The mean reflectance value is calculated once all pixels are assigned to a cluster and the process is repeated until no significant change occurs between pixel groupings. A histogram of the clusters (classes) is displayed for the user, who can now determine the appropriate number of clusters to generate through the classification process (Warner and Campagna, 2009; Eastman, 2012). The number of clusters to keep through the subsequent assigning of pixels to clusters depends upon the analyst. A small number of clusters (based upon the major break points in the histogram) will provide generalized land cover categories, necessitating little reassignment of clusters. In this case, a number of clusters approximately double that of major classes was selected (20-25 clusters) in order to capture some of the land covers that are not common. Next, a supervised

classification was performed and the clusters were assigned to land cover categories (Table 2.2), following the CORINE land cover technical guide (Bossard et al., 2000). However, not all CORINE categories (e.g. Class 4 – Wetlands) were utilized in this analysis. In this case, this decision is due to the limited nature of wetlands on Cyprus. Other subcategories were not utilized based upon their usefulness in classifying the Cypriot landscape and their ability to discern features. The CORINE land-cover classes are derived in a vector-based system (features are digitized on screen) at a minimum mapping unit of 25 hectares (note that future CORINE products will be produced in a semi-automated manner). Classes were renumbered (e.g. Class 13 in this system is Water bodies) to reflect exclusion of categories. The determination of land cover category was based upon the features highlighted in each of the spectral enhancements (image ratios, change images, NDVI, and tasseled cap) and a false color composite of each image date.

Table 3. Land cover classes that were expected across the Landsat images of Cyprus. Land cover classification scheme derived from CORINE land cover categories (Bossard et al., 2000).

Class number	Sub-class	Name	Description
1		Artificial areas	Includes urban areas and mine, industrial, and construction sites
2		Agricultural areas	Includes arable land, permanent crops, pastures, heterogeneous agricultural plots (more than one type of agricultural product in one area)
	3	Arable land	
	4	Permanent crops	
	5	Pastures	
	6	Heterogeneous agricultural areas	
7		Forest and semi-natural areas	Includes forests, shrub, and herbaceous cover. Also includes natural areas that are mostly open space with little vegetative cover
	8	Forests	

Class number	Sub-class	Name	Description
	9	Shrubs and/or herbaceous vegetation associations	
	10	Natural grassland	
	11	Open spaces	
	12	Bare rock/soil	
13		Water bodies	Includes inland waters, marine waters, and water courses (including canals)
14		Clouds	

Change analysis

Post-classification change detection is used to quantify differences between time periods. Changes are represented for each comparison (e.g. 1973 to 1984, 1984 to 1990, etc.) in a matrix illustrating "from-to" land cover classes and total number of pixels changed between classes. Land cover categories and areas of change are layered to create images that illustrate the geographical extent of each. Images created during pre-processing (change images) can also help to inform the areas of change.

An accuracy assessment is only viable for the 2011 classified image as reference images and on-the-ground field data are not available to serve as reference data for other classifications of other time steps. One hundred and fifty-one reference pixels were selected randomly from the on-the-ground observation data (27.7% of on-the-ground observation data). The reference pixel coordinates were then located on Google Earth imagery, aerial photos, and the pre-processing imagery for land cover categorization. An error matrix was constructed (Tables 4 and 5) to highlight errors within the classification

categories of the 2011 Landsat image based upon reference pixel categorization, and accuracy statistics were calculated (*cf.* Lillesand et al. 2004).

Table 4. Error matrix for the 2011 Landsat land cover classification scheme. Error matrix was constructed using 151 reference points. The reference points were randomly selected from on-the-ground survey points collected between 2008 and 2011.

			Reference Data				
Classified Data	**Background**	**Artificial areas**	**Agricultural Areas**	**Forests**	**Shrubs/ Herbaceous Cover**	**Bare Rock/ Soil**	**Classified (Row) Totals**
Background	0	0	2	0	2	0	4
Artificial Areas	0	7	1	0	0	0	8
Agricultural Areas	0	3	3	0	0	1	7
Forests	0	1	4	41	4	1	51
Shrubs/ Herbaceous Cover	0	6	22	17	23	4	72
Bare Rock/Soil	0	0	2	0	2	2	6
Column (Reference) Total	0	17	34	60	32	8	151

Table 5. Accuracy assessment summary statistics for each land cover category in the 2011 classified Landsat image. The Producer's accuracy is a measure of omission and the User's accuracy is a measure of commission.

Class Name	**Classified Totals**	**Number Correct**	**Producer's Accuracy**	**User's Accuracy**
Background	4	0	---	---
Artificial Areas	8	7	41.18%	87.50%
Agricultural Areas	7	3	8.82%	42.86%
Forests	51	41	68.33%	80.39%
Shrubs/Herbaceous Cover	72	23	71.88%	31.94%
Bare Rock/Soil	6	2	25.00%	33.33%
Totals	151	76		

Overall Classification Accuracy =50.33%
Overall Kappa Statistics = 0.3344

Landscape pattern analysis

Landscape pattern analysis is useful in analyzing changes in the distribution, number, size, and aggregation of land cover classes across the landscape. For use with data broken up into grids (e.g., based on remote sensing or aerial photography), Turner et al. (2001) define a patch as "a contiguous group of cells of the same mapped category." However, the analyst must determine what constitutes contiguous, with the most common guidelines being a four-neighbor rule (including cells that touch on the horizontal and vertical sides of the cell of interest) or an eight-neighbor rule (including the immediately surrounding horizontal, vertical, and diagonal cells). An eight-neighbor rule is applied to the classified imagery to capture landscape-scale heterogeneity; however, metrics are calculated at the class level to determine variation between land cover classes.

Specifically, metrics were employed at the class level that determined the area of patches, the diversity or evenness of land covers in a neighborhood (7x7 neighborhood size), the edge density, the change process and the compactness of patches (Eastman, 2012). The evenness index (diversity of land covers) ranges from 0 to 1 and is an indicator of how uniform the landscape is within a neighborhood (number of pixels under analysis). Values near 0 indicate that the land cover is uniform, while values near 1 indicate the maximum diversity of land cover categories. Edge density measures the fragmentation of the neighborhood under analysis and is calculated by comparing the number of adjacent pairs of pixels that are different from each other (in land cover category) relative to the maximum number of different pairs possible within the same neighborhood. The index ranges in value from 0 to 1 with values of 0 indicating that

there is very little fragmentation and values near one indicating maximum fragmentation (or number of edges) within the neighborhood. The change process metric is a means of comparing two images of different dates and measures the type of change occurring between time steps within each land cover category. The change process is determined by comparing the number of land cover patches present at each time step and calculates changes in their areas and perimeters (*cf*. Bogaert et al., 2004). The categories of change process are summarized in Table 6. The compactness index ranges from 0 to 1, where 0 indicates the land cover class of interest is maximally aggregated, while numbers near 1 indicate maximum disaggregation (Eastman, 2012).

Table 6. Types of change processes possible within IDRISI. Change process describes how land covers are changing between two time periods. Table based on Eastman (2012).

Change process	Description
Deformation	The shape of patches is changing
Shift	The position of patches is changing
Perforation	The number of patches remains constant but the area decreases
Shrinkage	The number of patches remains constant but the area and perimeter decrease
Enlargement	The number of patches is constant but the area increases
Attrition	The number of patches and area decrease
Aggregation	The number of patches decreases but area is constant or increasing
Creation	The number of patches and are increasing
Dissection	The number of patches is increasing and the area is decreasing
Fragmentation	The number of patches increases and the area is strongly decreasing

Results

Image classification and analysis

Landsat imagery was classified for five time steps (1973, 1984, 1990, 2001 and 2011) and evaluated for changes in land cover category and landscape configuration

between each time step. Each path/row of the Landsat images was classified separately to reduce effects from image capture at different dates, times and sensor. The land cover categories from the CORINE Land Cover Technical Guide (Bossard et al., 2000) were adapted for a pixel-based analysis resulting in six classification categories: artificial areas, agricultural areas, forests, shrubs and/or herbaceous vegetation, bare soils/rocks and water (see Table 6 for a description of the categories). The ISOCLUST classifier created groups of pixels with similar spectral responses and the groups were then assigned to a land cover category based on comparisons with the NDVI, Tasseled Cap and false-color composite images. Maps depicting the land cover for 1973, 1984, 1990, 2001 and 2011 are included as Figures 6, 7, 8, 9 and 10, respectively.

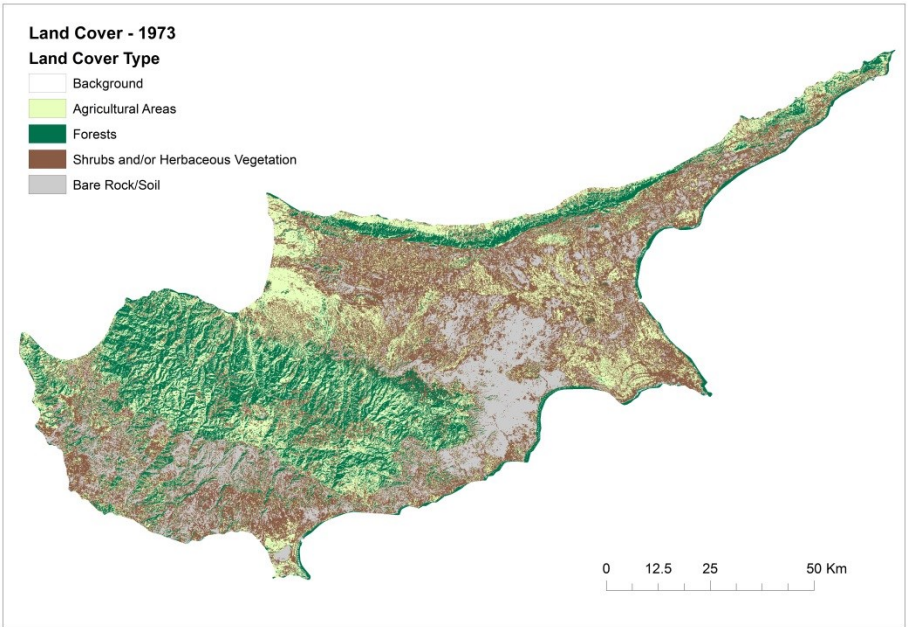

Figure 6. Map of the land cover classification for the mosaiced 1973 Landsat images, derived using an ISOCLUST classifier. In this image artificial areas are not evident at the scale of analysis (30 m pixels).

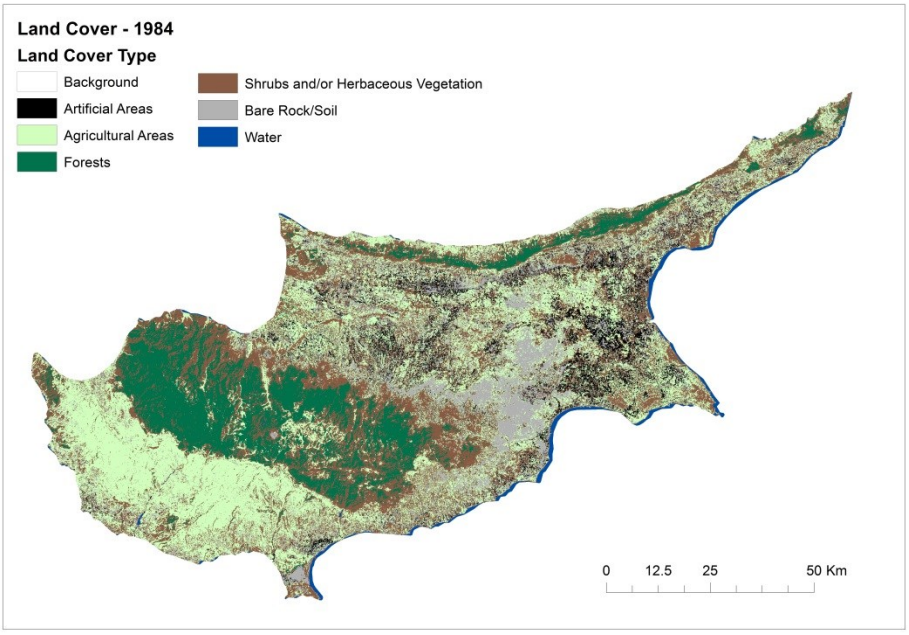

Figure 7. Map of the land cover classification for the mosaiced 1984 Landsat images, derived using an ISOCLUST classifier. Agricultural areas in the southeast of the country have increased in agricultural land covers.

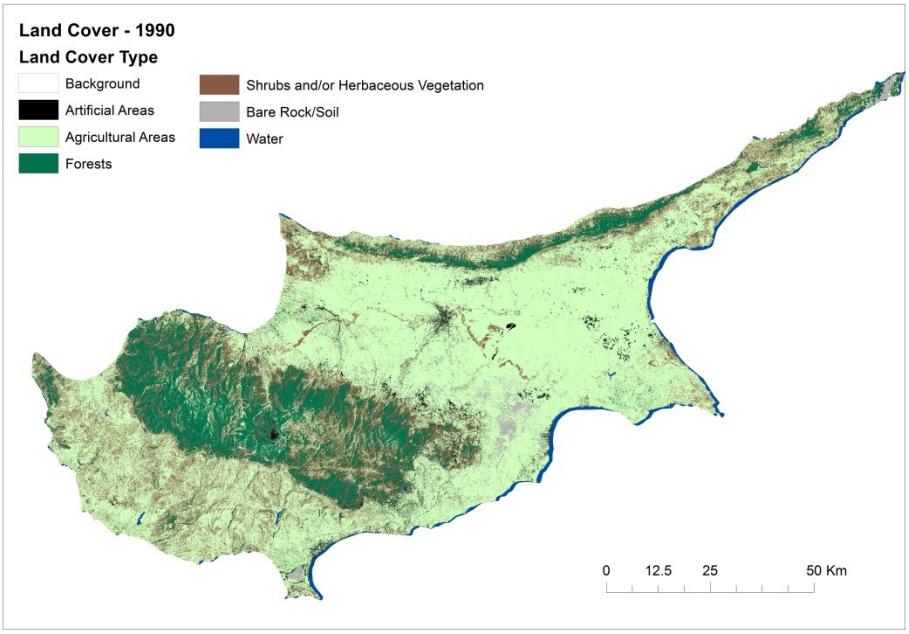

Figure 8. Map of the land cover classification for the mosaiced 1990 Landsat images, derived using an ISOCLUST classifier. The Mesaoria Plain shows an increase in agricultural land covers and the urban area of Nicosia evident in the plain.

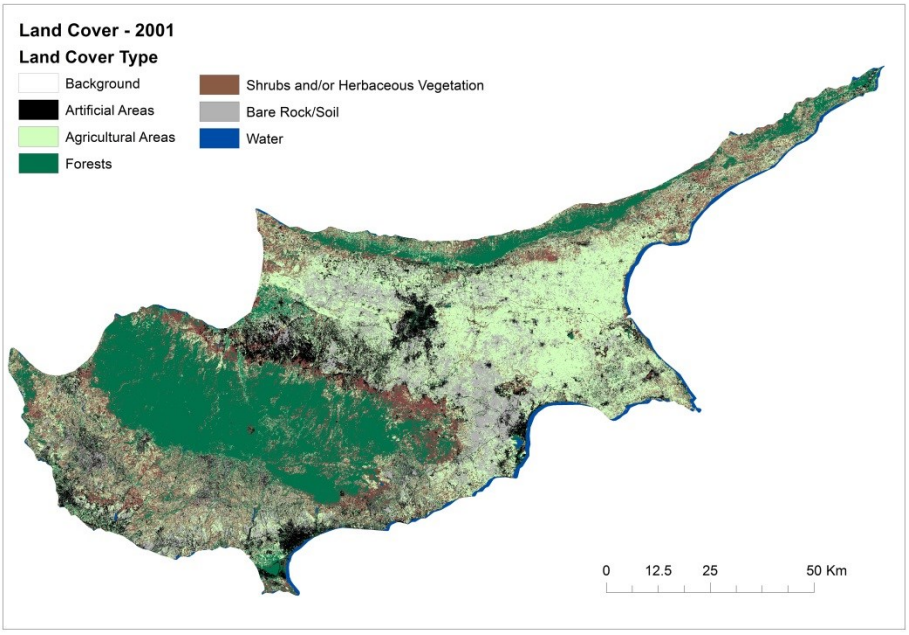

Figure 9. Map of the land cover classification for the mosaiced 2001 Landsat images, derived using an ISOCLUST classifier. The Troodos Range shows an increase in forests and the urban areas of Nicosia, Larnaka and Limasol are clearly delineated.

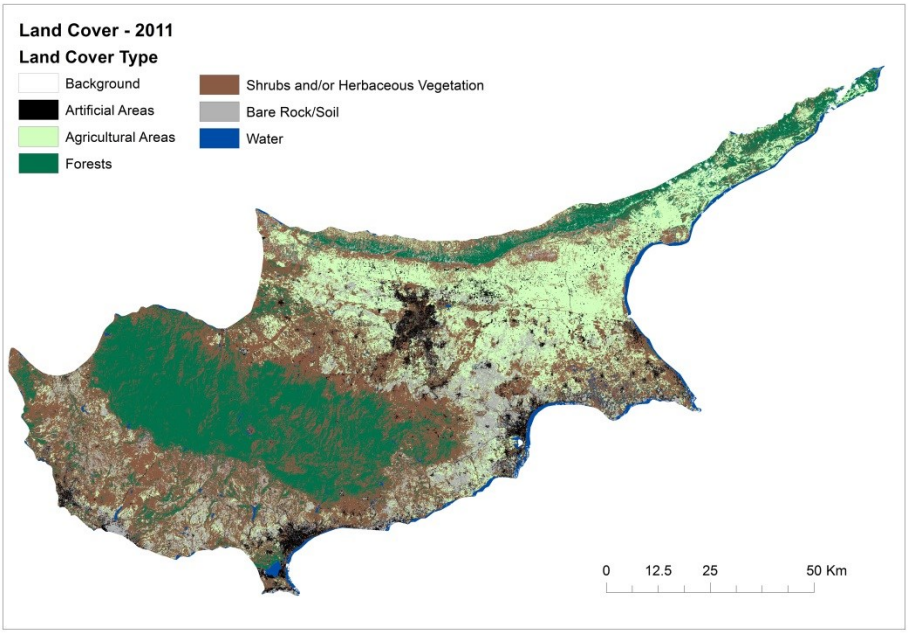

Figure 10. Map of the land cover classification for the mosaiced 2011 Landsat images, derived using an ISOCLUST classifier. The urban areas have increased in extent.

The 2011 classified image (Figure 10) was assessed for pixels that were misclassified through the construction of an error matrix that compares the classification of pixels to their actual land cover as verified on the ground or through higher resolution imagery (Congalton, 1991). Errors of commission (total number of correctly classified pixels in category/total number of pixels as classified belonging to the category) and errors of omission (total number of pixels correctly classified pixels/total number of pixels identified as the category from reference data) are calculated from the error matrix. Shrubs and/or herbaceous vegetation had a producer's accuracy (errors of omission) of 71.88% and forests were at 68.33% (Table 5), indicating the probability that reference pixels are successfully identified using the ISOCLUST algorithm. Artificial areas and forests had user's accuracies (errors of commission) of 87.50% and 80.39%, respectively. This is a measure of reliability that indicates the probability of a pixel identified as either of these classes actually belonging to the same class on the ground (Congalton, 1991).

Overall accuracy and a Kappa statistic also were calculated to evaluate the classification results further. Overall classification accuracy was 50.33% and the Kappa statistic (KHAT) was 33.44% (Table 5). Overall accuracy indicates that only half of the pixels are correctly classified when judged against reference data. The KHAT statistic measures the difference between the observed accuracy (agreement between the reference data and an automated classifier) and chance agreement (agreement between the reference data and a random classifier) (Lillesand and Kiefer, 2000). The KHAT statistic for the 2011 classified map indicates that it is 33% better than if the result had occurred

by chance and is ranked as fair in terms of strength of agreement (Landis and Koch, 1977).

Change analysis

Matrices were constructed to evaluate the changes in land cover categories between each time step (Tables 7 to 10). The cross-tabulation (from-to) matrix for 1973 to 1984 (Table 7) shows that 1.34% of shrub and/or herbaceous vegetation changed to artificial areas by 1984 and 3.74% of artificial areas in 1973 were classified as shrub and/or herbaceous cover in 1984. Agricultural areas comprise 9.76% of the landscape in 1973 but increase to 11.97% by 1984. Forests decline from7.08% in 1973 to 4.74% in 1984 with 2.34% of the change attributed to transition from forest to shrub and/or herbaceous vegetation.

Table 7. Proportional cross-tabulation of land cover categories. The table tabulates the portion of a class in 1973 (columns) that transition to each other class in 1984 (rows). Total proportional area for each category is shown along the bottom (1973 totals) and along the right side (1984 totals) of the table. See Table 3 for classification system.

		1973 Land Cover Classification (proportional area)					
		0	2	8	9	12	Total
1984 Land Cover Classification (proportional area)	0	0.6552	0.0008	0.001	0.0005	0.0001	0.6576
	1	0	0.0062	0.0004	0.0134	0.0037	0.0237
	2	0	0.0321	0.0089	0.052	0.0268	0.1197
	8	0.0006	0.0139	0.0317	0.0012	0	0.0474
	9	0	0.0374	0.0234	0.0322	0.0104	0.1035
	12	0	0.0071	0.0012	0.017	0.0181	0.0434
	13	0.0004	0.0001	0.0042	0	0.0001	0.0047
	Total	0.6562	0.0976	0.0708	0.1163	0.059	1

The 1984 to 1990 cross-tabulation (Table 8) shows an increase in agricultural areas from 11.97% of the landscape in 1984 to 21.18% of the landscape by 1990. A large

proportion of this change (5.79%) comes from forest transitioning into agricultural areas by 1990. The total area classified as bare soils/rocks in 1984 declines from 4.34% to 0.54% in 1990. A transition from soils to agriculture accounts for 3.56% of the changed area.

Table 8. Proportional cross-tabulation of land cover categories. The table tabulates the portion of a class in 1984 (columns) that transition to each other class in 1990 (rows). Total proportional area for each category is shown along the bottom (1984 totals) and along the right side (1990 totals) of the table. See Table 3 for classification system.

		1984 Land Cover Classification (proportional area)							
		0	1	2	8	9	12	13	Total
1990 Land Cover Classification (proportional area)	0	0.6552	0	0.0004	0	0.0001	0.0001	0	0.6558
	1	0.0001	0.001	0.0029	0.0001	0.0038	0.002	0	0.0101
	2	0.0005	0.0221	0.0933	0.0024	0.0579	0.0356	0	0.2118
	8	0.0006	0	0.0011	0.0369	0.0097	0	0	0.0484
	9	0.0004	0.0005	0.0209	0.008	0.0314	0.002	0	0.0632
	12	0.0004	0.0001	0.001	0	0.0003	0.0036	0	0.0054
	13	0.0003	0	0.0001	0	0.0004	0	0.0046	0.0054
Total		0.6576	0.0237	0.1197	0.0474	0.1035	0.0434	0.0047	1

In 1990, 21.18% of the landscape is under cultivation (Table 9); however, this declines to 11.17% by 2001. The decline is split between increase to artificial areas (change of 3.24% between 1990 and 2001), increase in bare soil/rock (change of 3.29%), and increase in shrub and/or herbaceous vegetation (change of 3.57% between the two time steps). Forested areas increase from 4.84% of the landscape in 1990 to 8.92% in 2001 with 2.48% of the change in transitions from shrub and/or herbaceous cover.

Agricultural areas decline from 11.17% of the landscape to 7.98% between 2001 and 2011, with a shift of 4.57% of land from agriculture to shrub and/or herbaceous vegetation (Table 10). Shrub and/or herbaceous cover increased overall, from 6.09% of

the landscape in 2001 to 12.79% in 2011. There also is a notable decline in artificial areas from 3.95% of the total land area in 2001 to 1.86% by 2011. This shift is seen in a transition to forests (change of 4.57%).

Table 9. Proportional cross-tabulation of land cover categories. The table tabulates the portion of a class in 1990 (columns) that transition to each other class in 2001 (rows). Total proportional area for each category is shown along the bottom (1990 totals) and along the right side (2001 totals) of the table. See Table 3 for classification system.

		1990 Land Cover Classification (proportional area)							
		0	1	2	8	9	12	13	Total
2001 Land Cover Classification (proportional area)	0	0.6552	0	0	0	0	0	0	0.6552
	1	0.0001	0.0028	0.0324	0.0002	0.0033	0.0006	0	0.0395
	2	0.0001	0.0019	0.0937	0.0012	0.0141	0.0007	0	0.1117
	8	0	0.002	0.0171	0.0446	0.0248	0.0005	0.0002	0.0892
	9	0.0001	0.0029	0.0357	0.0023	0.0197	0.0002	0	0.0609
	12	0.0002	0.0003	0.0329	0.0001	0.0013	0.0034	0	0.0382
	13	0	0.0001	0.0001	0	0	0.0001	0.0051	0.0054
	Total	0.6558	0.0101	0.2118	0.0484	0.0632	0.0054	0.0054	1

Table 10. Proportional cross-tabulation of land cover categories. The table tabulates the portion of a class in 2001 (columns) that transition to each other class in 2011 (rows). Total proportional area for each category is shown along the bottom (2001 totals) and along the right side (2011 totals) of the table. See Table 3 for classification system.

		2001 Land Cover Classification (proportional area)							
		0	1	2	8	9	12	13	Total
2011 Land Cover Classification (proportional area)	0	0.6552	0	0	0	0	0	0	0.6552
	1	0	0.009	0.0042	0.0008	0.001	0.0036	0.0001	0.0186
	2	0	0.0075	0.0479	0.0014	0.0082	0.0147	0	0.0798
	8	0	0.0004	0.0041	0.0667	0.0071	0.0002	0	0.0785
	9	0	0.0179	0.0457	0.0174	0.0412	0.0056	0	0.1279
	12	0	0.0041	0.0087	0.0006	0.002	0.0139	0.0001	0.0295
	13	0	0.0004	0.0006	0.001	0.0003	0.0002	0.0047	0.0073
	14	0	0.0001	0.0005	0.0012	0.001	0	0.0004	0.0033
	Total	0.6552	0.0395	0.1117	0.0892	0.0609	0.0382	0.0054	1

A cross-tabulation was also conducted for the time period of 1984 to 2001 to evaluate the changes that occurred after 1974 but prior to the opening of the UN

controlled buffer zone (Table 11). Over this time frame the largest change was observed in forest cover. In 1984 the landscape was composed of 4.74% forest and by 2001 forest cover increased to 8.92%. Shrub and/or herbaceous cover declined with transition of 3.07% to artificial cover and 2.92% to forests. Evaluation of this time period indicates relatively little overall change to the percentage of the landscape designated as artificial areas (increase from 2.37% to 3.95%).

Table 11. Proportional cross-tabulation of land cover categories. The table tabulates the portion of a class in 1984 (columns) that transition to each other class in 2001 (rows). Total proportional area for each category is shown along the bottom (1984 totals) and along the right side (2001 totals) of the table. See Table 3 for classification system.

		1984 Land Cover Classification (proportional area)							
		0	1	2	8	9	12	13	Total
2001 Land Cover Classification (proportional area)	0	0.6552	0	0	0	0	0	0	0.6552
	1	0.0002	0.0053	0.0173	0	0.0089	0.0077	0	0.0395
	2	0.0004	0.0131	0.0486	0.0009	0.0307	0.018	0	0.1117
	8	0.001	0.0004	0.0126	0.0443	0.0292	0.0015	0.0001	0.0892
	9	0.0004	0.0017	0.0247	0.0021	0.0272	0.0048	0	0.0609
	12	0.0001	0.0032	0.0165	0	0.0072	0.0112	0	0.0382
	13	0.0003	0	0.0001	0	0.0003	0.0001	0.0045	0.0054
	Total	0.6576	0.0237	0.1197	0.0474	0.1035	0.0434	0.0047	1

Transitions maps were created for artificial areas, agricultural areas, forests and shrub and/or herbaceous vegetation (Figures 11-14). These maps illustrate the spatial arrangement of area gained, lost or persisting between time steps for each land cover category individually. In the maps for 1973 to 1984 transitions (Figure 11a-d), agricultural areas in the Troodos appear to decline while increases in agriculture are most pronounced from the southwestern edge of the Troodos foothills to the coast. With this agricultural transition, shrubs and/or herbaceous vegetation increase around the entire

Troodos foothills and throughout the Mesaoria Plain. Additional areas of shrub and/or herbaceous vegetation increase along the foothills of the Kyrenia Range, the Karpas Peninsula and the Akamas Peninsula. Artificial areas appear to increase the most across the Mesaoria Plain and along the southeastern coastline. Forest areas decline in the northern portions of both the Troodos and Kyrenia ranges. Many slopes with a predominately south to southeast orientation show increases in forested areas.

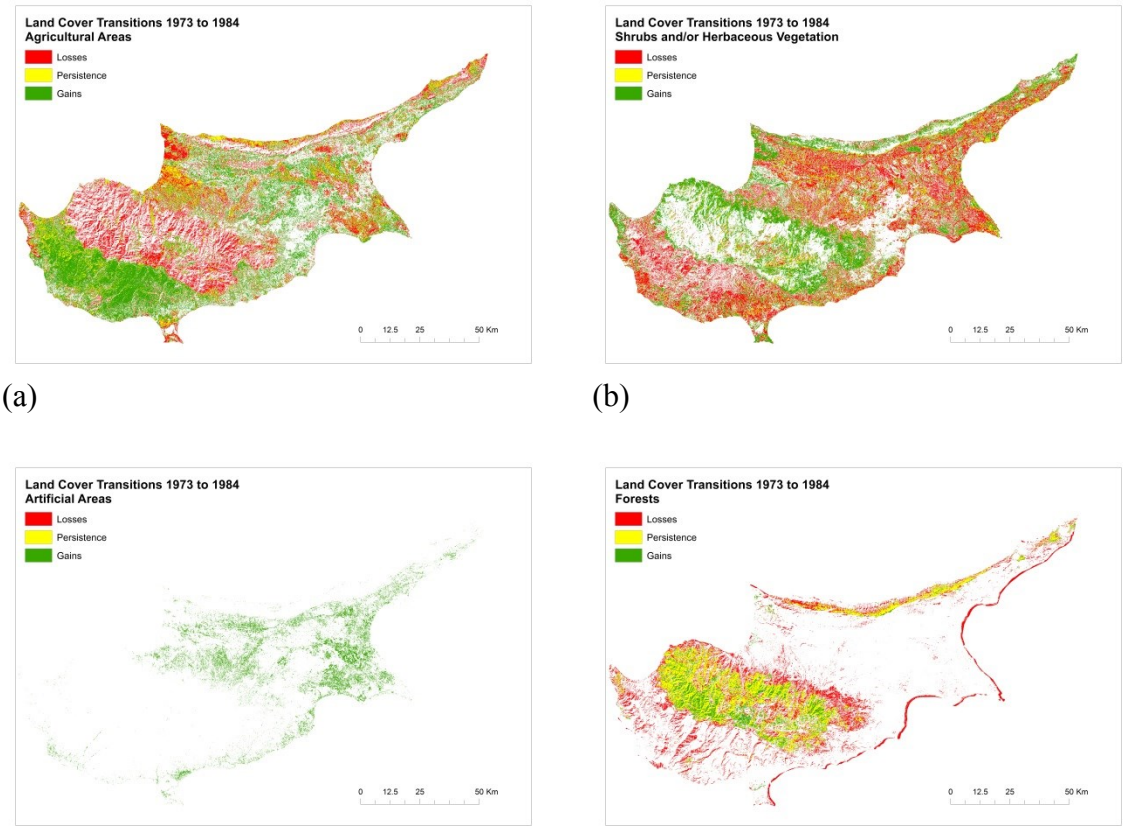

Figure 11. Transition maps for 1973 to 1984. Green areas are pixels of increase in the specific land cover, red areas are pixels of decrease and yellow areas are areas that stay the same land cover between the two time periods. Map a depicts changes to agricultural areas, b is changes to shrubs and/or herbaceous covers, c illustrates changes to artificial areas and d shows changes to forests.

The transition maps for 1984 to 1990 (Figure 12a-d) show further increases in agriculture across the Mesaoria Plain and extension northward onto the Karpas Peninsula with small declines near Nicosia. Changes to agricultural areas are not very pronounced along the southeastern side of the Troodos during this time period. Shrubs and/or herbaceous vegetation decline dramatically long the northern fringe of the Troodos and to a lesser extent, across the Mesaoria Plain. The southeastern foothills to the coast experience some increases in shrub and/or herbaceous cover. Artificial areas increase near Nicosia and Limasol. A large patch of artificial area is seen in the center of the Troodos around a mine site developed during this time period. Forest cover stabilizes between 1984 and 1990, with only a few patches of loss scattered throughout the Troodos.

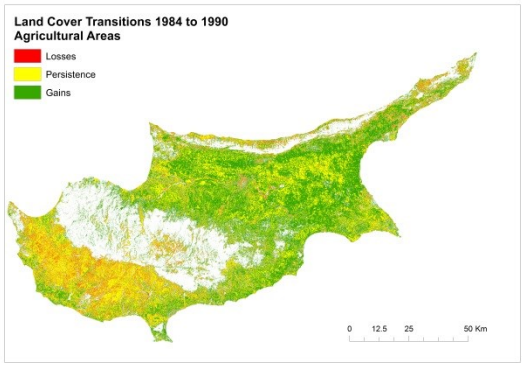

(a)

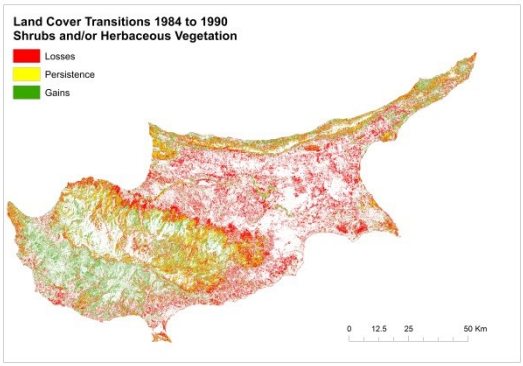

(b)

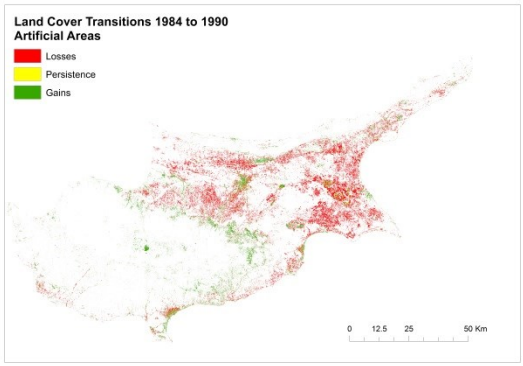

(c)

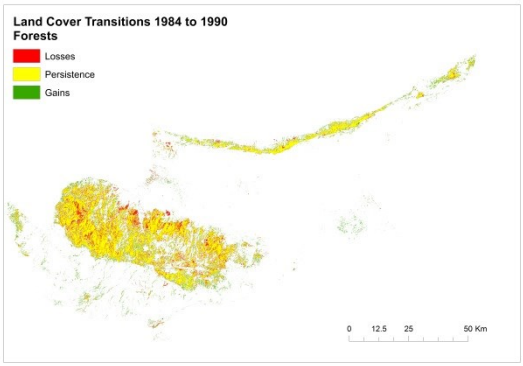

(d)

Figure 12. Transition maps for 1984 to 1990. Green areas are pixels of increase in the specific land cover, red areas are pixels of decrease and yellow areas are areas that stay the same land cover between the two time periods. Map a depicts changes to agricultural areas, b is changes to shrubs and/or herbaceous covers, c illustrates changes to artificial areas and d shows changes to forests.

Agricultural areas do not change much over the Mesaoria Plain between 1990 and 2001 (Figure 13a), although a large area of loss is evident near Nicosia, Limasol, Larnaka and in a patch of the northern foothills of the Troodos. Shrubs and/or herbaceous vegetation show a slight decline across the entire island, with a ribbon of decline evident along the buffer zone (Figure 13b). Artificial areas increase in the areas of agricultural decline (Figure 13c) and a network of roads becomes more apparent across the landscape.

Forests maintain their configuration between 1990 and 2001, with additions in the Troodos and Kyrenia Ranges and Morphou Bay (Figure 13d).

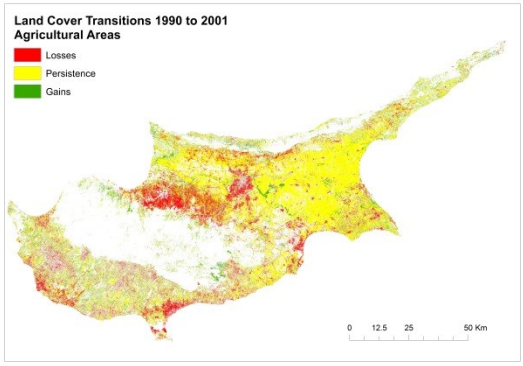

(a)

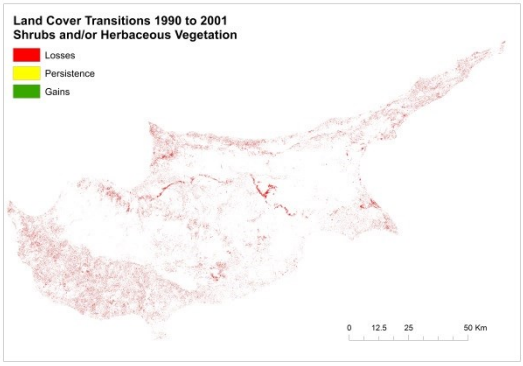

(b)

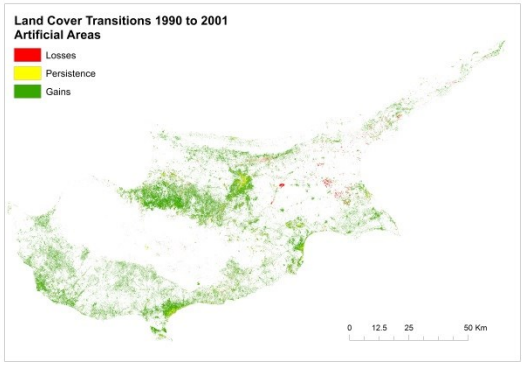

(c)

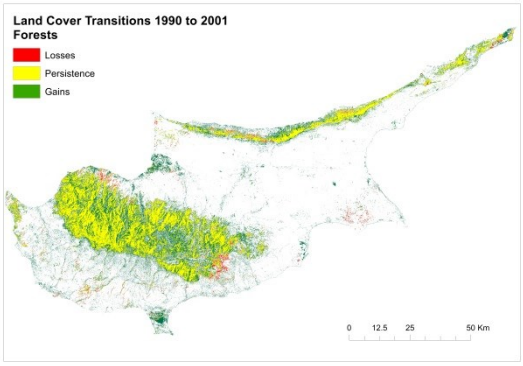

(d)

Figure 13. Transition maps for 1990 to 2001. Green areas are pixels of increase in the specific land cover, red areas are pixels of decrease and yellow areas are areas that stay the same land cover between the two time periods. Map a depicts changes to agricultural areas, b is changes to shrubs and/or herbaceous covers, c illustrates changes to artificial areas and d shows changes to forests.

The Karpas Peninsula experiences an increase in agricultural areas between 2001 and 2011 while the southeast end of the Mesaoria Plain shows a decline (Figure 14a). Much of the Mesaoria Plain is stable over this time period and does not increase or decrease in agricultural land cover. Shrubs and/or herbaceous vegetation appear to experience the most dramatic changes between 2001 and 2011 with increases in cover

across much of the island (Figure 14b). Increases are particularly high along the southeast and northwest ends of the Mesaoria Plain. Much of the southwestern side of the Troodos, extending to the coast, maintains shrub and/or herbaceous cover between 2001 and 2011, however many areas in this region also experience an increase in this cover type. There is still evidence of growth in artificial areas near Nicosia, Larnaka and Limasol, with additional coastal areas along the south also increasing in this land cover type (Figure 14c). Forest areas are largely maintained with increases to forest cover along the Karpas Peninsula (Figure 14d).

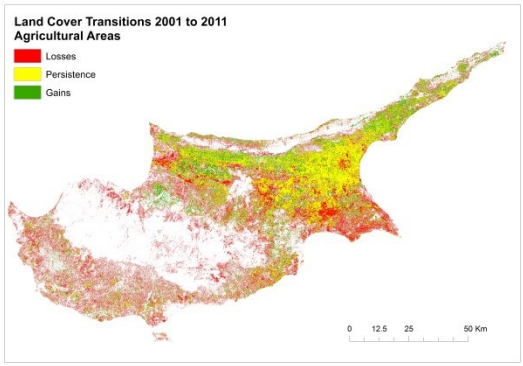

(a)

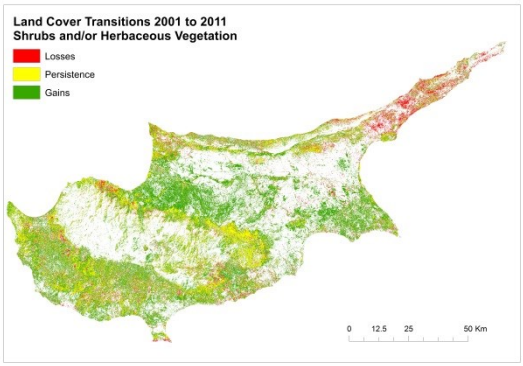

(b)

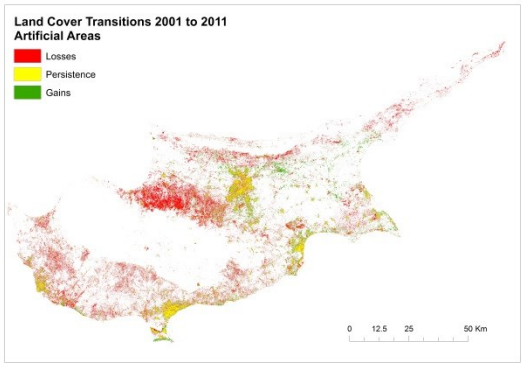

(c)

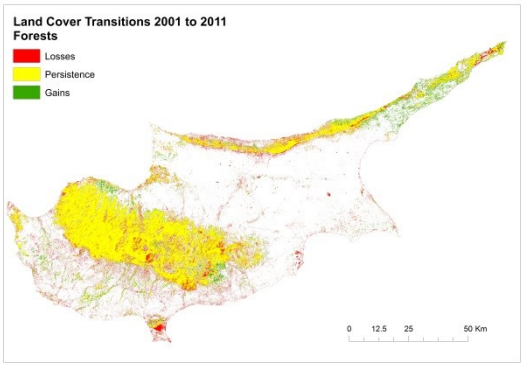

(d)

Figure 14. Transition maps for 2001 to 2011. Green areas are pixels of increase in the specific land cover, red areas are pixels of decrease and yellow areas are areas that stay the same land cover between the two time periods. Map a depicts changes to agricultural areas, b is changes to shrubs and/or herbaceous covers, c illustrates changes to artificial areas and d shows changes to forests.

Changes in northern and southern Cyprus

To examine changes occurring on different parts of the island, the UN controlled buffer zone was used as a boundary to divide Cyprus into northern and southern portions. Over the entire period of evaluation (1973-2011) large shifts in land cover categories are not evident (Table 12). The largest change is in the shrub and/or herbaceous cover, which experienced a decline from 4.99% to 3.26% of the entire landscape. A majority of the difference is in transition to agricultural land covers (2.88%). In 1973 artificial areas are

not evident across the entire island, and by 2011 they constitute only 0.46% of the northern area (1189.28 km^2). When the time period since 1974 (1984-2011 images) is considered more details emerge (Table 13). For example, an increase in forests occurs from 1984 to 2011, increasing from 3.92% to 5.53% of northern Cyprus. Agricultural areas increase from 3.92% to 5.53% of the northern area, while artificial areas decrease from 1.29% to 0.46%. In southern Cyprus, agricultural areas decline from 6.20% in 1973 to 2.44% in 2011 (Table 14), while forested area increase in extent over the same period (from 5.61% to 6.16%). Shrub and/or herbaceous vegetation cover experiences the largest change between time periods, with an increase from 6.64% in 1973 to 9.53% in 2011. Between 1984 and 2011 agricultural areas declined from 8.05% of the southern landscape to 2.44%; much of this transition was to shrub and/or herbaceous vegetation (4.51%) (Table 15). Forests also experienced noticeable change during this time period, gaining 2.06% of the landscape. Looking at just the time between closing and re-opening of the buffer zone (1984-2001 image dates), forest areas experienced an increase in extent, growing from 6.20% in 1984 to 7.19% in 2001.

Table 12. Proportional cross-tabulation of land cover categories for northern Cyprus from 1973 to 2011. The table tabulates the portion of a class in 1973 (columns) that transition to each other class in 2011 (rows). Total proportional area for each category is shown along the bottom (1973 totals) and along the right side (2011 totals) of the table. See Table 3 for classification system.

		1973 Land Cover Classification (proportional area)					
		0	2	8	9	12	Total
2011 Land Cover Classification (proportional area)	0	0.8805	0	0	0	0	0.8805
	1	0	0.001	0.0001	0.0024	0.0011	0.0046
	2	0	0.0127	0.0009	0.0288	0.013	0.0553
	8	0.0001	0.006	0.0077	0.0028	0.0003	0.0169
	9	0	0.014	0.0029	0.0132	0.0025	0.0326
	12	0	0.0006	0.0001	0.0019	0.0023	0.0048
	13	0.0002	0.0002	0.002	0.0001	0	0.0025
	14	0	0.0013	0.0008	0.0006	0.0001	0.0028
	Total	0.8807	0.0356	0.0146	0.0499	0.0192	1

Table 13. Proportional cross-tabulation of land cover categories for northern Cyprus from 1984 to 2001. The table tabulates the portion of a class in 1984 (columns) that transition to each other class in 2001 (rows). Total proportional area for each category is shown along the bottom (1984 totals) and along the right side (2001 totals) of the table. See Table 3 for classification system.

		1984 Land Cover Classification (proportional area)							
		0	1	2	8	9	12	13	Total
2001 Land Cover Classification (proportional area)	0	0.8805	0	0	0	0	0	0	0.8805
	1	0.0002	0.0015	0.0033	0	0.0023	0.002	0	0.0093
	2	0.0004	0.0087	0.0209	0.0003	0.0156	0.0112	0	0.0572
	8	0.001	0.0001	0.0029	0.0057	0.0071	0.0004	0	0.0172
	9	0.0004	0.0009	0.0069	0.0004	0.0089	0.0025	0	0.0201
	12	0.0001	0.0017	0.0052	0	0.0028	0.0035	0	0.0133
	13	0.0003	0	0	0	0.0001	0	0.0019	0.0024
	Total	0.8829	0.0129	0.0392	0.0064	0.0369	0.0196	0.0019	1

Table 14. Proportional cross-tabulation of land cover categories for southern Cyprus from 1973 to 2011. The table tabulates the portion of a class in 1973 (columns) that transition to each other class in 2011 (rows). Total proportional area for each category is shown along the bottom (1973 totals) and along the right side (2011 totals) of the table. See Table 3 for classification system.

2011 Land Cover Classification (proportional area)	1973 Land Cover Classification (proportional area)					
	0	2	8	9	12	Total
0	0.7748	0	0	0	0	0.7748
1	0	0.0027	0.0005	0.0067	0.0041	0.014
2	0	0.0043	0.0006	0.011	0.0086	0.0244
8	0.0005	0.0205	0.0354	0.0048	0.0004	0.0616
9	0	0.0317	0.0164	0.0351	0.012	0.0953
12	0	0.0021	0.0006	0.008	0.014	0.0247
13	0.0002	0.0007	0.0023	0.0007	0.0007	0.0047
14	0	0	0.0003	0	0.0001	0.0004
Total	0.7756	0.062	0.0561	0.0664	0.0399	1

Table 15. Proportional cross-tabulation of land cover categories for southern Cyprus from 1984 to 2001. The table tabulates the portion of a class in 1984 (columns) that transition to each other class in 2001 (rows). Total proportional area for each category is shown along the bottom (1984 totals) and along the right side (2001 totals) of the table. See Table 3 for classification system.

2001 Land Cover Classification (proportional area)	1984 Land Cover Classification (proportional area)							
	0	1	2	8	9	12	13	Total
0	0.7748	0	0	0	0	0	0	0.7748
1	0	0.0038	0.014	0	0.0066	0.0057	0	0.0301
2	0	0.0044	0.0276	0.0006	0.0151	0.0068	0	0.0545
8	0	0.0003	0.0097	0.0387	0.022	0.0011	0.0001	0.0719
9	0	0.0007	0.0178	0.0017	0.0182	0.0023	0	0.0408
12	0	0.0015	0.0113	0	0.0044	0.0077	0	0.025
13	0	0	0	0	0.0002	0.0001	0.0026	0.0029
Total	0.7748	0.0108	0.0805	0.041	0.0665	0.0237	0.0027	1

Landscape pattern analysis

Five metrics describing landscape patterns were employed to examine how landscapes have changed in Cyprus from 1973 to 2011. Each metric produces a map, with values at each pixel indicating the measure for the patch to which the pixel belongs. On the maps for each index, low values are indicated by cooler colors while high values are indicated by warmer colors. Patch areas (Figures 15a-e) remain similar from 1973 to 2011 but patch areas change in their distribution over time. For example in 1973 slightly larger patches occur across the Mesaoria Plain (Figure 15a) but by 2011 the largest patches are occurring in the foothills of the Troodos and Kyrenia Ranges (Figure 15e). In 1990 (Figure 15c) large patches are occurring across most of the island and indicate that land cover categories covering these regions are becoming more contiguous and aggregated.

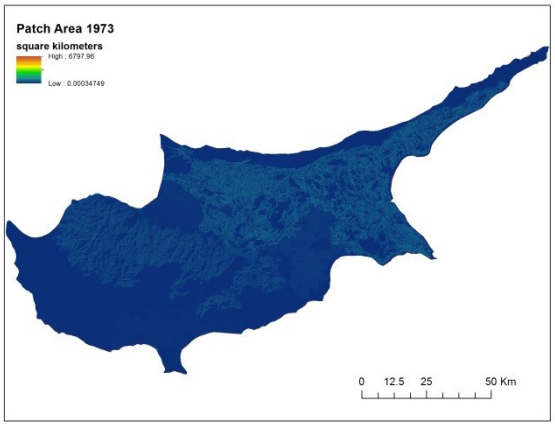

(a)

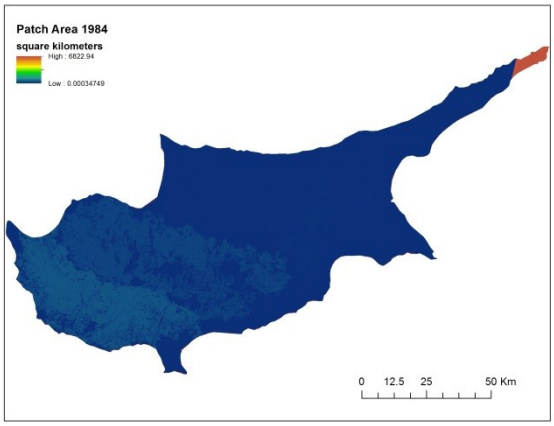

(b)

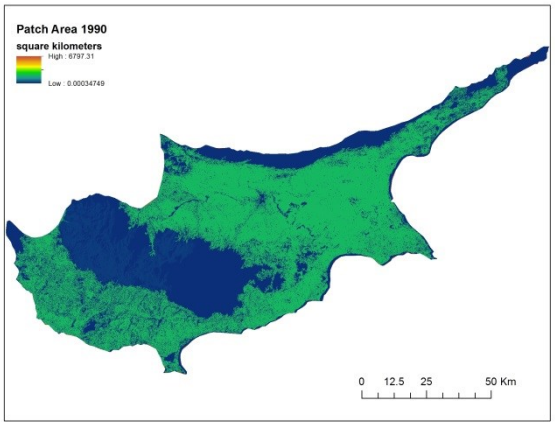

(c)

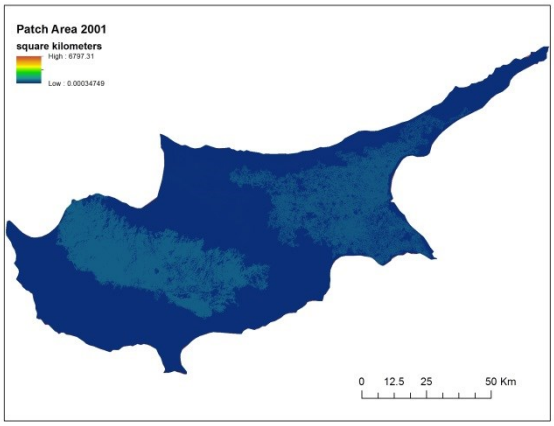

(d)

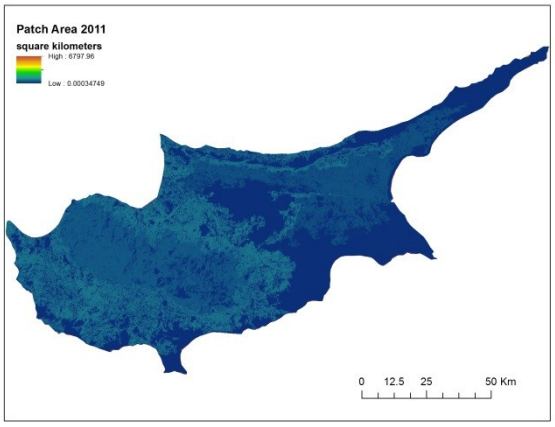

(e)

Figure 15. Patch area for each time step from 1973 to 2011. Locations of the largest patch area shift from the Mesaoria Plain to the foothills of the Troodos and Kyrenia Ranges.

Land cover diversity was evaluated using the normalized entropy (also known as Shannon's Diversity index or Evenness Index). This measure ranges from 0 to 1 and indicates how the land cover categories are distributed across the neighborhood with 1 representing more evenness (or land covers that are approximately evenly distributed across the landscape within the neighborhood and represents the highest diversity of land covers) and 0 indicating less evenness (one land cover is prevalent, thus the distribution is more uniform) (Turner et al., 2001). In 1973 the areas of highest evenness occur in the

Troodos foothills while the areas that are most uniform in land cover are located in the northwestern and southeastern parts of the Mesaoria Plain (Figure 16a). In 1984 the pattern shifts, with the highest evenness occurring across the Mesaoria Plain, the southern side of the Kyrenia Range and the southern coastline (Figure 16b). Regions of the Troodos, particularly to the north and west, show large regions of low land cover diversity, with prevalence of forest and agricultural land covers. This indicates that across the Mesaoria Plain land covers are changing and increasing the heterogeneity of the landscape. By 1990 the Mesaoria Plain has stabilized and evenness has declined, while areas around Nicosia and in and around the Troodos have the highest evenness, with nodes and linear features appearing in the landscape (Figure 16c). This indicates that land covers are transitioning with a distinctive increase in artificial areas and roads radiating from those areas (nodes and linear features). In 2001, evenness is highest along the southern foothills of the Troodos and many linear features are visible in this area and the Mesaoria Plain (Figure 16d). This indicates the road network is still increasing and development along the south coast is common. Evenness in 2011 is the highest near and along the southern coastlines and urban centers (Figure 16e) indicating transitions to artificial areas are still progressing, creating heterogeneous landscapes as they grow.

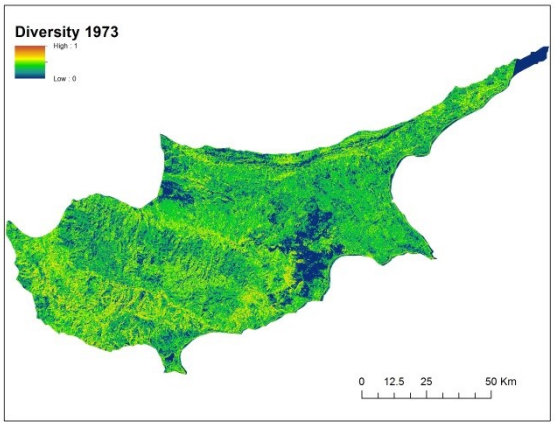
Diversity 1973
High : 1
Low : 0
0 12.5 25 50 Km

(a)

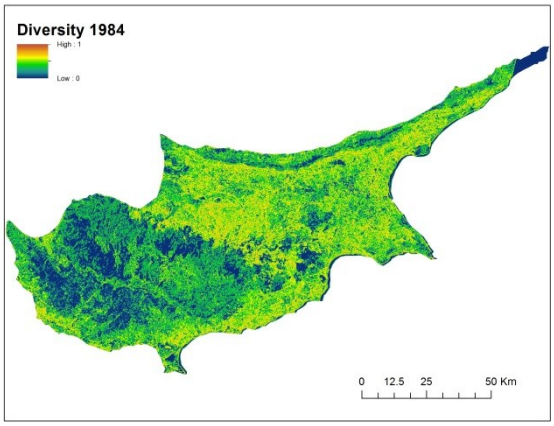
Diversity 1984
High : 1
Low : 0
0 12.5 25 50 Km

(b)

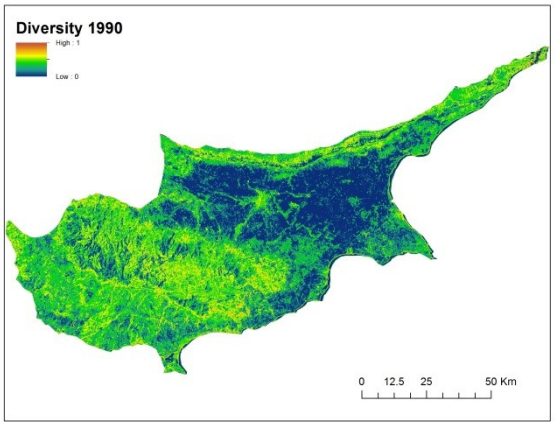
Diversity 1990
High : 1
Low : 0
0 12.5 25 50 Km

(c)

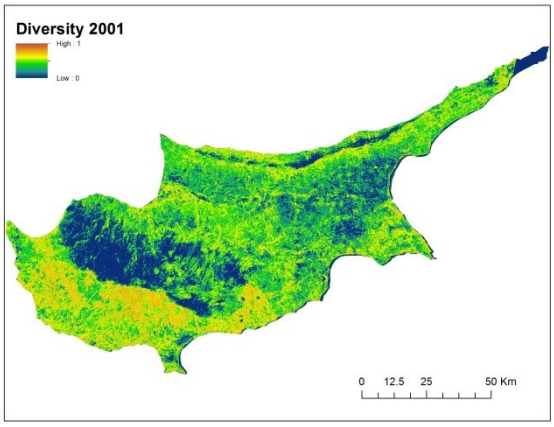
Diversity 2001
High : 1
Low : 0
0 12.5 25 50 Km

(d)

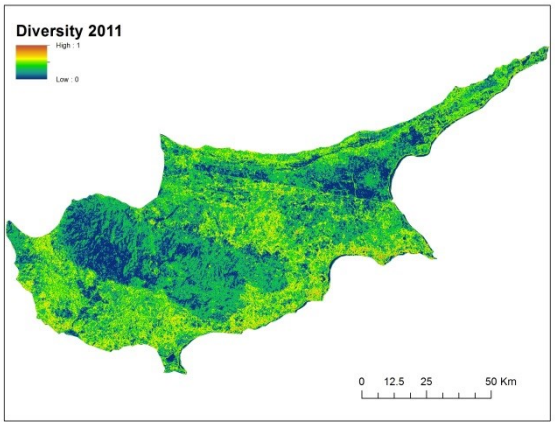

(e)

Figure 16. Land cover diversity or Evenness Index. Higher values indicate areas where land covers are more evenly distributed across the 7x7 pixel neighborhood and represent the highest diversity of land covers possible in that neighborhood. Low values indicate that the land cover in the neighborhood is more uniform and fewer land cover types occur in the neighborhood and one or two cover types dominate the neighborhood.

Edge density was calculated to examine the level of fragmentation with values near 0 indicating very little fragmentation and 1 indicating maximum fragmentation in the neighborhood under analysis. Edge density does not change much between 1973 and 1984 (Figures 17a and 17b), with the notable areas of change are in the Troodos and Mesaoria Plain. In 1984 the Troodos have decreased in edge density (become less fragmented) while the Mesaoria Plain increases in fragmentation. However, by 1990 (Figure 17c) the Mesaoria Plain has very little fragmentation but fragmentation has increased across all other parts of the island. The urban center of Nicosia stands out in the Mesaoria Plain as a region of fragmentation. Fragmentation is high along the Troodos foothills in 2001 (Figure 17d) but has continued to decline within the Troodos and along the northern parts of the Kyrenia Range. The map illustrating the distribution of fragmentation in 2011 (Figure 17e) looks similar to distributions in the 1973 and 1984

maps (Figures 17a and 17b); however, fragmentation is slightly higher across most of the island with values lower than either of those years in the Troodos.

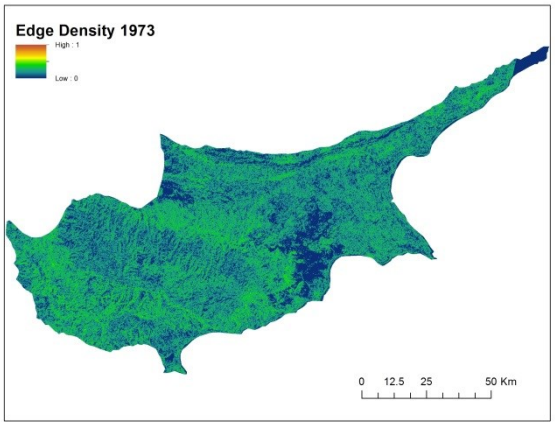

(a)

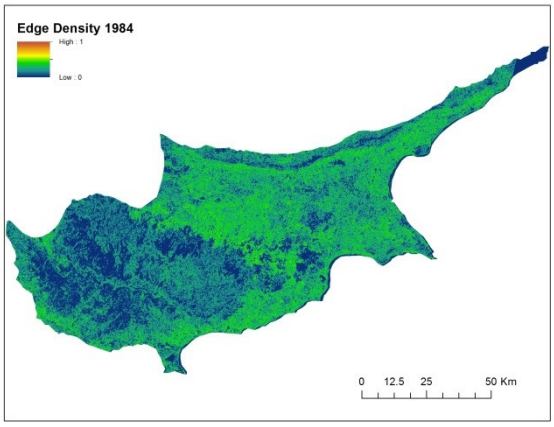

(b)

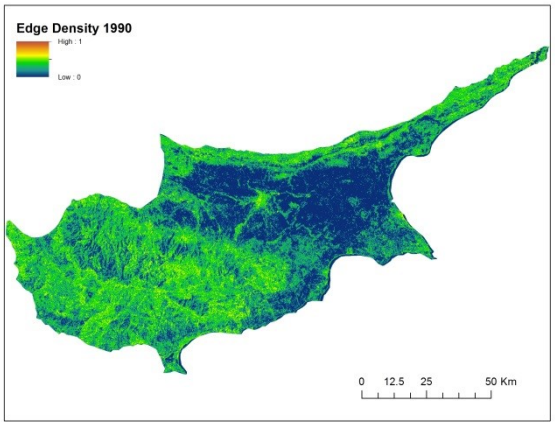

(c)

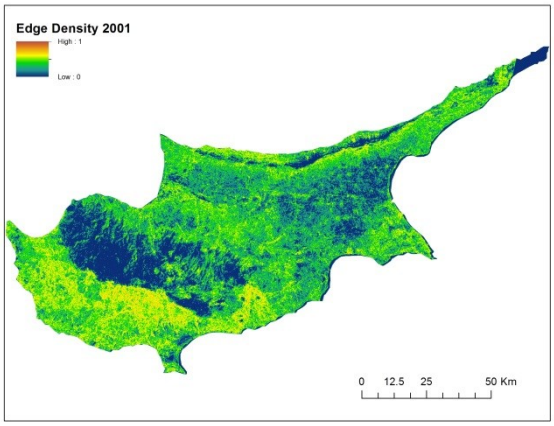

(d)

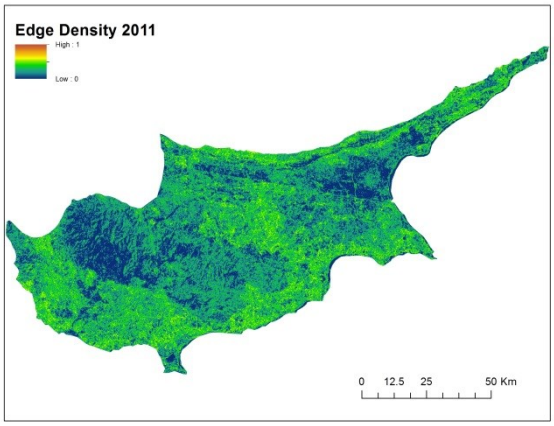

(e)

Figure 17. Edge density measures the level of fragmentation in the 7x7 pixel neighborhood. Higher values indicate that more edges exist in the neighborhood, thus the neighborhood is fragmented.

The compactness index indicates aggregation of land cover categories with values that range from 0 to 1. Maximum aggregation is indicated by values near 0, while maximum disaggregation is indicated by values near 1. Patch compactness for each year (Figures 18a-e) follows the trends highlighted for edge density (Figures 17a-e). It logically follows that these two measures are similar as an increase in fragmentation (values near one for patch compactness) would increase the edge density measurements as dissimilar cover types are now adjacent to each other.

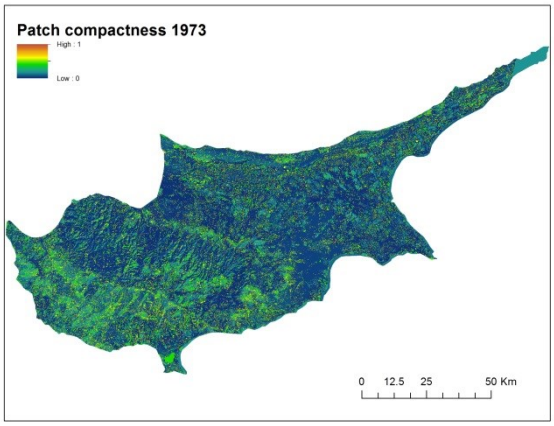

(a)

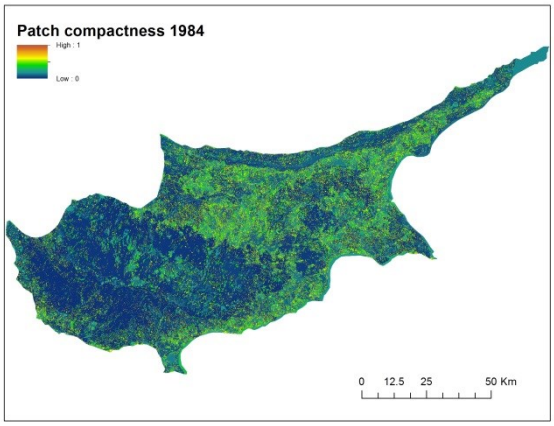

(b)

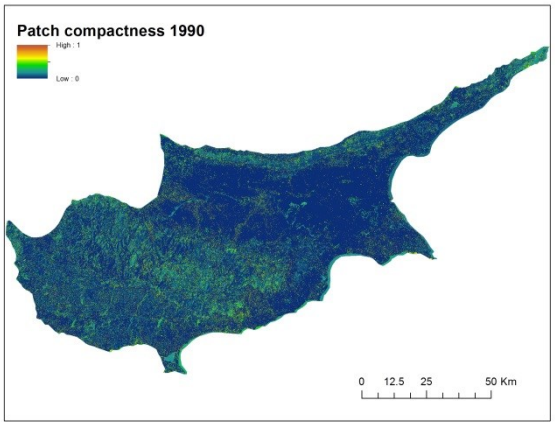

(c)

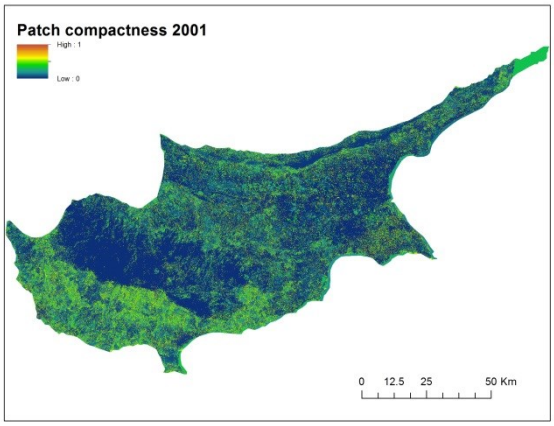

(d)

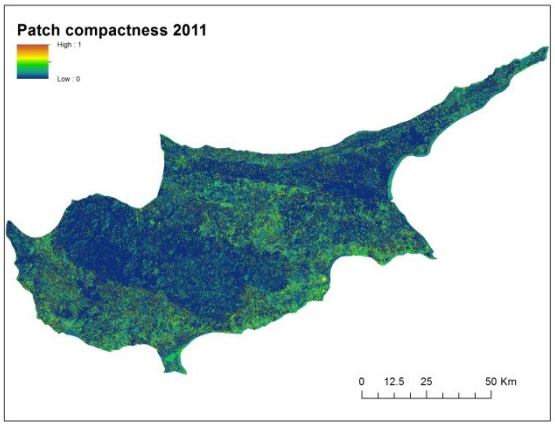

(e)

Figure 18. Patch compactness is a measure of aggregation of the patches in a 7x7 neighborhood. Values near 0 represent maximum aggregation of patches, while values near 1 represent maximum disaggregation. Areas with high values of patch compactness are areas where multiple land covers occur within an area, so patches are very small and fragmented in nature.

The change process metric compares images of two different dates and indicates the type of change that occurs over the time period of interest. Changes to the area and perimeter of overlapping land covers determines the dominant change process for each land cover (see Table 6). In Cyprus, four change processes occur over the time steps between 1973 and 2011 (Figures 19a-d); creation, attrition, aggregation and dissection.

Between 1973 and 1984 (Figure 19a), attrition of land covers is the dominant process across the Troodos and northern parts of the Kyrenia Ranges. This indicates that the number of patches and area of patches are decreasing. Southeast of the Troodos the dominant pattern is aggregation, indicting the number of patches is decreasing and that the area of each patch remains constant or increases. Across the Mesaoria Plain and in the foothills of the Troodos and Kyrenia Ranges dissection is the dominant land change process, indicating an increase in the number of patches with decreases in the area of patches. Creation, or an increase in the number and area of patches, occurs scattered across the Mesaoria Plain and into the Karpas Peninsula. Between 1984 and 1990 (Figure 19b), creation is the dominant change process across a majority of the island with scattered areas of dissection in the Troodos and surrounding foothills, in and around Nicosia and along the northern side of the Kyrenia Range. Creation as the dominant change process indicates a homogenization of the landscape as patch sizes increase. Creation, dissection and attrition occur between 1990 and 2001 (Figure 19c). Creation occurs in areas of high dissection in the map from 1984-1990 (Figure 19b). Dissection is predominately located on the eastern end of the Mesaoria Plain, while areas of attrition are scattered across the entire island. Over the last time period covering 2001-2011 (Figure 19d) attrition and aggregation are the main processes, with aggregation occurring in the Kyrenia Range, the eastern tip of the Mesaoria Plain and surrounding the Troodos. Attrition occurs across the Troodos, the Mesaoria Plain and into the Karpas Peninsula. Areas of creation are evident as small patches, most of which occur along the southern

side of the Troodos. A majority of these are reservoirs, which introduces a new land cover and increases the number and area of patches in these locations.

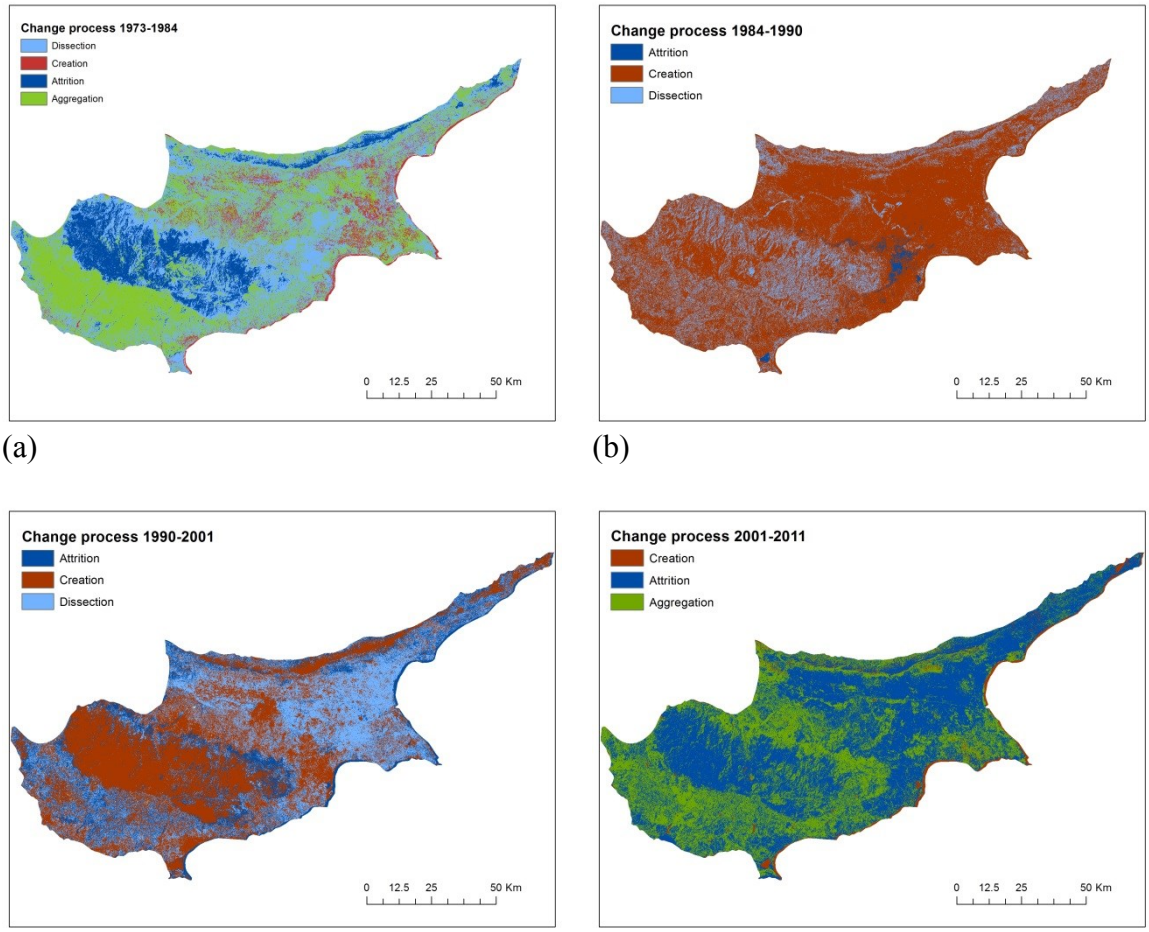

Figure 19. Change process between each set of time steps.

Discussion

Landsat imagery was used to classify land cover and to evaluate the transitions in land cover from 1973 to 2011. The hybrid classification technique ISOCLUST created groupings of land cover based on reflectance values of the Landsat data. The clusters were then assigned to a land cover category derived from the CORINE Land Cover Technical Guide (Bossard et al., 2000). CORINE land cover categories were selected

based upon their presence in the Cypriot landscape and a determination of which features are discernible from the Landsat images. The purpose of classifying land cover and evaluating the type of transitions and how they are occurring was to address the following questions and predicted landscape responses:

How has the Cypriot landscape changed over approximately the last 50 years (island-wide)?

1. Due to population movements and a change in the economic base of Cyprus, urban areas are expected to have expanded, while outlying villages are expected to have declined in extent. Development along the coast is expected to have increased in response to a larger tourism sector. In addition, it is expected that agricultural plots have shifted from small, multi-crop plots to larger, single-species plots.

Are there differences between the northern and southern portions of the island? If so, how do they differ in terms of land cover composition and change over time?

2. Differences are expected across the island with coasts developing more quickly and extensively in the southern portion of the island. Along this same line of reasoning, urban expansion is expected to be greater in the southern areas of the island. It is also expected that agricultural plots remained similar in size and configuration in the northern area due to limited trade and economic development after 1974.
3. In terms of landscape configuration, less heterogeneity is predicted in the south as urban areas and size of agricultural plots increase.

Evaluating research questions and predictions

Prediction 1

Political events beginning in the late 1950s led to the partition of Cyprus in 1974 and the resettlement of an estimated 200,000 Greek and Turkish Cypriots. This event is proposed to accelerate the processes of agricultural abandonment and urban expansion on the island post-1974. Based on the results of land cover change analyses, urban areas increase, most notably in Nicosia, Larnaka and Limasol. Agricultural areas decline, particularly in southern Cyprus. By 1984 artificial land cover across the island was increasing (Table 7), with an increase to 1.29% of the study area in northern Cyprus (Table 13) and 1.08% in southern Cyprus (Table 15). Urban areas are more apparent by 1990 (Figure 8) with the most development around Nicosia and Limasol. Urban areas continue to grow through 2011 (Figures 9 and 10), with increases to urban extent around Nicosia, Larnaka and Limasol. The urban area of Kyrenia is most apparent in Figures 8 and 9, (1990 and 2001). Development is highest along the southern coastline between 1990 and 2001 (Figure 13c) and stretches from Ayia Napa to Paphos, as well as in Polis to the west of the Troodos. Additional development is seen along the Karpas Peninsula during the same time frame.

Urban growth is easier to quantify and observe on land cover maps than transitions to larger agricultural plots. The long-term trend is a general loss of agricultural land cover, from 9.76% of the landscape in the study area (Table 7) to 7.98% (Table 10) with much of this loss occurring in the southern portions of the island (Figures 11a – 14a). Coupled with the decrease in agricultural land covers is an increase in shrub and/or

herbaceous covers, indicating a trend of agricultural abandonment and not fallow areas. The patch area of agricultural areas increases between 1973 and 2011 but only across the Mesaoria Plain and into the lower portions of the Karpas Peninsula. This may indicate that in places where agriculture was not abandoned around the Troodos foothills, the topography restricts the consolidation of many agricultural plots. However, the Mesaoria and lower portions of the Karpas are relatively flat and open, allowing for the increase in plot size. Due to the spatial resolution of the Landsat images and the inability to discern between types of agricultural land covers, it is not possible to determine if crop production has shifted from multi-species plots to single-species production in a plot.

Prediction 2

Prediction 2 looked to examine rates and type of land cover changes between the northern and southern parts of the island after the political division in 1974 utilizing land cover maps from 1984 to 2011 to calculate the changes that occurred post-1974. Comparisons of change within land cover categories reveals changes in the opposite direction between northern and southern Cyprus, with the exception of forest cover. Agricultural areas increased in the northern portion of the island, with most of the transition to agricultural lands coming from areas that were previously covered by shrub and/or herbaceous vegetation (Table 13). Forested areas more than double from 1984 to 2001, with an increase from 0.64% of the study area to 1.72%. In 2011, artificial areas have declined from 1984 or 2001 land cover classifications (Tables 12 and 13). Shrub and/or herbaceous cover increases by 2011, to approximately the same extent as 1984

(3.26% and 3.69%, respectively) while forested areas remain relatively unchanged from 2001 extents.

In southern Cyprus, agricultural land covers decline from 8.05% of the study area in 1984 to 5.45% in 2001 (Table 15). A majority (1.78%) of the transition is to shrub and/or herbaceous cover, indicating a permanent change from agricultural production in these areas and encroachment by shrub dominated plant communities. Overall, shrub and/or herbaceous cover declines from 6.65% of the study area in 1984 to 4.08% in 2001. There is a large increase in artificial area extent between 1984 and 2001 (1.08% and 3.01%, respectively). Forested areas also experience a large increase in extent over this time period, expanding from 4.1% of the southern region to 7.19%. By 2011, artificial extents have declined to 1.4% of the southern areas with further declines in agricultural areas (2.44%) (Table 14). Shrubs and/or herbaceous cover increases to 9.53% of the southern portion of the island, indicating a 27-year increase in this land cover type in line with agricultural declines over the same period (1984-2011).

The extent of development along the southern coastline from 1984-2001 is demonstrated in Figure 13c, which depicts not only the growth of the coastal cities of Larnaka, Limasol and Paphos, but also the increase in development across the entire coastline during this period. In addition, development is noticeable along the northern coastline near Kyrenia and onto the Karpas Peninsula. The decline of artificial areas is predominately in the Troodos foothills and along the northern extent of the Troodos (Figure 14c). The decline in the southern portions of the foothills may indicate an actual loss of developed areas as people continue to move away from the villages into the urban

centers. The decline in artificial areas along the northern Troodos foothills is likely an artifact due to the difference in reflectance of calcareous soils between 2001 and 2011. Agricultural patches shift in terms of where larger patches are located between 1984 and 2001. Larger patches occur in the south in 1984 and shift to the eastern part of the Mesaoria Plain of both north and south Cyprus and into the Karpas Peninsula of northern Cyprus by 2001. This follows the larger trend of agricultural abandonment in the southern portion of Cyprus; however it contradicts the prediction that patches would remain of similar size and configuration in northern Cyprus during closure of the buffer zone.

Prediction 3

Prediction 3 anticipated the increase of agricultural plot sizes in the southern parts of Cyprus. However, as discussed in Prediction 2 agricultural patches decline in size across most of the southern portions of Cyprus, only increasing along the eastern extent of the Mesaoria Plain. Comparison of the results for the 1984 and 2001 evenness index (Figures 16b and 16c) indicate an increase in land cover diversity along the southern edge of the Troodos. This is expected as agricultural areas are abandoned and those areas transition to shrub and/or herbaceous cover types and as coastal development causes transitions from one land cover type to another type. A small decline in evenness occurs along the eastern part of the Mesaoria Plain near Famagusta, in the same region where patch size and agricultural land covers are increasing. Land cover evenness decreases across a large portion of the Troodos, but also along the northern slopes of the Kyrenia Range. Small declines in evenness are discernible in the urban area of Nicosia. Edge

density also plays a role in heterogeneity and indicates the level of fragmentation. Figures 17b and 17d illustrate that the southern part of the island are more fragmented in 2001 than they were in 1984; however fragmentation has increased in much of northern Cyprus as well.

Accuracy assessments for the classified 2011 Landsat image were low, with overall accuracy of 50.33% and a Kappa statistic (KHAT) of 33.44%. Landis and Koch (1977) consider the KHAT statistic as fair in terms of strength of agreement between observed accuracy and chance agreement. The error matrix and accuracy assessment (Tables 4 and 5, respectively) reveal cases of misclassification For example, 22 points that were classified as shrubs/herbaceous cover where identified as agricultural areas in the reference data and 17 forest reference points were incorrectly classified as shrub/agricultural areas (Table 4). Gong et al. (2013) consider misidentification between forests, shrubs and grasslands as "typical confusions" and also state that their study had issues in correctly separating grasslands from bare croplands. The results of Gong et al.'s study (2013), as well as the results discussed above highlight general issues in large area land use and land cover mapping that influence classification accuracies. Examples of these issues include spectral confusion, where two different land covers have similar or overlapping reflectance values (e.g. croplands and grasslands or orchards and open deciduous forests); mixed pixels, where pixels within the image are larger than land cover categories and thus contain multiple land covers; and underrepresentation or other inadequacies in the selection of training samples for land cover categories. In the case of the 2011 Landsat classified map, both spectral confusion and mixed pixels are an issue.

Land covers in Cyprus are often smaller in size than the pixels used to represent them, thus the land cover with the dominant spectral reflectance is assigned to the entire pixel. When the land cover category for this pixel is compared to ground truth data, the two may or may not agree, which may influence the accuracy assessment of the image. Other large area land-cover and land-use mapping projects (e.g. National Land Cover Dataset) have provided initial estimates of accuracy between 70 and 98% (Homer et al., 2007) and Selkowitz and Stehman (2011) found that overall accuracies were higher when both a primary and alternate reference label were compared to the sample pixel. However, when just comparing the sample pixel to the primary reference label, accuracies declined to 59.4% for Level II classification and 69.3% for Level I classification (see Selkowitz and Stehman, 2011, for a description of the classification hierarchy). Overall accuracy of 50.33% for Cyprus' 2011 land cover classification was calculated considering only a primary reference label, resulting in a similar overall accuracy to the Selkowitz and Stehman (2011) study.

Conclusions

Across Cyprus a slight increase in forests was noted for the entire study period (1973-2011), with declines that occurred from 1973 to 1984 (Table 7) and 2001 to 2011. Hadjikyraikou (2000) reports that 7770 hectares of forest were burnt between 1990 and 1999 in the southern forests, which may contribute to the decline noticed in forested areas from 2001 to 2011. A transition from shrub and/or herbaceous cover to agriculture occurred between 1984 and 1990 (Table 8) but a transition from agriculture to bare rock/soil and shrub and/or herbaceous cover occurs by 2011 to near 1973 extents (Tables

7 and 10). However, the distribution of agricultural and shrub and/or herbaceous land cover types changes from 1973 to 2011 (Figures 6-10).

Evaluation of Predictions 1 through 3 found differences in land cover transitions and types between the northern and southern portions of Cyprus. Land cover transitions occurred as anticipated with increased development along the coast and increase in urban areas. In the eastern portion of the Mesaoria Plain, agricultural plots shifted to larger patches but much of the southern portion of the island transitioned to smaller patches of agriculture with replacement by shrub and/or herbaceous cover. Coastlines did develop extensively in the southern portion of the island between 1984 and 2011 as well as in Kyrenia, and to a small extent along the Karpas Peninsula. Evaluation of land cover diversity and edge density in land covers indicates that the southern portion of the island is more heterogeneous in 2011 than in 1984 due to multiple types of land conversions during this time period (Figure 16).

Continuation of the overall trends of land cover transitions would indicate further coastal development, even along the northern coast, contrary to the remote sensing analysis. Growth of the urban areas of Nicosia, Larnaka, Limasol, Paphos and Kyrenia is expected to continue as fewer people choose to live in the smaller villages, especially villages far removed from the urban areas. Continued transition to shrubs in areas of agricultural decline is anticipated, with eventual growth of *Pinus brutia* and other forest types where conditions allow for the reintroduction of forest species.

Chapter 4

MAXENT MODELING OF MODERN VEGETATION

Introduction

Species distribution models (SDMs) incorporate a broad range of statistical methods, data types, and applications. SDMs are known by a variety of names in scientific literature, such as climate envelope models, bioclimatic models, ecological niche models and habitat suitability models (Elith and Graham, 2009; Elith and Leathwick, 2009; Franklin, 2009). The resulting models are used to predict the current distribution or range of plant or animal species and the future range of species as a means of applying rules for the management of the species, whether this is reintroduction of species, preservation of suitable habitat, or mitigation of responses to changes in habitat availability, habitat quality and climate change (e.g. Franklin, 1995, 2009; Guisan and Zimmerman, 2000; Manel et al., 2001; Rushton et al., 2004; Guisan and Thuiller, 2005; Barry and Elith, 2006; Elith and Graham, 2009; Warren and Seifert, 2011).

Biogeographers have a long history of describing species distributions based upon climate or other environmental factors (Von Humboldt, 1805/1807; Merriam and Steineger, 1890; Grinnell, 1904). However, these early attempts at mapping species (or community) distributions were primarily descriptive. As ecological and geographical theory advanced, quantitative methods for combining field-based observations of species with environmental conditions were developed to produce the suite of models available today. Common model types include generalized linear models (GLMs), generalized additive models (GAMs) and machine learning methods (Elith and Graham, 2009; Elith

and Leathwick, 2009; Franklin, 2009). All of these models produce predicted species distributions by correlating field observations with environmental variables at observation points to predict distributions across space and/or time. Many of these models require the use of presence/absence data, which reduces their applicability, since an increasing number of published data sets provide predominately presence-only data (e.g. museum collections or historical surveys) (Graham et al., 2004; Elith et al., 2006; Phillips and Dudík, 2008; Franklin, 2009; Elith et al., 2011). Modeling based on presence-only data presents a series of challenges such as: How well does the model tie to ecological theory? How does the model perform against presence/absence models or other presence-only models? Which model is best suited to address the intended question(s) and or application(s)? (Elith and Graham, 2009). Table 16 summarizes commonly used presence-only methods, their primary characteristics, the modeling tool or method, and pertinent literature (based on Elith et al., 2006; Phillips et al., 2006; Pearson, 2008; Franklin, 2009; Soto-Berelov, 2011).

Table 16. Commonly used presence-only species distribution methods, major features of each method and literature where first described or implemented. Table is based on based on Elith et al., 2006; Phillips et al., 2006; Pearson, 2008; Franklin, 2009; Soto-Berelov, 2011

Model Type	Software/ Model	Features/Method	Background/pseudo -absence samples	Source (as applied in SDMs)
Environmental/ climate envelope	BIOCLIM	Parallelepiped classifier; potential range is the multi-dimensional environmental space bounded by the minimum and maximum values of the defined set of presences (e.g. 100%); produces a binary classification (suitable vs. unsuitable)	No	Busby, 1986, 1991
	HABITAT	Convex hull; the relative density of presences within subareas determines membership of each subregion to the range of the species		Walker & Cocks, 1991

Model Type	Software/ Model	Features/Method	Background/pseudo -absence samples	Source (as applied in SDMs)
Environmental distance	DOMAIN	Gower metric; compares the site of interest to the nearest presence record to estimate the environmental similarity	No	Carpenter et al., 1993
Discriminative models	GAMs (Generalized additive model)	Non-parametric; multiple regression model; categorical data can be used; linear and non-linear functions can both be used	Yes	Hastie & Tibshirani, 1990
	GLMs (Generalized linear models)	Parametric; general category of models that includes linear regression; categorical data can be used; multiple link functions available (e.g. linear, polynomial); link function describes the relationship between the response (species data) and the predictors	Yes	McCullagh & Nelder, 1989
	MARS (Multivariate adaptive regression splines)	Piece-wise linear basis functions; non-linear regression method	Yes	Friedman, 1991; Hastie & Tibshirani, 1996
	ENFA (Ecological niche factor analysis)	Multivarigate ordination; niche based the magnitude of difference between the species' mean and the complete range of environmental conditions in the background sample	Yes	Hirzel et al., 2002
Generative models	GARP	Genetic algorithm; uses four tools to identify relationships between occurrences and environmental data	Yes	Stockwell & Noble, 1992; Stockwell & Peters, 1999
	Maxent (Maximum entropy)	Machine-learning or maximum-likelihood method; categorical data can be used; linear and non-linear functions can be used; prediction based on the probability distribution of maximum entropy, subject to constraints based upon the environmental data	Yes	Phillips et al., 2004

Presence-only methods of modeling potentially suitable habitat are of particular interest for this study, which utilizes presence-only observations and a combination of differing sampling methods, sample sizes and sampling dates. Based on the full range of

observed data, twenty-two woody shrub and tree species representing conservation, agricultural, cultural and indicator species were chosen for modeling (Table 17). Modeling of these species will examine their current suitable areas, assess modeling platform performance and produce binary suitability maps. These models will provide the base conditions necessary to predict future suitable areas based on two climate change scenarios over three time periods, and will combine these future scenarios with land-use change predictions derived from the land cover transitions presented in Chapter 3.

From the presence-only methods listed in Table 16, Maxent[4] was selected to create models representing the potentially suitable areas for the selected species. Maxent is a modeling platform based on ecological niche-theory (Hutchinson, 1957), which creates potential geographic distribution models from presence-only data (Phillips et al., 2004; Phillips et al., 2006; Elith et al., 2011). Maxent uses environmental covariates, in conjunction with the species observations and a background sample to estimate the environmental space (or niche) that is the most uniform while adhering to environmental constraints (Phillips et al., 2004; Phillips et al., 2006; Elith et al., 2011). Maxent was selected for this study based on its ties to ecological theory, ability to create projections of suitable areas based upon future environmental variables, and its performance when using small sample sizes, correlated variables and biased data.

[4] http://www.cs.princeton.edu/~schapire/maxent/

Table 17. A list of the twenty-two species chosen for species distribution modeling, their respective habitat types, and the various ways each species is important to the landscapes of Cyprus. Cultural uses of each plant are from Tsintides et al., 2002.

Taxon	Habitat Type	Indicator Species	Species of Concern	Other Characteristics	Cultural uses
Arbutus andrachne	Forests (Q. alnifolia and P. brutia forests)			Indigenous; Cultural	Edible fruit; liquor production; charcoal and firewood
Cedrus brevifolia	Forests (C. brevifolia forest)	Yes	Vulnerable; Habitats Directive	Endemic; Cultural	Ornamental; insect repellent; icon production
Cistus creticus	Forests and shrublands			Indigenous; Cultural	Labdanum production
Cistus parviflorus	Forests and shrublands			Indigenous	
Cistus salviifolius	Forests and shrublands			Indigenous	
Ficus carica	Forests			Indigenous; Cultivated; Cultural	Fruit production; symbolic (ties to ancient Greece)
Helianthemum obtusifolium	Forests and shrublands			Endemic	
Juniperus foetidissima	Forests		Habitats Directive for endemic forests, coastal dunes, and arborescent matorral with Juniperus	Indigenous	
Juniperus phoenicea	Shrublands		Habitats Directive for endemic forests, coastal dunes, and arborescent matorral with Juniperus	Indigenous	
Olea europaea	Forests			Indigenous; Cultivated; Cultural	Fruit and oil production; symbolic (ties to ancient Greece); ornamental; firewood
Pinus brutia	Forests	Yes		Indigenous	

Taxon	Habitat Type	Indicator Species	Species of Concern	Other Characteristics	Cultural uses
Pinus nigra	Forests ((Sub)Mediterranean pine forest with endemic black pine)	Yes		Indigenous	
Pistacia atlantica				Indigenous; Cultivated; Cultural	Resin production
Pistacia lentiscus	Forests and sand dunes			Indigenous; Cultural	Fruit production; ornamental
Pistacia terebinthus	Pine forest and shrublands			Indigenous; Cultural	Fruit production; dye; ornament
Prunus dulcis				Adventive; Cultivated	
Pterocephalus multiflorus	Forests and shrublands			Endemic	
Punica granatum				Naturalized; Cultivated; Cultural	Fruit production; ornamental; dye; symbolic
Quercus alnifolia	Forests (Scrub and low forest vegetation)	Yes	Habitats directive for scrub and low forests vegetation with Q. alnifolia	Endemic	
Quercus coccifera	Forests and shrublands			Indigenous	
Sarcopoterium spinosum	Forests and shrublands	Yes		Indigenous	
Thymus capitatus	Forests and shrublands	Yes		Indigenous	

Niche-based models represent the realized niche of modeled species, based on observed data, environmental data and the study area under consideration (Phillips et al., 2006). This definition of niche-based models, including Maxent, implies that the species of interest inhabit areas based upon interactions with other species (including humans), environmental limiters (e.g. resources or geographic barriers), and the ability of a species to disperse to other areas (Guisan and Thuiller, 2005; Phillips et al., 2006; Soberón, 2007). Many SDMs, however, are static and do not model interactions and dispersal abilities explicitly (Guisan and Thuiller, 2005; Elith and Leathwick, 2009; Franklin, 2009). Bias is an issue across all model types, since presence data often is assumed incorrectly to represent unbiased samples from across the distribution of a species (Reddy and Daválos, 2003; Phillips and Dudík, 2008). In light of the potential bias in presence-only methods, resulting models can estimate biased distributions for the species under study (Phillips and Dudík, 2008). Models that implement the use of a background sample with the same sampling bias as the species of interest can reduce the impact of bias on predicted distributions (Dudík et al., 2005; Phillips and Dudík, 2008; Phillips et al., 2009). Another way to reduce sampling bias is to create a grid to correct for the bias by coding the grid according to relative sampling effort (Phillips, 2010; Elith et al., 2011).

Elith et al. (2006) evaluated sixteen approaches to presence-only SDMs based on 54 species with varying geographic extents and prevalence across six regions of the world. Using independent presence/absence data to evaluate their models, the authors found that Maxent performed competitively, ranking among the top-performing presence-only methods using the area under the Receiver Operating Characteristic curve (AUC;

see Methods, Threshold-independent validation for a discussion of the AUC) and a Pearson's correlation coefficient as measures of model performance (Elith et al., 2006; Elith et al., 2011). Additionally, Maxent performs well with small sample sizes (Phillips et al. 2004; Phillips et al., 2006, Dudík et al., 2007; Phillips and Dudík, 2008) and it handles correlated variables well, thereby requiring only the removal of non-relevant variables (Elith et al., 2011). Elith and Leathwick (2009) still recommend reducing the number of variables and focusing on direct (or proximal) variables rather than indirect (or distal) variables, particularly when the model will be used to project to novel areas or climates.

Methods

Data acquisition

Field sampling

This study incorporates presence-only observations of perennial plant species along with environmental variables at 660 locations on the island of Cyprus. Vegetation data were collected over four field seasons during the summers of 2008-2011 at 564 locations (Figure 5); observations from 114 historical data points based on herbarium collections sampled between 1747 and 1974 (Miekle, 1977, 1985) expand these observations to include areas that were less disturbed in the past and species that were less represented in our database (see Figure 5). Initially, the perennial plant species were recorded at 131 randomly selected points from a sample transect beginning near Limasol on the southern coast of Cyprus, into the foothills of the Troodos Mountains, across the Mesaoria Plain, over the Kyrenia Range, and to the north coast of Cyprus (see random

points shown on Figure 5). A hand-held global positioning system receiver (GPS) was used to locate all the sample points (e.g., latitude and longitude).

Since many of the randomly generated sample points fell on urban or heavily modified landscapes, and in order to more fully characterize the distribution of the perennial plant species in Cyprus, comparable data on the woody plant species and environmental variables were collected at 390 additional non-random sample points. The non-randomly generated sample points come from a series of transects that traverse the full elevational range of the island from sea level to the summit of the Troodos Massif (Figure 5). These non-random sample points were selected where vegetation was the least disturbed, where the sample transects could record indigenous woody plants and capture environmental variability (elevation and substrate) within Cyprus. Sample locales were chosen to cover a variety of vegetation types, ranging from coastal scrub to orchards to the maquis and forested landscapes of the higher elevations. Again, the location of each point was determined with a GPS. Perennial plant species for both the random and non-randomly selected locations were recorded over an area of about 100 m diameter. In addition, aspect, substrate, plant species present and estimated vegetation cover were collected at each point. Nomenclature follows *Trees and Shrubs in Cyprus* (Tsintides et al., 2002), *Flora of Cyprus* (Miekle, 1977, 1985), and *An Illustrated Flora of North Cyprus* (Viney, 1994).

Climate data

Climate data for potential inclusion as covariates for present-day and future distribution models were downloaded from WorldClim[5]. These data consist of 19 bioclimatic variables that are derived from monthly mean, minimum, and maximum temperatures, and precipitation (Hijmans et al., 2005). In addition, soil and surface geology raster surfaces were created for inclusion as model variables, utilizing environmental grids with approximately 1-km^2 pixels, since some species were reported to be restricted to specific substrates (Meikle 1977, 1985; Tsintides et al., 2002). Prior to model creation, a correlation matrix (using Pearson's r) was constructed for all covariates (Appendix A), and highly correlated ($r \geq 0.85$) or redundant variables were pruned to reduce the number of variables used in model building (Table 18).

Table 18. Pruned environmental variables utilized in modern and future model creation for species of interest.

Variable	Description
BIO1	Mean Annual Temperature
BIO2	Mean Diurnal Range (mean of monthly temperature (maximum temperature – minimum temperature))
BIO3	Isothermality ((BIO2/BIO7)*100)
BIO4	Temperature Seasonality (standard deviation*100)
BIO7	Annual Temperature Range (BIO5 (maximum temperature of the warmest month) – BIO6 (minimum temperature of the coldest month))
BIO8	Mean Temperature of the Wettest Quarter
BIO10	Mean Temperature of the Warmest Quarter
BIO12	Annual Precipitation
BIO15	Precipitation Seasonality (coefficient of variation)

[5] http://www.worldclim.org/bioclim

BIO16	Precipitation of the Wettest Quarter
BIO17	Precipitation of the Driest Quarter
Geology	Surface geology (based on Geological Map of Cyprus, 1995)
Bias grid	Grid representing sampling effort to reduce sampling bias

A bias grid was constructed as a continuous surface across the entire study area. This surface represents sampling effort across the area of interest and is helpful in reducing bias introduced during sampling (Phillips, 2010; Elith et al., 2011). In this study, many samples are non-random and are located near roads, thus the bias grid was constructed from the road network of Cyprus, and indicates that *a priori* sampling probabilities were higher along the roadways, but does not exclude sampling outside of these areas (Phillips, 2010).

Maxent modeling

Species distribution models were created using a bootstrapping method of data partitioning for modeling test/train data. The observation data were partitioned into a training data set consisting of 70% of the observations; the remaining 30% were used as testing data. The models were replicated 10 times and the test/train data were resampled with each model run (see Phillips et al., 2006). The final mapped distribution represents the average of all model runs.

Models were calibrated in the same manner for each species modeled. For each model run a random seed was selected and all samples were added to the background, with all other options set at the recommended default values. Phillips and Dudík (2008) suggest adding the observation samples to the background when correcting for bias to

ensure that the background sample contains all of the environmental constraints present in the observation data. In the current version of Maxent (v 3.3.3k), the default output is a logistic format that assigns a value ranging from 0 to 1 to each pixel in the output map. In the best case scenario, the interpretation of each pixel is the probability of species presence in that pixel, with pixels that represent the characteristic environment of the species having a logistic output near 0.5 (Elith et al., 2011). In practice the logistic output is below 1 and is related to the default setting in Maxent of 0.5 for species prevalence (indicating the probability of presence within a pixel given "typical" conditions for the species of interest) but in presence-only sampling, actual species prevalence often cannot be determined. Thus, careful interpretation of the logistic output is necessary, especially when comparing species that differ in sampling intensity or rarity (Elith et al., 2011). With regard to Cypriot vegetation, cross-comparisons are not the purpose of the study, thus the default value of species prevalence of 0.5 was utilized. A more conservative approach, and the one applied to the species distributions discussed here, is to interpret the output as relative suitability for the species of interest, with higher pixel values indicating higher suitability for the species (Phillips et al., 2006).

Model validation

Threshold-dependent validation

Threshold-dependent validation of the output maps requires implementation of a threshold rule to create a binary (suitable vs. unsuitable locations) map for each species. Maxent's output for individual runs includes a list of the logistic threshold value, threshold rules, training/testing omission rates, and the *p*-values associated with each

rule. Guidelines for selection of an appropriate threshold vary according to the expected use of the model output, often with a consideration for balancing sensitivity (fraction of true presences accurately predicted) with specificity (fraction of true absences accurately predicted) (Franklin, 2009).

The threshold of maximum training (sensitivity + specificity) was selected (Table 19). This threshold represents the highest possible value of the sum of sensitivity and specificity (Manel et al., 2001) and can also be determined from the point along the Receiver Operating Curve (ROC) whose tangent is equal to 1 (Franklin, 2009). Freeman and Moisen (2008) determined that this threshold also minimizes the mean error rate of presences and absences. In addition, the application of a threshold allows for the evaluation of model performance using the *omission rate* and the *proportional predicted area* (Phillips et al., 2006) (Table 19). A one-tailed binomial test is used to determine if the model output is different from a randomly selected model with the same proportional predicted area (Phillips et al., 2006; resulting *p*-values are found in Table 19).

Threshold-independent validation

Models also were evaluated using the area under the ROC curve (AUC). The ROC plots are created by plotting predicted values for *1-Specificity* along the x-axis versus predicted *Sensitivity* values along the y-axis. The AUC is calculated as the area occurring under the constructed ROC plot (Hanley and McNeil, 1982). The use of the AUC as a measure of model success is contested (e.g. Pearson et al., 2007); however, Phillips et al. (2006) argue that instead of interpreting the AUC as distinguishing presence from absence, in Maxent the AUC is interpreted as distinguishing presences

from a random background sample. Using this interpretation, AUC values range from 0.5 (random) to 1.0, with values above 0.5 indicating model performance better than random prediction (Table 19).

Table 19. Species selected for modeling, sample size, and model building statistics. Grey shading indicates models that were not statistically significantly different from a random prediction across the same proportional area.

Taxon	n	Training AUC	Training AUC std dev	Test AUC	Test AUC std dev	Threshold value	Proportional predicted area	p-value	Success Rate (%)
Juniperus foetidissima	7	0.9922	0.007884314	0.9341	0.1406922	0.3209	0.03	5.91E-02	97.5
Cedrus brevifolia	14	0.9587	0.003462138	0.9718	0.0284749	0.1393	0.0559	6.69E-04	36.67
Pinus nigra	16	0.9911	0.003173894	0.9902	0.0058824	0.1533	0.0315	1.22E-04	71.67
Pterocephalus multiflorus	38	0.9703	0.0063454	0.9519	0.0219887	0.2132	0.096	3.18E-08	78.89
Arbutus andrachne	40	0.9668	0.007074185	0.9367	0.0249914	0.1938	0.1177	2.69E-08	70
Quercus alnifolia	68	0.9614	0.00309466	0.9447	0.014658	0.1894	0.1241	7.22E-15	72.22
Cistus parviflorus	13	0.8911	0.04501413	0.7481	0.1415193	0.4376	0.1778	4.44E-01	60
Juniperus phoenicea	14	0.955	0.026151933	0.8838	0.0481401	0.4342	0.0749	3.04E-02	72.22
Pistacia lentiscus	62	0.9137	0.009118772	0.8233	0.0434874	0.3294	0.1977	1.98E-05	70.56
Helianthemum obtusifolium	10	0.9039	0.047604521	0.6297	0.1827858	0.4471	0.1641	6.16E-01	92.5
Pistacia atlantica	14	0.9093	0.024162624	0.7048	0.1500549	0.3577	0.2074	6.05E-01	65.72
Cistus salviifolius	32	0.9414	0.00685335	0.8804	0.0427038	0.3907	0.1518	6.77E-04	47.5
Quercus coccifera	43	0.9262	0.01768758	0.8469	0.0428579	0.311	0.2072	7.48E-04	79.74
Thymus capitatus	74	0.8519	0.01151646	0.7518	0.0522338	0.4085	0.2349	6.95E-05	73.45
Prunus dulcis	92	0.8715	0.01533566	0.8162	0.0303333	0.365	0.2826	1.34E-07	63.64
Sarcopoterium spinosum	117	0.8736	0.01651319	0.7787	0.0306031	0.4419	0.1936	4.52E-06	59.62
Pistacia terebinthus	128	0.9009	0.010691324	0.8448	0.0184346	0.3697	0.2486	3.98E-12	93
Pinus brutia	195	0.8793	0.01317369	0.8041	0.3544322	0.3754	0.2462	2.69E-14	84.17
Cistus creticus	122	0.8938	0.011838095	0.8258	0.0356002	0.389	0.2174	1.24E-09	60
Punica granatum	11	0.8641	0.04560805	0.6308	0.2604714	0.4092	0.2703	6.11E-01	56.57
Ficus carica	49	0.8964	0.020666771	0.7717	0.075179	0.3834	0.2096	5.53E-04	62.5
Olea europaea	177	0.8393	0.0172573	0.7341	0.0481401	0.4485	0.2652	9.38E-07	85.46

Results

Maps of suitable areas

Maxent produces a continuous surface of suitability for each species modeled, with potential values ranging from 0 to 1 across the study area (Figure 20). As indicated in the discussion of methods (see Data Acquisition), these models are not meant to compare species, but they do permit modeling of future species distributions based on climate changes (see Chapter 5) in which use of a standardized scale can lead to intuitive comparisons between species distributions. The final species distribution maps were created with a threshold value calculated from the maximum training sensitivity + specificity, since use of a threshold allows for the calculation of *p*-values to assist in validation of the modern-day models (Figure 21).

Figure 21 reveals models that fit the distribution of species observations, but do not create predictions that are restricted to the training data nor provide poor predictive ability across testing data, thus avoiding overfitting of the models across all species. When assessed using the AUC, the species models performed well with both training and testing data (Table 19). Visual examination of the models also reveals that models performed well based on historical descriptions of species distributions and did not exclude observations from areas described as a core area by previous authors (e.g. Meikle 1977, 1985; Tsintides et al., 2002; see Table 17).

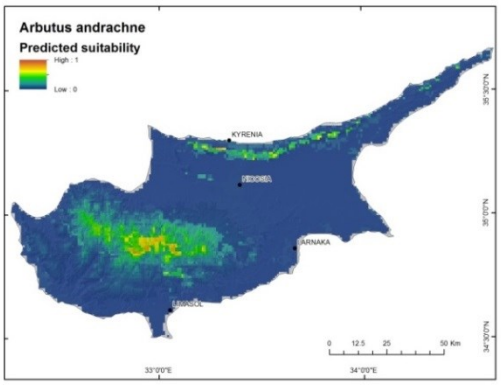
Arbutus andrachne
Predicted suitability
High : 1
Low : 0
KYRENIA
LEFKOSIA
LARNAKA
LIMASSOL
0 12.5 25 50 Km
33°0'0"E
34°0'0"E
35°0'0"N
34°30'0"N

(a)

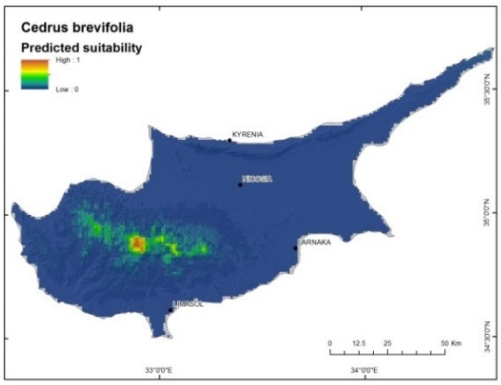
Cedrus brevifolia
Predicted suitability
High : 1
Low : 0
KYRENIA
LEFKOSIA
LARNAKA
LIMASSOL
0 12.5 25 50 Km
33°0'0"E
34°0'0"E
35°0'0"N
34°30'0"N

(b)

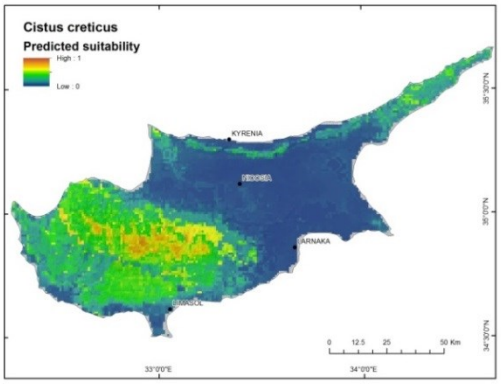
Cistus creticus
Predicted suitability
High : 1
Low : 0
KYRENIA
LEFKOSIA
LARNAKA
LIMASSOL
0 12.5 25 50 Km
33°0'0"E
34°0'0"E
35°0'0"N
34°30'0"N

(c)

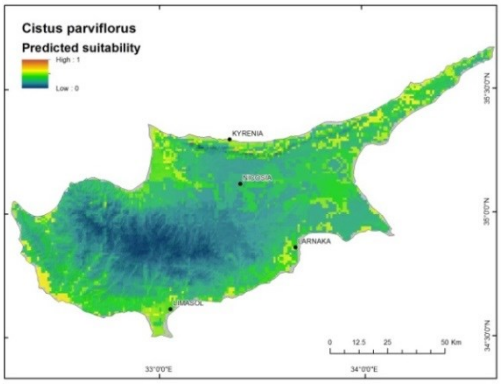
Cistus parviflorus
Predicted suitability
High : 1
Low : 0
KYRENIA
LEFKOSIA
LARNAKA
LIMASSOL
0 12.5 25 50 Km
33°0'0"E
34°0'0"E
35°0'0"N
34°30'0"N

(d)

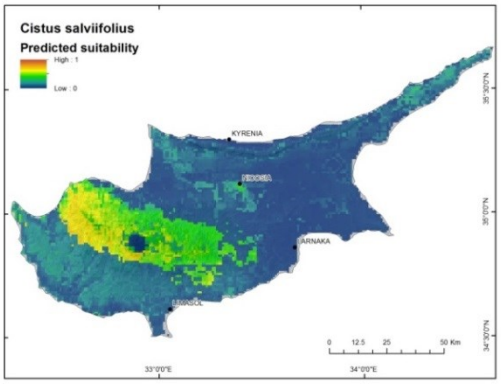
Cistus salviifolius
Predicted suitability
High : 1
Low : 0
KYRENIA
LEFKOSIA
LARNAKA
LIMASSOL
0 12.5 25 50 Km
33°0'0"E
34°0'0"E
35°0'0"N
34°30'0"N

(e)

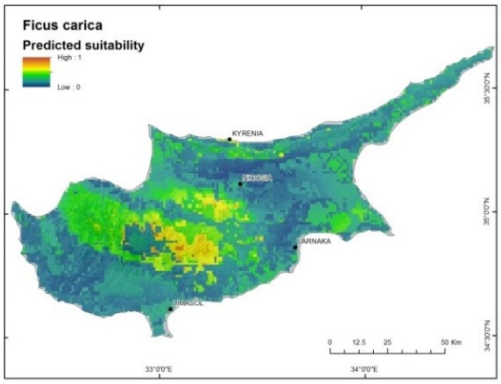
Ficus carica
Predicted suitability
High : 1
Low : 0
KYRENIA
LEFKOSIA
LARNAKA
LIMASSOL
0 12.5 25 50 Km
33°0'0"E
34°0'0"E
35°0'0"N
34°30'0"N

(f)

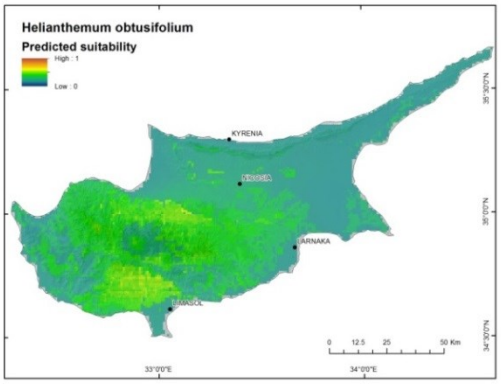
Helianthemum obtusifolium
Predicted suitability
High : 1
Low : 0
KYRENIA
LARNAKA
LIMASSOL
0 12.5 25 50 Km
33°0'0"E
34°0'0"E

(g)

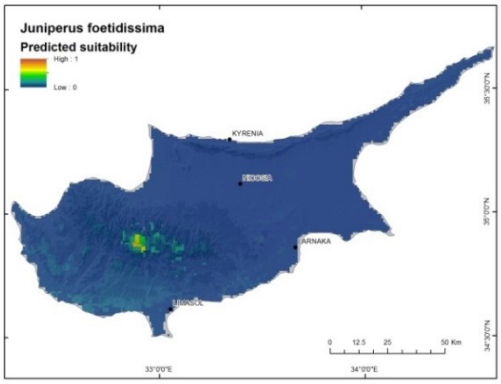
Juniperus foetidissima
Predicted suitability
High : 1
Low : 0
KYRENIA
LARNAKA
LIMASSOL
0 12.5 25 50 Km
33°0'0"E
34°0'0"E

(h)

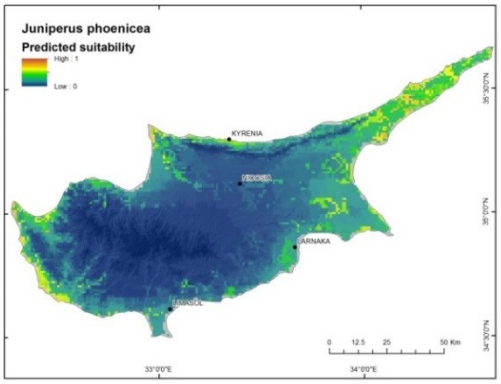
Juniperus phoenicea
Predicted suitability
High : 1
Low : 0
KYRENIA
LARNAKA
LIMASSOL
0 12.5 25 50 Km
33°0'0"E
34°0'0"E

(i)

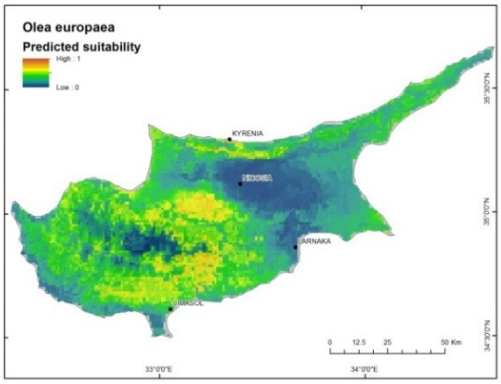
Olea europaea
Predicted suitability
High : 1
Low : 0
KYRENIA
LARNAKA
LIMASSOL
0 12.5 25 50 Km
33°0'0"E
34°0'0"E

(j)

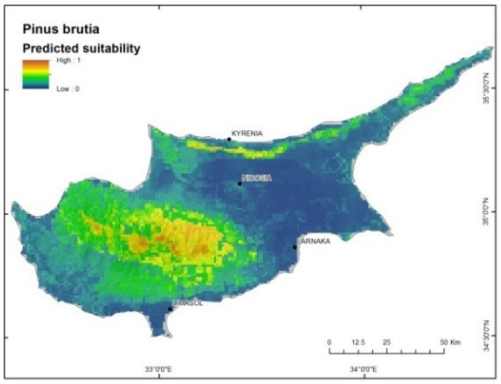
Pinus brutia
Predicted suitability
High : 1
Low : 0
KYRENIA
LARNAKA
LIMASSOL
0 12.5 25 50 Km
33°0'0"E
34°0'0"E

(k)

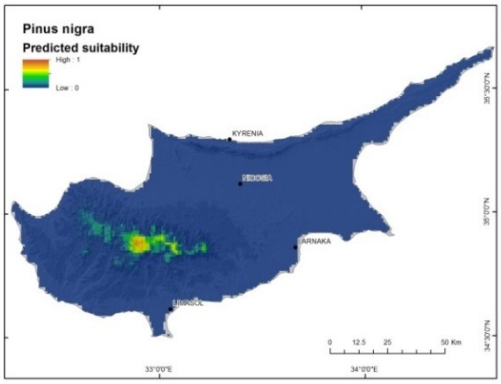
Pinus nigra
Predicted suitability
High : 1
Low : 0
KYRENIA
LARNAKA
LIMASSOL
0 12.5 25 50 Km
33°0'0"E
34°0'0"E

(l)

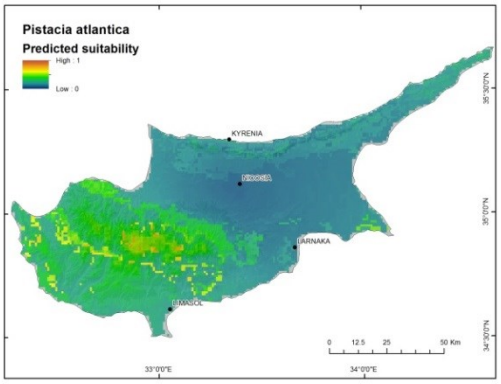
Pistacia atlantica
Predicted suitability
High : 1
Low : 0
KYRENIA
LIMASOL
0 12.5 25 50 Km
33°0'0"E
34°0'0"E

(m)

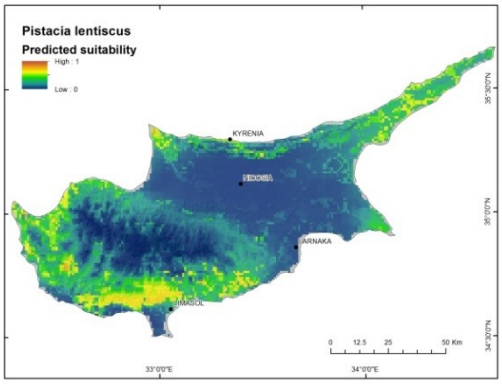
Pistacia lentiscus
Predicted suitability
High : 1
Low : 0
KYRENIA
LIMASOL
0 12.5 25 50 Km
33°0'0"E
34°0'0"E

(n)

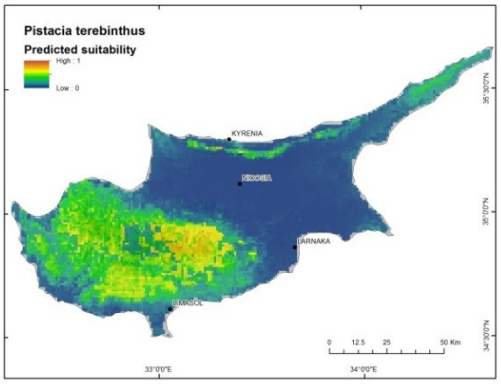
Pistacia terebinthus
Predicted suitability
High : 1
Low : 0
KYRENIA
LIMASOL
0 12.5 25 50 Km
33°0'0"E
34°0'0"E

(o)

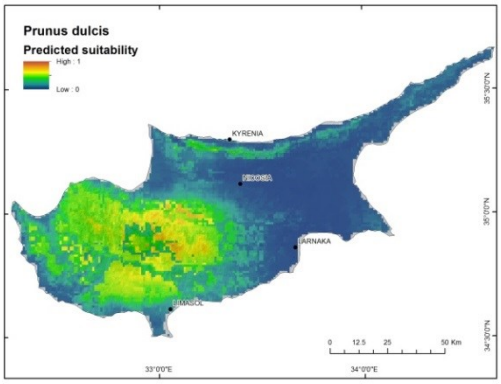
Prunus dulcis
Predicted suitability
High : 1
Low : 0
KYRENIA
LIMASOL
0 12.5 25 50 Km
33°0'0"E
34°0'0"E

(p)

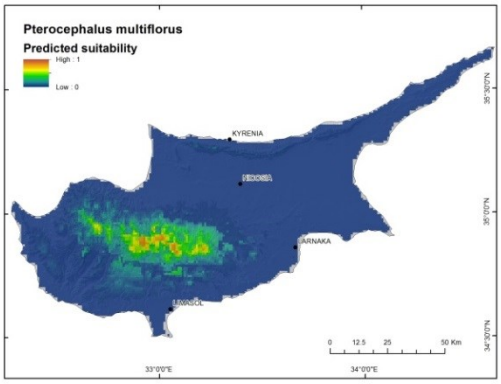
Pterocephalus multiflorus
Predicted suitability
High : 1
Low : 0
KYRENIA
LIMASOL
0 12.5 25 50 Km
33°0'0"E
34°0'0"E

(q)

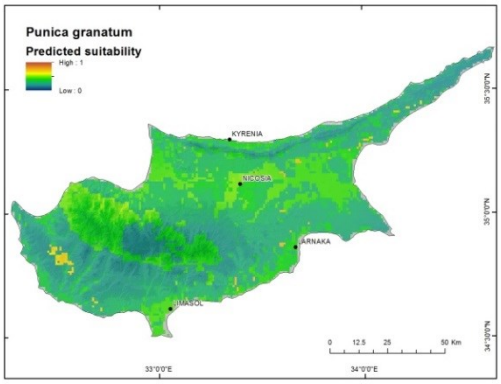
Punica granatum
Predicted suitability
High : 1
Low : 0
KYRENIA
LIMASOL
0 12.5 25 50 Km
33°0'0"E
34°0'0"E

(r)

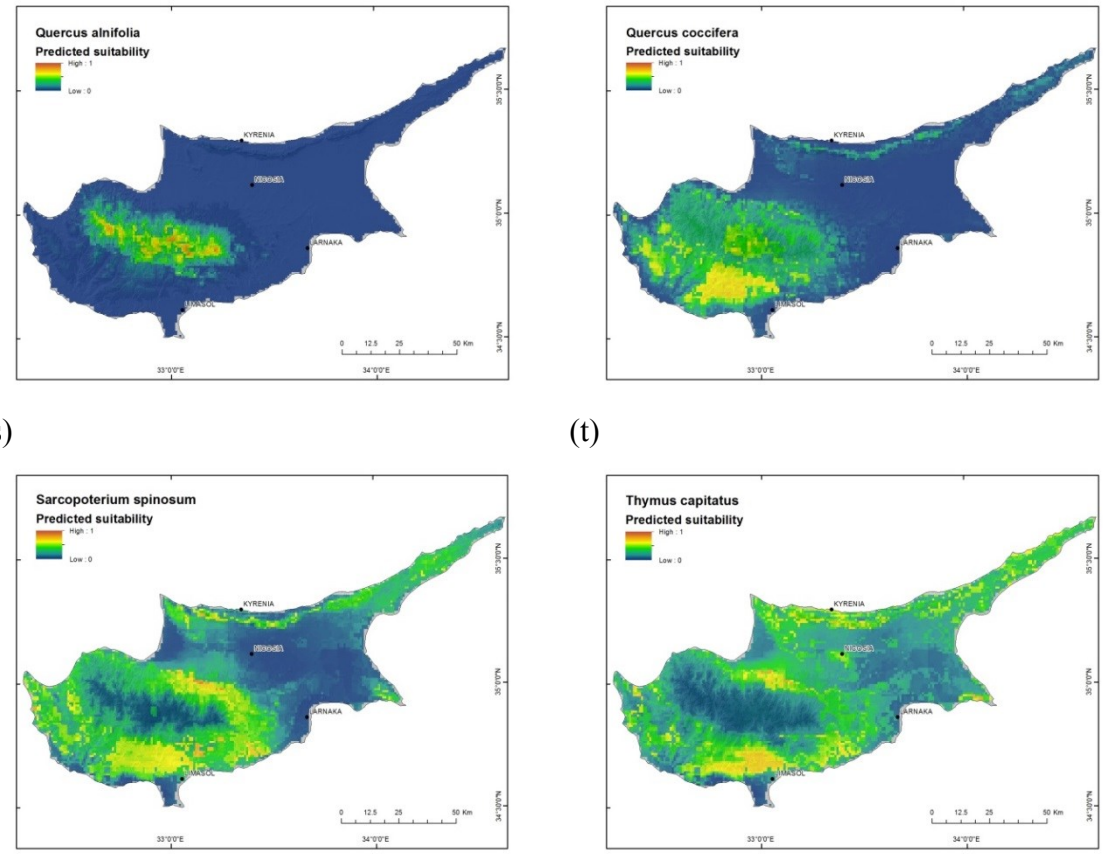

(s) (t)

(u) (v)

Figure 20. Continuous suitability maps for twenty-two species occurring on Cyprus. The maps have a standardized scale, where 1 (warmer colors) indicate that the model predicts higher suitability at that pixel. Cooler colors (near 0) indicate that the pixel is not predicted as environmentally suitable by the model.

Environmental variable contribution

The percent contribution by environmental variable for each species is summarized in Table 20. Geological substrate contributed as a variable in model construction for each species. Among the most interesting results regarding geology, modeling of *Quercus alnifolia* incorporated only an 11.3% contribution from the geology variable, even though previous studies indicate this species is highly associated with, and

often restricted to, igneous formations (Meikle, 1977, 1985). In contrast, geology played a large role in model building for *Cistus parviflorus* (69.4%), *Ficus carica* (65.6%), *Helianthemum obtusifolium* (77.7%), *Pistacia atlantica* (64.8%) and *Punica granatum* (73.4%). Among these taxa, only *Cistus parviflorus* is mentioned by Meikle (1977, 1985) as influenced by geological substrate.

Pinus nigra's model construction was most influenced by a 53.5% contribution by BIO12, annual precipitation. BIO12 influenced all models except those for *Cistus parviflorus*, *Helianthemum obtusifolium,* and *Punica granatum*. BIO1, mean annual temperature, and BIO17, precipitation of the driest quarter, also contributed to a majority of the models. BIO7, annual temperature range, was only included in modeling *Olea europaea,* as an 8.5% contributing variable.

Table 20. Percent contribution of the top five environmental variables to predictive suitability model construction for each species.

Taxon	Geology	BIO1	BIO2	BIO3	BIO4	BIO7	BIO8	BIO10	BIO12	BIO15	BIO16	BIO17	Top 5 variable contribution (%)
Arbutus andrachne	31.2	18.2							9.5		13.8	14.1	86.8
Cedrus brevifolia	24.6	7.2							36.3		4.8	12.3	85.2
Cistus creticus	17.8	6.1							42.1		12.9	6.2	85.1
Cistus parviflorus	69.4	3.3	2.5					1.2				21.8	98.2
Cistus salviifolius	54.5	8.4							17.9	4.7		6.3	91.8
Ficus carica	65.6	7			12.4				4.1		5.8		94.9
Helianthemum obtusifolium	77.7	2.9	4.2					2.9				6.2	93.9
Juniperus foetidissima	62.2	7.6		8.2				6.4	5.7				90.1
Juniperus phoenicea	49.3		3.8	5.4					3.4			30.7	92.6
Olea europaea	23.7	9.5				8.5			20.6		13		75.3
Pinus brutia	15.7	14.3					15.3	9.3	17.4				72
Pinus nigra	5.1			5.1					53.8		6.6	12.7	83.3
Pistacia atlantica	64.8							2.7	13.2	3.3	13.8		97.8
Pistacia lentiscus	37.2				9.1				29.2		5.8	8.8	90.1
Pistacia terebinthus	15.2	9.7						8.1	24.9		24.1		82
Prunus dulcis	21.2	30.3						28.8	7.9			3	91.2
Pterocephalus multiflorus	10			14.3					18.3		7	36.7	86.3
Punica granatum	73.4		3.4	9.3	6.6					3.3			96
Quercus alnifolia	11.3	8.5							32.8		3.6	38.2	94.4
Quercus coccifera	30.9	29.3		3.1				19.9	13.2				96.4
Sarcopoterium spinosum	28.4							8.6	22.3		17.9	8.6	85.8
Thymus capitatus	56.4				3.7				13.9		8.9	5.3	88.2

Model validation

Threshold-dependent validation

The selection of a logistic threshold allows the creation of a binary distribution (suitable vs. unsuitable) map for each species (Figure 21), in which values above the threshold are considered to indicate suitable areas and those under the threshold are excluded from the prediction. A threshold of maximum training sensitivity + specificity was chosen for all species. The binomial probability is calculated by Maxent (or an approximation thereof when training samples are greater than 25), producing a *p*-value, which indicates if the model produced a significantly better prediction than random. In this case, the null hypothesis states that the model is no better than a random prediction over the same proportional area (Phillips et al., 2006).

The binomial probability for eighteen models resulted in *p*-values less than 0.05, indicating that the model results were better than a randomly predicted distribution over the same proportional predicted area (Table 19). Binomial probabilities for *Quercus alnifolia, Pinus brutia* and *Pistacia terebinthus* were the most significant at 7.22×10^{-15}, 2.69×10^{-14} and 3.98×10^{-12}, respectively. Models for cultivated orchard species that occur in mid- to low-elevations also tended to perform well when evaluated using the binomial probability. Models constructed for *Olea europaea, Ficus carica* and *Prunus dulcis* had *p*-values of 9.38×10^{-7}, 5.53×10^{-4} and 1.34×10^{-7}, respectively. Success rates indicate how often a model correctly predicted a test point as occurring within the predicted suitable area for the threshold of maximum training sensitivity + specificity. Overall, modeling success rates varied from 36.67% (for *Cedrus brevifolia*) to 97.5% (for *Juniperus foetidissima*). *Quercus alnifolia, Pinus brutia* and *Pistacia terebinthus* (best performing

in terms of *p*-value) had success rates of 72.22%, 84.17% and 93%, respectively, thus performing well when using success rates as indicators of model performance. Models for cultivated species *Olea europaea, Ficus carica* and *Prunus dulcis* had success rates of 85.46%, 62.5% and 63.64%, respectively, (Table 19).

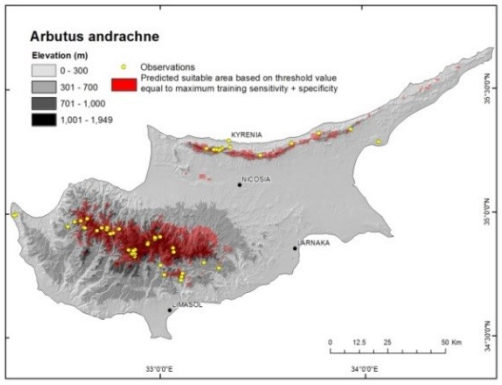

(a)

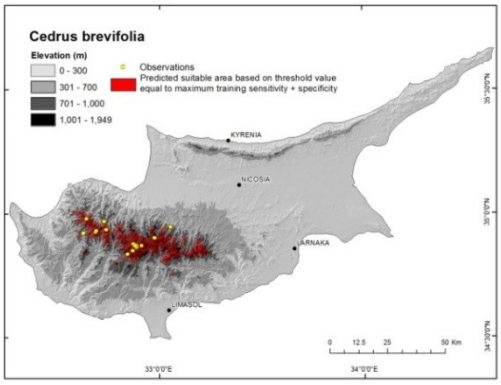

(b)

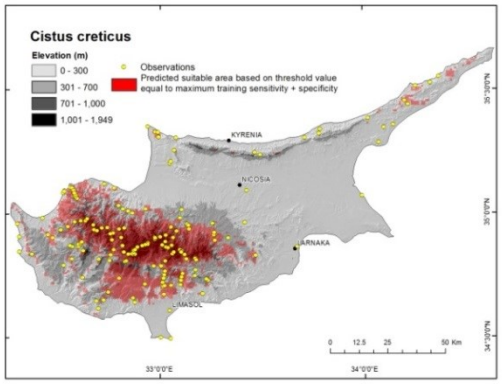

(c)

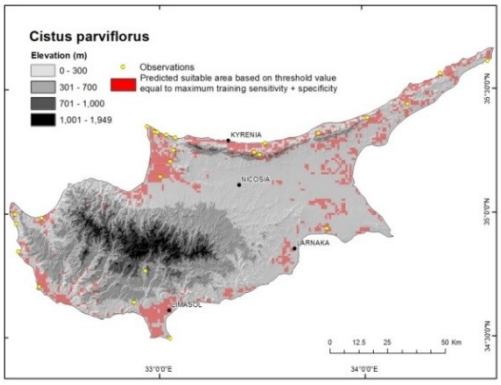

(d)

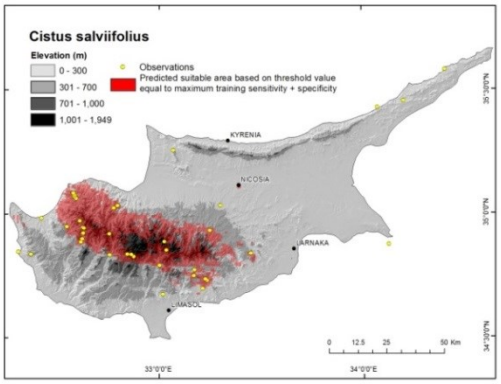
Cistus salviifolius
Elevation (m)
0 - 300
301 - 700
701 - 1,000
1,001 - 1,949
Observations
Predicted suitable area based on threshold value equal to maximum training sensitivity + specificity
KYRENIA
NICOSIA
ARNAKA
LIMASOL
0 12.5 25 50 Km
33°0'0"E
34°0'0"E
35°0'0"N
34°30'0"N

(e)

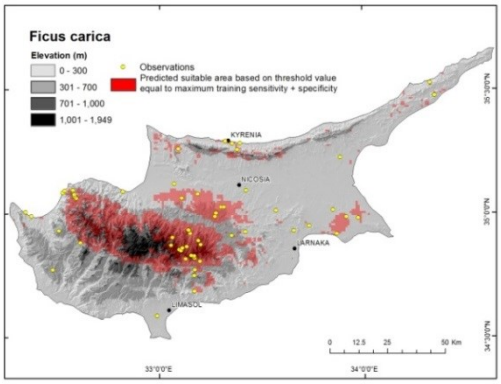
Ficus carica
Elevation (m)
0 - 300
301 - 700
701 - 1,000
1,001 - 1,949
Observations
Predicted suitable area based on threshold value equal to maximum training sensitivity + specificity
KYRENIA
NICOSIA
ARNAKA
LIMASOL
0 12.5 25 50 Km
33°0'0"E
34°0'0"E
35°0'0"N
34°30'0"N

(f)

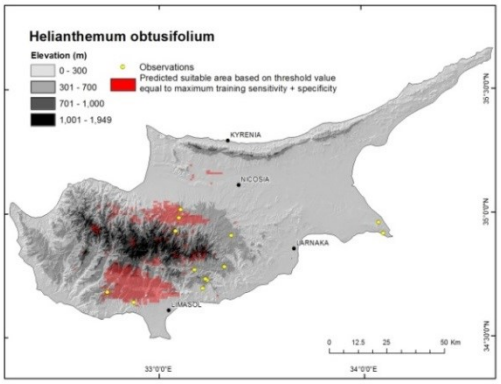
Helianthemum obtusifolium
Elevation (m)
0 - 300
301 - 700
701 - 1,000
1,001 - 1,949
Observations
Predicted suitable area based on threshold value equal to maximum training sensitivity + specificity
KYRENIA
NICOSIA
ARNAKA
LIMASOL
0 12.5 25 50 Km
33°0'0"E
34°0'0"E
35°0'0"N
34°30'0"N

(g)

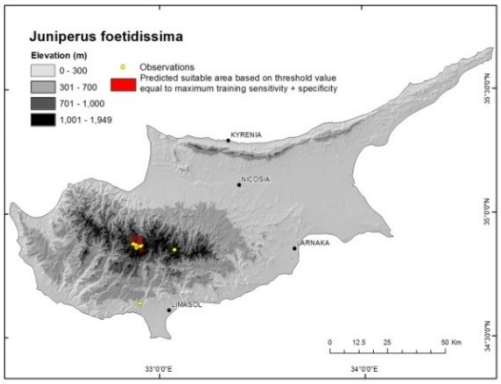
Juniperus foetidissima
Elevation (m)
0 - 300
301 - 700
701 - 1,000
1,001 - 1,949
Observations
Predicted suitable area based on threshold value equal to maximum training sensitivity + specificity
KYRENIA
NICOSIA
ARNAKA
LIMASOL
0 12.5 25 50 Km
33°0'0"E
34°0'0"E
35°0'0"N
34°30'0"N

(h)

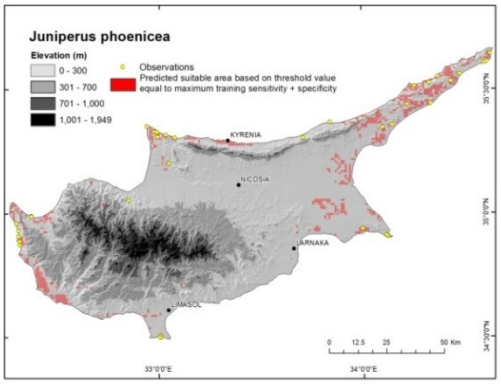
Juniperus phoenicea
Elevation (m)
0 - 300
301 - 700
701 - 1,000
1,001 - 1,949
Observations
Predicted suitable area based on threshold value equal to maximum training sensitivity + specificity
KYRENIA
NICOSIA
ARNAKA
LIMASOL
0 12.5 25 50 Km
33°0'0"E
34°0'0"E
35°0'0"N
34°30'0"N

(i)

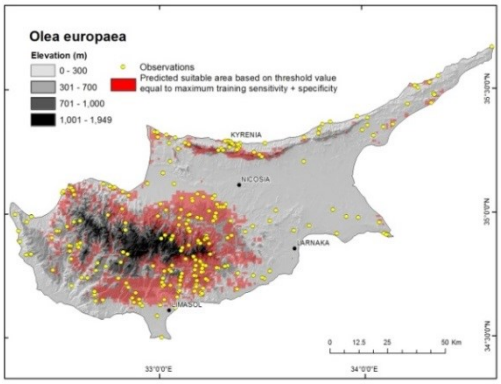
Olea europaea
Elevation (m)
0 - 300
301 - 700
701 - 1,000
1,001 - 1,949
Observations
Predicted suitable area based on threshold value equal to maximum training sensitivity + specificity
KYRENIA
NICOSIA
ARNAKA
LIMASOL
0 12.5 25 50 Km
33°0'0"E
34°0'0"E
35°0'0"N
34°30'0"N

(j)

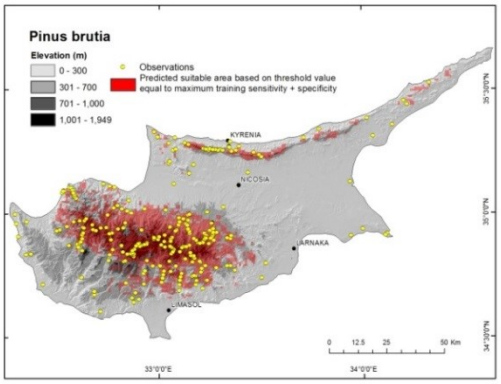
Pinus brutia
Elevation (m)
0 - 300
301 - 700
701 - 1,000
1,001 - 1,949
Observations
Predicted suitable area based on threshold value equal to maximum training sensitivity + specificity
KYRENIA
NICOSIA
ARNAKA
LIMASOL
0 12.5 25 50 Km
33°0'0"E
34°0'0"E
35°0'0"N
34°30'0"N

(k)

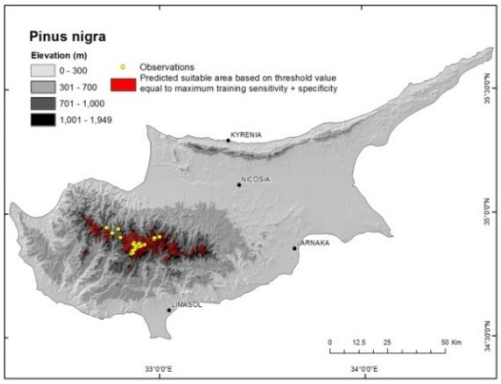
Pinus nigra
Elevation (m)
0 - 300
301 - 700
701 - 1,000
1,001 - 1,949
Observations
Predicted suitable area based on threshold value equal to maximum training sensitivity + specificity
KYRENIA
NICOSIA
ARNAKA
LIMASOL
0 12.5 25 50 Km
33°0'0"E
34°0'0"E
35°0'0"N
34°30'0"N

(l)

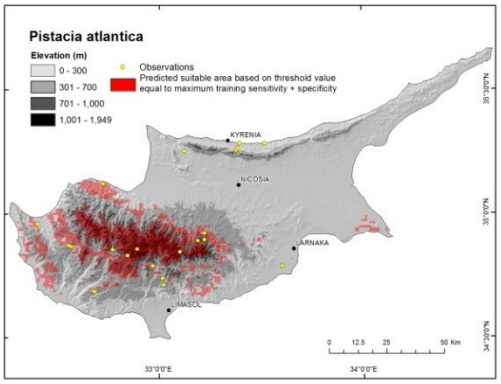
Pistacia atlantica
Elevation (m)
0 - 300
301 - 700
701 - 1,000
1,001 - 1,949
Observations
Predicted suitable area based on threshold value equal to maximum training sensitivity + specificity
KYRENIA
NICOSIA
ARNAKA
LIMASOL
0 12.5 25 50 Km
33°0'0"E
34°0'0"E
35°0'0"N
34°30'0"N

(m)

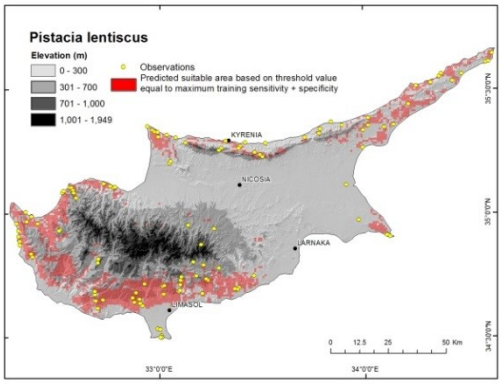
Pistacia lentiscus
Elevation (m)
0 - 300
301 - 700
701 - 1,000
1,001 - 1,949
Observations
Predicted suitable area based on threshold value equal to maximum training sensitivity + specificity
KYRENIA
NICOSIA
ARNAKA
LIMASOL
0 12.5 25 50 Km
33°0'0"E
34°0'0"E
35°0'0"N
34°30'0"N

(n)

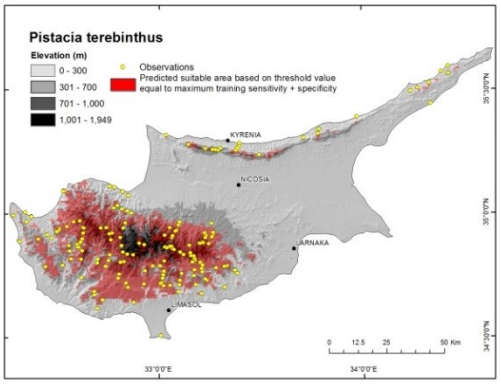
Pistacia terebinthus
Elevation (m)
0 - 300
301 - 700
701 - 1,000
1,001 - 1,949
Observations
Predicted suitable area based on threshold value equal to maximum training sensitivity + specificity
KYRENIA
NICOSIA
ARNAKA
LIMASOL
0 12.5 25 50 Km
33°0'0"E
34°0'0"E
35°0'0"N
34°30'0"N

(o)

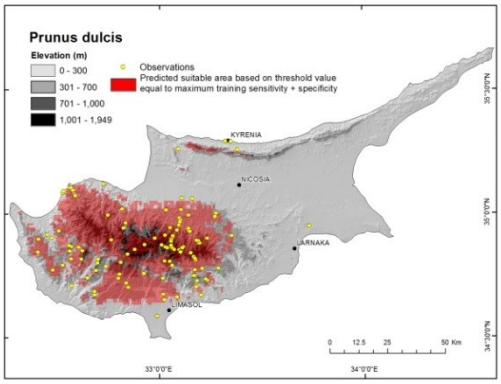
Prunus dulcis
Elevation (m)
0 - 300
301 - 700
701 - 1,000
1,001 - 1,949
Observations
Predicted suitable area based on threshold value equal to maximum training sensitivity + specificity
KYRENIA
NICOSIA
ARNAKA
LIMASOL
0 12.5 25 50 Km
33°0'0"E
34°0'0"E
35°0'0"N
34°30'0"N

(p)

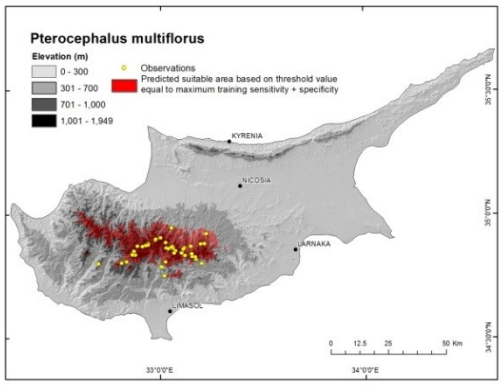

(q)

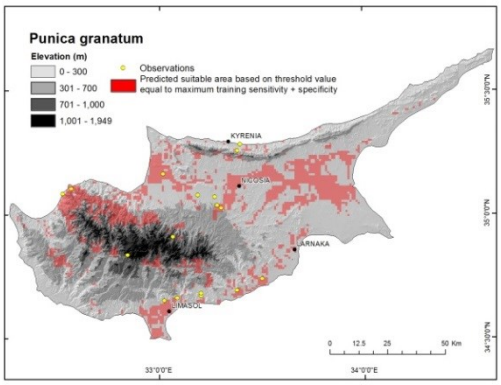

(r)

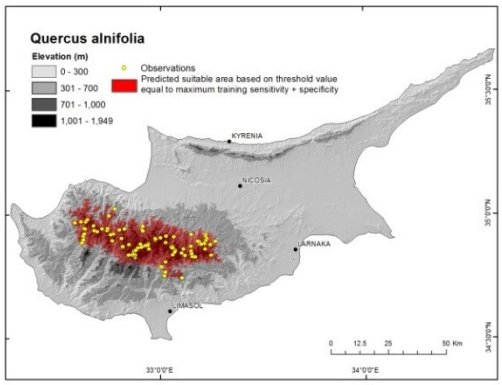

(s)

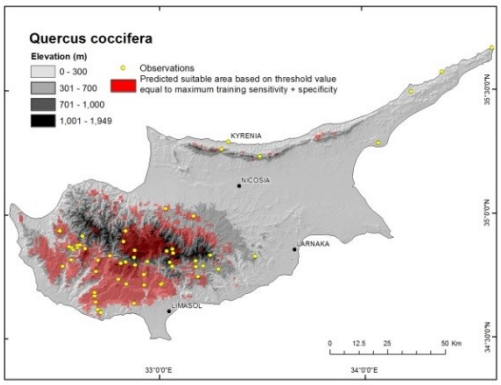

(t)

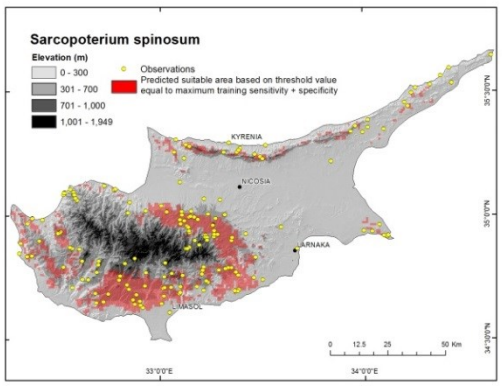

(u)

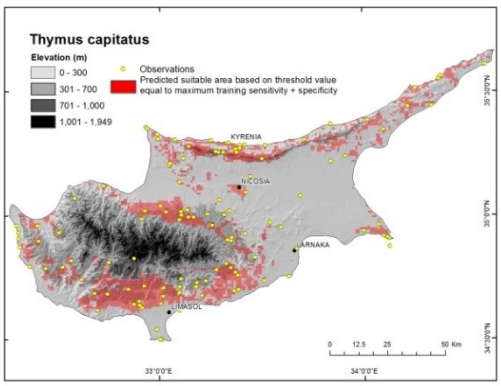

(v)

Figure 21. Red areas indicate the binary predicted suitable areas of occurrence based on a threshold of maximum training sensitivity + specificity. Yellow points are field observations for the specific species mapped.

Threshold-independent validation

Threshold-independent validation is based on the AUC for training and test data. The AUC indicates how well the model predicts presences in comparison to a random background sample; values above 0.5 are considered to indicate models that perform better than a random prediction. Training AUC (Table 19) ranged from 0.8393 for *Olea europaea* to 0.9922 for *Juniperus foetidissima*, indicating that the models perform well in predicting the occurrence of the data they are trained on (or created with) as the AUC is much higher than 0.5 and hence, model performance is much better than randomly predicted distributions for these species. Test AUC (Table 19) ranged from 0.6297 for *Helianthemum obtusifolium* to 0.9902 for *Pinus nigra*, indicating model performance better than random prediction for all species. Higher AUC values also demonstrate that models perform well when applied to withheld data and that they are not overly specific to the training data or constrained by the environmental predictors, an indicator that the models may perform well under new conditions. All species with fewer than 14 observations had test AUCs under 0.7481, with the exception of *Juniperus foetidissima* (test AUC=0.9341). *Pistacia atlantica* (n=14) had the lowest test AUC (0.7048) of species with 14 or more observations. There is no apparent correlation between training AUC values and the number of observations for each species.

Discussion

This study has produced continuous and binary suitability maps, while determining the effectiveness of Maxent in modeling of plant species distributions on Cyprus. This study attempts to predict the future distribution of twenty-two species, based upon their status as conservation, agricultural, cultural, or indicator species on

Cyprus; all are key taxa for maintaining vegetation habitats and biological diversity. (see Table 17). Conservation species are indicated by their occurrence on the European Red List of Vascular Plants (Bilz et al., 2011) or as a species that occur within a priority habitat according to Annex I of the Habitats Directive (Council of the European Communities, Council Directive 92/43/EEC, 2007). Cyprus is made up of seven general habitat categories: Coastal and Halophytic Habitats, Coastal Sand Dunes and Island Dunes, Freshwaters Habitats, Sclerophyllous Scrub (Matorral), Rocky Habitats and Caves, Natural and Semi-Natural Grassland Formations, and Forests. Four of the 15 priority habitats occur within Coastal and Halophytic Habitats and four within the Forest Habitats. Indicator species are species that are considered to define a particular habitat type. Four species of orchard trees, *Punica granatum* (pomegranate)*, Prunus dulcis* (almond)*, Olea europaea* (olive) and *Ficus carica* (fig) were selected to represent the agricultural species of Cyprus (Table 17). These trees were selected on the basis of their long history as cultivars on the island and as sources of present-day agricultural products. In addition to *Punica granatum, Olea europaea* and *Ficus carica, Arbutus andrachne, Cistus creticus, Cedrus brevifolia, Pistacia lentiscus* and *Pistacia terebinthus* are species of cultural importance. Examples of cultural uses include wood for icon production, dye extraction or symbolic ties to ancient Greece.

Maxent was selected as the modeling tool/platform, partially due to its ability to create effective models of species from relatively few observations. In this study, Maxent's ability to create high performing models was demonstrated in models for high elevation species such as *Juniperus foetidissima, Cedrus brevifolia, Quercus alnifolia* and *Pinus nigra*. These species may have low sampling observations due to restrictions in

extent or detectability. However when evaluated using a threshold of maximum training sensitivity + suitability and a binomial probability, they produced binary prediction maps that produce better than random predictions over the same area (Table 19). Additionally these models performed exceptionally well when evaluated using both the test and training AUCs (all higher than 0.90). *Juniperus foetidissima, Cedrus brevifolia, Quercus alnifolia* and *Pinus nigra* are considered a species of concern under Annex I of the Habitats Directive, and *Cedrus brevifolia* has been declared a vulnerable species (European Red List, 2011). High performing models are required to model the current distributions of these and similar species to insure their survival and maintain species diversity. Additionally, models can be utilized to conduct targeted surveys in areas of predicted suitability, to assist in decision-making for establishing conservation or reserve areas, and to model the expected distribution of the species under future climate conditions. Although not currently on any lists for monitoring, high performing models for other high elevation species such as *Pterocephalus multiflorus* (an endemic species) and *Arbutus andrachne* (used historically) are important when considering the potential impacts of climate change, as these species will not be able to migrate elevationally in response to predicted changes in temperature and precipitation.

Mid- and low-elevation species follow the overall trend of high performing models when evaluated using both threshold-dependent and –independent measures of performance. Models constructed for *Cistus parviflorus, Helianthemum obtusifolium, Pistacia atlantica* and *Punica granatum* did not produce models that are different from a model constructed over the same proportional predicted area using a random sampling of background points. In other words, these models do not differ significantly from

randomly constructed models. They tend to have lower (0.6297 to 0.7481) test AUCs but there is not a relationship between threshold-dependent and –independent measures of performance. Although these species have low observation numbers (Table 19), these results may reflect the parameterization of the models. For example, the suite of environmental variables selected for this study may not be those best suited to create predictions of habitat suitability for these particular species. In addition, the selection of a different method of thresholding the continuous predicted suitability maps may produce *p*-values that are statistically significant. Finally, the use of a cross-validation method (e.g. Phillips et al., 2006; Elith et al., 2011) for partitioning data into train/test datasets may increase the AUC for each of these species.

As a means of evaluating field observations for accuracy, identified species were compared against the botanical regions described by Meikle (1977). Misidentification of species may result in models that predict species for areas in which they are not environmentally compatible, or it may skew results toward misidentified sites, potentially impacting management decisions. Meikle's botanical regions were created through his personal observations, and with reference to other previously published observations. When possible, Meikle visited botanical collections and verified the species' classification, noting where the plant was collected (if available) for inclusion in his description of a species and its distribution on Cyprus (see Meikle 1977, 1985; further description in Chapter 2).Several species (*Cistus creticus*, *Ficus carica*, *Juniperus foetidissima*, *Juniperus phoenicea*, *Pinus brutia*, and *Thymus capitatus*) were observed outside of their historical botanical regions, as described by Meikle (1977, 1985). For example, the observation of *C. parviflorus* in Division 5 is not easily explained, since *C.*

parviflorus was not noted by Meikle (1977, 1985) in this division. Observations occurring in Division 5 may represent a range extension of the species, or depending upon the area of observation (e.g. urban, suburban, roadside, forest, etc.), the observations may reflect plantings for roadside beautification/revegetation projects or landscaping plantings in yards or other urban features. *Thymus capitatus* was described as occurring in Region 8 and *Ficus carica* in Region 3 by Hand (2004). The observation of *Juniperus foetidissima* in Region 2 and *Pinus brutia* in Division 4 may represent a planted specimen or a misclassification (*P. brutia* is often misidentified as *P. halepensis* as their botanical classification is often discussed; see Hand, Hadjikyriakou, and Christodoulou, 2011). *Juniperus phoenicea* was described in Division 7 by Farjon (2005). Thus, with the exception of *C. parviflorus* many of the species observations still fall within their documented botanical regions based upon updates since the publication of Meikle's books (1977, 1985).

The percent contribution of environmental variables may help to determine limiting factors in the distribution of a species. For the species modeled here, geology was a contributing variable in the development of all the models and may help direct conservation efforts, particularly for species of agricultural interest (i.e. *Ficus carica* and *Punica granatum*) where targeted substrate improvements are more likely to occur. Many predictions were also influenced by BIO12, annual precipitation, and BIO17, precipitation of the driest quarter, indicating that many of the Cypriot species are restricted by either low annual or seasonal precipitation, which may have potential consequences under climate change predictions of lower rainfall and higher temperatures (IPCC, 2007; EEA, 2010; Zacharidis, 2012). BIO1, annual mean temperature range, also

played a role in model construction for 14 of the 22 species, most notably *Prunus dulcis* and *Quercus coccifera* (29.3% and 30.3% contribution, respectively), indicating that the distributions of these species are influenced by temperature extremes (high or low temperature annually).

Quercus alnifolia has been noted as being restricted to the igneous rocks of the Troodos Range and as occurring above 760m (Meikle 1977, 1985); however, geology only accounted for 11.3% of variable contribution, whereas BIO12, annual precipitation, and BIO17, precipitation of the driest quarter, accounted for 32.8% and 38.2%, respectively. This may indicate that the environmental requirements of *Q. alnifolia* require further study, as Tsintides et al. (2002) notes that this species can occur at elevations as low as 300m. With the results of the Maxent models, further study on the moisture requirements of *Q. alnifolia* would be interesting, in order to determine if moisture is indeed the limiting variable (as elevation can indicate changes to other environmental gradients in addition to precipitation).

The models created for the 22 species listed in Table 17 are the starting point to evaluate the impact of climate scenarios for 2030, 2050, and 2070 on habitat suitability in Cyprus, an area that currently lacks such predictions. Current modeling efforts have focused on the Mediterranean as a region, but it is important to look at Cyprus individually due to the high number of endemic species, many of which are species of concern.

Conclusions

A majority of models (18 of 22) constructed to predict the present-day habitat suitability of selected plant species on Cyprus were statistically significant (at $p < 0.05$),

indicating that they perform better than random predictions for each of these species. Models for high elevation species *Juniperus foetidissima, Cedrus brevifolia, Pinus nigra, Pterocephalus multiflorus, Arbutus andrachne* and *Quercus alnifolia* performed well when evaluated using the AUC, a threshold-independent metric. The combined results of threshold-dependent (binomial probability) and threshold-independent methods of evaluation indicate these models are reliable and increase the credibility of their use for prediction into new climate scenarios.

Models for three of the four orchard species (*Olea europaea, Ficus carica* and *Prunus dulcis*) were also high performing, with *p*-values from the binomial probability indicating they function better than a random prediction over the same proportional predicted area. The test and training AUCs suggest that these models are well suited to predict into novel climate conditions, as the models performed well when predicting areas of suitability for test data. Mid-elevation species (*Cistus salviifolius, Quercus coccifera, Thymus capitatus, Sarcopoterium spinosum, Pistacia terebinthus* and *Cistus creticus*) and low elevation species (*Juniperus phoenicea* and *Pistacia lentiscus*) follow the same trend, with significant *p*-values and good to excellent test and training AUC values.

Several species with few observations did not have high test AUCs, indicating that additional tweaks to the models might be warranted. Although models for *C. parviflorus*, *H. obtusifolium*, *P. atlantica* and *P. granatum* are not statistically significant using the maximum training specificity + sensitivity rule at a 0.05 significance level, this does not mean these models cannot be used to predict future suitable areas; it only indicates that under this particular threshold rule the results are insignificant. Overall,

Maxent produced valuable models to use as a starting point in evaluating the impacts of climate change scenarios on habitat suitability, evaluation of potentially suitable habitat for conservation and preservation, refining survey data and supplementing other data for management decisions.

Chapter 5

MAXENT MODELING OF FUTURE VEGETATION 2030-2070

Introduction

Mediterranean ecosystems contain approximately 20 percent of the Earth's vascular plants (Heywood and Watson, 1995; Cowling et al., 1996; Groombridge and Jenkins, 2002; Yates et al., 2010). The Mediterranean Basin is described as a biodiversity hotspot, as it is high in endemic species, although the region experiences various pressures, including climate change, that threaten the persistence of species (Myers et al., 2000). In Cyprus, approximately 2000 plant taxa have been identified, with 144 endemic species, many of which are local endemics to one of the island's two large mountain ranges. Bilz et al. (2011) included 45 Cypriot endemics in the European Red List of Vascular Plants, categorizing 10 plants as critically endangered (*Allium marathasicum, Arabis kennedyae, Astragalus macrocarpus, Centaurea akamantis, Crypsis hadjikyriakou, Delphinium caseyi, Limonium mucronulatum, Maresia nana* var. *glabra, Salvia veneris* and *Scilla morrisii*), 5 as endangered (*Brassica hilarionis, Onosma troodi, Peucedanum kyriakae, Solenopsis antiphonitis* and *Tulipa cypria*), 25 as vulnerable (*Allium exaltatum, Arum sintenisii, Astragalus echinus* var. *chionistrae, Brachypodium glaucovirens, Cedrus brevifolia, Clinopodium troodi, Crocus cyprius, Cynoglossum troodi, Cyperus cyprius, Erysimum kykkoticum, Ferula cypria, Hedysarum cypruim, Lactuca tetrantha, Onosma caepitosa, Origanum cardiofolium, Papaver cyprium, Ranunculus kykkoensis, Scilla lochiae, Sedum microstachyum, Serapias politisii, Sideritis cypria, Silene gemmate, Taraxacum aphrogenes* and *Taraxacum holmboei*), 1 as near

threatened (*Ophrys kotschyi*), and 4 as data deficient (*Alyssum akamasicum, Phlomis brevibracteata, Phlomis cypria* and *Phlomis cypria* subsp. *cypria*).

Anthropogenic climate change is expected to increase mean annual temperatures in Europe at a rate greater than the global mean (increases of 1.8°C to 4.0°C), with temperatures predicted to increase between 1.1°C and 6.4°C between the present (1980-1999 average) and the end of the 21st century, depending upon the climate scenario under consideration (IPCC, 2007; EEA, 2010). The Mediterranean is most likely to experience the predicted increase in temperature over the summer months, with a decrease of 5-20% in mean annual precipitation across the Mediterranean Basin (IPCC, 2007; EEA, 2010). The Meteorological Service of Cyprus (2013) recorded a 17% decrease in mean annual precipitation from 1901-1930 (559 mm) to 1971-2000 (462 mm). In addition, temperature increases were noted across the island, with a 1°C increase since the beginning of the 20th century.

The predicted changes in temperature and precipitation are expected to have profound effects on ecosystem function; the diversity and composition of communities; and the distribution, dispersal, and abundance of individual species (Parmesan and Yohe, 2003; Rosenzweig et al., 2008; Yates et al., 2010; Butler et al., 2012). Future changes in species distributions are not unexpected, given species' responses to past changes in climate. For example, in the Holocene, dispersal events that crossed large physical barriers over long distances have been recorded in the pollen record (Pitelka, 2004; Thomas et al., 2004). Within the past 30 years, species have shifted their ranges to higher elevations or toward the poles (Parmesan, 2006), restricted their ranges (Thuiller et al., 2005), changed in abundance (Parmesan and Yohe, 2003; Root et al., 2003), and possibly

gone extinct (Pounds et al., 1999) in response to climate changes. Thomas et al. (2004) projected species extinction rates of 11% or 34% by 2050 based on assumptions regarding species' ability to disperse to projected areas of suitable environmental conditions under conditions of mean temperature increase of 0.8°C to 1.7°C and CO2 increase by 500 parts per million by volume (ppmv), a scenario less severe than the IPCC (2007) has predicted for mean changes in temperature. Mediterranean species are predicted to decline by as much as 62% in response to increased temperatures and decreased precipitation (Zacharidis, 2012).

This study attempts to predict the future distribution of twenty-two species, based upon their status as conservation, agricultural, cultural, or indicator species on Cyprus (see Table 17). Conservation species are indicated by their occurrence on the European Red List of Vascular Plants (2011) or as a species that occurs within a priority habitat according to Annex I of the Habitats Directive (Council of the European Communities, Council Directive 92/43/EEC, 2007). Cyprus is made up of seven general habitat categories: Coastal and Halophytic Habitats, Coastal Sand Dunes and Island Dunes, Freshwaters Habitats, Sclerophyllous Scrub (Matorral), Rocky Habitats and Caves, Natural and Semi-Natural Grassland Formations, and Forests. Four of the 15 priority habitats occur within the Coastal and Halophytic Habitats and four within the Forest Habitats categories. Indicator species are species that define a particular habitat type. Four species of orchard trees *Punica granatum* (pomegranate)*, Prunus dulcis* (almond)*, Olea europaea* (olive) and *Ficus carica* (fig) represent the agricultural species of Cyprus (Table 17). These trees were selected due their long history as cultivars on the island and their importance for present-day agricultural products. In addition to *Punica granatum,*

Olea europaea and *Ficus carica, Arbutus andrachne, Cistus creticus, Cedrus brevifolia, Pistacia lentiscus* and *Pistacia terebinthus* are species of cultural importance. Examples of cultural uses include wood for icon production, dye extraction or symbolic ties to ancient Greece.

Cyprus presents itself as an interesting case study due to its species diversity and for its potential for habitat loss and species extinctions due to climate change. More specifically, the following question will be addressed:

How will the current species' distributions change with respect to IPCC AR4 A1b and A2 climate scenarios for 2030, 2050, and 2070?

This question produces the following predictions (see Methods for a description of the scenarios):

1. Under an A1b scenario: We would expect minimal changes to most species distributions with the exceptions of high elevation or coastal species. For high-elevation species, Cyprus has only two major mountain ranges, both of which are relatively low in elevation (1952 m maximum). Thus, movement to higher elevation is not possible as a response to global warming for some of the higher elevation species. Similarly, there is no adaptive option for species to spread northward, since Cyprus' latitude only varies by approximately 250 km. With increases in temperature and sea level, species currently restricted to the coast will likely expand their ranges inland.
2. Under an A2 scenario: We would expect species that are limited by high temperature or low precipitation to disperse to higher elevation. For some species this may cause a restriction in modern distributions. Generalists will

likely expand into new habitats currently unavailable to them due to resource competition or other limiting factors. We would expect the loss of high elevation species and species with modern limited distributions by the end of the 21st century.

Methods

Selection of climate scenarios and model

Future IPCC Assessment Report 4 (AR4) gas-emission scenarios (from the IPCC Special Report on Emissions Scenarios; SRES, 2000) are grouped into four qualitative categories (A1, A2, B1, and B2) with differing driving forces and resulting greenhouse gas (GHG) emissions. The A1 storyline depicts rapid economic growth, population that peaks mid-century, and rapid introduction of new and efficient technologies. This storyline is further divided into three scenarios, A1FI, A1T and A1b, to explore differing approaches to energy system technologies (IPCC, 2000). To model future distributions of Cypriot vegetation, SRES scenarios A1b and A2 were selected. Like all A1 scenarios, the A1b scenario depicts rapid economic growth, global population peaking mid-century with declines later in the century, and the quick introduction and adoption of new and more efficient technology. This scenario assumes a balanced approach (versus fossil intensive – A1FI or non-fossil energy sources – A1T) to use of all available energy sources, with new technologies and improvements applying to all forms of energy supply. The A2 scenario depicts a heterogeneous world, with high population growth rates, slow economic development, and slow technological change (IPCC, 2000). Based on ensemble predictions of future climate, the A1b scenario's most likely estimate of temperature change between 2090 and 2099 (relative to 1980-1999) is 2.8°C, with a range of 1.7°-

4.4°C for the Mediterranean. The A2 scenario's most likely estimate of temperature change over the same time period is 3.4°C, with a range of 2.0°-5.4°C (IPCC, 2007). These two story lines represent mid- and high-emissions scenarios, with minimal differences in temperature predictions by 2050, but diverging temperatures thereafter (Wilby et al., 2009; Jones and Thornton, 2013). At the time of data acquisition, B1 scenarios (low-emissions scenario) were not available at the selected data resolution and time slices.

In addition to selection of the GHG-emissions scenarios, decisions on the appropriate atmosphere-ocean global climate model(s) (AOGCM) were required. Twenty-three models were utilized in the IPCC AR4 (2007) to create ensemble predictions of future climate conditions; however, not all models are available at the desired resolution of 1 km^2, at time slices of 2030, 2050, and 2070 (representing the time periods of 2021-2040, 2041-2060, and 2061-2080, respectively), or include the option to download the derived bioclimatic variables. From the remaining available models, MRI-CGCM2.3.2 (Meteorological Research Institute, Japan; Yukimoto et al., 2006) was selected as it reliably simulates current climate (Yukimoto et al., 2006) and was the most conservative model available during data acquisition, providing more conservative estimates of temperature increase than the ensemble best estimate predictions, with an average temperature increase of 2.4°C for SRES A1b and 2.7°C for SRES A2 over the period of 2080-2099.

Bioclimatic grids were downloaded from the Climate Change, Agriculture and Food Security (CCAFS) Global Climate Model (GCM) Data Portal[6] and consist of 19 bioclimatic variables derived from the monthly estimates of precipitation and maximum and minimum temperatures (Ramírez-Villegas and Bueno-Cabrera, 2009) at approximately 1 km^2 resolution (30-arc second x 30-arc second), matching the resolution of modern species predictions (see Chapter 3). These data are downscaled from the original 100 to 200 km resolution AOGCM projections using the delta method of statistical downscaling (Ramirez-Villegas and Jarvis, 2010). This methodology does not improve data accuracy, but in the absence of a regional climate model, or the long-term meteorological data necessary to produce a regional climate model or use a different downscaling method, this is the best option for agricultural, species distribution and other ecological/biological assessments that require higher spatial resolution data as predictor variables (Ramirez-Villegas and Jarvis, 2010). The delta downscaling method applies a thin-plate spline spatial interpolation to the original AOGCM outputs. To create the new climate surfaces, the anomalies from the 1961-1990 baseline data are calculated for each time step and then applied to the higher spatial resolution baseline data. This method is based on the assumptions that changes in climate vary over large distances, and that relationships between climatic variables are maintained throughout time. These assumptions, however, may not hold true in landscapes of highly variable topography (Ramirez-Villegas and Jarvis, 2010).

[6] http://www.ccafs-climate.org/

Maxent and future prediction of species distributions

Predictions of future distributions were created for 22 species (see Table 17) using the same predictive bioclimatic variables as modern models (see Chapter 4) after determining that correlations between variables were not highly variable over time (Appendices B through G) (see Elith et al., 2010) and were not indirect environmental predictors of species occurrence (e.g. monthly estimates of bioclimatic variables or elevation) (Phillips et al., 2006). Geology was assumed to remain constant across time slices. Since the modern models were constructed using a bootstrapping method of data partitioning and replicated 10 times, future scenarios also were generated for each model run. Prediction of future climates often involves novel conditions that are not sampled in the training of the model, thus Maxent performs "clamping," by restricting values for future environmental variables to the maximum value encountered in the same variable used during training (Elith et al., 2011). The final mapped distribution represents the average of all model runs. These data are first presented as continuous surfaces of predicted suitability. Thresholds are applied to the continuous predictions (see Table 19 for threshold values) and a binary presence/absence map is created for any species maintaining predicted suitable areas above threshold values throughout the time steps (Table 21). The presence/absence maps allow for the calculation of change in area occupied as well as the examination of any shifts in species distribution. Any species without predicted suitable habitat above the threshold values at any time step are assumed to not persist to subsequent time steps, thus losing all suitable areas of occurrence.

Model validation

Unlike modern models, future models of species distributions are difficult to validate since these distributions cannot be observed. However, Maxent features built-in applications that allow for the visualization of similarities between modern and future climate conditions (multivariate environmental similarity surfaces, MESS). Maxent maps the variable in each grid cell that is most dissimilar, and displays the effect of constraining the data ("clamping") to training data maximum values (Phillips et al., 2006; Phillips and Dudík, 2008; Elith et al., 2010; Elith et al., 2011).

Table 21. Predicted suitable area for each species modeled. Models were constructed using climate scenarios A1b and A2 and species responses were modeled across three time steps: 2030, 2050 and 2070.

	Predicted suitable area (square km) for each time slice/climate scenario								
Taxon	**Modern**	**2030 A1b**	**2050 A1b**	**2070 A1b**	**2030 A2**	**2050 A2**	**2070 A2**	**Overall change in suitable area (Modern - A1B 2070; %)**	**Overall change in suitable area (Modern - A2 2070; %)**
Arbutus andrachne	1088.8427	0	0	0	79.37840506	0	0	-100	-100
Cedrus brevifolia	517.1309	0	0	0	0	0	0	-100	-100
Cistus creticus	2011.1674	0	0	0	0	0	0	-100	-100
Cistus parviflorus	1644.8278	0	0	0	0	0	0	-100	-100
Cistus salviifolius	1404.3018	0	0	0	0	0	0	-100	-100
Ficus carica	1939.0096	252.2818616	8550.861852	4503.349119	6132.571235	7174.707523	8166.544624	132.2499651	321.1709227
Helianthemum obtusifolium	1518.0891	158.7568101	0	0	0	0	0	-100	-100
Juniperus foetidissima	277.53	0	0	0	0	0	0	-100	-100
Juniperus phoenicea	692.8999	0	0	0	0	0	0	-100	-100
Olea europaea	2453.3652	4316.299016	3656.122182	1005.983747	2636.777713	2452.085384	3377.904802	-58.9957603	37.68454862
Pinus brutia	2277.5962	76.23470585	2171.51023	0	1309.350721	535.2147906	1404.447622	-100	-38.33640826
Pinus nigra	291.4065	0	0	0	0	0	0	-100	-100
Pistacia atlantica	1918.6574	0	0	0	0	0	0	-100	-100
Pistacia lentiscus	1828.9227	4251.067257	4269.143528	2779.816027	5466.892927	3269.447179	3353.541133	51.99199107	83.36155665
Pistacia terebinthus	2299.7986	2371.921054	382.7453789	1894.078774	2878.842552	139.1086901	2085.844426	-17.64153721	-9.303170021
Prunus dulcis	2614.3326	4390.961872	4798.856845	9101.795139	6132.571235	8190.122368	6703.938566	248.1498543	156.4302096
Pterocephalus multiflorus	888.096	0	0	0	0	0	0	-100	-100
Punica granatum	2500.5453	1457.890509	92.73912671	92.73912671	92.73912671	0	0	-96.29124389	-100
Quercus alnifolia	1148.0491	74.66285625	0	0	0	0	0	-100	-100
Quercus coccifera	1916.8072	0	0	0	0	0	0	-100	-100
Sarcopoterium spinosum	1790.9936	1865.785481	249.9240872	3561.025281	6917.710112	6009.966965	4522.211314	98.82959272	152.4973464
Thymus capitatus	2173.0599	3264.73163	756.8455849	3708.779143	4658.176305	1131.731716	4849.156032	70.67081968	123.1487513

Results

Trends

The overall trends were examined visually from the continuous prediction maps (Figures 22-43) and the binary presence/absence maps (Figures 44-52). The continuous prediction maps provide probability of suitability for species occurrence at each pixel across the entire study area. This type of map is helpful when comparing areas of suitability for a single species across multiple time slices. Since the predictions of suitability cover the study area, it is possible to visually discern changes to the overall pattern of potential distribution. The continuous maps are important for inclusion as the source for thresholds used to create binary presence/absence maps. When examining the continuous prediction maps for A1b scenarios, *Cistus parviflorus, Ficus carica, Helianthemum obtusifolium, Olea europaea, Pinus brutia, Pistacia lentiscus, Pistacia terebinthus, Prunus dulcis, Punica granatum, Sarcopoterium spinosum, and Thymus capitatus* all appear to persist throughout all time steps (Figures 22-43). Suitable areas are not predicted in 2050 for *C. parviflorus* (Figure 25d). It does, however, appear along the coastline in the 2070 prediction, but is more restricted in range, and habitat suitability scores are lower than modern predictions (Figure 25f). *Pinus brutia* also appears to expand its range by 2050 (Figure 32d), particularly toward the Akamas Peninsula and along the northern reaches of the Karpas Peninsula, but the suitability scores decline by 2070 (Figure 32f). *Ficus carica, P. lentiscus, P. terebintus, P. dulcis, S. spinosum,* and *T. capitatus* all appear to expand into new suitable areas by 2070. The A2 scenario produces similar results, with *F. carica, H. obtusifolium, O. europaea, P. lentiscus, P. terebinthus, P. dulcis, P. granatum, S. spinosum,* and *T. capitatus* appearing to maintain

suitable areas through all time steps (Figures 22-43). *Cistus parviflorus* (Figure 25g) does have suitable areas predicted in 2070, and *P. brutia* (Figure 32g) is added to the list of species with suitable areas by this time.

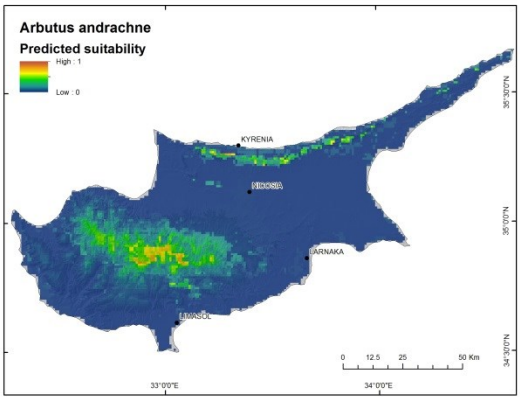

(a)

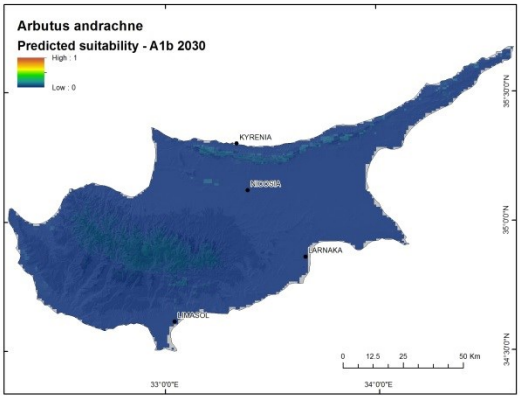

(b)

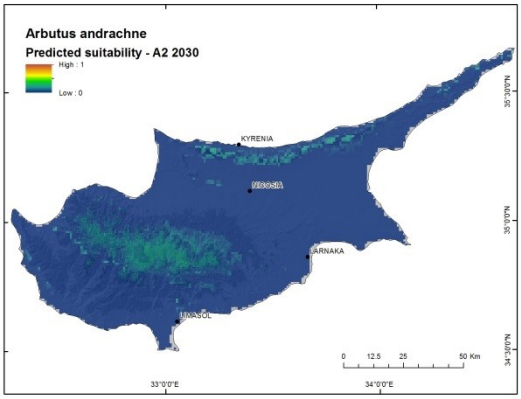

(c)

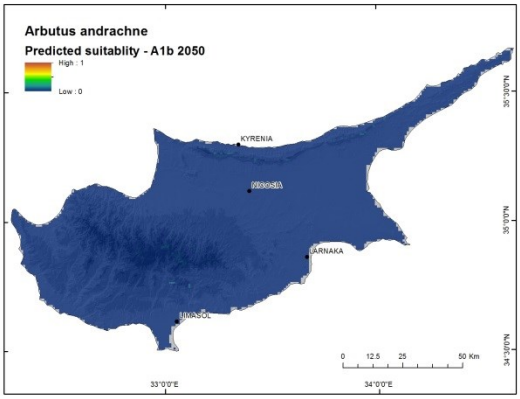

(d)

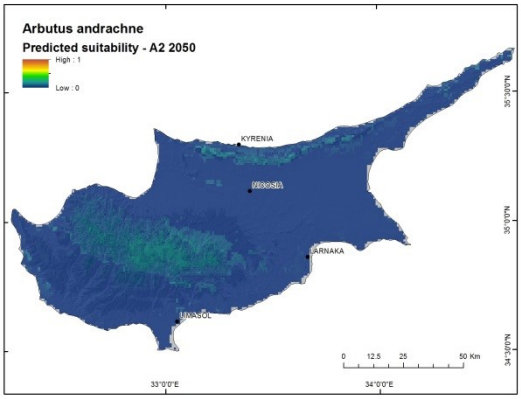

(e)

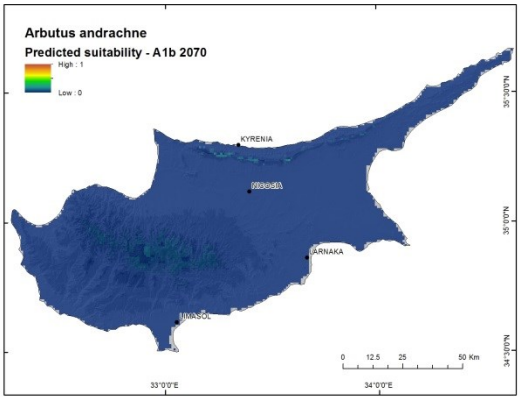

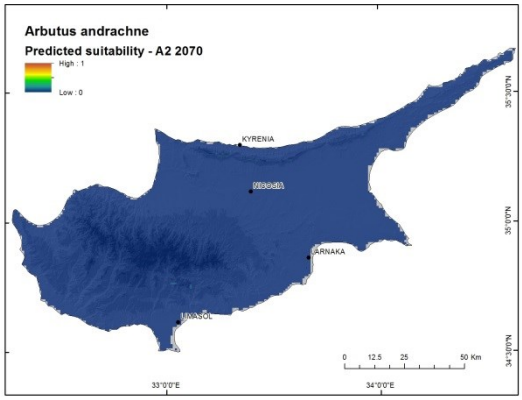

(f) (g)

Figure 22. Continuous suitability maps for *Arbutus andrachne* from present (Figure 22a) through 2070 A1b (Figure 22f) and A2 (Figure 22g) climate scenarios. Warmer colors indicate predicted suitability at a pixel to be near 1 (completely suitable for occurrence) and cooler colors indicate suitability predictions closer to 0 (completely unsuitable for occurrence).

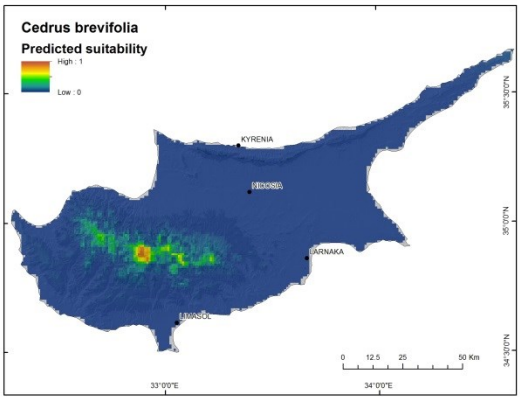

(a)

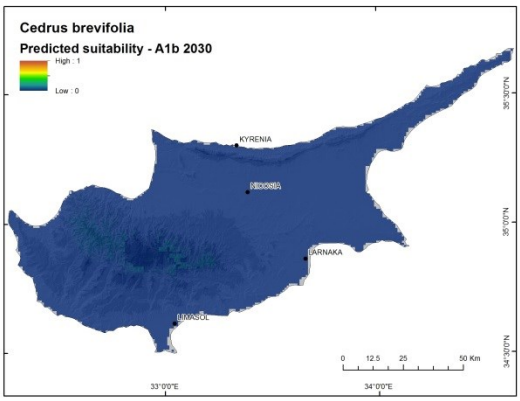

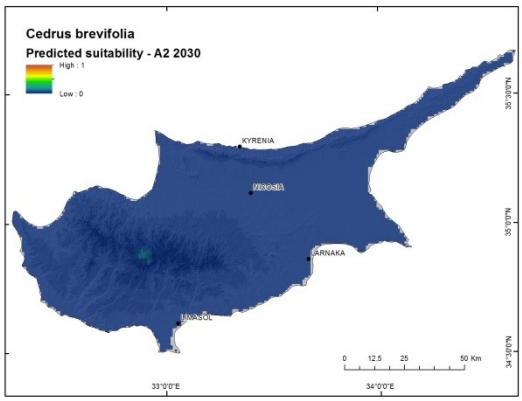

(b) (c)

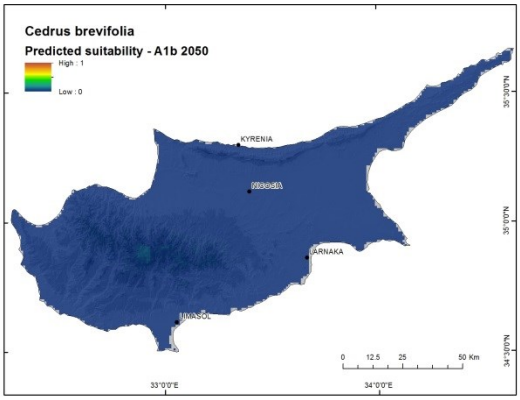

(d)

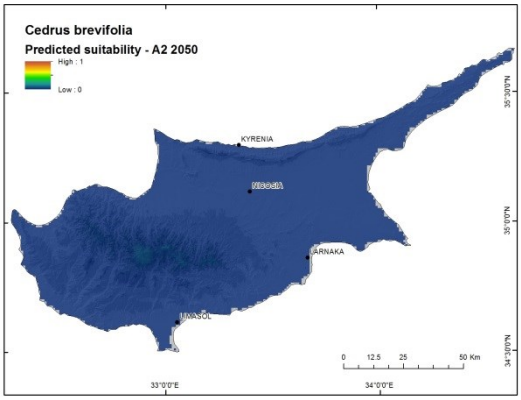

(e)

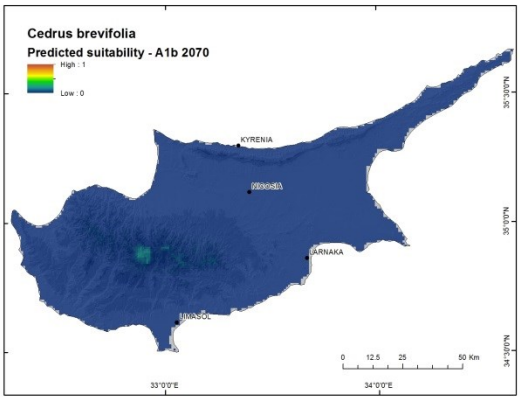

(f)

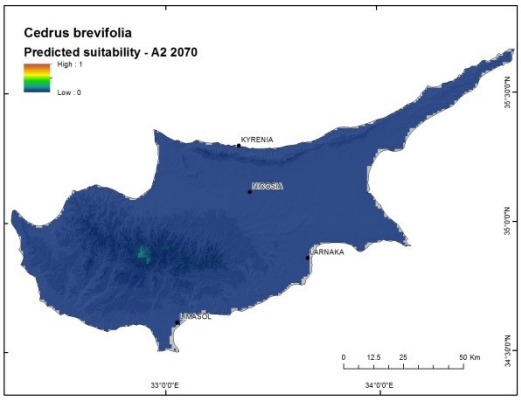

(g)

Figure 23. Continuous suitability maps for *Cedrus brevifolia* from present (Figure 23a) through 2070 A1b (Figure 23f) and A2 (Figure 23g) climate scenarios. Warmer colors indicate predicted suitability at a pixel to be near 1 (completely suitable for occurrence) and cooler colors indicate suitability predictions closer to 0 (completely unsuitable for occurrence).

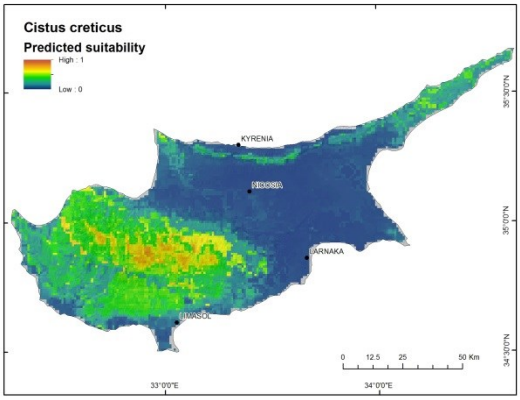
Cistus creticus
Predicted suitability
High : 1
Low : 0
KYRENIA
NIKOSIA
LARNAKA
LIMASOL
0 12.5 25 50 Km
33°0'0"E
34°0'0"E
35°30'0"N
35°0'0"N
34°30'0"N

(a)

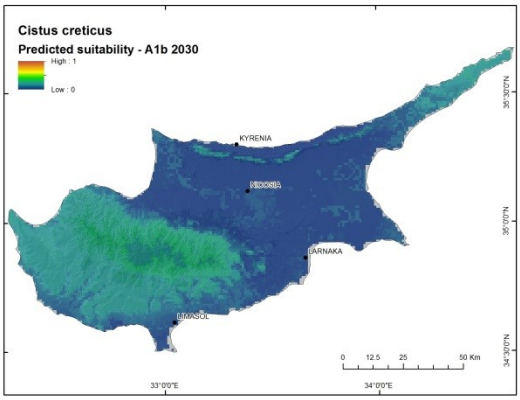
Cistus creticus
Predicted suitability - A1b 2030
High : 1
Low : 0
KYRENIA
NIKOSIA
LARNAKA
LIMASOL
0 12.5 25 50 Km
33°0'0"E
34°0'0"E
35°30'0"N
35°0'0"N
34°30'0"N

(b)

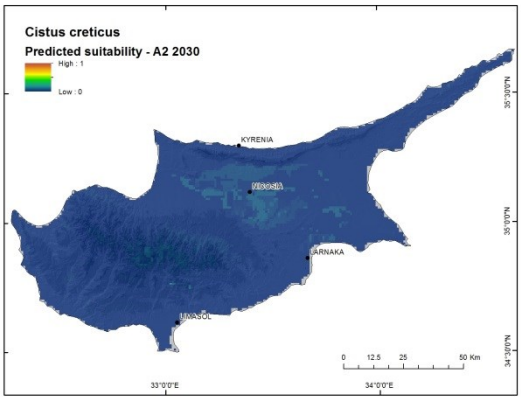
Cistus creticus
Predicted suitability - A2 2030
High : 1
Low : 0
KYRENIA
NIKOSIA
LARNAKA
LIMASOL
0 12.5 25 50 Km
33°0'0"E
34°0'0"E
35°30'0"N
35°0'0"N
34°30'0"N

(c)

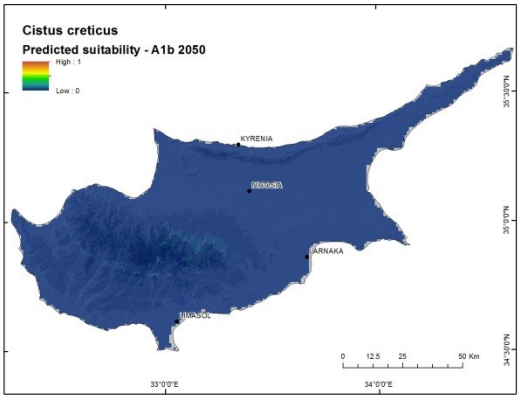
Cistus creticus
Predicted suitability - A1b 2050
High : 1
Low : 0
KYRENIA
NIKOSIA
LARNAKA
LIMASOL
0 12.5 25 50 Km
33°0'0"E
34°0'0"E
35°30'0"N
35°0'0"N
34°30'0"N

(d)

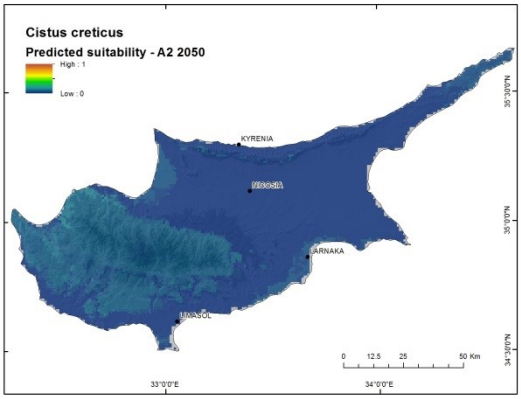
Cistus creticus
Predicted suitability - A2 2050
High : 1
Low : 0
KYRENIA
NIKOSIA
LARNAKA
LIMASOL
0 12.5 25 50 Km
33°0'0"E
34°0'0"E
35°30'0"N
35°0'0"N
34°30'0"N

(e)

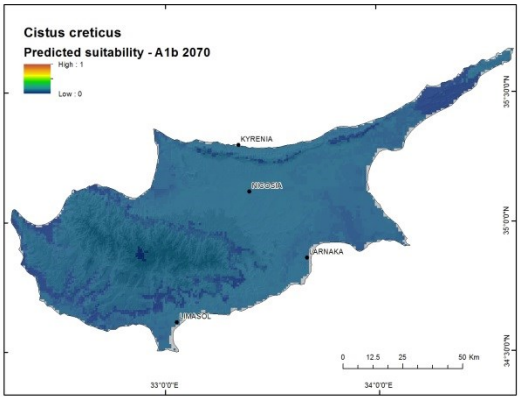

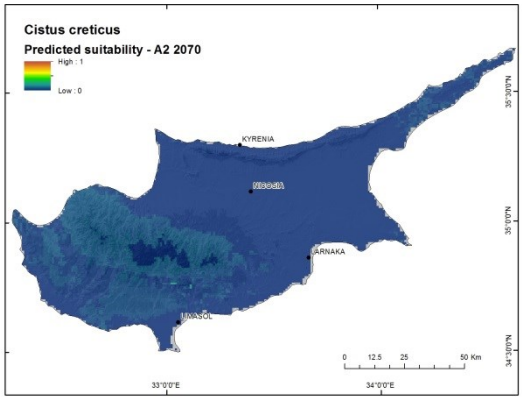

(f) (g)

Figure 24. Continuous suitability maps for *Cistus creticus* from present (Figure 24a) through 2070 A1b (Figure 24f) and A2 (Figure 24g) climate scenarios. Warmer colors indicate predicted suitability at a pixel to be near 1 (completely suitable for occurrence) and cooler colors indicate suitability predictions closer to 0 (completely unsuitable for occurrence).

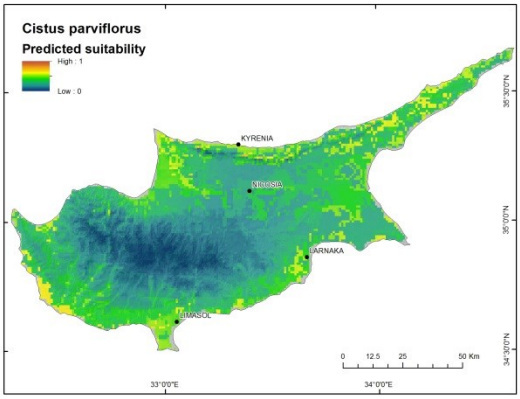

(a)

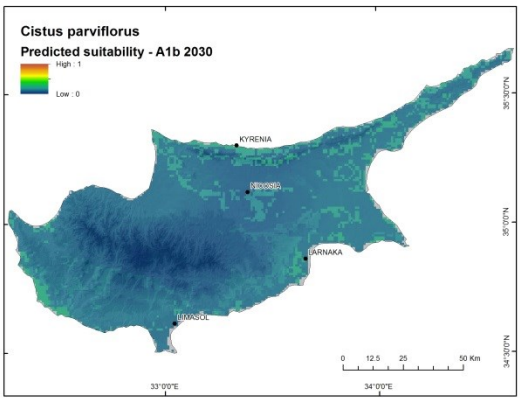

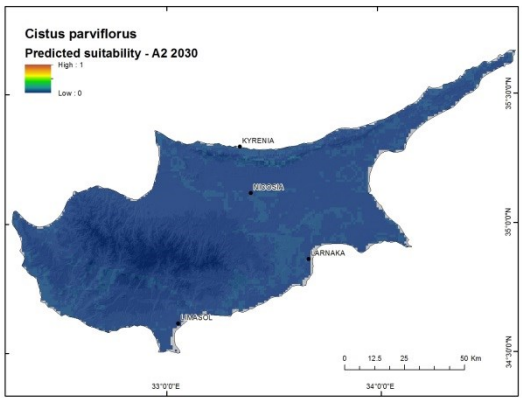

(b) (c)

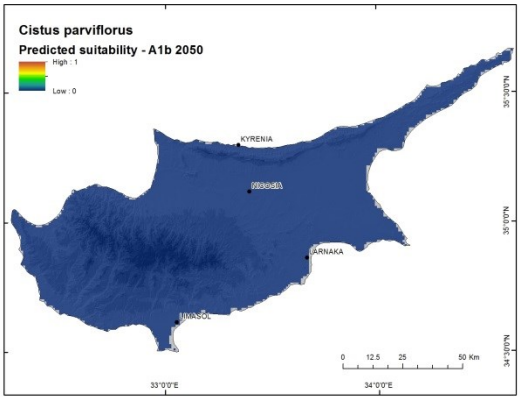

(d)

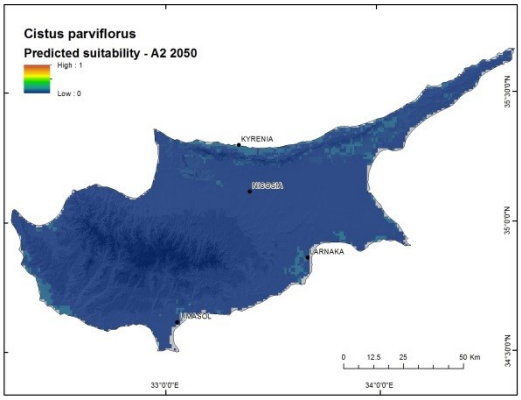

(e)

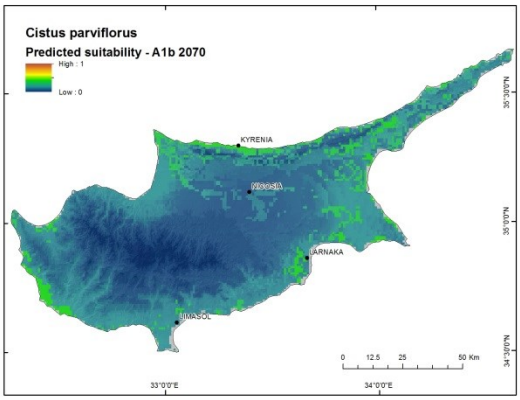

(f)

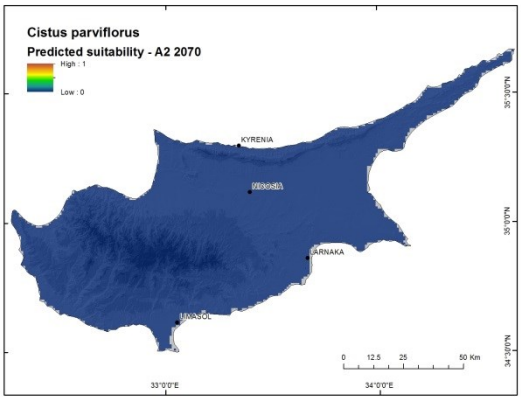

(g)

Figure 25. Continuous suitability maps for *Cistus parviflorus* from present (Figure 25a) through 2070 A1b (Figure 25f) and A2 (Figure 25g) climate scenarios. Warmer colors indicate predicted suitability at a pixel to be near 1 (completely suitable for occurrence) and cooler colors indicate suitability predictions closer to 0 (completely unsuitable for occurrence).

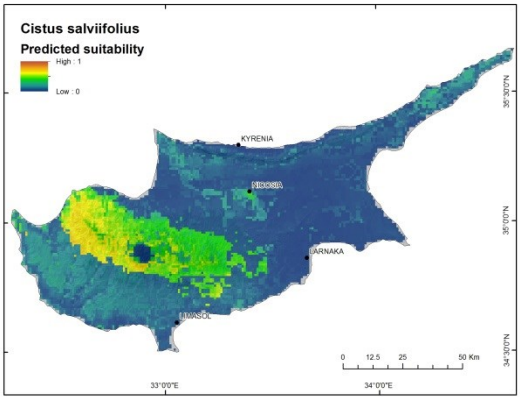
Cistus salviifolius
Predicted suitability
High : 1
Low : 0
KYRENIA
NICOSIA
ARNAKA
LIMASOL
0 12.5 25 50 Km
33°0'0"E
34°0'0"E
35°30'0"N
35°0'0"N
34°30'0"N

(a)

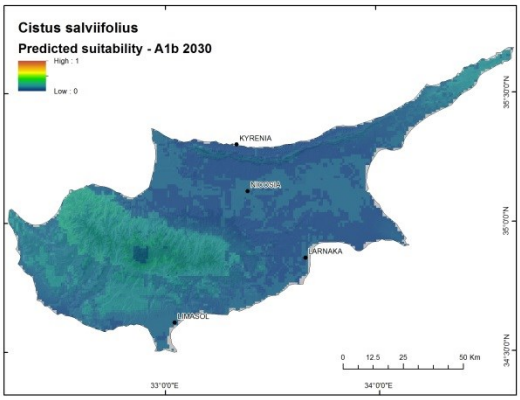
Cistus salviifolius
Predicted suitability - A1b 2030
High : 1
Low : 0
KYRENIA
NICOSIA
ARNAKA
LIMASOL
0 12.5 25 50 Km
33°0'0"E
34°0'0"E
35°30'0"N
35°0'0"N
34°30'0"N

(b)

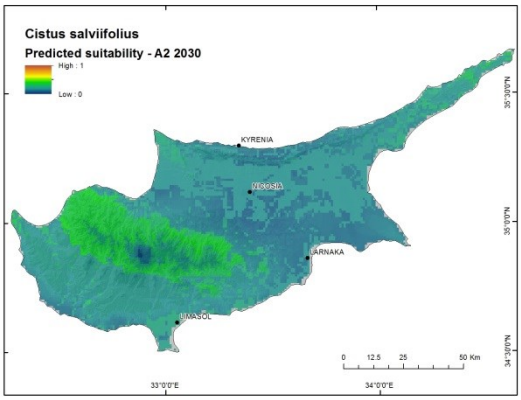
Cistus salviifolius
Predicted suitability - A2 2030
High : 1
Low : 0
KYRENIA
NICOSIA
ARNAKA
LIMASOL
0 12.5 25 50 Km
33°0'0"E
34°0'0"E
35°30'0"N
35°0'0"N
34°30'0"N

(c)

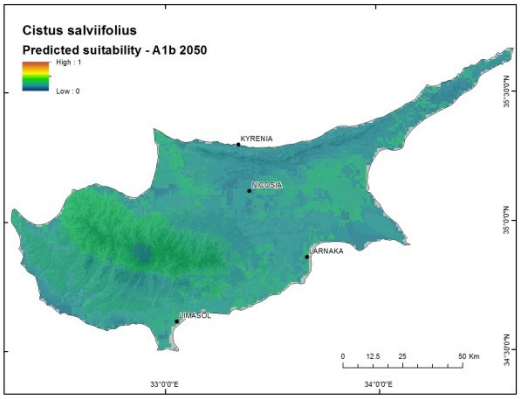
Cistus salviifolius
Predicted suitability - A1b 2050
High : 1
Low : 0
KYRENIA
NICOSIA
ARNAKA
LIMASOL
0 12.5 25 50 Km
33°0'0"E
34°0'0"E
35°30'0"N
35°0'0"N
34°30'0"N

(d)

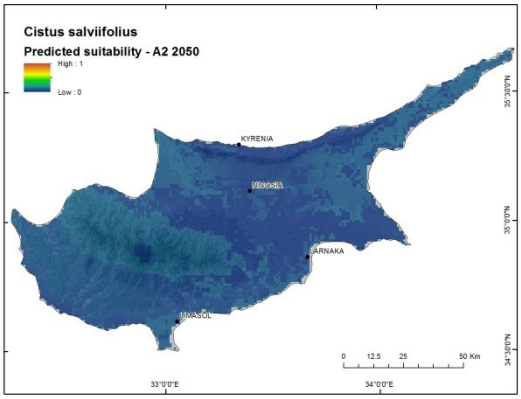
Cistus salviifolius
Predicted suitability - A2 2050
High : 1
Low : 0
KYRENIA
NICOSIA
ARNAKA
LIMASOL
0 12.5 25 50 Km
33°0'0"E
34°0'0"E
35°30'0"N
35°0'0"N
34°30'0"N

(e)

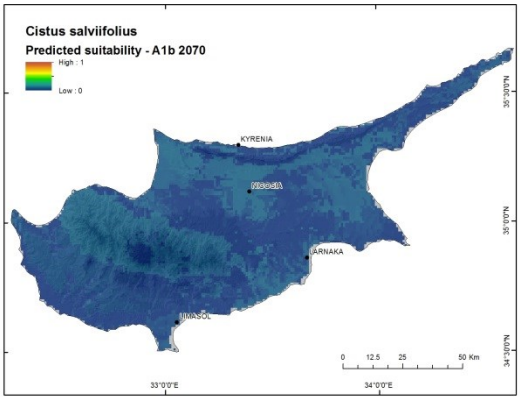

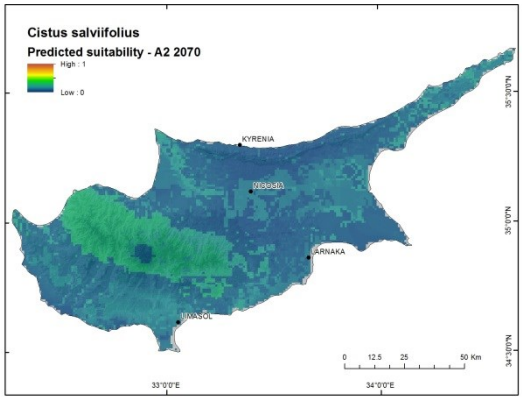

(f) (g)

Figure 26. Continuous suitability maps for *Cistus salviifolius* from present (Figure 26a) through 2070 A1b (Figure 26f) and A2 (Figure 26g) climate scenarios. Warmer colors indicate predicted suitability at a pixel to be near 1 (completely suitable for occurrence) and cooler colors indicate suitability predictions closer to 0 (completely unsuitable for occurrence).

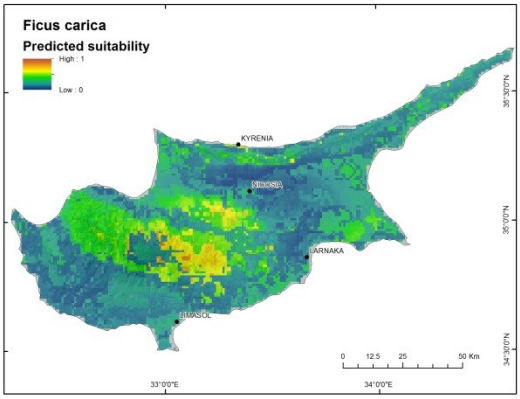

(a)

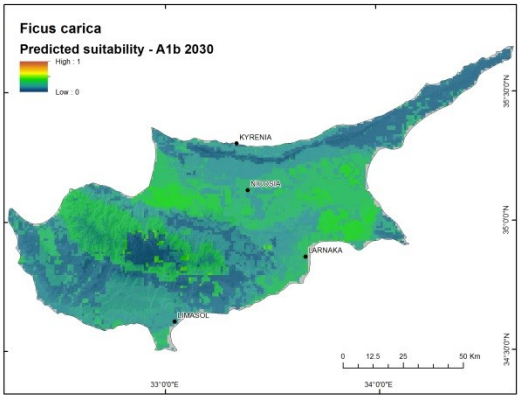

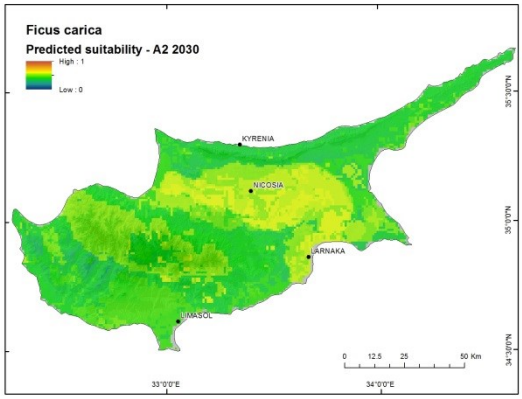

(b) (c)

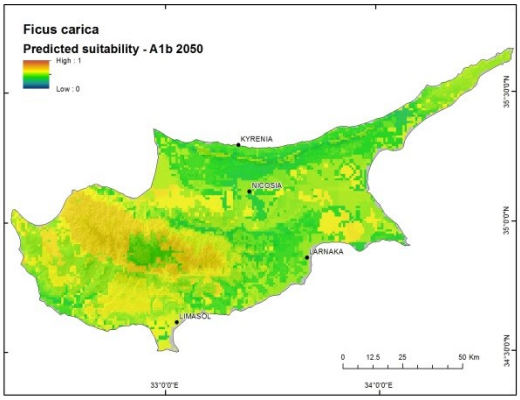

(d)

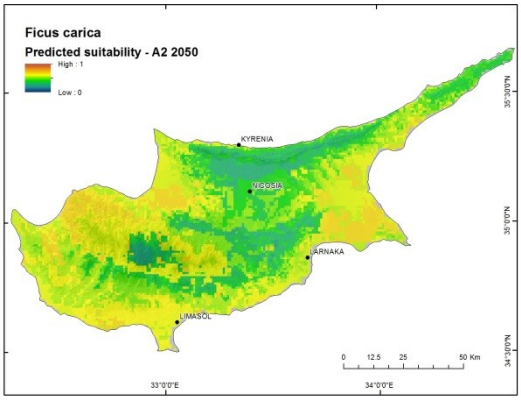

(e)

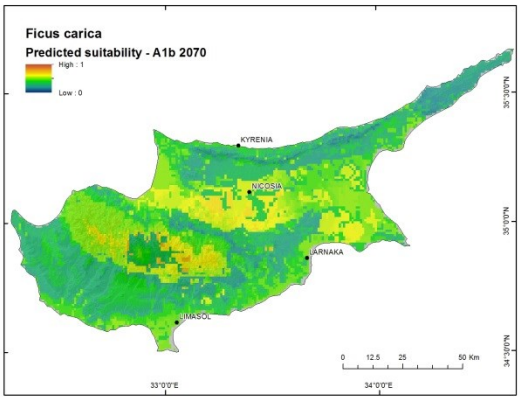

(f)

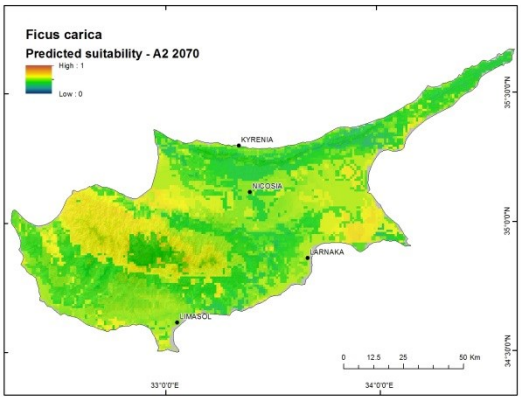

(g)

Figure 27. Continuous suitability maps for *Ficus carica* from present (Figure 27a) through 2070 A1b (Figure 27f) and A2 (Figure 27g) climate scenarios. Warmer colors indicate predicted suitability at a pixel to be near 1 (completely suitable for occurrence) and cooler colors indicate suitability predictions closer to 0 (completely unsuitable for occurrence).

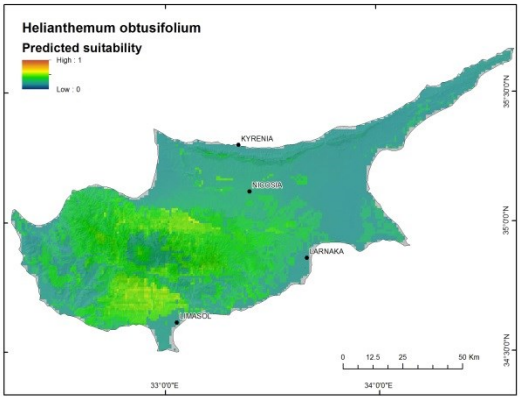
Helianthemum obtusifolium
Predicted suitability
High : 1
Low : 0
KYRENIA
NICOSIA
ARNAKA
LIMASOL
0 12.5 25 50 Km
33°0'0"E
34°0'0"E
35°30'0"N
35°0'0"N
34°30'0"N

(a)

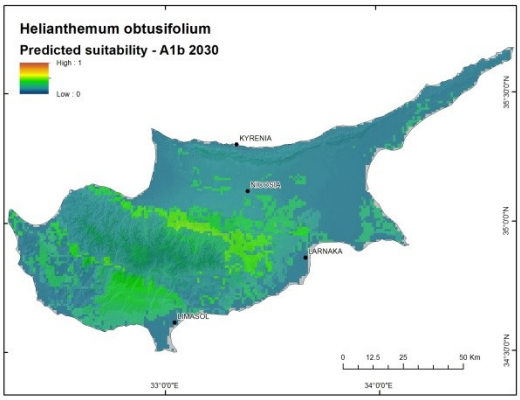
Helianthemum obtusifolium
Predicted suitability - A1b 2030
High : 1
Low : 0
KYRENIA
NICOSIA
ARNAKA
LIMASOL
0 12.5 25 50 Km
33°0'0"E
34°0'0"E
35°30'0"N
35°0'0"N
34°30'0"N

(b)

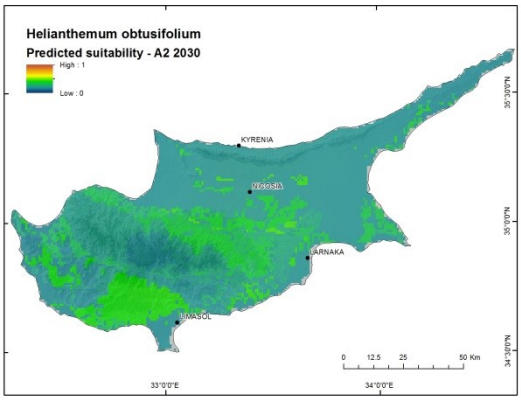
Helianthemum obtusifolium
Predicted suitability - A2 2030
High : 1
Low : 0
KYRENIA
NICOSIA
ARNAKA
LIMASOL
0 12.5 25 50 Km
33°0'0"E
34°0'0"E
35°30'0"N
35°0'0"N
34°30'0"N

(c)

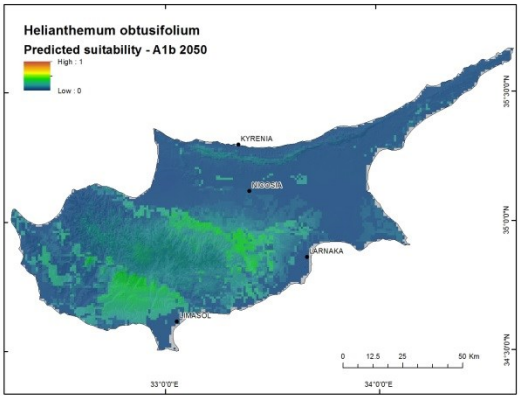
Helianthemum obtusifolium
Predicted suitability - A1b 2050
High : 1
Low : 0
KYRENIA
NICOSIA
ARNAKA
LIMASOL
0 12.5 25 50 Km
33°0'0"E
34°0'0"E
35°30'0"N
35°0'0"N
34°30'0"N

(d)

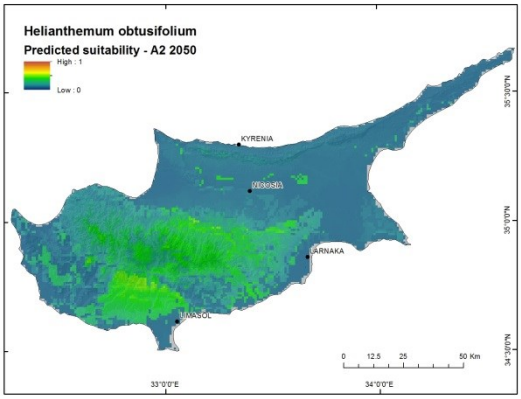
Helianthemum obtusifolium
Predicted suitability - A2 2050
High : 1
Low : 0
KYRENIA
NICOSIA
ARNAKA
LIMASOL
0 12.5 25 50 Km
33°0'0"E
34°0'0"E
35°30'0"N
35°0'0"N
34°30'0"N

(e)

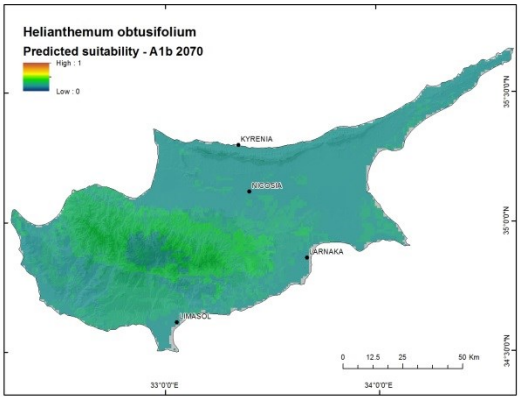

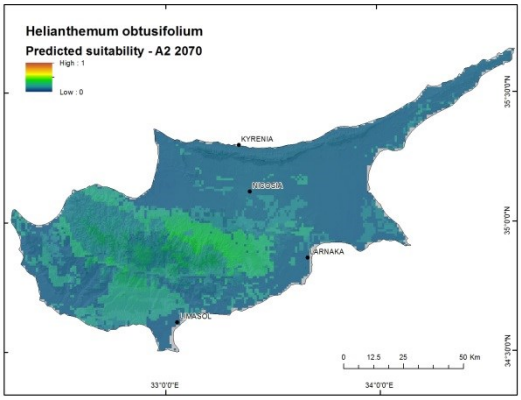

(f) (g)

Figure 28. Continuous suitability maps for *Helianthemum obtusifolium* from present (Figure 28a) through 2070 A1b (Figure 28f) and A2 (Figure 28g) climate scenarios. Warmer colors indicate predicted suitability at a pixel to be near 1 (completely suitable for occurrence) and cooler colors indicate suitability predictions closer to 0 (completely unsuitable for occurrence).

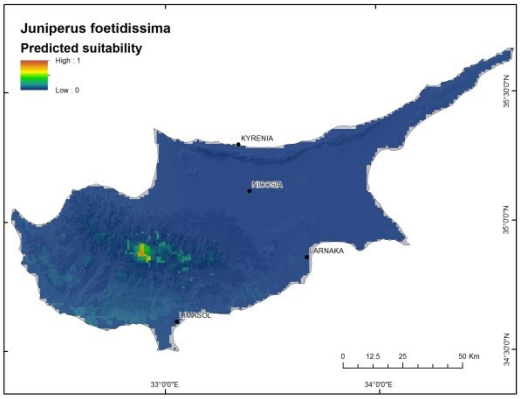

(a)

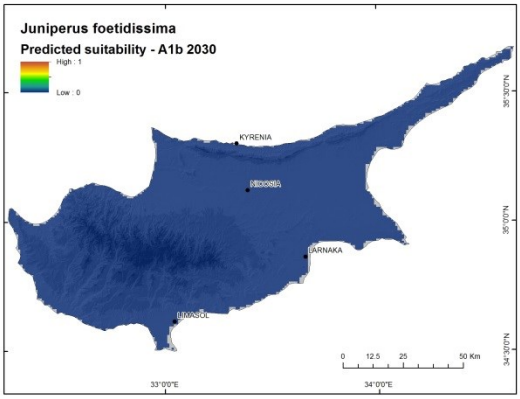

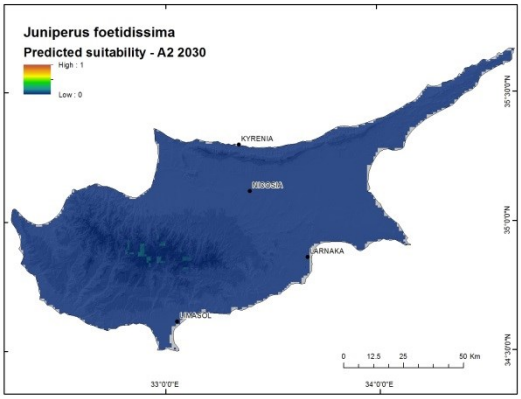

(b) (c)

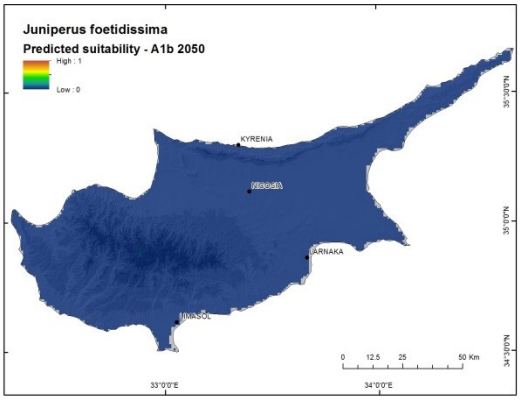

(d)

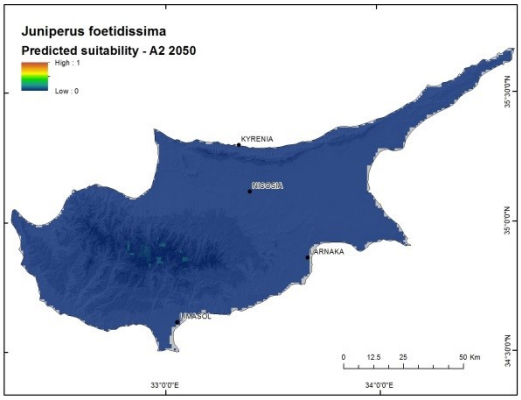

(e)

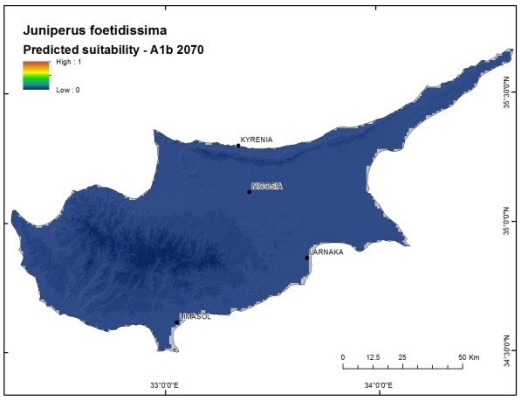

(f)

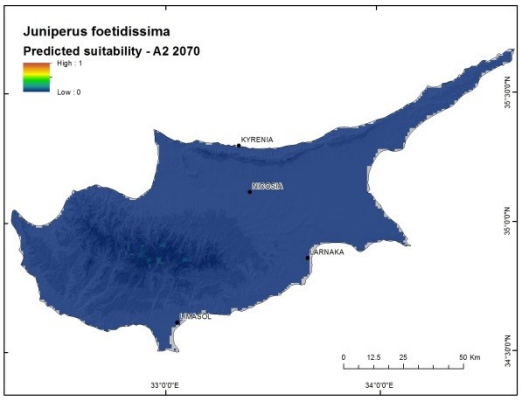

(g)

Figure 29. Continuous suitability maps for *Juniperus foetidissima* from present (Figure 29a) through 2070 A1b (Figure 29f) and A2 (Figure 29g) climate scenarios. Warmer colors indicate predicted suitability at a pixel to be near 1 (completely suitable for occurrence) and cooler colors indicate suitability predictions closer to 0 (completely unsuitable for occurrence).

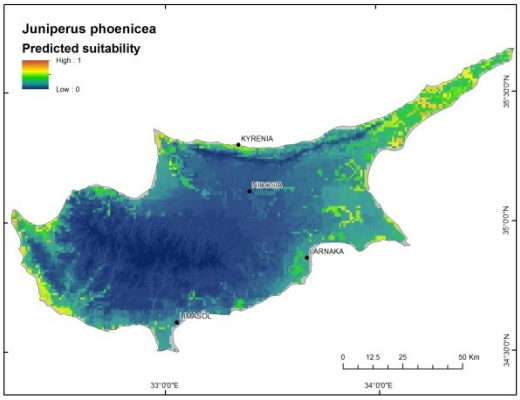
Juniperus phoenicea
Predicted suitability
High : 1
Low : 0
KYRENIA
LIMASOL
0 12.5 25 50 Km
33°0'0"E
34°0'0"E

(a)

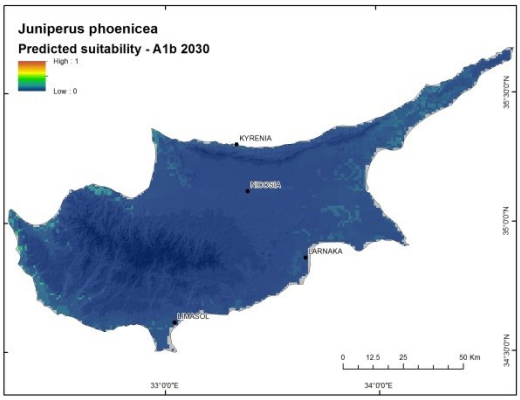
Juniperus phoenicea
Predicted suitability - A1b 2030
High : 1
Low : 0
KYRENIA
LIMASOL
0 12.5 25 50 Km
33°0'0"E
34°0'0"E

(b)

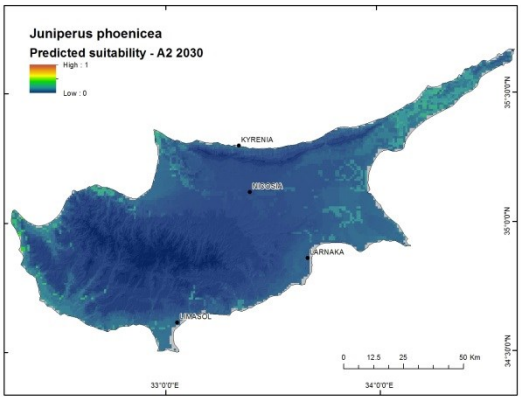
Juniperus phoenicea
Predicted suitability - A2 2030
High : 1
Low : 0
KYRENIA
LIMASOL
0 12.5 25 50 Km
33°0'0"E
34°0'0"E

(c)

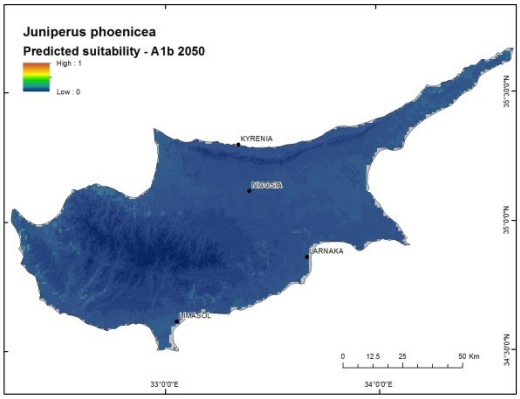
Juniperus phoenicea
Predicted suitability - A1b 2050
High : 1
Low : 0
KYRENIA
LIMASOL
0 12.5 25 50 Km
33°0'0"E
34°0'0"E

(d)

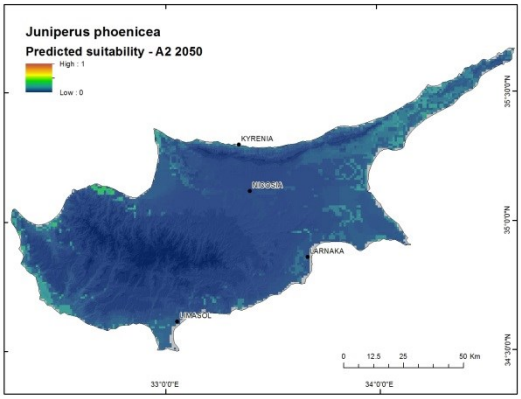
Juniperus phoenicea
Predicted suitability - A2 2050
High : 1
Low : 0
KYRENIA
LIMASOL
0 12.5 25 50 Km
33°0'0"E
34°0'0"E

(e)

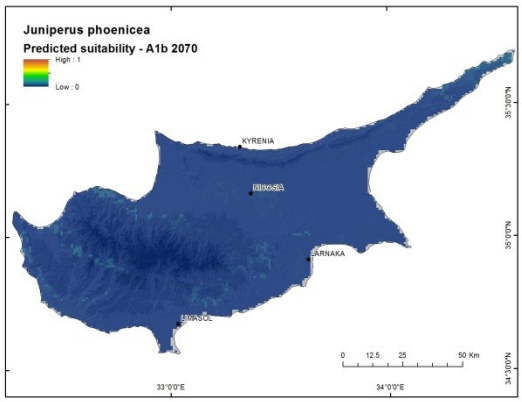

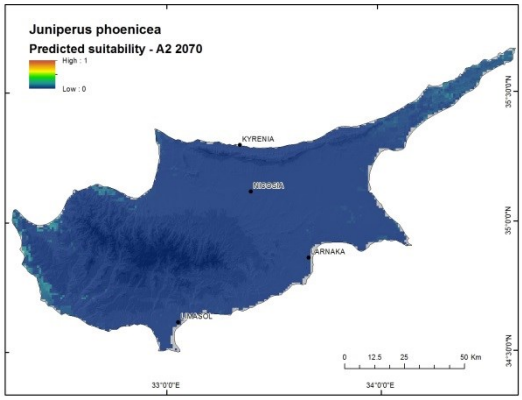

(f) (g)

Figure 30. Continuous suitability maps for *Juniperus phoenicea* from present (Figure 30a) through 2070 A1b (Figure 30f) and A2 (Figure 30g) climate scenarios. Warmer colors indicate predicted suitability at a pixel to be near 1 (completely suitable for occurrence) and cooler colors indicate suitability predictions closer to 0 (completely unsuitable for occurrence).

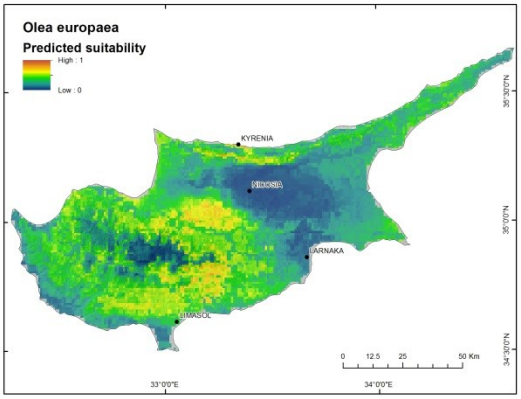

(a)

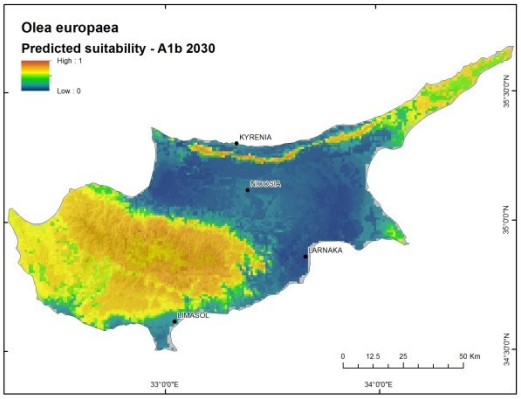

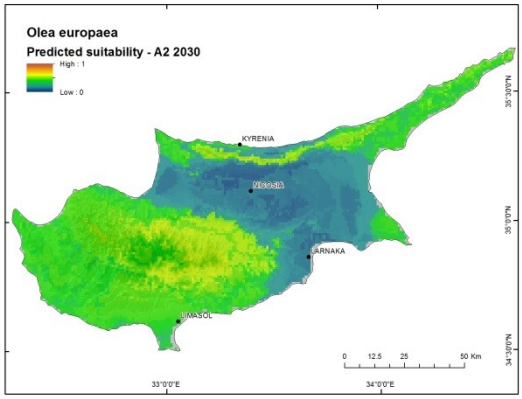

(b) (c)

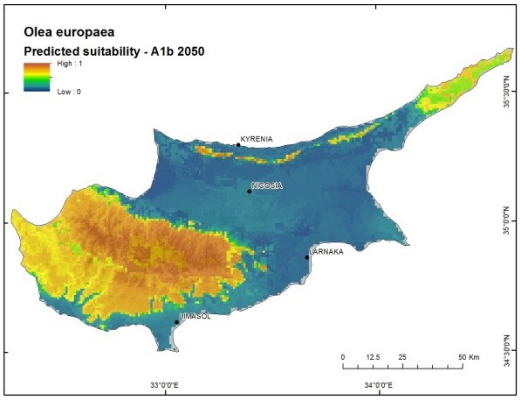

(d)

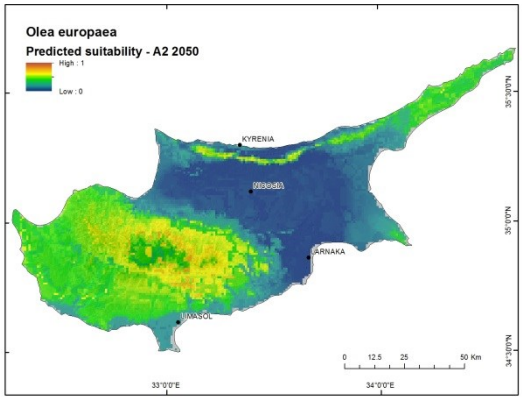

(e)

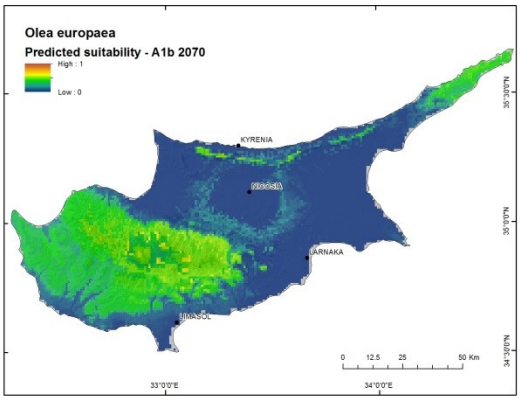

(f)

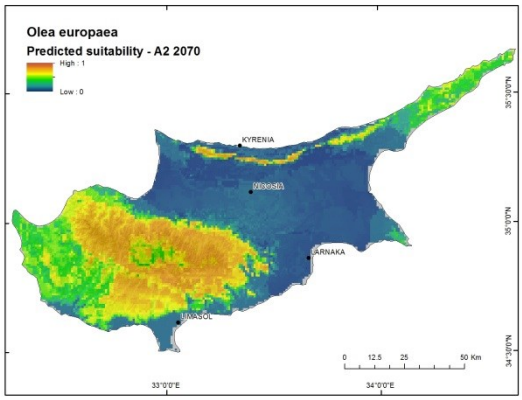

(g)

Figure 31. Continuous suitability maps for *Olea europaea* from present (Figure 31a) through 2070 A1b (Figure 31f) and A2 (Figure 31g) climate scenarios. Warmer colors indicate predicted suitability at a pixel to be near 1 (completely suitable for occurrence) and cooler colors indicate suitability predictions closer to 0 (completely unsuitable for occurrence).

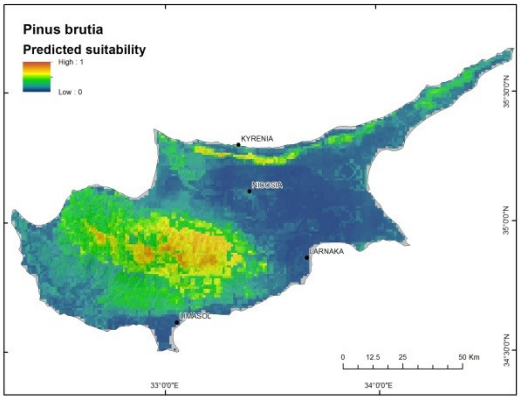
Pinus brutia
Predicted suitability
High : 1
Low : 0
KYRENIA
LIMASOL
0 12.5 25 50 Km
33°0'0"E
34°0'0"E

(a)

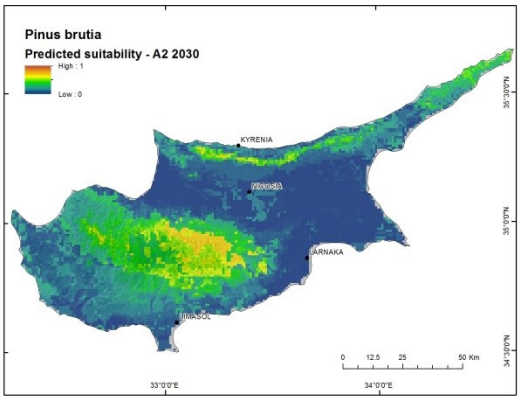
Pinus brutia
Predicted suitability - A2 2030
High : 1
Low : 0
KYRENIA
LIMASOL
0 12.5 25 50 Km
33°0'0"E
34°0'0"E

(b)

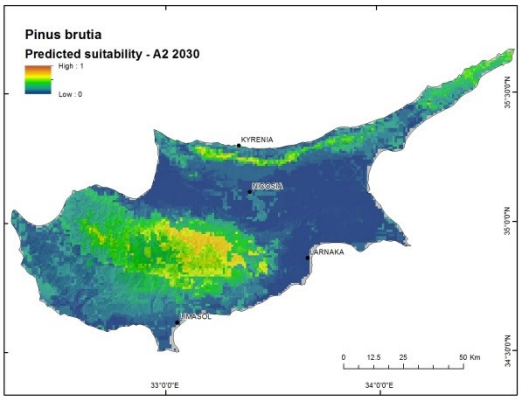
Pinus brutia
Predicted suitability - A2 2030
High : 1
Low : 0
KYRENIA
LIMASOL
0 12.5 25 50 Km
33°0'0"E
34°0'0"E

(c)

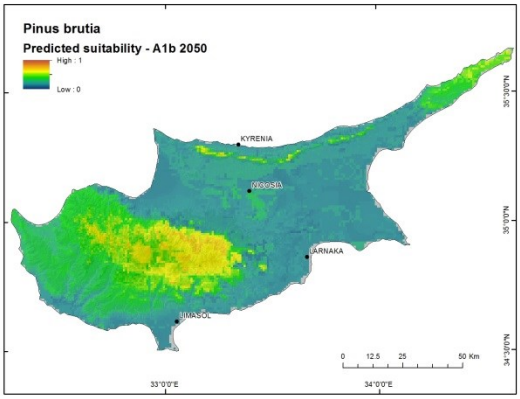
Pinus brutia
Predicted suitability - A1b 2050
High : 1
Low : 0
KYRENIA
LIMASOL
0 12.5 25 50 Km
33°0'0"E
34°0'0"E

(d)

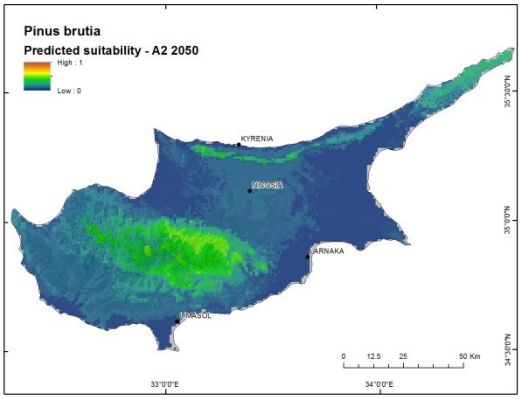
Pinus brutia
Predicted suitability - A2 2050
High : 1
Low : 0
KYRENIA
LIMASOL
0 12.5 25 50 Km
33°0'0"E
34°0'0"E

(e)

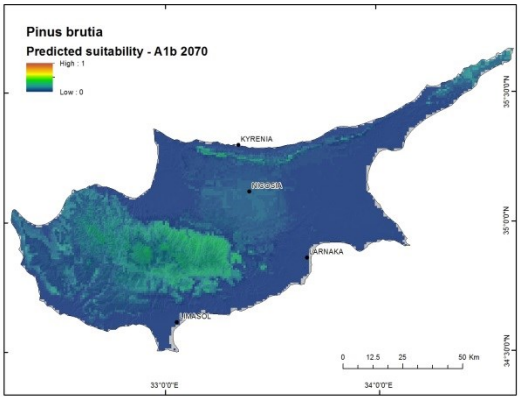

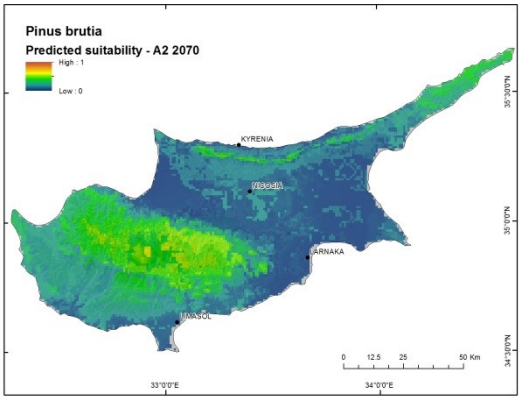

(f) (g)

Figure 32. Continuous suitability maps for *Pinus brutia* from present (Figure 32a) through 2070 A1b (Figure 32f) and A2 (Figure 32g) climate scenarios. Warmer colors indicate predicted suitability at a pixel to be near 1 (completely suitable for occurrence) and cooler colors indicate suitability predictions closer to 0 (completely unsuitable for occurrence).

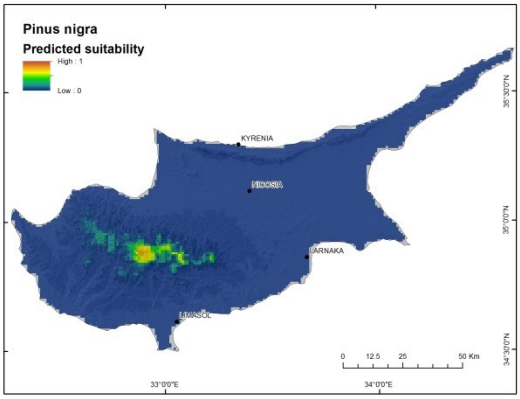

(a)

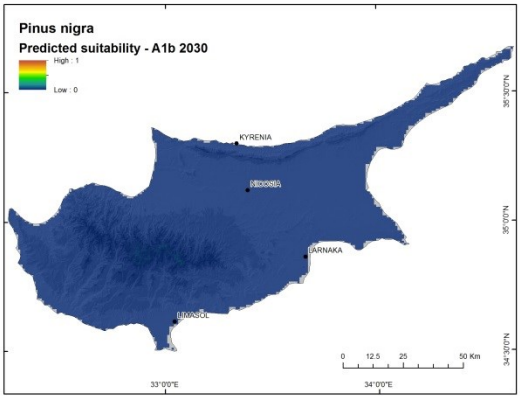

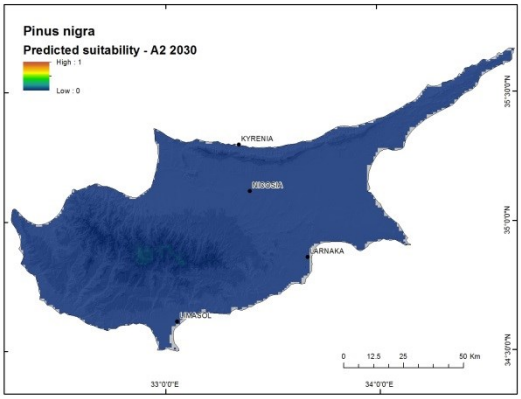

(b) (c)

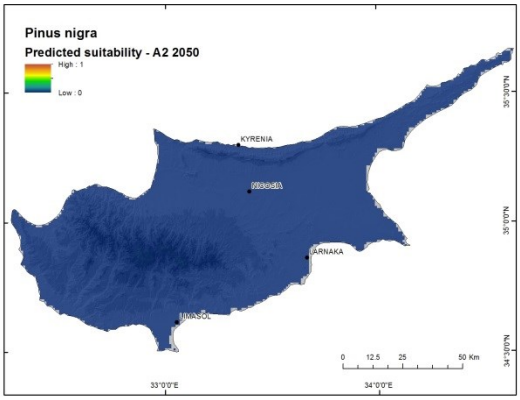

(d)

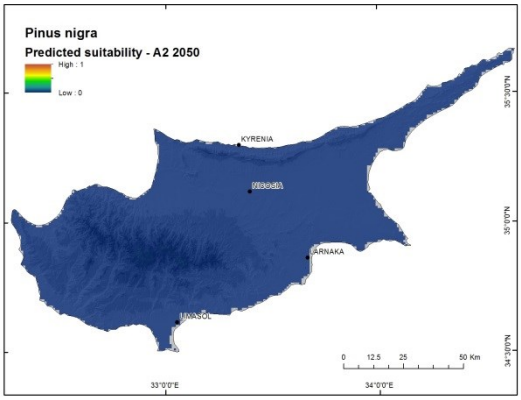

(e)

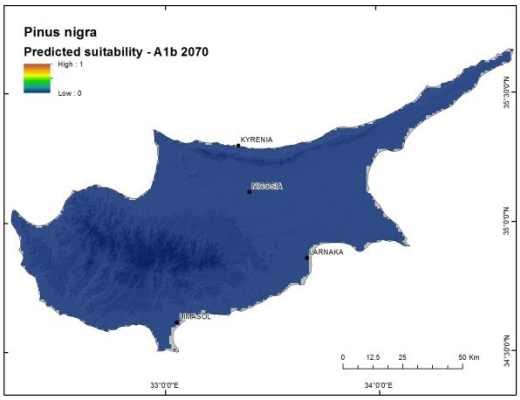

(f)

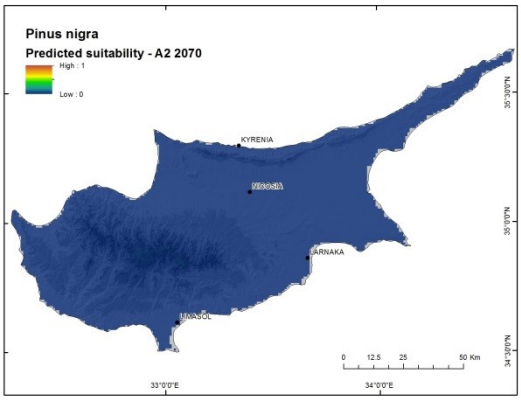

(g)

Figure 33. Continuous suitability maps for *Pinus nigra* from present (Figure 33a) through 2070 A1b (Figure 33f) and A2 (Figure 33g) climate scenarios. Warmer colors indicate predicted suitability at a pixel to be near 1 (completely suitable for occurrence) and cooler colors indicate suitability predictions closer to 0 (completely unsuitable for occurrence).

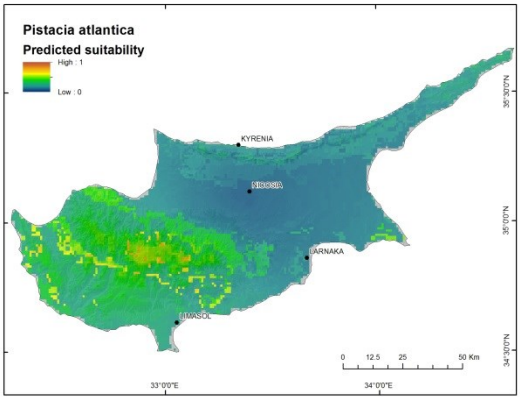
Pistacia atlantica
Predicted suitability
High : 1
Low : 0
KYRENIA
NICOSIA
LARNAKA
LIMASOL
0 12.5 25 50 Km
33°0'0"E
34°0'0"E
35°30'0"N
35°0'0"N
34°30'0"N

(a)

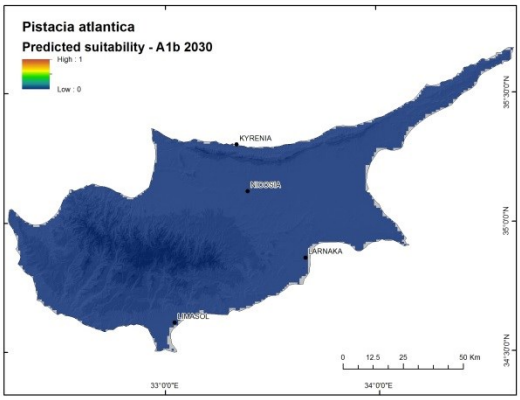
Pistacia atlantica
Predicted suitability - A1b 2030
High : 1
Low : 0
KYRENIA
NICOSIA
LARNAKA
LIMASOL
0 12.5 25 50 Km
33°0'0"E
34°0'0"E
35°30'0"N
35°0'0"N
34°30'0"N

(b)

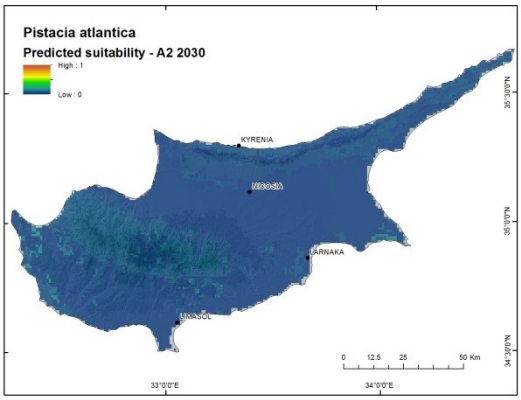
Pistacia atlantica
Predicted suitability - A2 2030
High : 1
Low : 0
KYRENIA
NICOSIA
LARNAKA
LIMASOL
0 12.5 25 50 Km
33°0'0"E
34°0'0"E
35°30'0"N
35°0'0"N
34°30'0"N

(c)

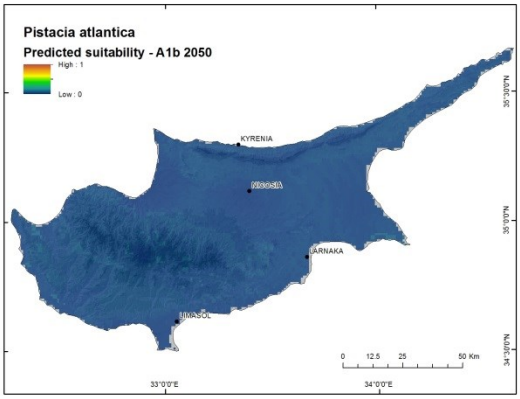
Pistacia atlantica
Predicted suitability - A1b 2050
High : 1
Low : 0
KYRENIA
NICOSIA
LARNAKA
LIMASOL
0 12.5 25 50 Km
33°0'0"E
34°0'0"E
35°30'0"N
35°0'0"N
34°30'0"N

(d)

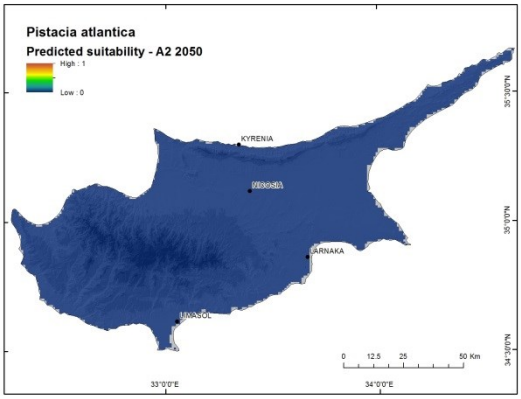
Pistacia atlantica
Predicted suitability - A2 2050
High : 1
Low : 0
KYRENIA
NICOSIA
LARNAKA
LIMASOL
0 12.5 25 50 Km
33°0'0"E
34°0'0"E
35°30'0"N
35°0'0"N
34°30'0"N

(e)

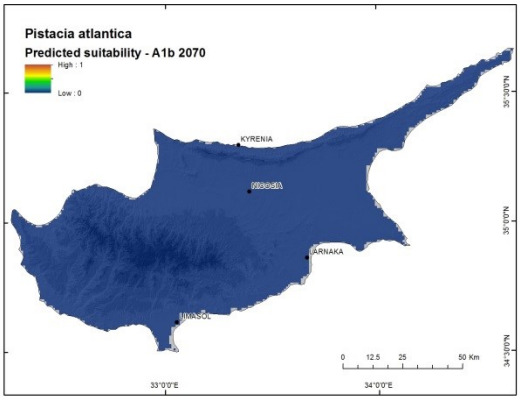

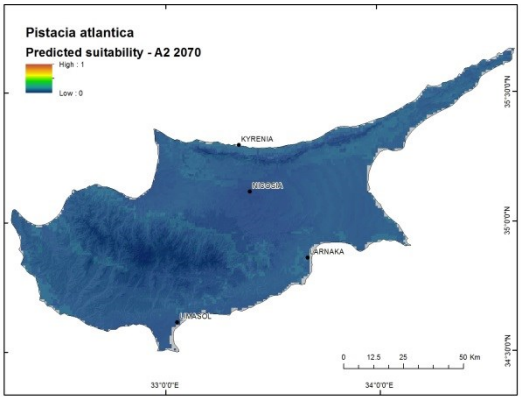

(f) (g)

Figure 34. Continuous suitability maps for *Pistacia atlantica* from present (Figure 34a) through 2070 A1b (Figure 34f) and A2 (Figure 34g) climate scenarios. Warmer colors indicate predicted suitability at a pixel to be near 1 (completely suitable for occurrence) and cooler colors indicate suitability predictions closer to 0 (completely unsuitable for occurrence).

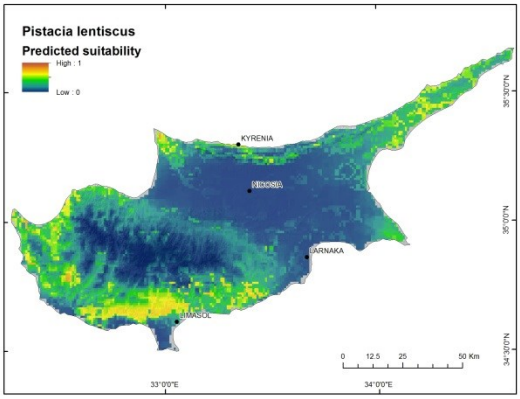

(a)

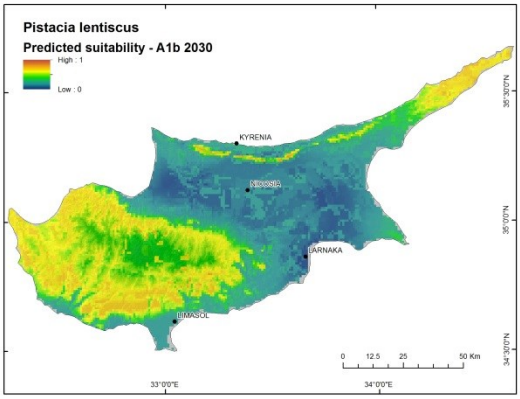

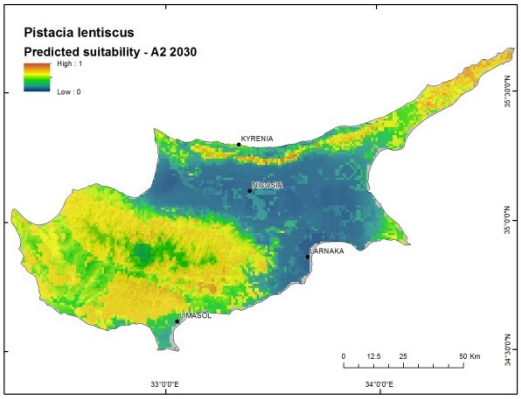

(b) (c)

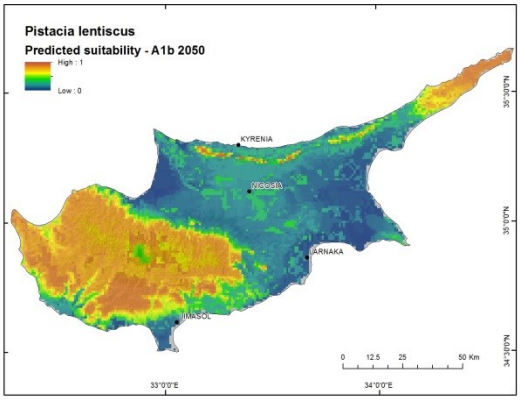

(d)

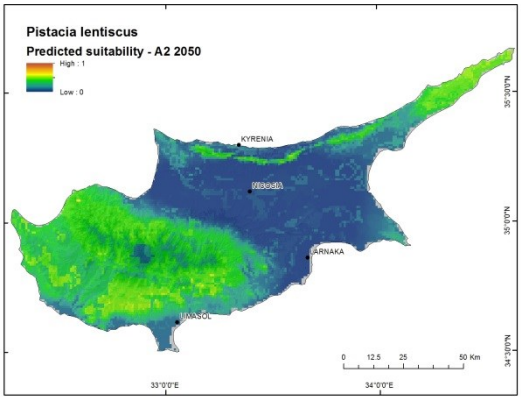

(e)

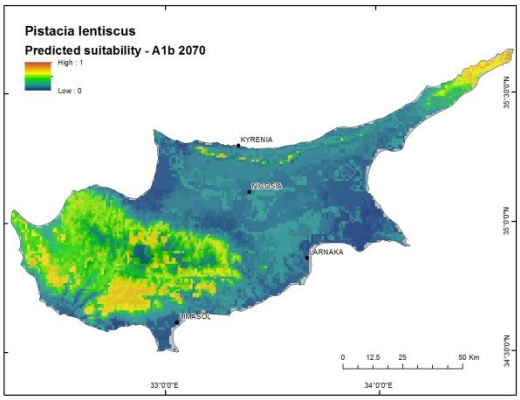

(f)

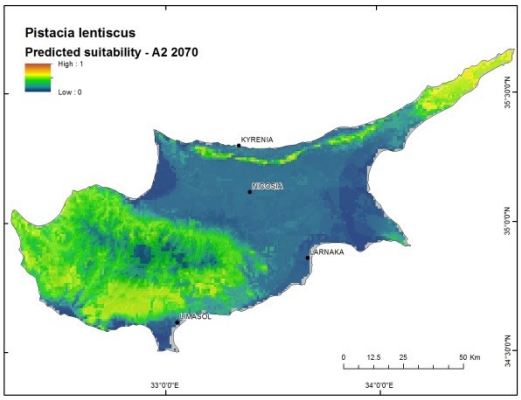

(g)

Figure 35. Continuous suitability maps for *Pistacia lentiscus* from present (Figure 35a) through 2070 A1b (Figure 35f) and A2 (Figure 35g) climate scenarios. Warmer colors indicate predicted suitability at a pixel to be near 1 (completely suitable for occurrence) and cooler colors indicate suitability predictions closer to 0 (completely unsuitable for occurrence).

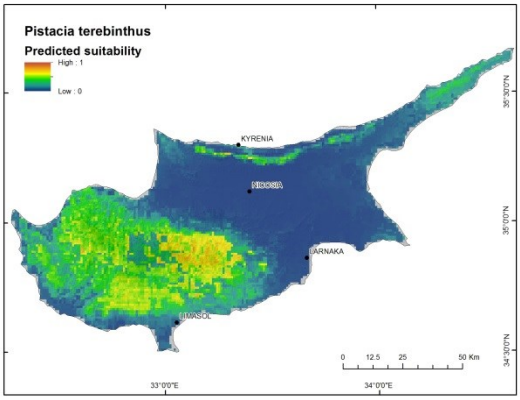
Pistacia terebinthus
Predicted suitability
High : 1
Low : 0
KYRENIA
NICOSIA
LARNAKA
LIMASOL
0 12.5 25 50 Km
33°0'0"E
34°0'0"E
35°30'0"N
35°0'0"N
34°30'0"N

(a)

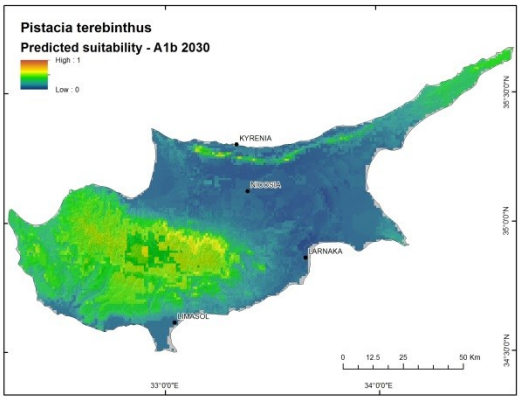
Pistacia terebinthus
Predicted suitability - A1b 2030
High : 1
Low : 0
KYRENIA
NICOSIA
LARNAKA
LIMASOL
0 12.5 25 50 Km
33°0'0"E
34°0'0"E
35°30'0"N
35°0'0"N
34°30'0"N

(b)

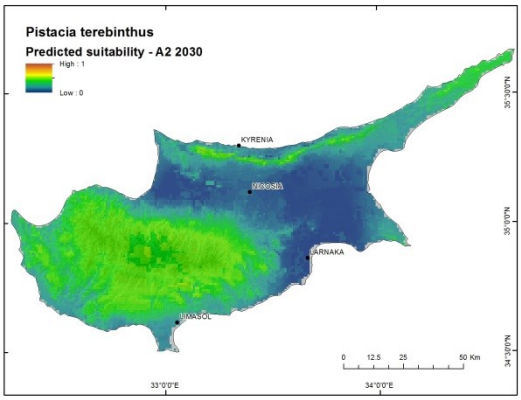
Pistacia terebinthus
Predicted suitability - A2 2030
High : 1
Low : 0
KYRENIA
NICOSIA
LARNAKA
LIMASOL
0 12.5 25 50 Km
33°0'0"E
34°0'0"E
35°30'0"N
35°0'0"N
34°30'0"N

(c)

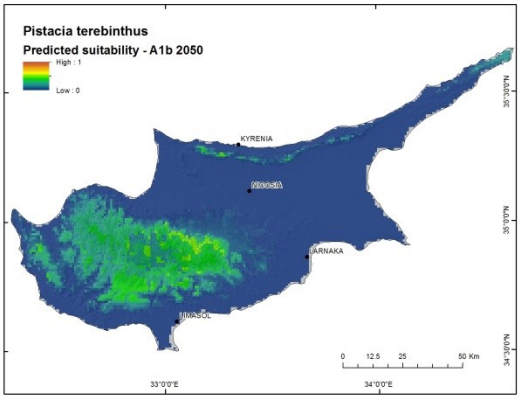
Pistacia terebinthus
Predicted suitability - A1b 2050
High : 1
Low : 0
KYRENIA
NICOSIA
LARNAKA
LIMASOL
0 12.5 25 50 Km
33°0'0"E
34°0'0"E
35°30'0"N
35°0'0"N
34°30'0"N

(d)

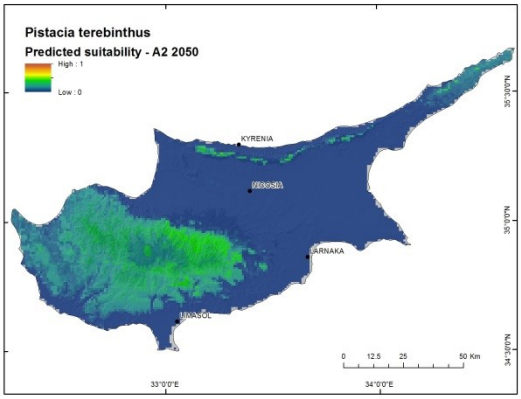
Pistacia terebinthus
Predicted suitability - A2 2050
High : 1
Low : 0
KYRENIA
NICOSIA
LARNAKA
LIMASOL
0 12.5 25 50 Km
33°0'0"E
34°0'0"E
35°30'0"N
35°0'0"N
34°30'0"N

(e)

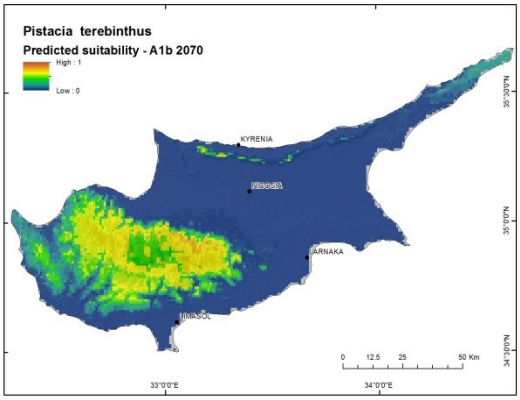

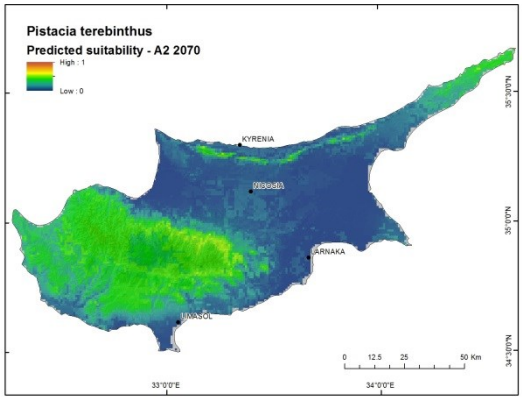

(f) (g)

Figure 36. Continuous suitability maps for *Pistacia terebinthus* from present (Figure 36a) through 2070 A1b (Figure 36f) and A2 (Figure 36g) climate scenarios. Warmer colors indicate predicted suitability at a pixel to be near 1 (completely suitable for occurrence) and cooler colors indicate suitability predictions closer to 0 (completely unsuitable for occurrence).

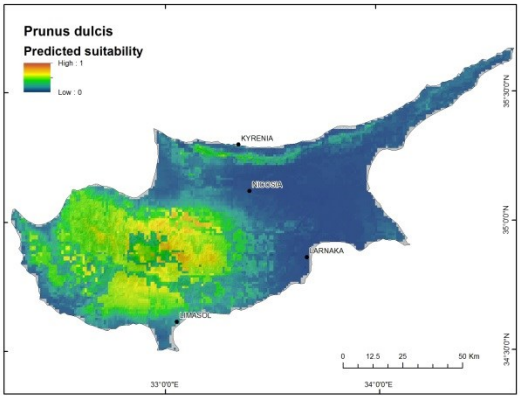

(a)

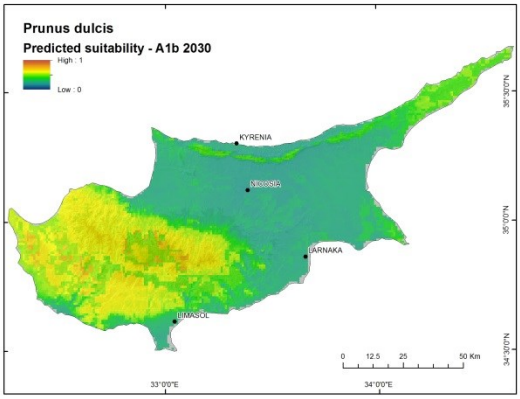

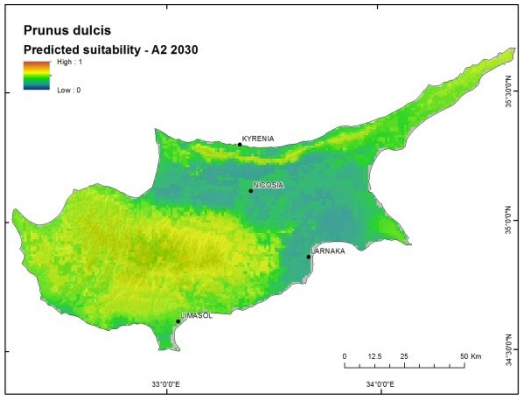

(b) (c)

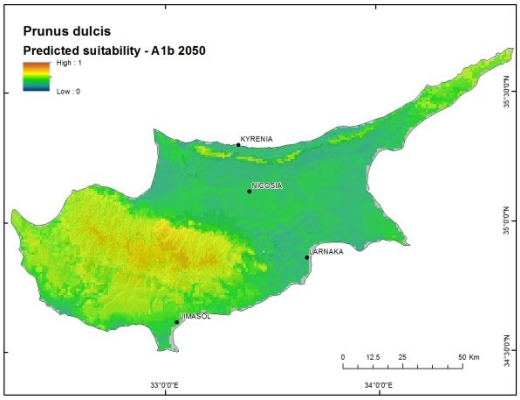

(d)

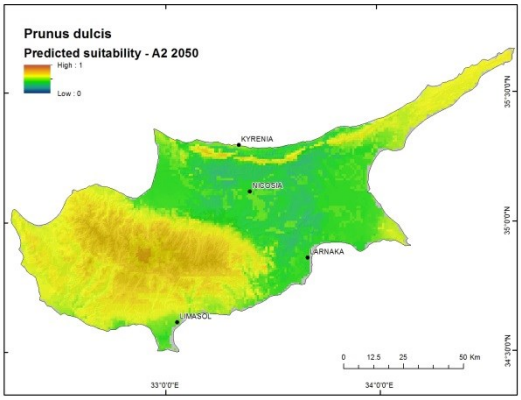

(e)

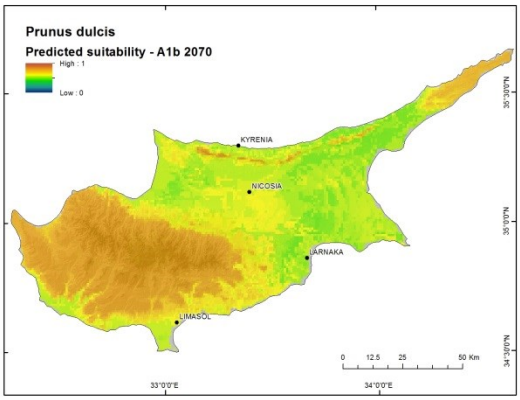

(f)

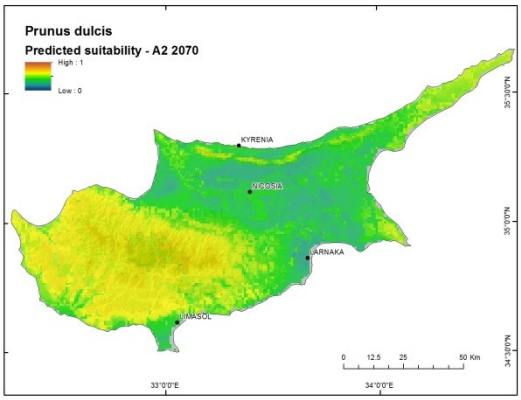

(g)

Figure 37. Continuous suitability maps for *Prunus dulcis* from present (Figure 37a) through 2070 A1b (Figure 37f) and A2 (Figure 37g) climate scenarios. Warmer colors indicate predicted suitability at a pixel to be near 1 (completely suitable for occurrence) and cooler colors indicate suitability predictions closer to 0 (completely unsuitable for occurrence).

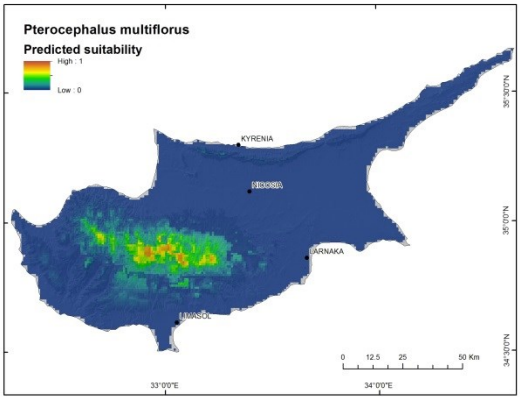
Pterocephalus multiflorus
Predicted suitability
High : 1
Low : 0
KYRENIA
NICOSIA
LARNAKA
LIMASOL
0 12.5 25 50 Km
33°0'0"E
34°0'0"E
35°30'0"N
35°0'0"N
34°30'0"N

(a)

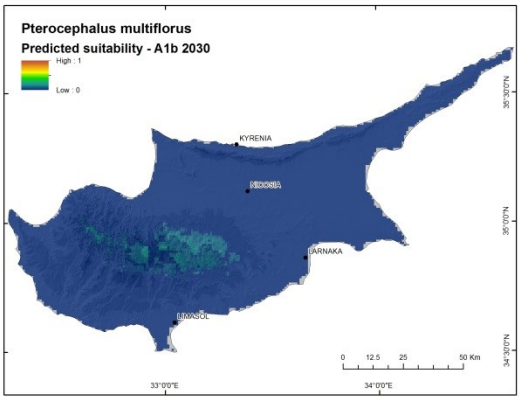
Pterocephalus multiflorus
Predicted suitability - A1b 2030
High : 1
Low : 0
KYRENIA
NICOSIA
LARNAKA
LIMASOL
0 12.5 25 50 Km
33°0'0"E
34°0'0"E
35°30'0"N
35°0'0"N
34°30'0"N

(b)

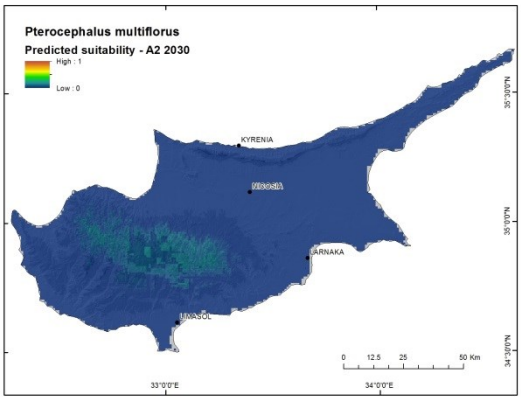
Pterocephalus multiflorus
Predicted suitability - A2 2030
High : 1
Low : 0
KYRENIA
NICOSIA
LARNAKA
LIMASOL
0 12.5 25 50 Km
33°0'0"E
34°0'0"E
35°30'0"N
35°0'0"N
34°30'0"N

(c)

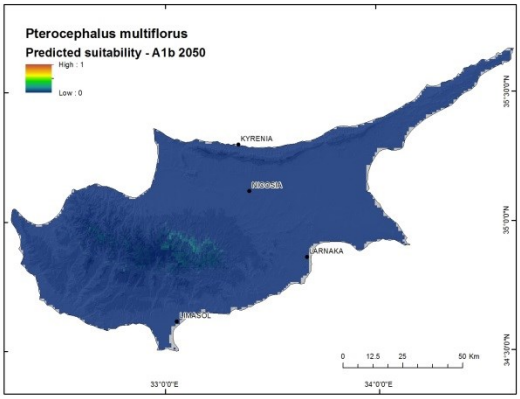
Pterocephalus multiflorus
Predicted suitability - A1b 2050
High : 1
Low : 0
KYRENIA
NICOSIA
LARNAKA
LIMASOL
0 12.5 25 50 Km
33°0'0"E
34°0'0"E
35°30'0"N
35°0'0"N
34°30'0"N

(d)

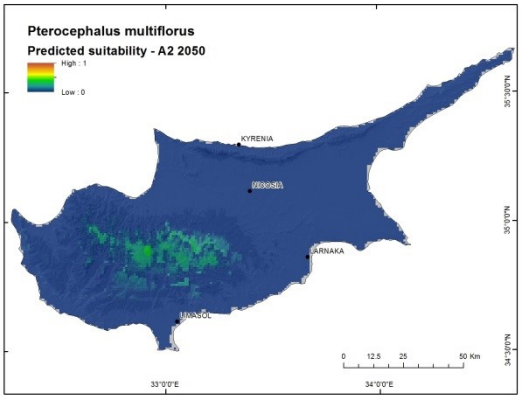
Pterocephalus multiflorus
Predicted suitability - A2 2050
High : 1
Low : 0
KYRENIA
NICOSIA
LARNAKA
LIMASOL
0 12.5 25 50 Km
33°0'0"E
34°0'0"E
35°30'0"N
35°0'0"N
34°30'0"N

(e)

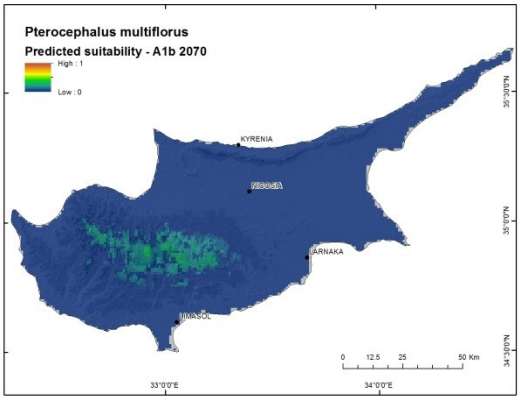

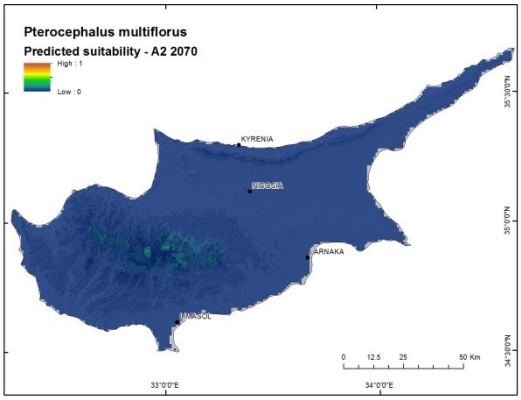

(f) (g)

Figure 38. Continuous suitability maps for *Pterocephalus multiflorus* from present (Figure 38a) through 2070 A1b (Figure 38f) and A2 (Figure 38g) climate scenarios. Warmer colors indicate predicted suitability at a pixel to be near 1 (completely suitable for occurrence) and cooler colors indicate suitability predictions closer to 0 (completely unsuitable for occurrence).

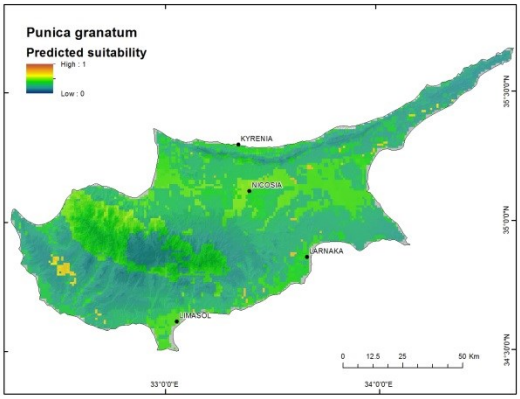

(a)

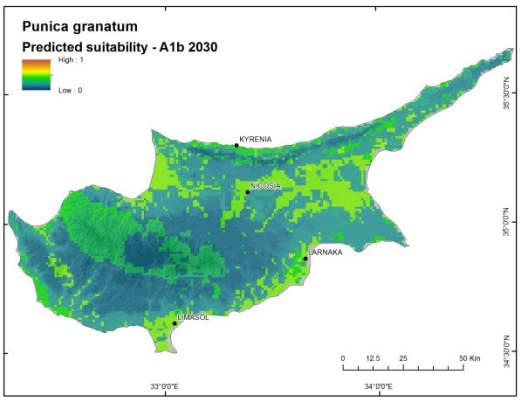

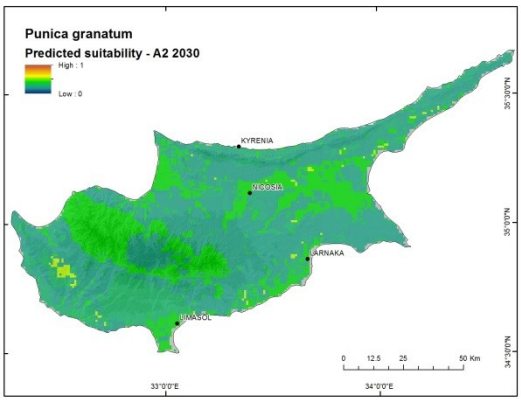

(b) (c)

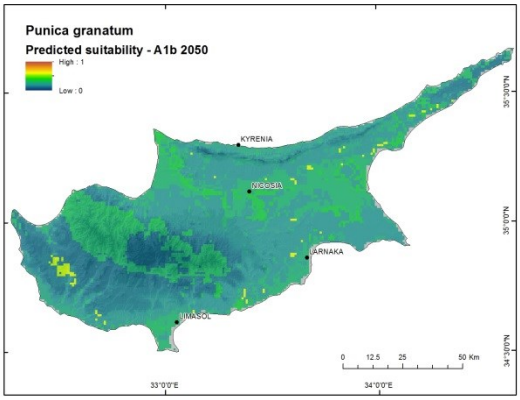

(d)

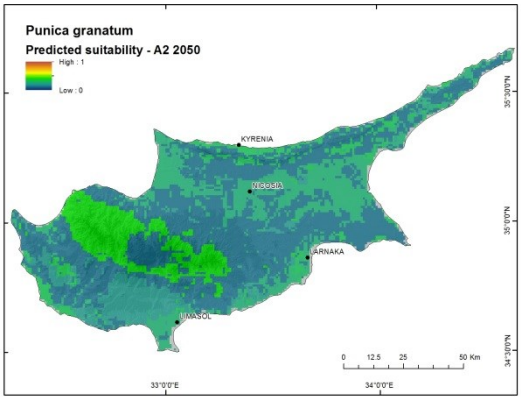

(e)

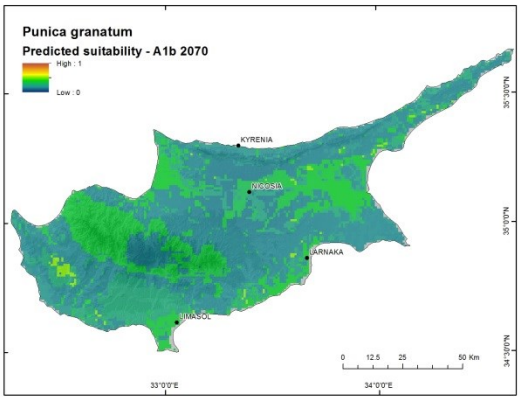

(f)

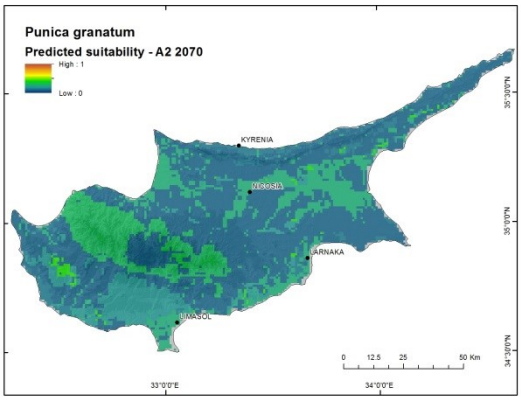

(g)

Figure 39. Continuous suitability maps for *Punica granatum* from present (Figure 39a) through 2070 A1b (Figure 39f) and A2 (Figure 39g) climate scenarios. Warmer colors indicate predicted suitability at a pixel to be near 1 (completely suitable for occurrence) and cooler colors indicate suitability predictions closer to 0 (completely unsuitable for occurrence).

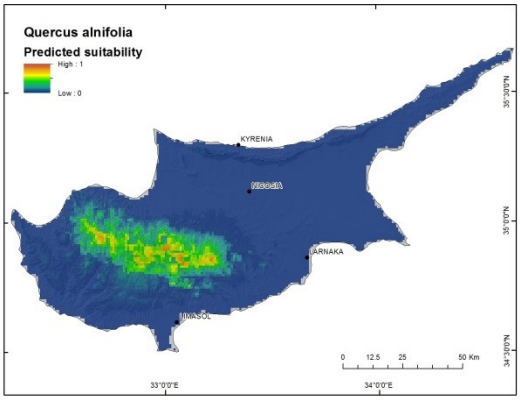
Quercus alnifolia
Predicted suitability
High : 1
Low : 0
KYRENIA
LEFKOŞA
LARNAKA
LIMASOL
0 12.5 25 50 Km
33°0'0"E
34°0'0"E
35°30'0"N
35°0'0"N
34°30'0"N

(a)

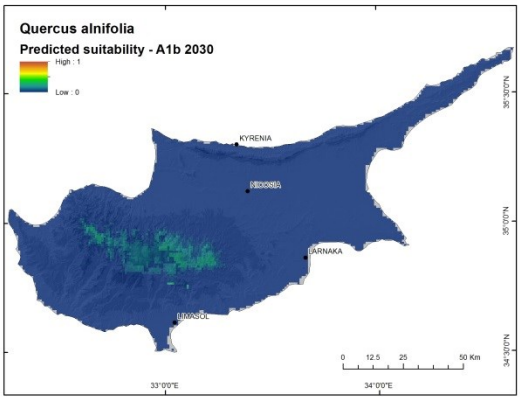
Quercus alnifolia
Predicted suitability - A1b 2030
High : 1
Low : 0
KYRENIA
LEFKOŞA
LARNAKA
LIMASOL
0 12.5 25 50 Km
33°0'0"E
34°0'0"E
35°30'0"N
35°0'0"N
34°30'0"N

(b)

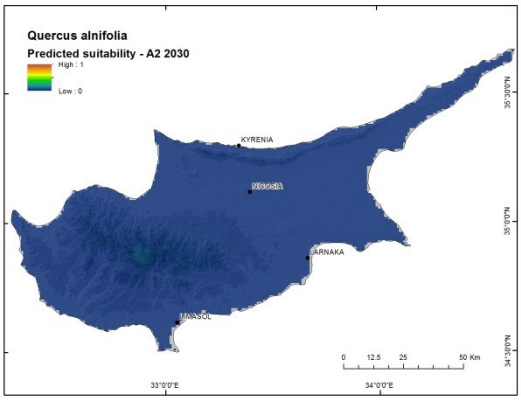
Quercus alnifolia
Predicted suitability - A2 2030
High : 1
Low : 0
KYRENIA
LEFKOŞA
LARNAKA
LIMASOL
0 12.5 25 50 Km
33°0'0"E
34°0'0"E
35°30'0"N
35°0'0"N
34°30'0"N

(c)

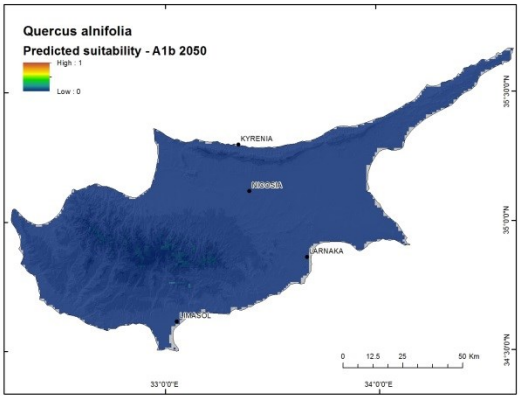
Quercus alnifolia
Predicted suitability - A1b 2050
High : 1
Low : 0
KYRENIA
LEFKOŞA
LARNAKA
LIMASOL
0 12.5 25 50 Km
33°0'0"E
34°0'0"E
35°30'0"N
35°0'0"N
34°30'0"N

(d)

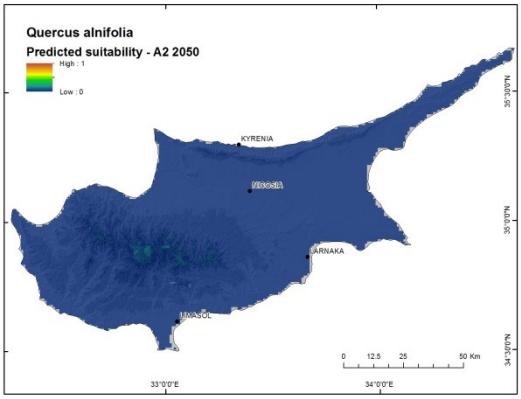
Quercus alnifolia
Predicted suitability - A2 2050
High : 1
Low : 0
KYRENIA
LEFKOŞA
LARNAKA
LIMASOL
0 12.5 25 50 Km
33°0'0"E
34°0'0"E
35°30'0"N
35°0'0"N
34°30'0"N

(e)

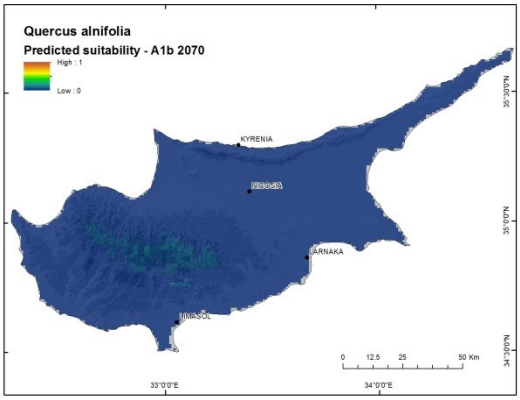

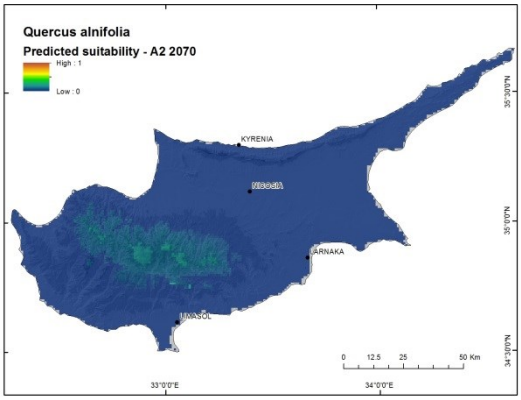

(f) (g)

Figure 40. Continuous suitability maps for *Quercus alnifolia* from present (Figure 40a) through 2070 A1b (Figure 40f) and A2 (Figure 40g) climate scenarios. Warmer colors indicate predicted suitability at a pixel to be near 1 (completely suitable for occurrence) and cooler colors indicate suitability predictions closer to 0 (completely unsuitable for occurrence).

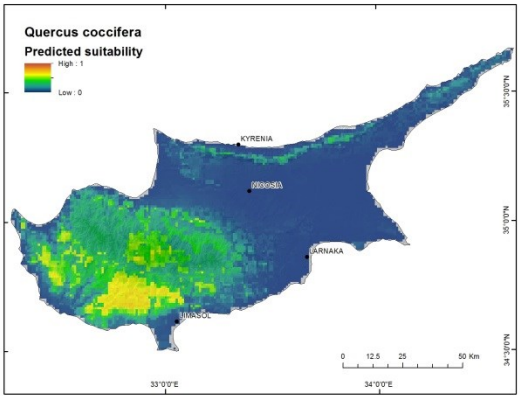

(a)

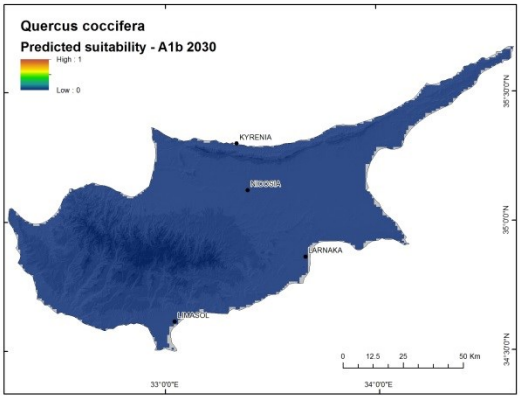

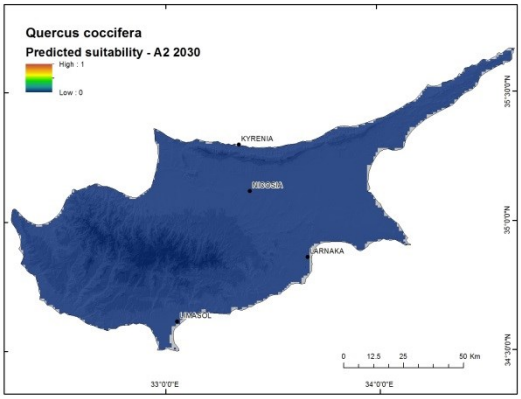

(b) (c)

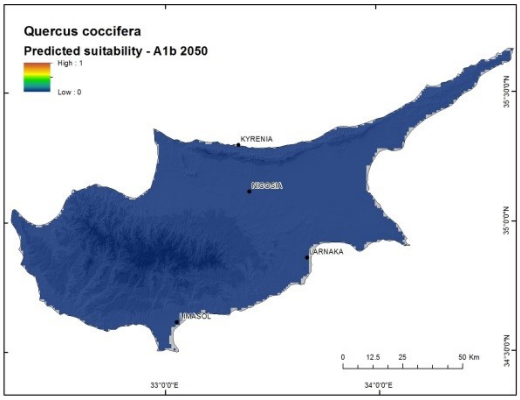

(d)

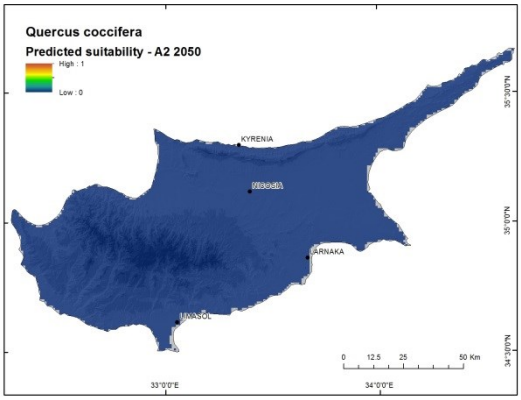

(e)

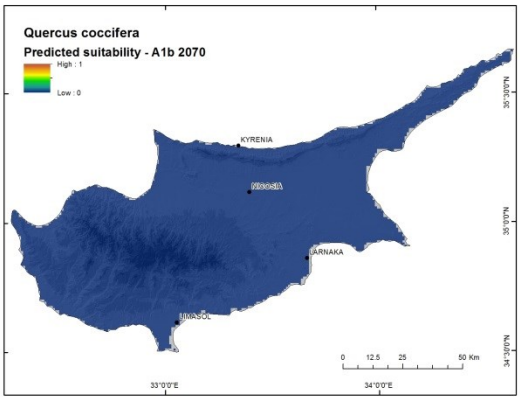

(f)

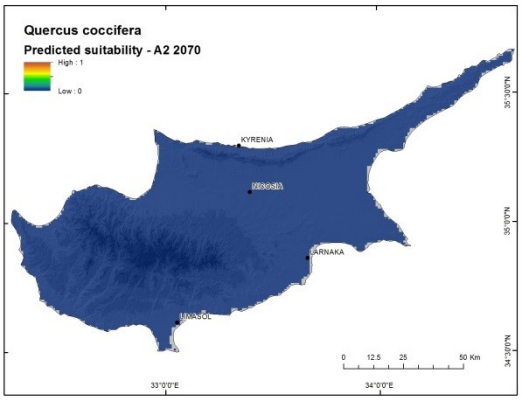

(g)

Figure 41. Continuous suitability maps for *Quercus coccifera* from present (Figure 41a) through 2070 A1b (Figure 41f) and A2 (Figure 41g) climate scenarios. Warmer colors indicate predicted suitability at a pixel to be near 1 (completely suitable for occurrence) and cooler colors indicate suitability predictions closer to 0 (completely unsuitable for occurrence).

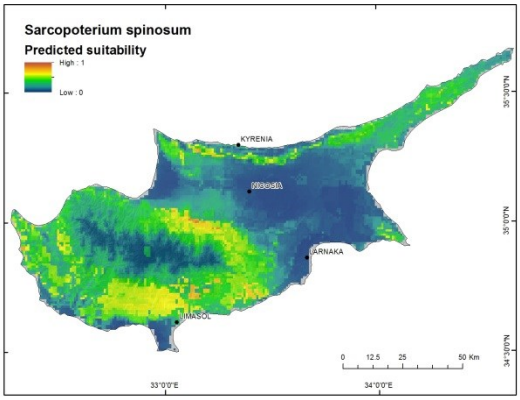
Sarcopoterium spinosum
Predicted suitability
High : 1
Low : 0
KYRENIA
LIMASOL
0 12.5 25 50 Km
33°0'0"E
34°0'0"E

(a)

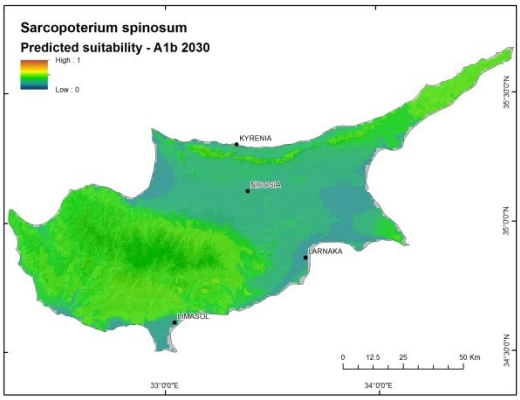
Sarcopoterium spinosum
Predicted suitability - A1b 2030
High : 1
Low : 0
KYRENIA
LIMASOL
0 12.5 25 50 Km
33°0'0"E
34°0'0"E

(b)

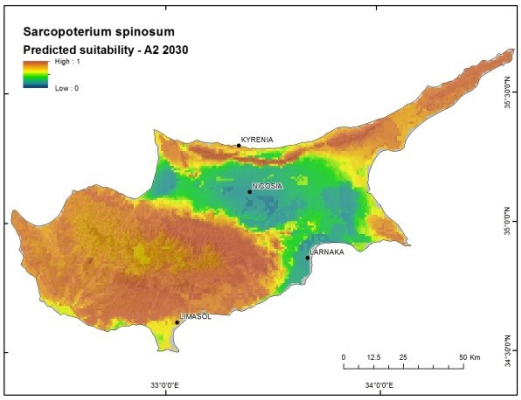
Sarcopoterium spinosum
Predicted suitability - A2 2030
High : 1
Low : 0
KYRENIA
LIMASOL
0 12.5 25 50 Km
33°0'0"E
34°0'0"E

(c)

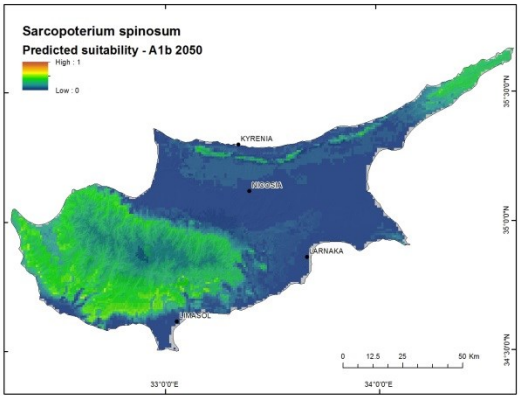
Sarcopoterium spinosum
Predicted suitability - A1b 2050
High : 1
Low : 0
KYRENIA
LIMASOL
0 12.5 25 50 Km
33°0'0"E
34°0'0"E

(d)

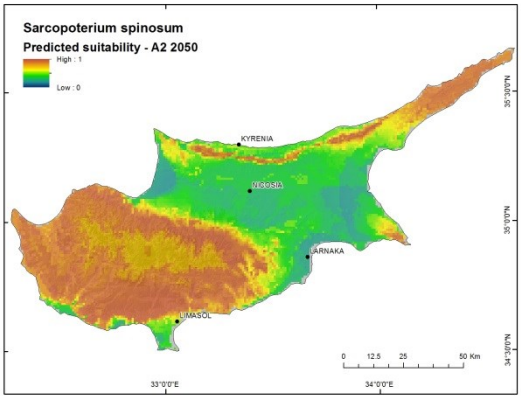
Sarcopoterium spinosum
Predicted suitability - A2 2050
High : 1
Low : 0
KYRENIA
LIMASOL
0 12.5 25 50 Km
33°0'0"E
34°0'0"E

(e)

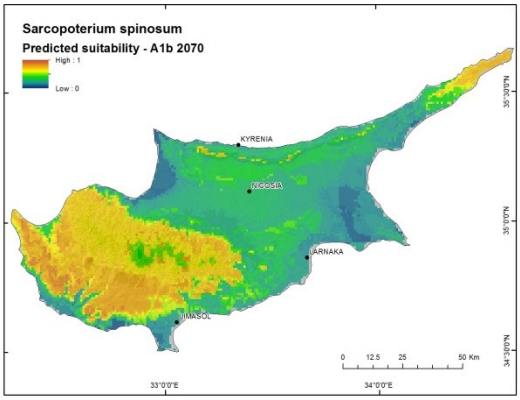

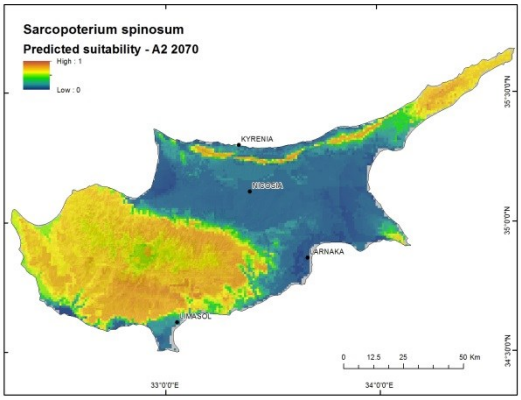

(f) (g)

Figure 42. Continuous suitability maps for *Sarcopoterium spinosum* from present (Figure 42a) through 2070 A1b (Figure 42f) and A2 (Figure 42g) climate scenarios. Warmer colors indicate predicted suitability at a pixel to be near 1 (completely suitable for occurrence) and cooler colors indicate suitability predictions closer to 0 (completely unsuitable for occurrence).

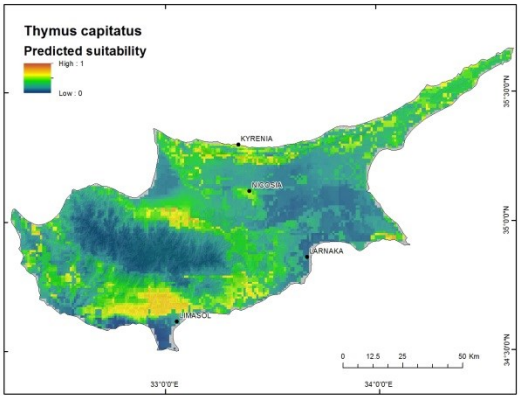

(a)

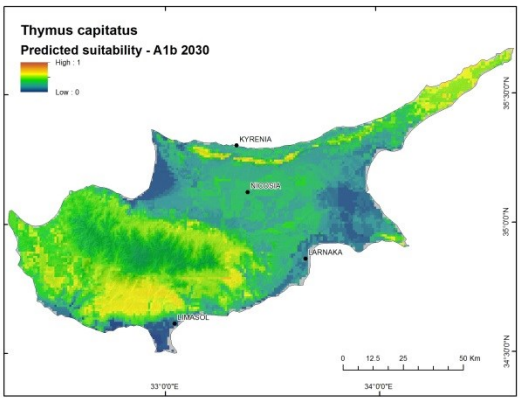

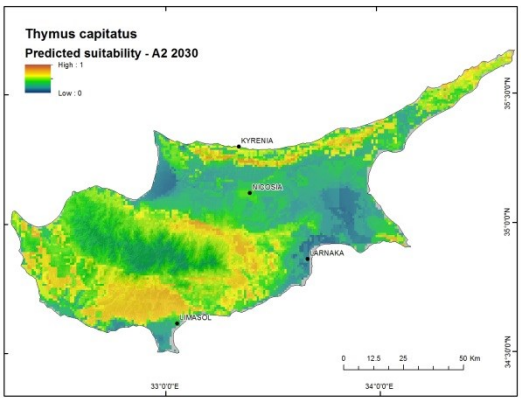

(b) (c)

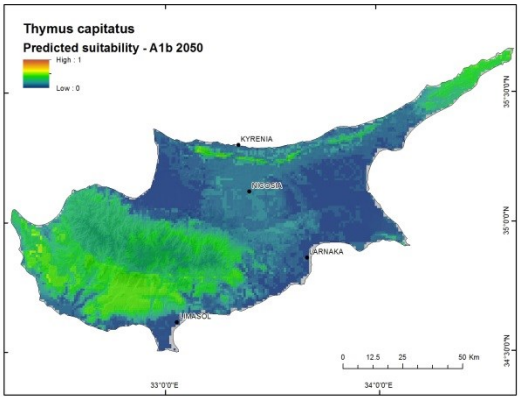

(d)

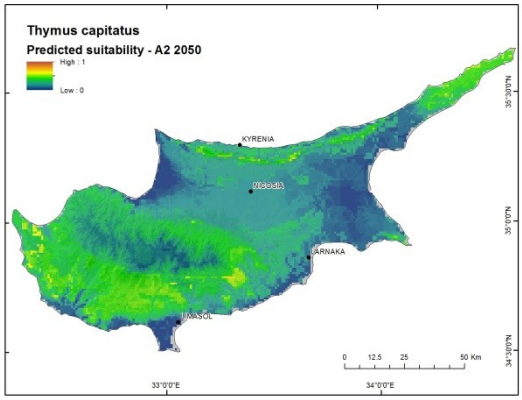

(e)

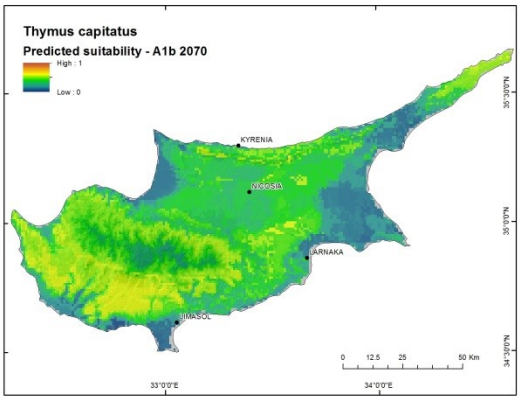

(f)

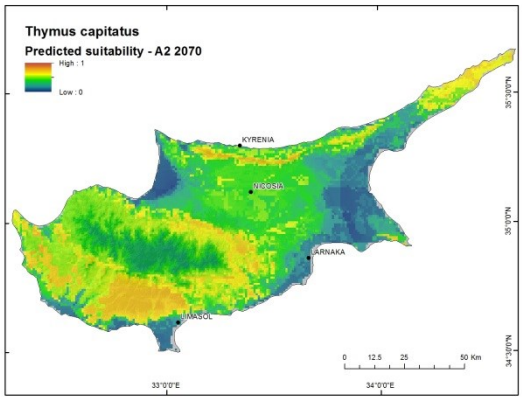

(g)

Figure 43. Continuous suitability maps for *Thymus capitatus* from present (Figure 43a) through 2070 A1b (Figure 43f) and A2 (Figure 43g) climate scenarios. Warmer colors indicate predicted suitability at a pixel to be near 1 (completely suitable for occurrence) and cooler colors indicate suitability predictions closer to 0 (completely unsuitable for occurrence).

The presence/absence maps are produced by applying a logistic threshold to the continuous prediction to create a binary map that only shows pixel values (probability of suitability for occurrence) above the threshold as suitable and pixel values below the threshold as unsuitable for the species of interest. The presence/absence maps are useful for calculating changes to the predicted area of suitability over multiple time slices. Each end-use of the presence/absence map (e.g. planning for future conservation sites, selecting species for protection or creating a network of protected areas) will dictate the

type of threshold applied to the continuous suitability maps. In this case, the application of a threshold of maximum training sensitivity + specificity produced interesting results under the selected climate scenarios in that areas predicted as suitable first contract and then expand for several species (Figures 44-52). For example, under the A1b scenario, *Olea europaea's* distribution contracts and advances to higher elevations under the A1b scenario, but expands its distribution under the A2 scenario, both to the southeast and to higher elevation. *Ficus carica* expands in suitable areas from 2030 to 2050, but its distribution is reduced by 2070, although this distribution is more widespread than at present. *Ficus carica* continuously expands across the landscape under all A2 scenarios, and suitable areas are predicted over most of the island by 2070. *Pinus brutia* appears to experience a large range extension between 2030 and 2050 under the A1b scenario. However, when the 2050 prediction is compared to the modern prediction the change is not very pronounced, and *P. brutia* does not have any predicted suitable areas by 2070. The overall range of *Pinus brutia* does not change dramatically from the present to 2070 under the A2 scenario. *Pistacia lentiscus* increases its range in extent and elevation under both climate scenarios, stretching up a large portion of the Troodos Range, the Kyrenia Mountains, and along the Karpas Peninsula. *Pistacia terebinthus* experiences a reduction in suitable areas in 2050 under both climate scenarios, with an increase in its area of suitability by 2070. Predicted areas of suitability under the A2 scenario do not differ substantially from the modern predicted suitable area. *Prunus dulcis, Sarcopoterium spinosum,* and *Thymus capitatus* fare well under both climate scenarios, expanding across the Troodos Range and foothills, the Karpas Peninsula, and Kyrenia Mountains.

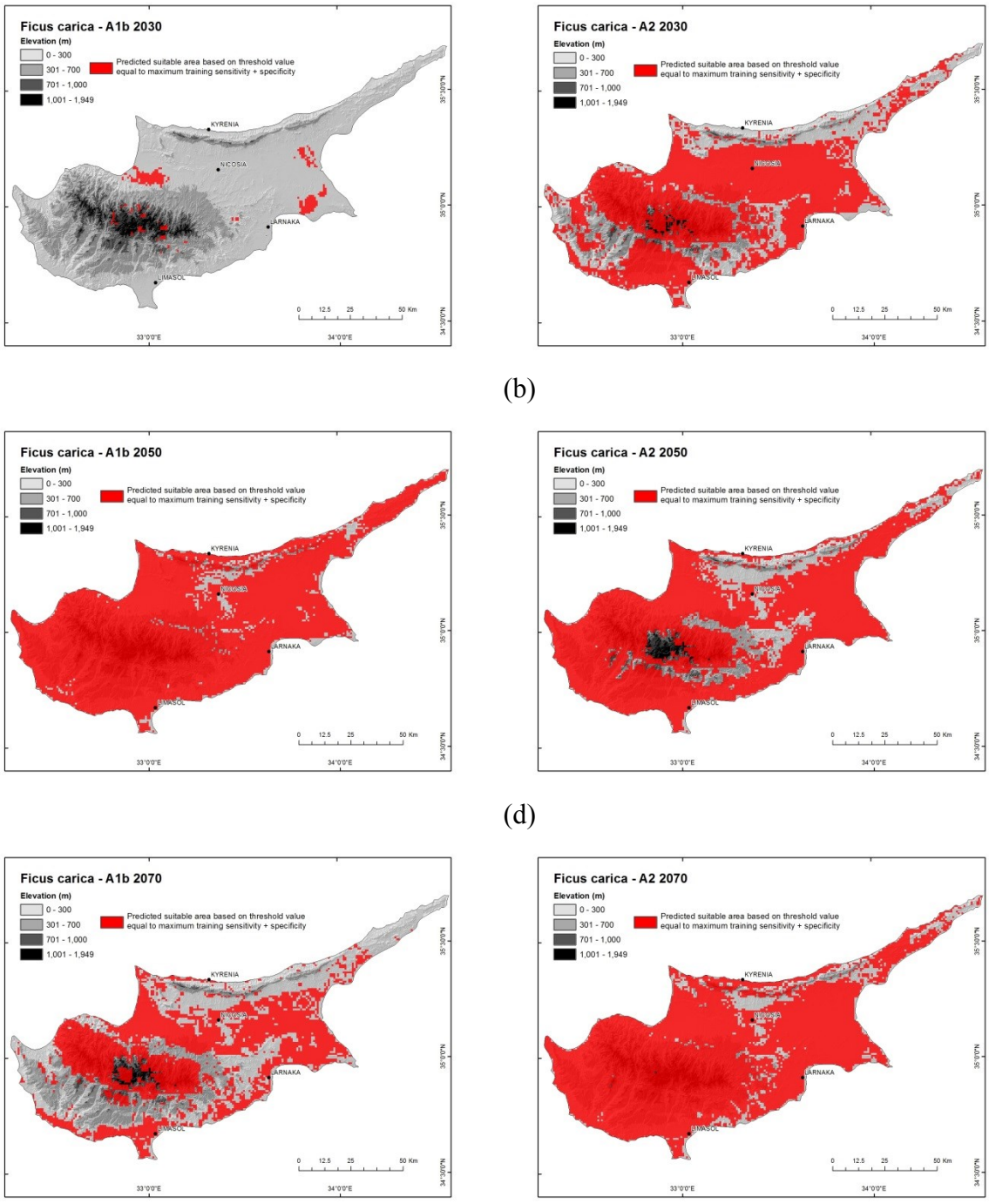

Figure 44. Binary suitability (presence/absence) maps for *Ficus carica* under climate scenarios A1b and A2 for 2030, 2050 and 2070. The area marked in red indicates the area of predicted suitability for occurrence based on a logistic threshold of maximum training sensitivity + specificity.

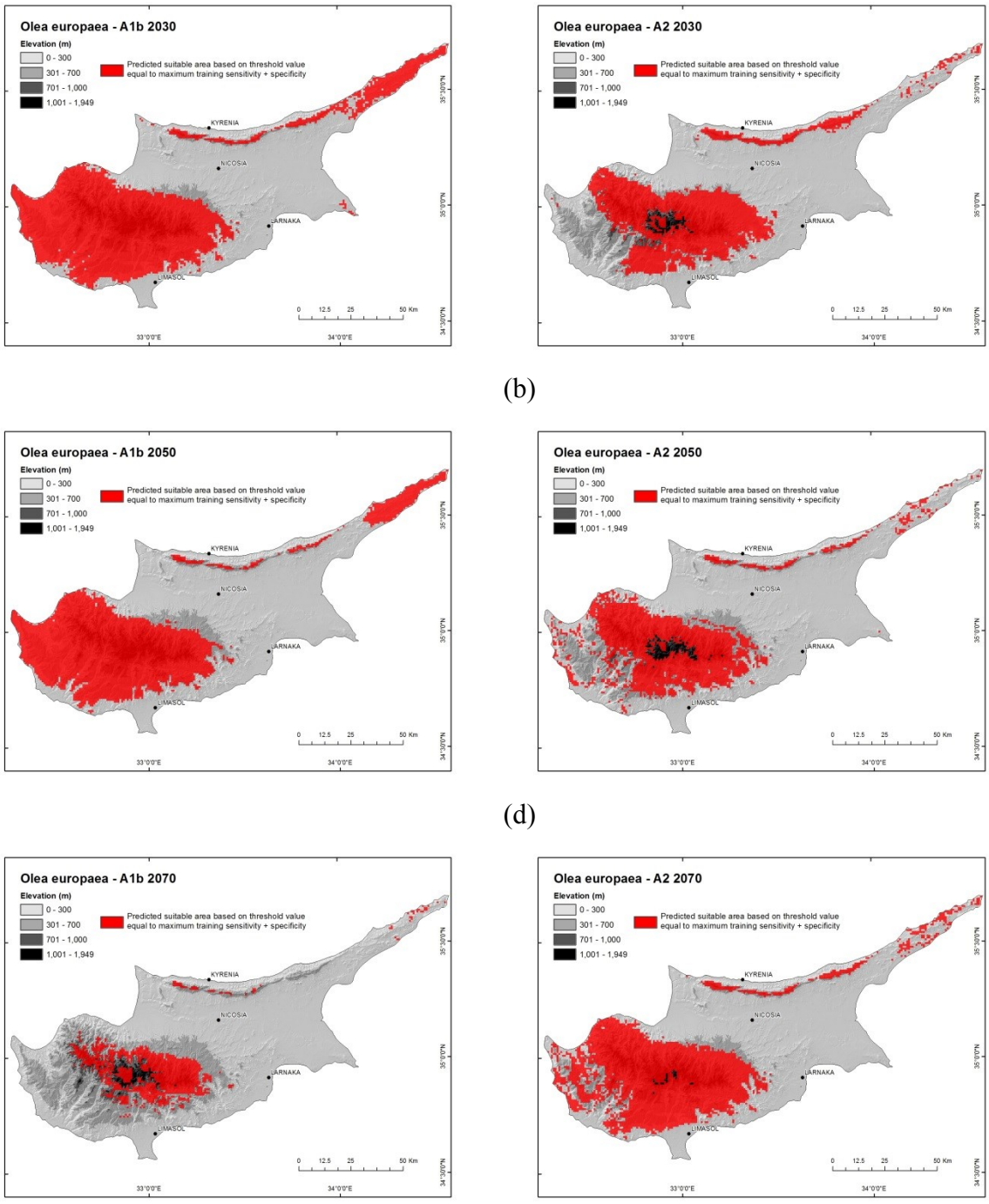

Figure 45. Binary suitability (presence/absence) maps for *Olea europaea* under climate scenarios A1b and A2 for 2030, 2050 and 2070. The area marked in red indicates the area of predicted suitability for occurrence based on a logistic threshold of maximum training sensitivity + specificity.

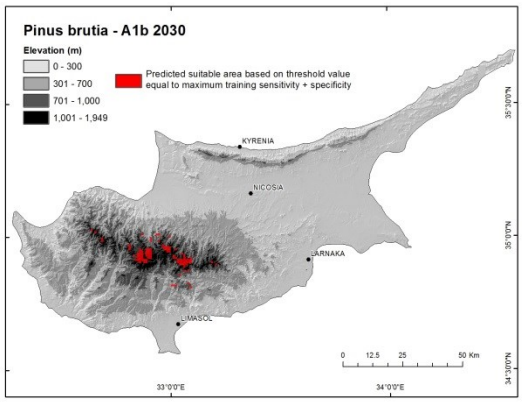

(a)

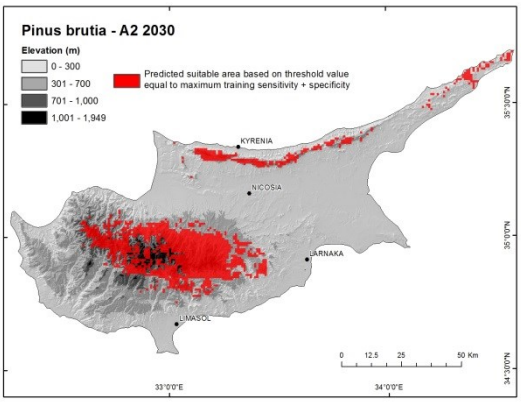

(b)

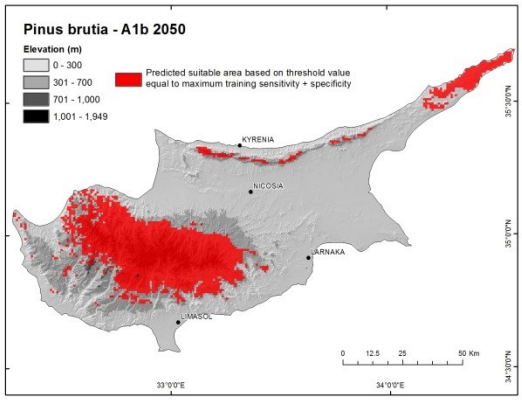

(c)

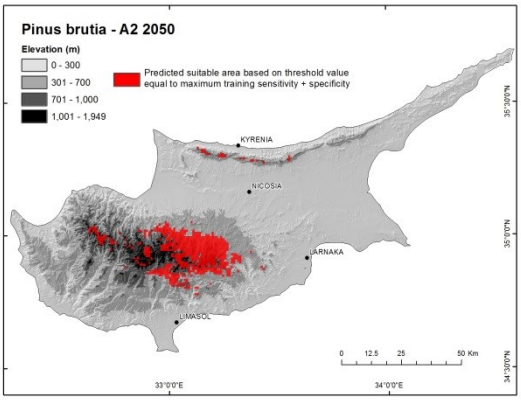

(d)

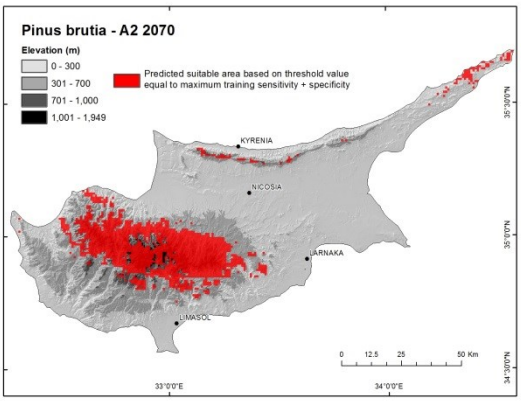

(e)

Figure 46. Binary suitability (presence/absence) maps for *Pinus brutia* under climate scenarios A1b and A2 for 2030, 2050 and 2070. The area marked in red indicates the area of predicted suitability for occurrence based on a logistic threshold of maximum training sensitivity + specificity.

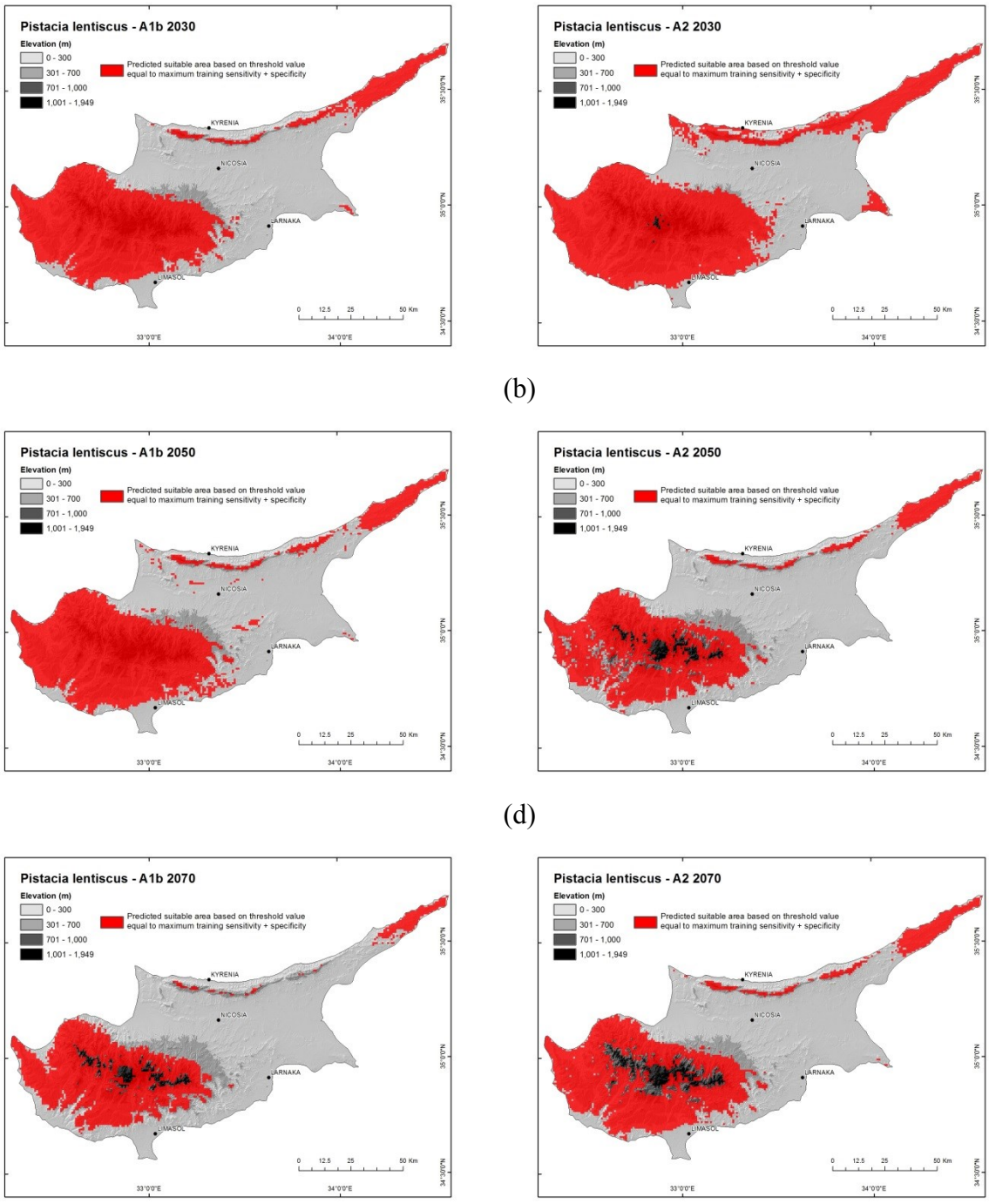

(a) (b)

(c) (d)

(e) (f)

Figure 47. Binary suitability (presence/absence) maps for *Pistacia lentiscus* under climate scenarios A1b and A2 for 2030, 2050 and 2070. The area marked in red indicates the area of predicted suitability for occurrence based on a logistic threshold of maximum training sensitivity + specificity.

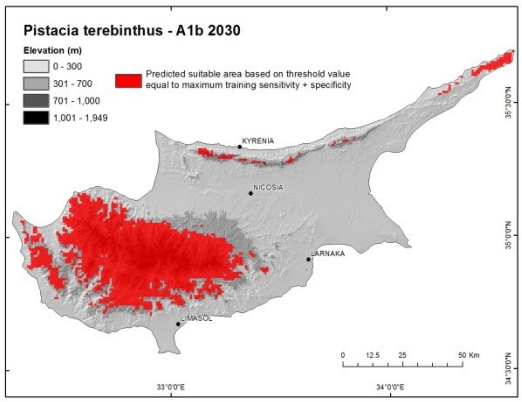

(a)

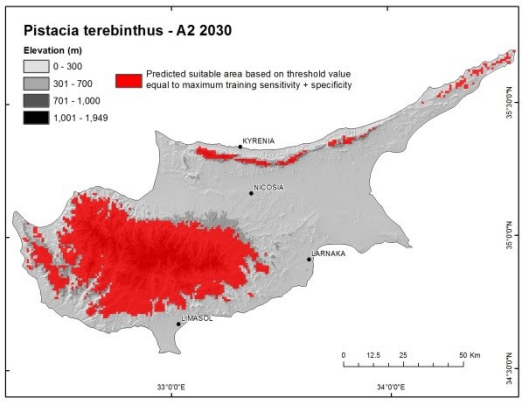

(b)

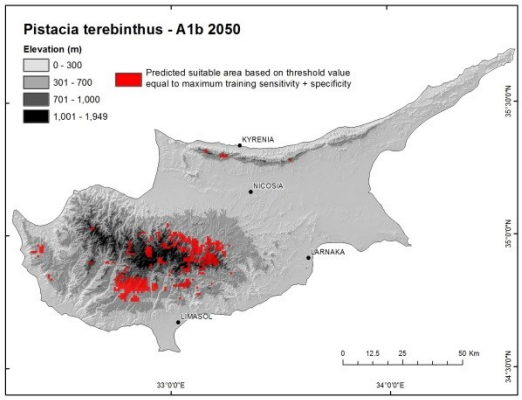

(c)

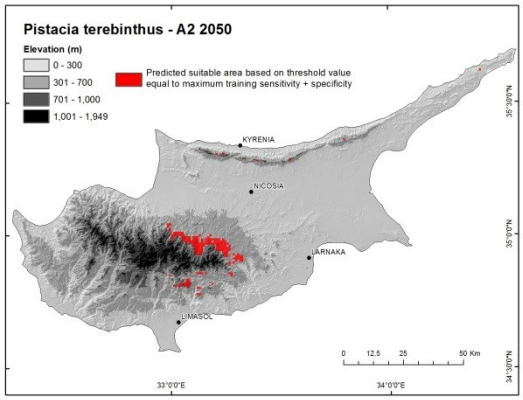

(d)

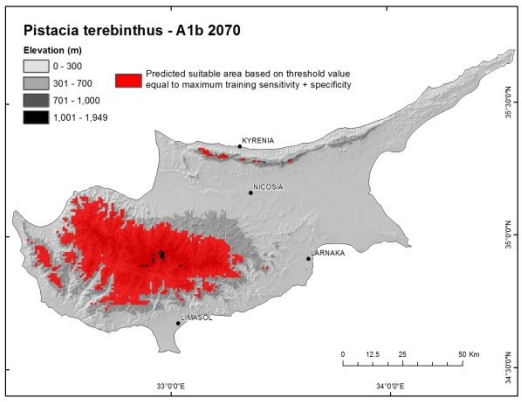

(e)

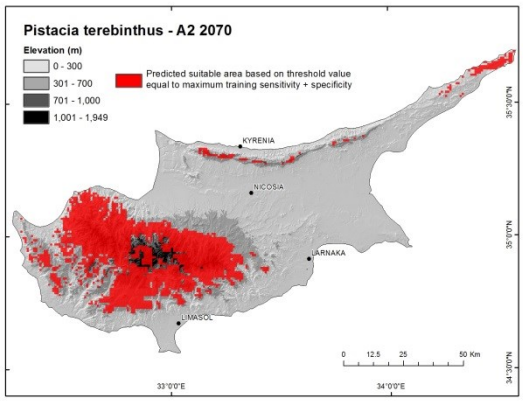

(f)

Figure 48. Binary suitability (presence/absence) maps for *Pistacia terebinthus* under climate scenarios A1b and A2 for 2030, 2050 and 2070. The area marked in red indicates the area of predicted suitability for occurrence based on a logistic threshold of maximum training sensitivity + specificity.

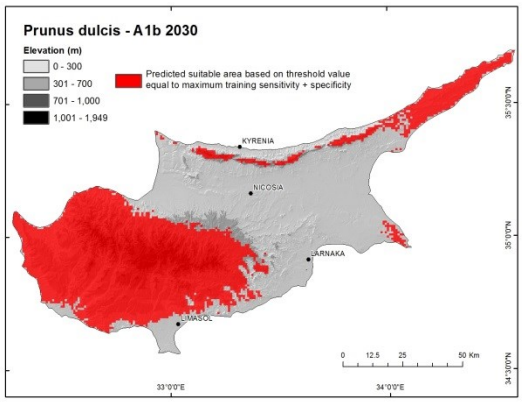

(a)

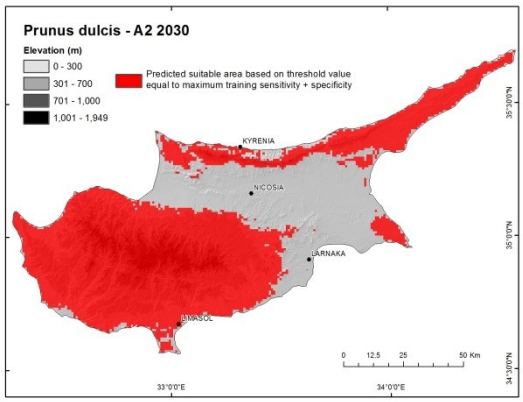

(b)

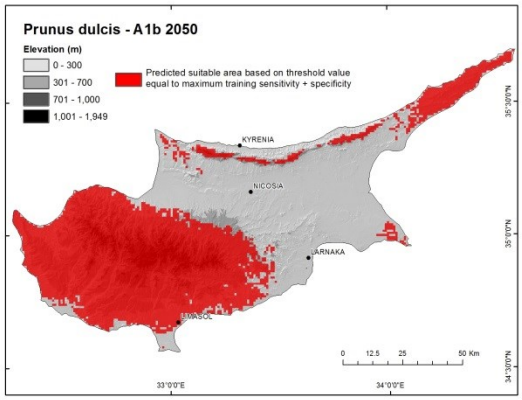

(c)

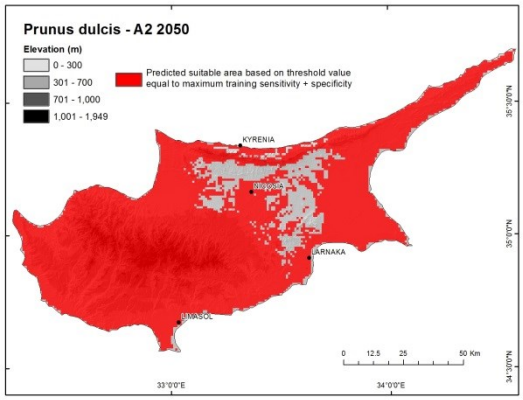

(d)

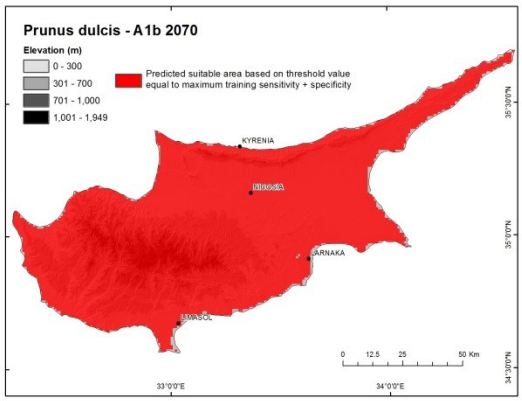

(e)

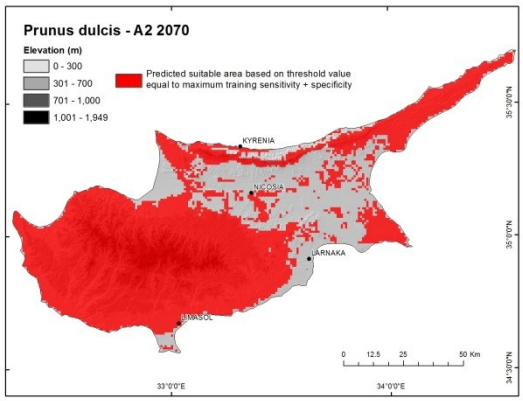

(f)

Figure 49. Binary suitability (presence/absence) maps for *Prunus dulcis* under climate scenarios A1b and A2 for 2030, 2050 and 2070. The area marked in red indicates the area of predicted suitability for occurrence based on a logistic threshold of maximum training sensitivity + specificity.

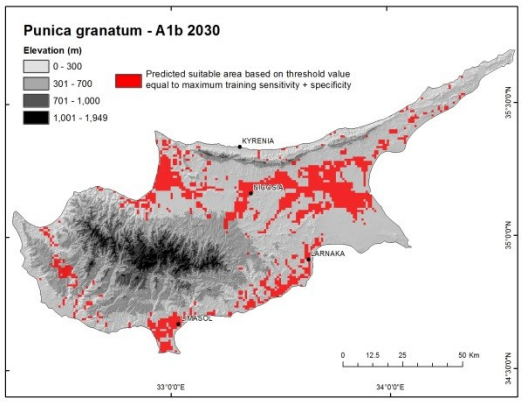

(a)

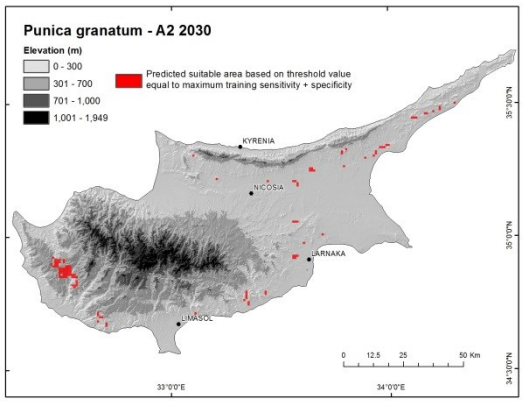

(b)

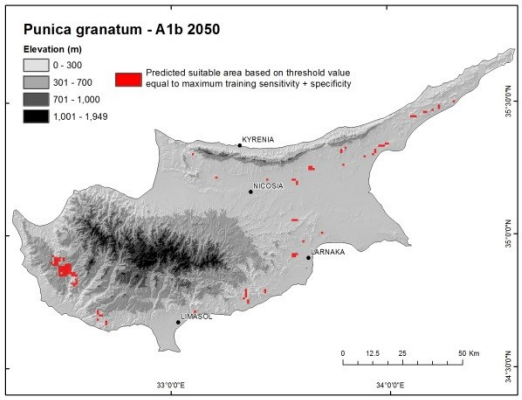

(c)

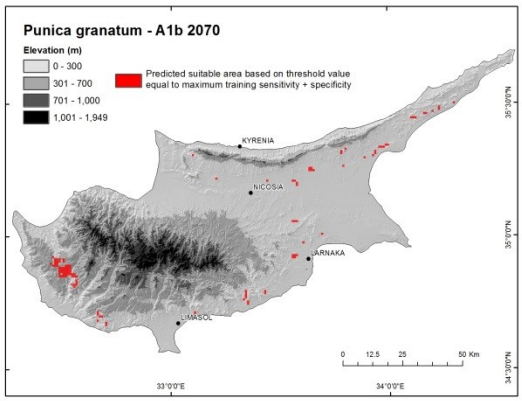

(d)

Figure 50. Binary suitability (presence/absence) maps for *Punica granatum* under climate scenarios A1b and A2 for 2030, 2050 and 2070. The area marked in red indicates the area of predicted suitability for occurrence based on a logistic threshold of maximum training sensitivity + specificity.

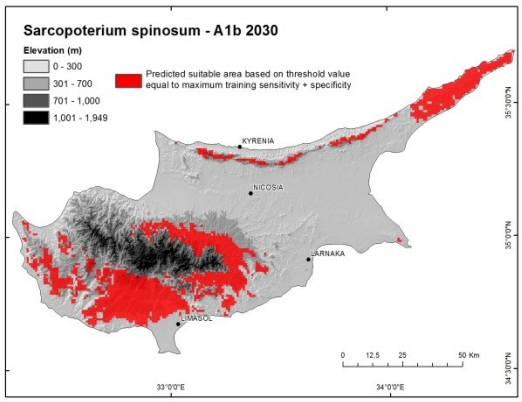

(a)

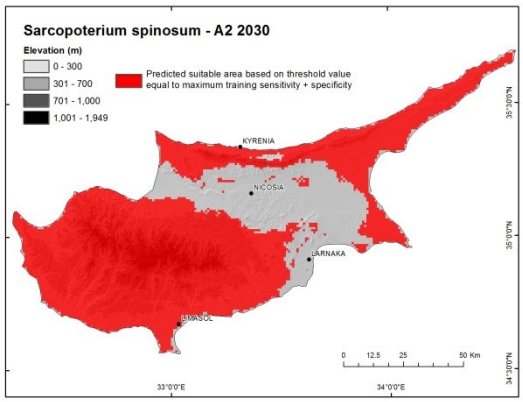

(b)

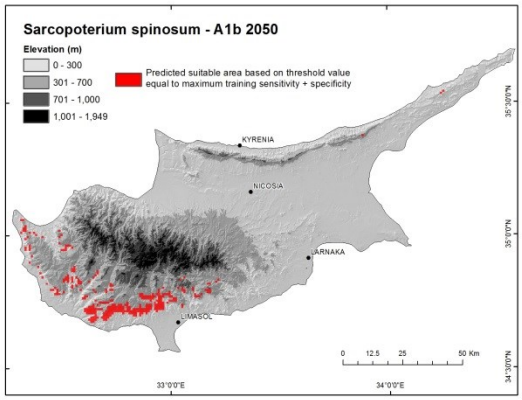

(c)

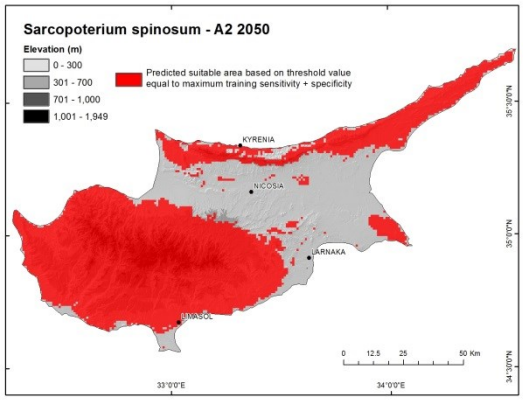

(d)

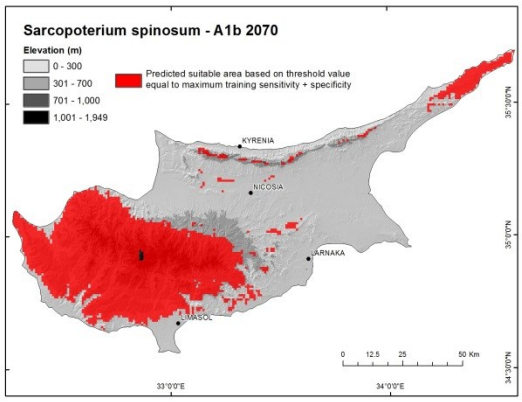

(e)

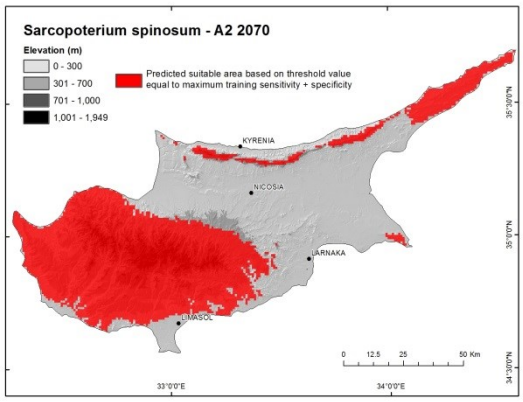

(f)

Figure 51. Binary suitability (presence/absence) maps for *Sarcopoterium spinosum* under climate scenarios A1b and A2 for 2030, 2050 and 2070. The area marked in red indicates the area of predicted suitability for occurrence based on a logistic threshold of maximum training sensitivity + specificity.

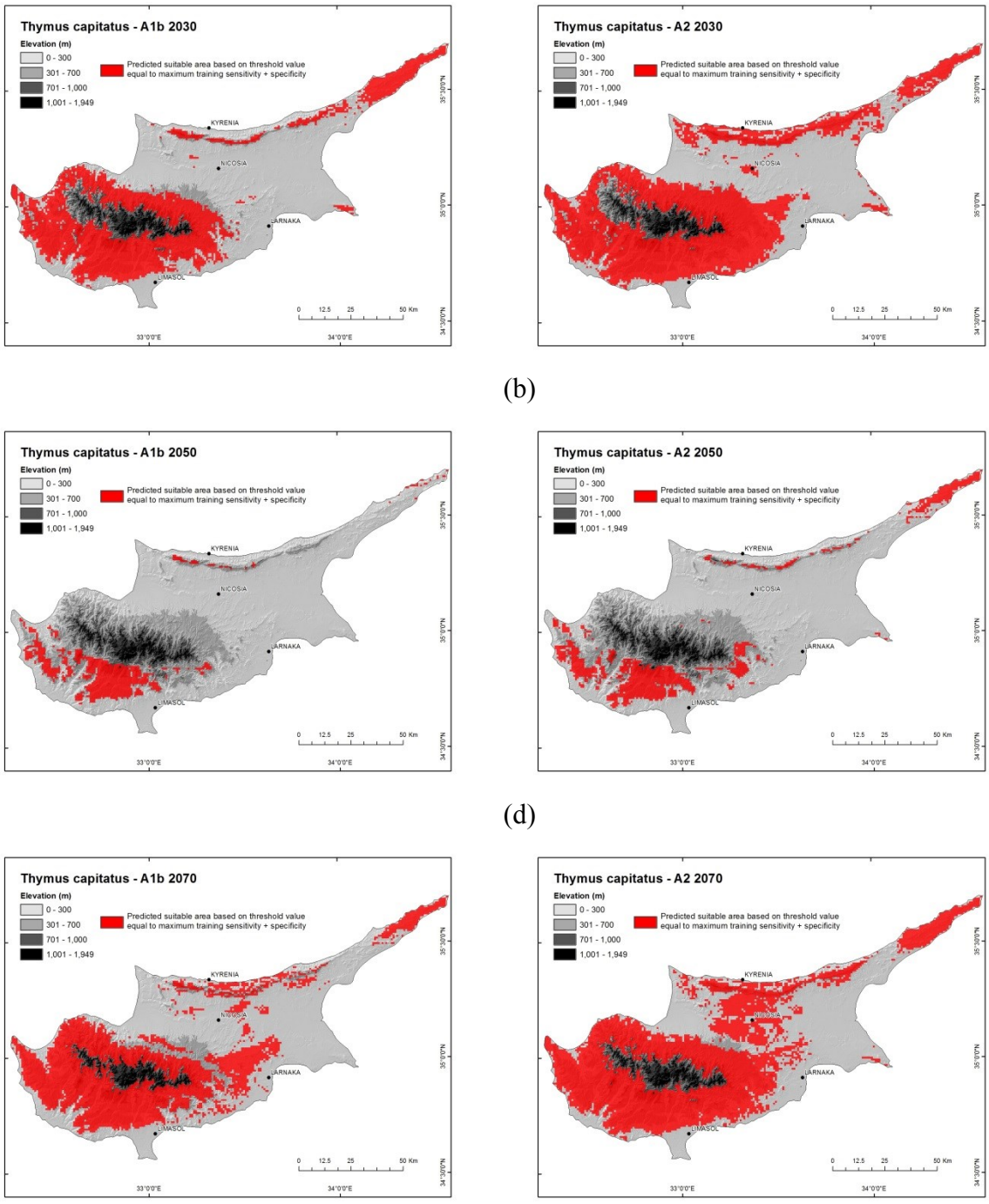

Figure 52. Binary suitability (presence/absence) maps for *Thymus capitatus* under climate scenarios A1b and A2 for 2030, 2050 and 2070. The area marked in red indicates the area of predicted suitability for occurrence based on a logistic threshold of maximum training sensitivity + specificity.

Table 21 provides the estimated areas (km^2) for the presence/absence maps and the overall change (%) between the modern prediction and each of the 2070 predictions. If a species did not persist above the threshold value at a time step, it was assumed that the species would not occur in the next time step. Eight species persisted through the A1b scenario; however only five increased their areas of predicted suitability (*F. carica, P. lentiscus, P. dulcis, S. spinosum,* and *T. capitatus*). The same number of species persisted through the A2 scenario; however, *O. europaea* increased in suitable area, *P. brutia* declined by approximately 38% (instead of 100%), and *P. granatum* lost all suitable area (as opposed to losing approximately 96% under A1b).

Model validation

Clamping

Clamping maps (Figures 53-74) indicate pixels and/or regions where future covariate values were constrained to the maximum or minimum values found in the training data. Clamping is necessary as SDMs can potentially behave in ways that are ecologically unviable under new climate conditions (Elith et al., 2010). Under new environmental conditions that are outside of the training range of the environmental covariates, the model is response is constant, or forced to behave in a predictable manner and remain within the range of known values in the training data. Thus models may predict species into areas that are considered suitable for occurrence only because the environmental covariates are constrained to the training data for that species. The predicted area of occurrence may contain environmental covariate values that overlap with the training data, but the predicted range extends outside that of the training data, meaning the location is potentially not suitable for species occurrence. The clamping

maps indicate areas of clamping with warmer colors highlighting the areas where the prediction is potentially influenced by covariates outside of the training range. Maps for *C. salviifolius* indicate clamping across a large proportion of the island, but values within the area of the modern prediction remain low. In addition, *H. obtusifolium, J. phoenicea, O. europaea, P. brutia, P. lentiscus, P. terebinthus, Pterocephalus multiflorus, S. spinosum,* and *T. capitatus* exhibited clamping across a portion of the island.

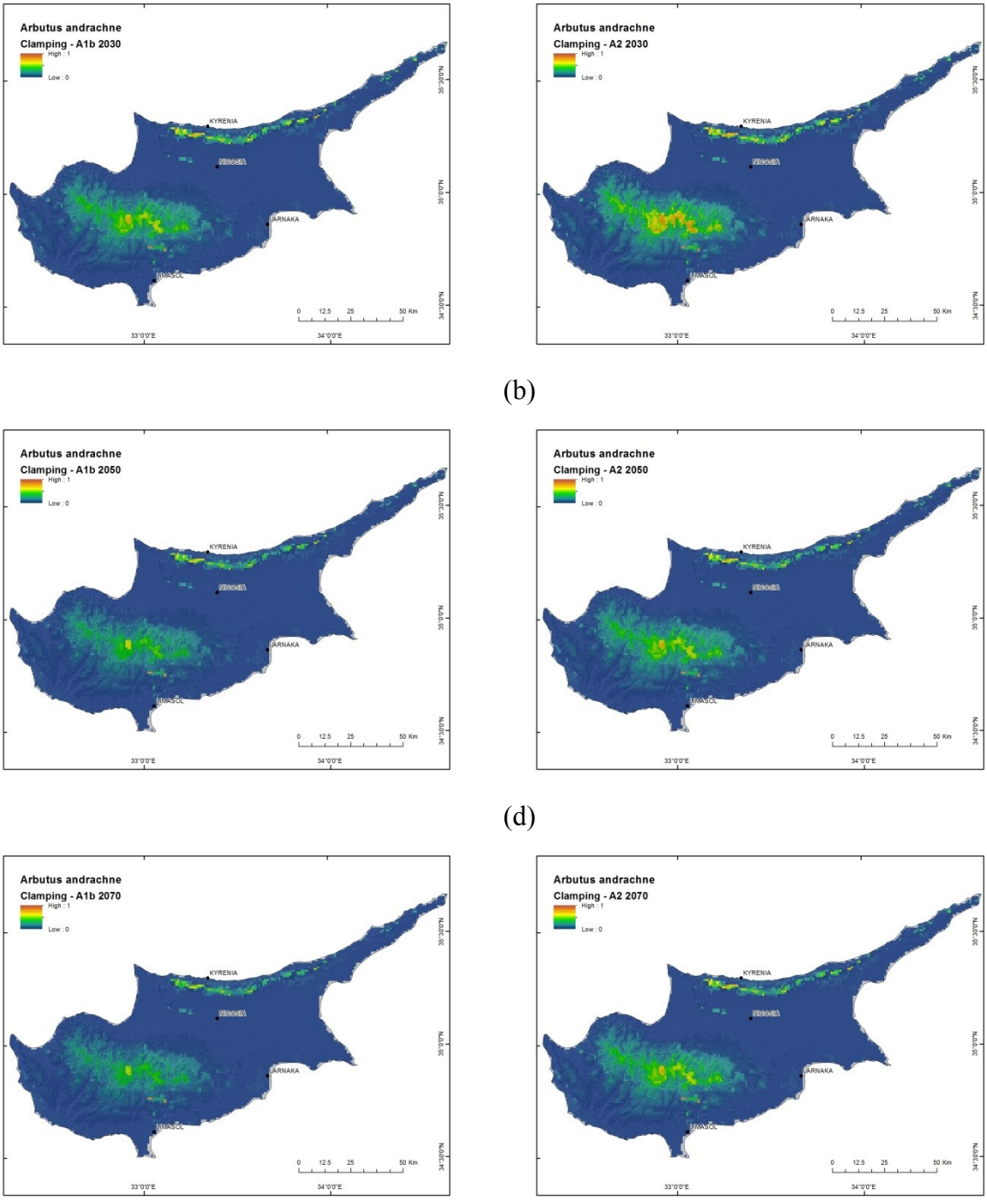

Figure 53. Clamping maps for *Arbutus andrachne* under climate scenarios A1b and A2 for 2030, 2050 and 2070. Warmer colors indicate areas where clamping, or restriction of environmental variables used to create the predictions to their values in the training data for present-day vegetation, has occurred.

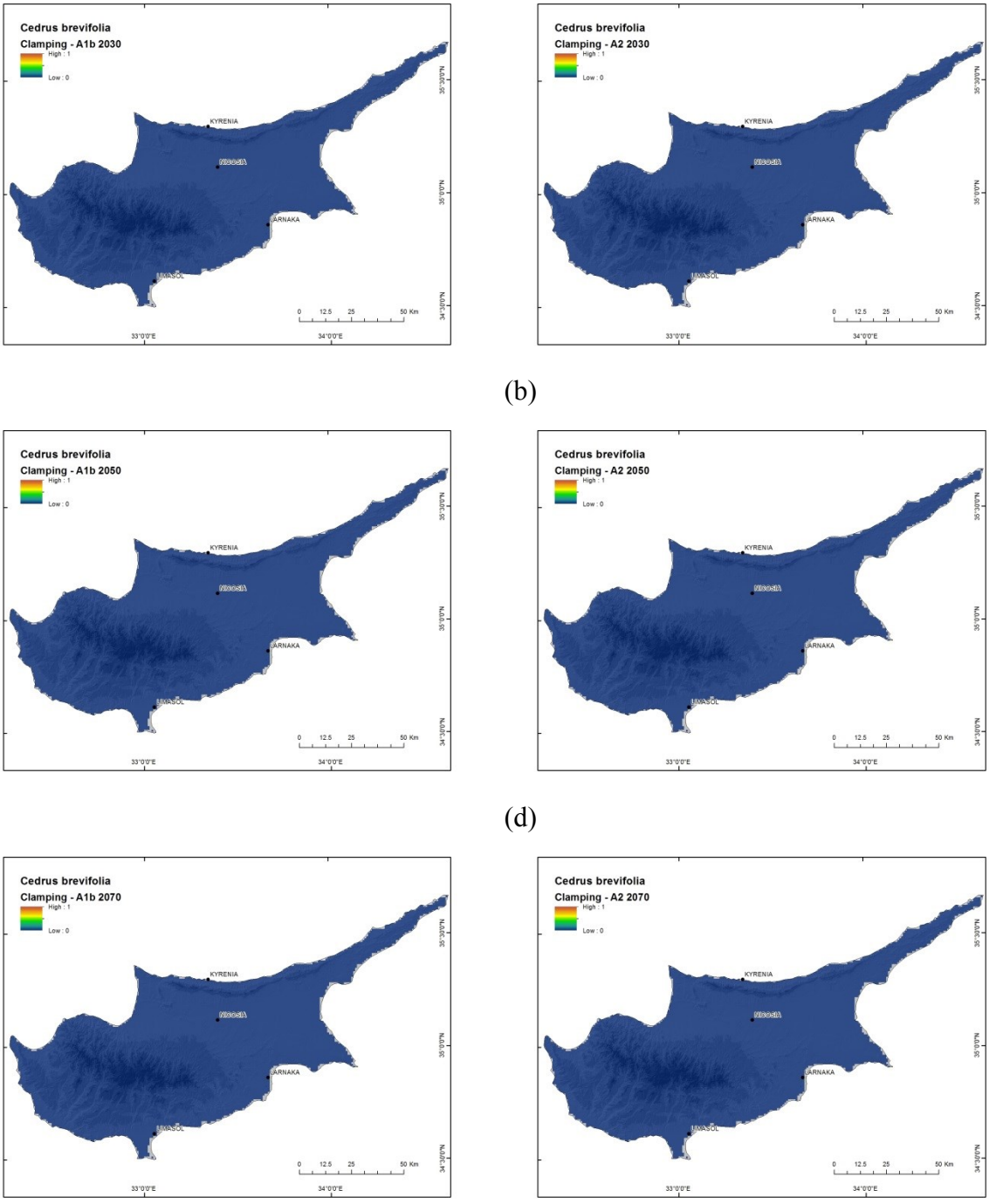

Figure 54. Clamping maps for *Cedrus brevifolia* under climate scenarios A1b and A2 for 2030, 2050 and 2070. Warmer colors indicate areas where clamping, or restriction of environmental variables used to create the predictions to their values in the training data for present-day vegetation, has occurred.

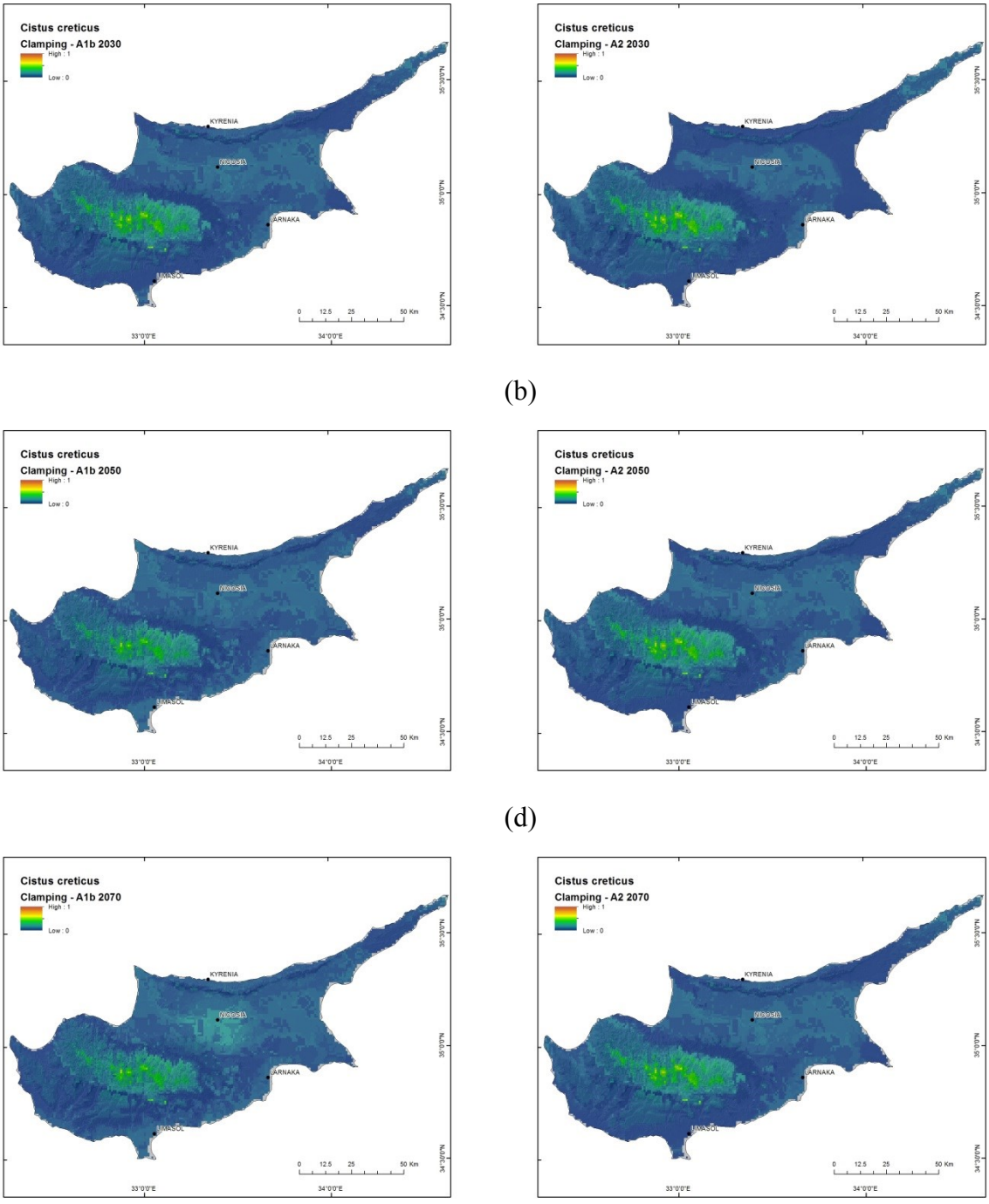

Figure 55. Clamping maps for *Cistus creticus* under climate scenarios A1b and A2 for 2030, 2050 and 2070. Warmer colors indicate areas where clamping, or restriction of environmental variables used to create the predictions to their values in the training data for present-day vegetation, has occurred.

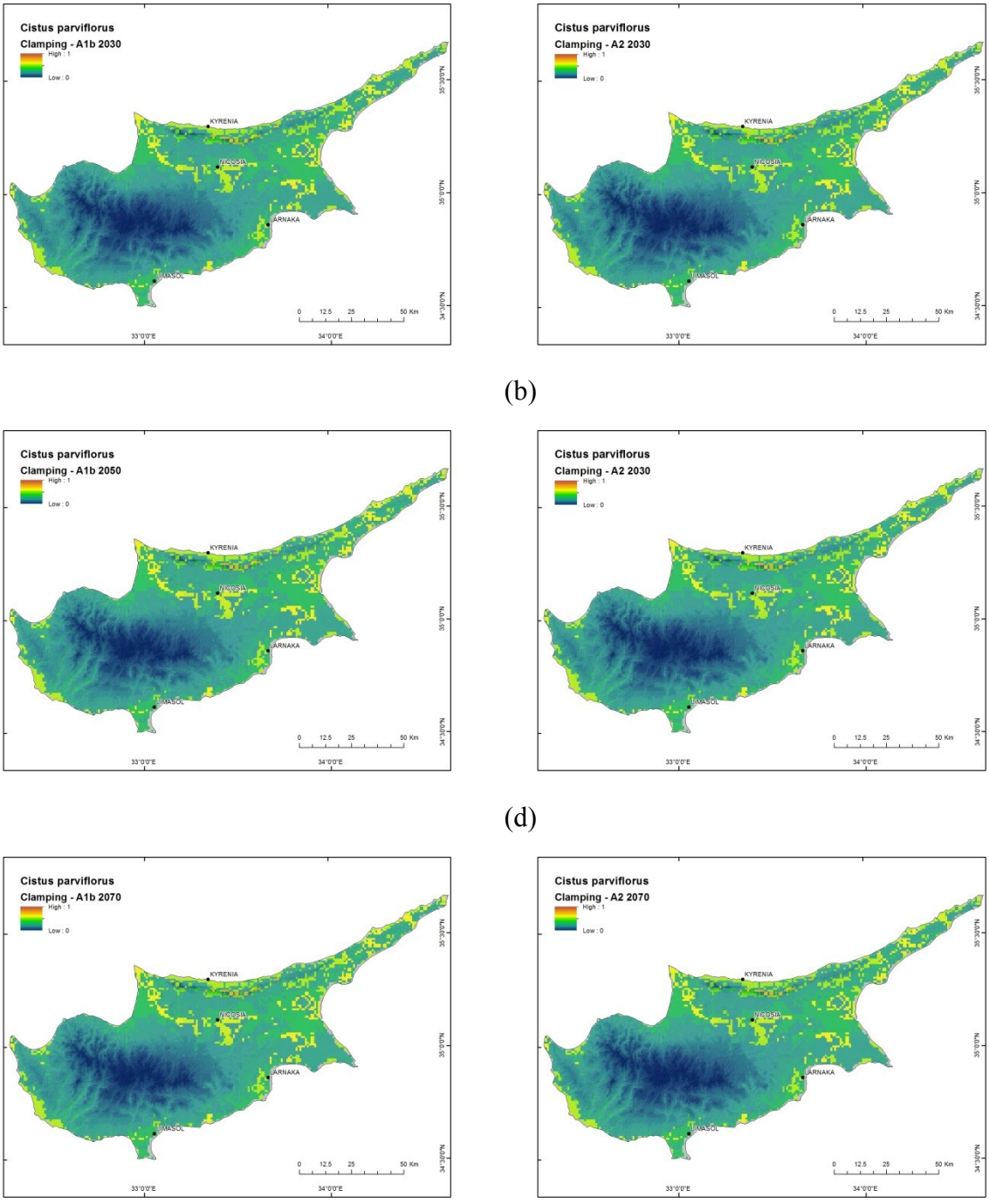

Figure 56. Clamping maps for *Cistus parviflorus* under climate scenarios A1b and A2 for 2030, 2050 and 2070. Warmer colors indicate areas where clamping, or restriction of environmental variables used to create the predictions to their values in the training data for present-day vegetation, has occurred.

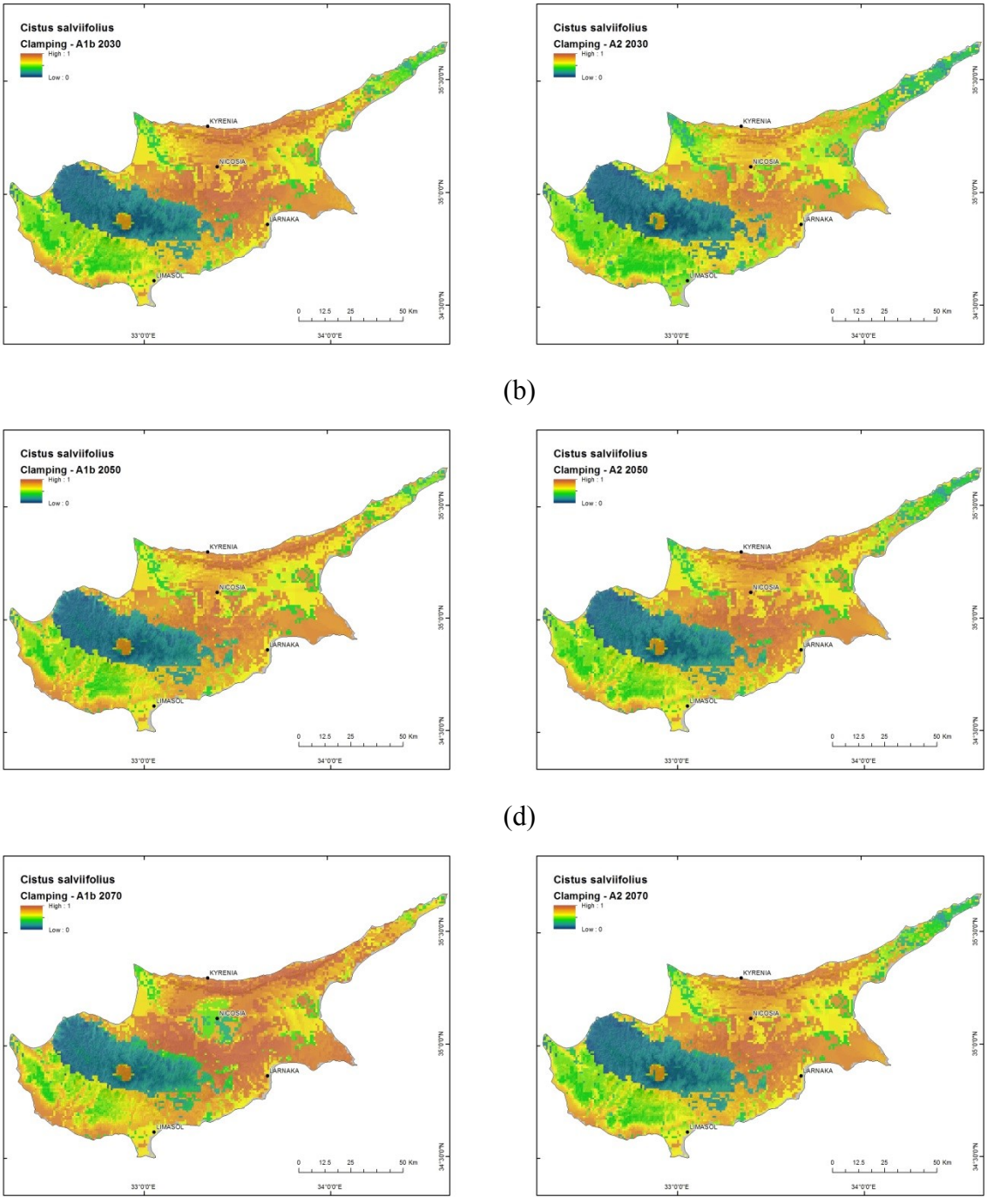

Figure 57. Clamping maps for *Cistus salviifolius* under climate scenarios A1b and A2 for 2030, 2050 and 2070. Warmer colors indicate areas where clamping, or restriction of environmental variables used to create the predictions to their values in the training data for present-day vegetation, has occurred.

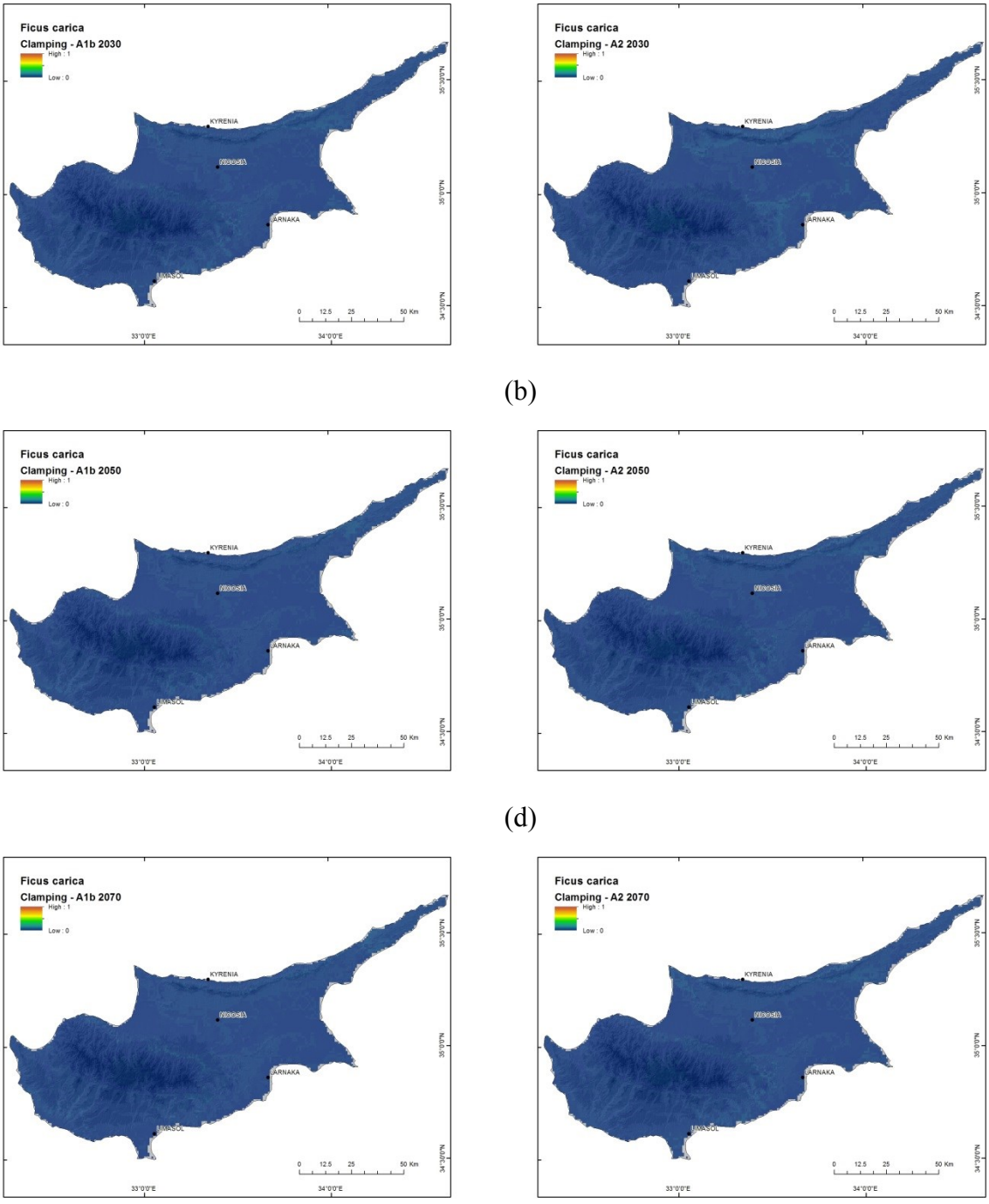

Figure 58. Clamping maps for *Ficus carica* under climate scenarios A1b and A2 for 2030, 2050 and 2070. Warmer colors indicate areas where clamping, or restriction of environmental variables used to create the predictions to their values in the training data for present-day vegetation, has occurred.

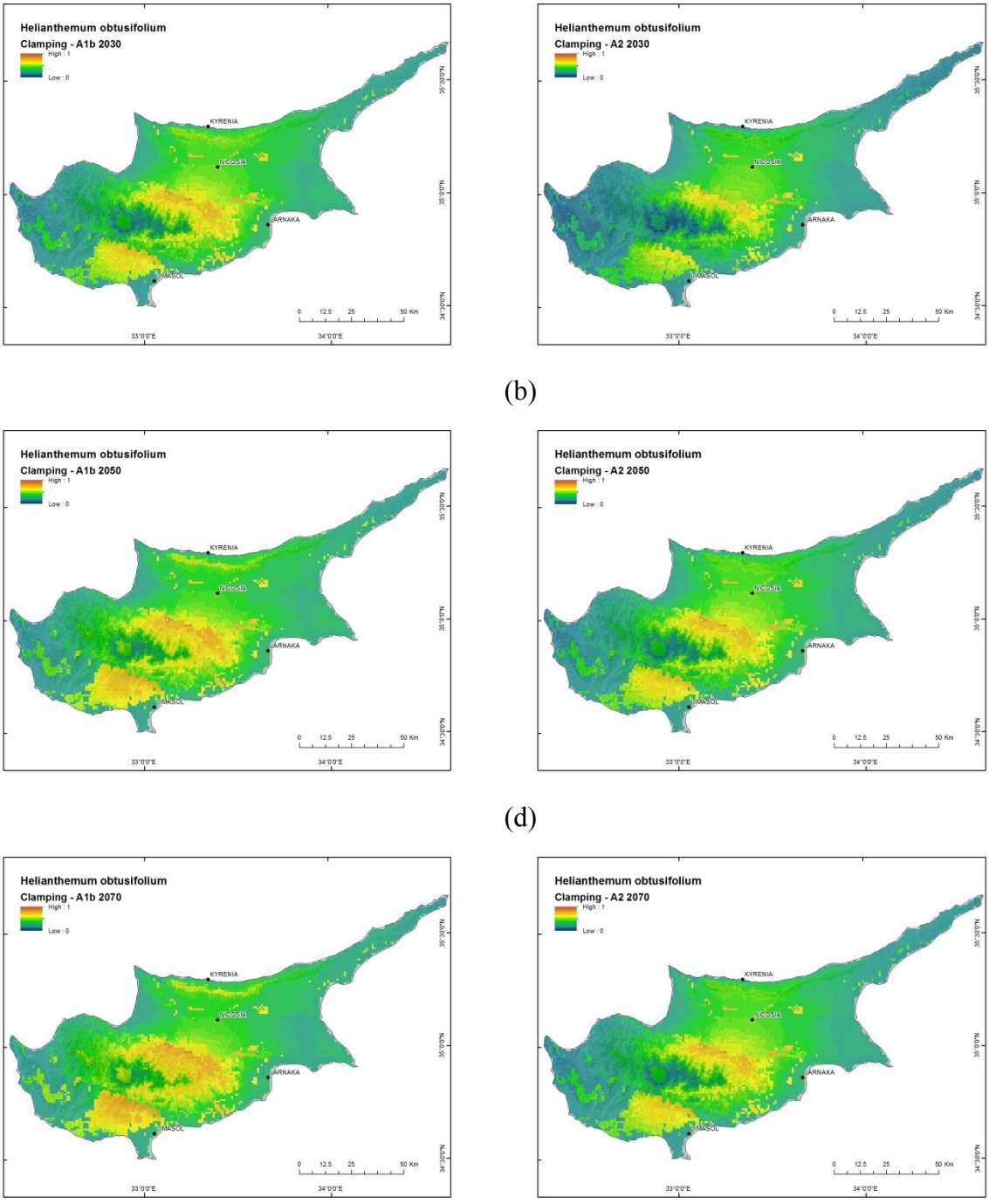

Figure 59. Clamping maps for *Helianthemum obtusifolium* under climate scenarios A1b and A2 for 2030, 2050 and 2070. Warmer colors indicate areas where clamping, or restriction of environmental variables used to create the predictions to their values in the training data for present-day vegetation, has occurred.

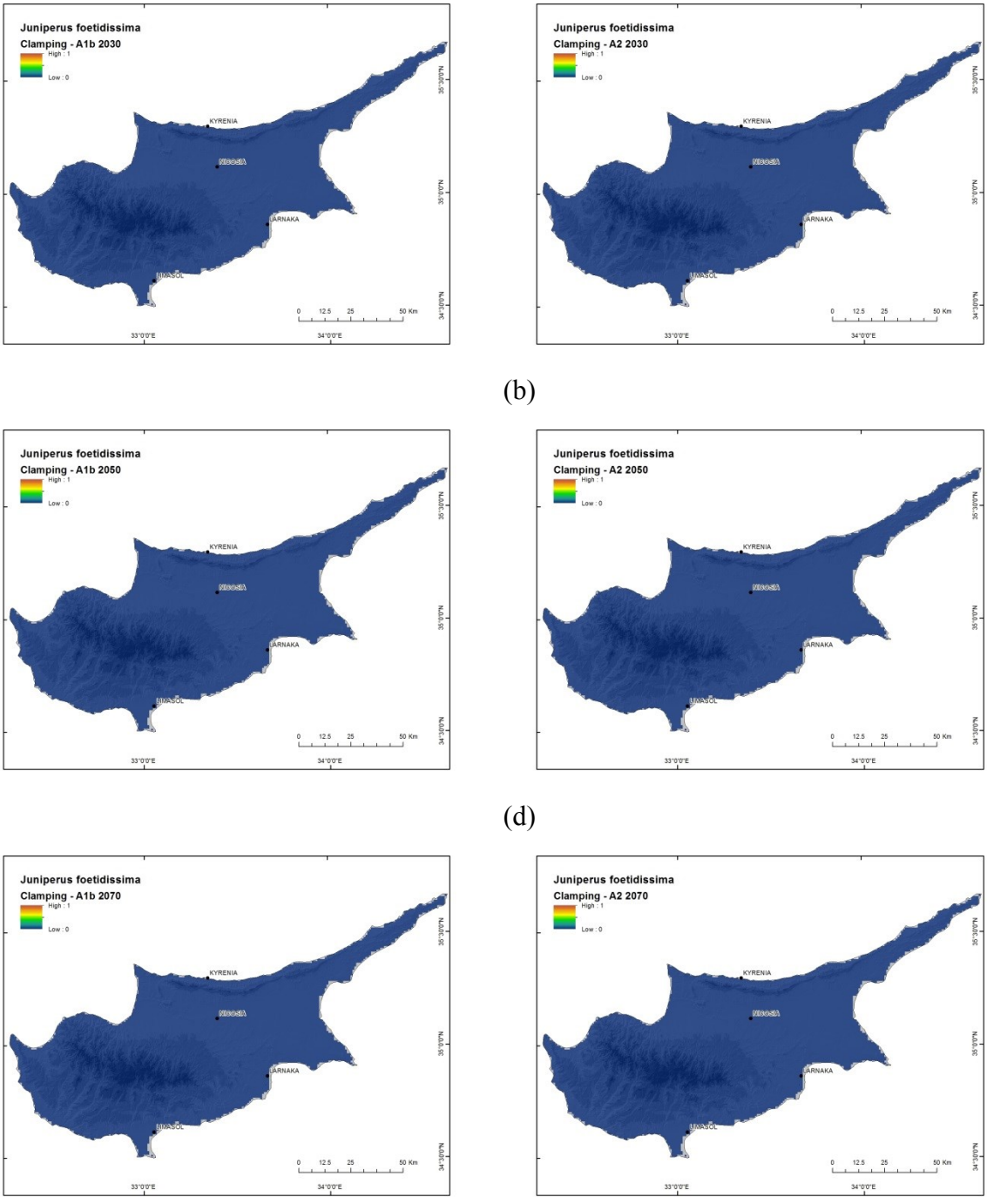

Figure 60. Clamping maps for *Juniperus foetidissima* under climate scenarios A1b and A2 for 2030, 2050 and 2070. Warmer colors indicate areas where clamping, or restriction of environmental variables used to create the predictions to their values in the training data for present-day vegetation, has occurred.

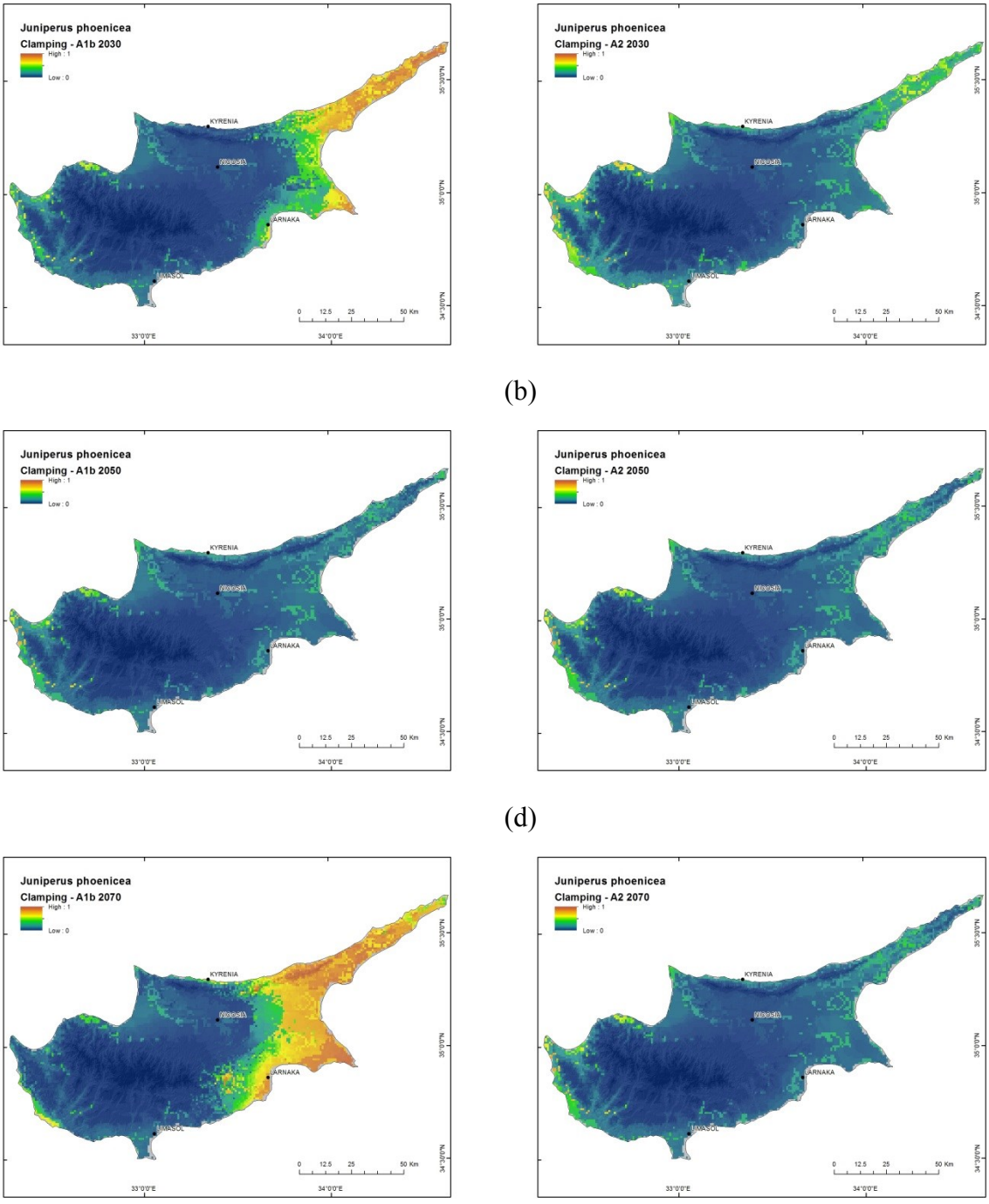

Figure 61. Clamping maps for *Juniperus phoenicea* under climate scenarios A1b and A2 for 2030, 2050 and 2070. Warmer colors indicate areas where clamping, or restriction of environmental variables used to create the predictions to their values in the training data for present-day vegetation, has occurred.

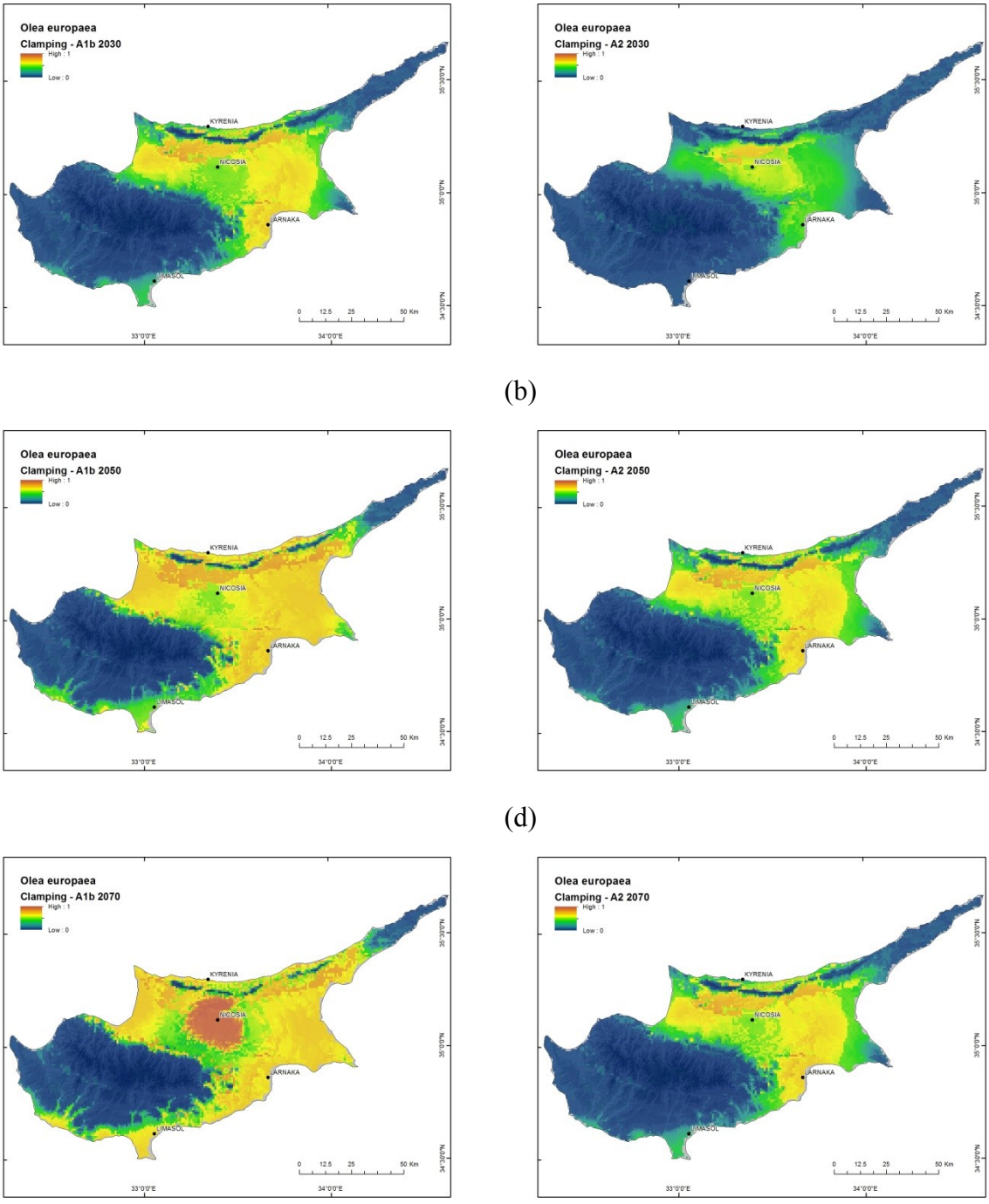

Figure 62. Clamping maps for *Olea europaea* under climate scenarios A1b and A2 for 2030, 2050 and 2070. Warmer colors indicate areas where clamping, or restriction of environmental variables used to create the predictions to their values in the training data for present-day vegetation, has occurred.

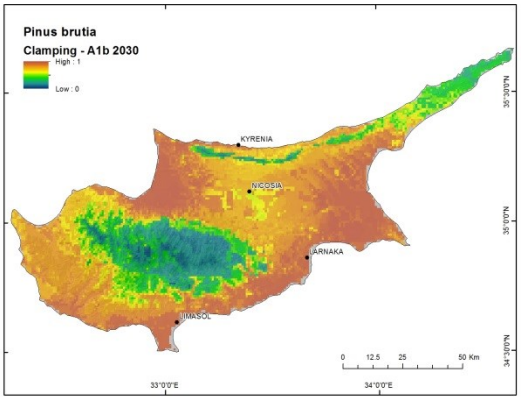

(a)

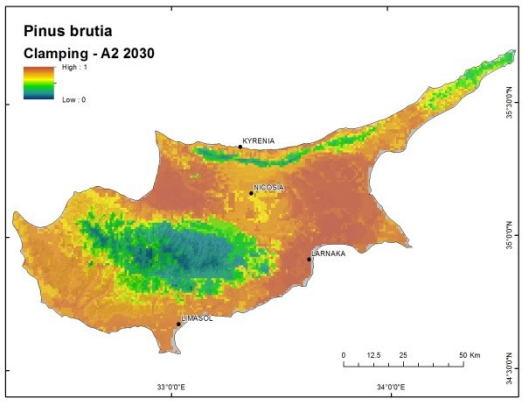

(b)

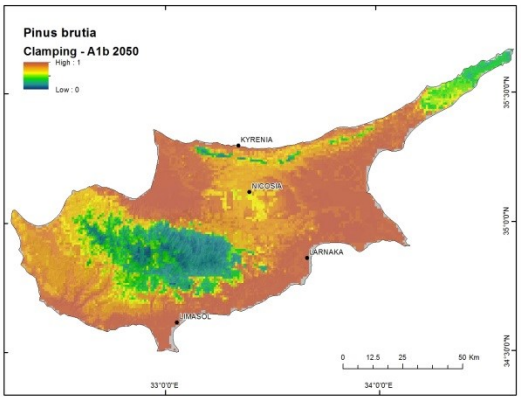

(c)

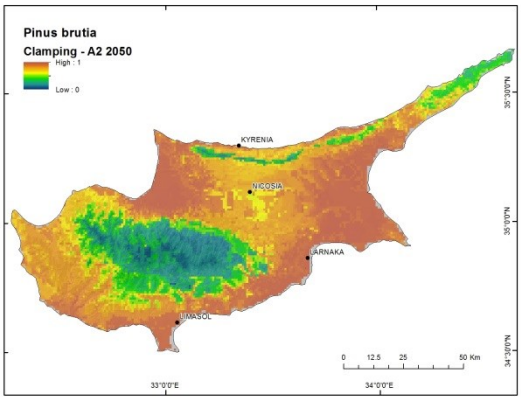

(d)

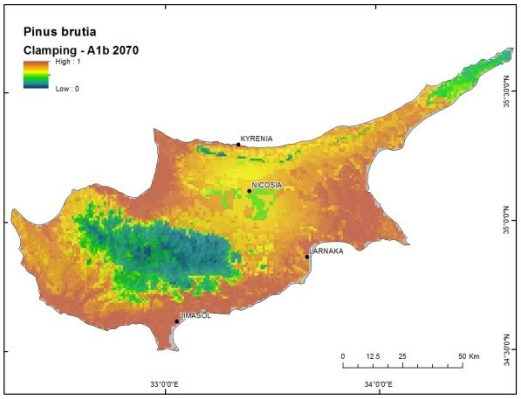

(e)

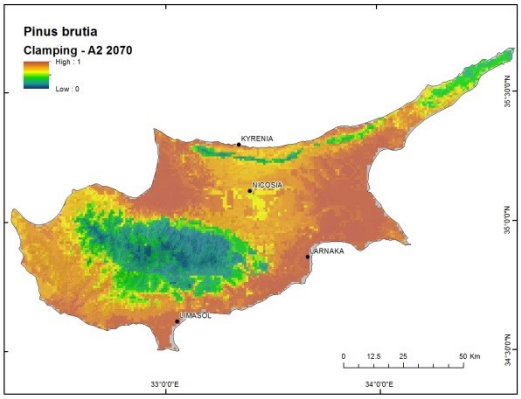

(f)

Figure 63. Clamping maps for *Pinus brutia* under climate scenarios A1b and A2 for 2030, 2050 and 2070. Warmer colors indicate areas where clamping, or restriction of environmental variables used to create the predictions to their values in the training data for present-day vegetation, has occurred.

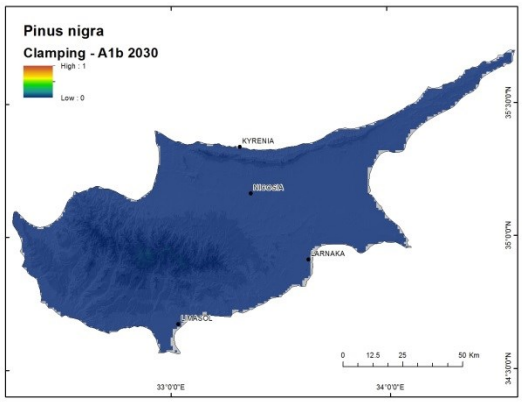

(a)

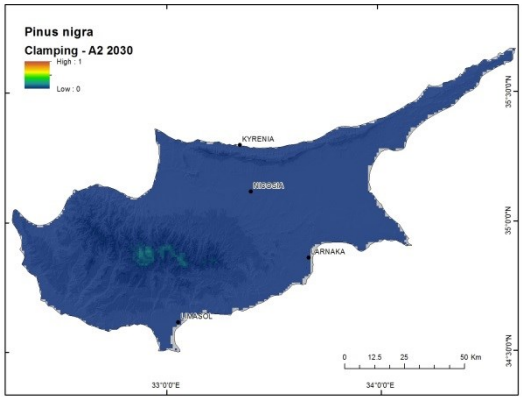

(b)

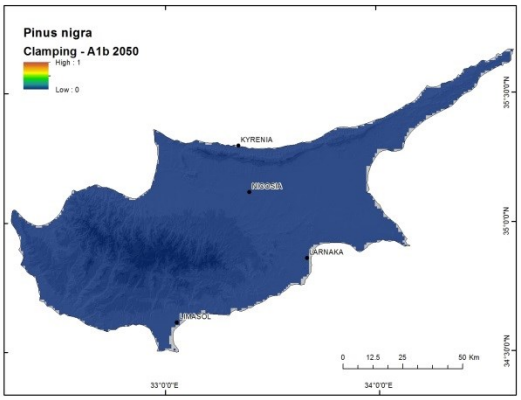

(c)

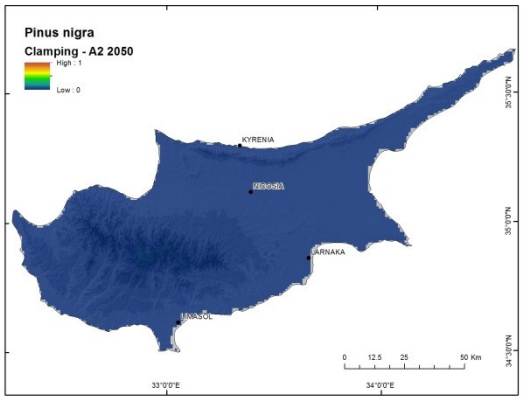

(d)

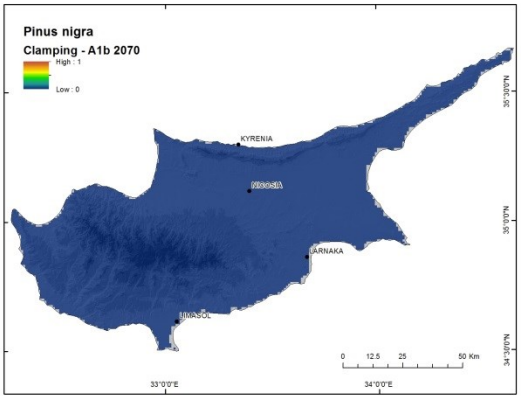

(e)

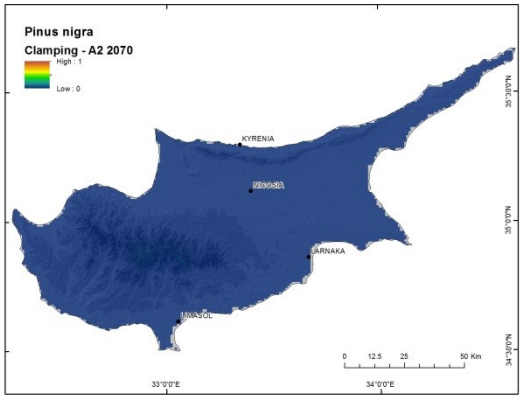

(f)

Figure 64. Clamping maps for *Pinus nigra* under climate scenarios A1b and A2 for 2030, 2050 and 2070. Warmer colors indicate areas where clamping, or restriction of environmental variables used to create the predictions to their values in the training data for present-day vegetation, has occurred.

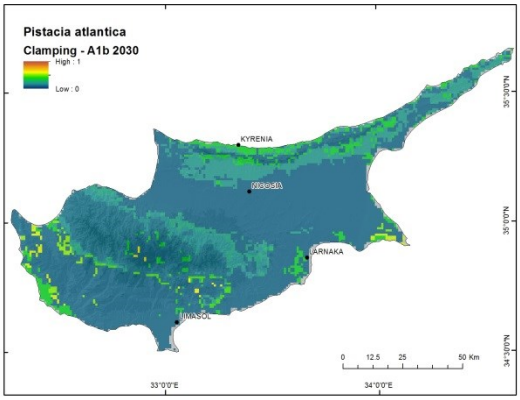

(a)

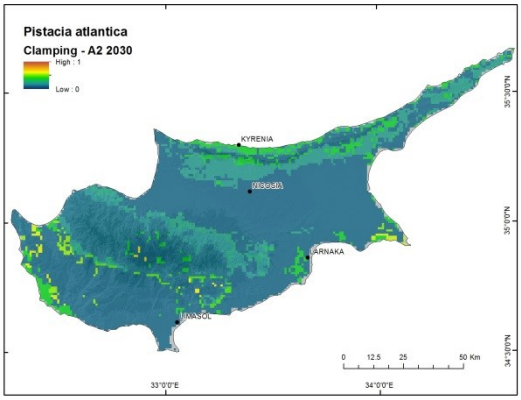

(b)

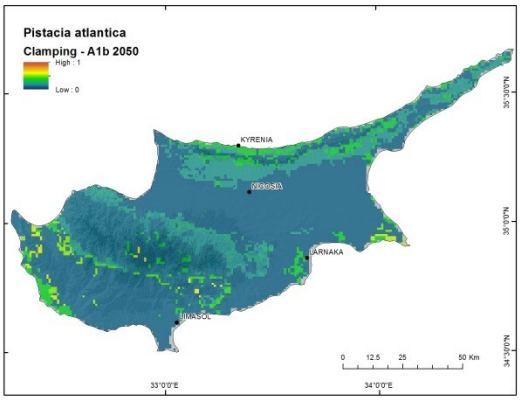

(c)

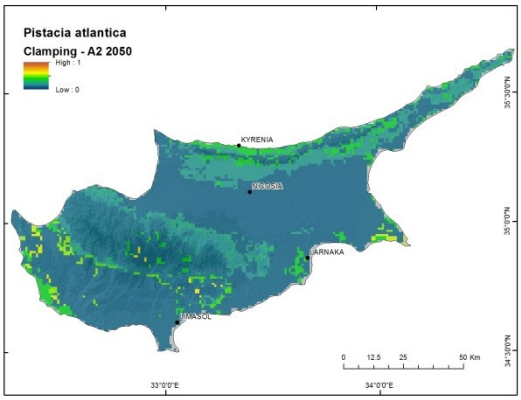

(d)

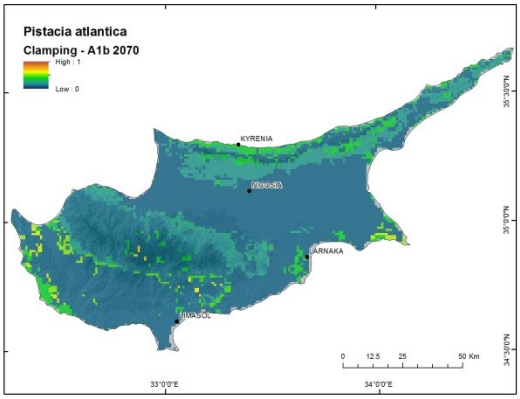

(e)

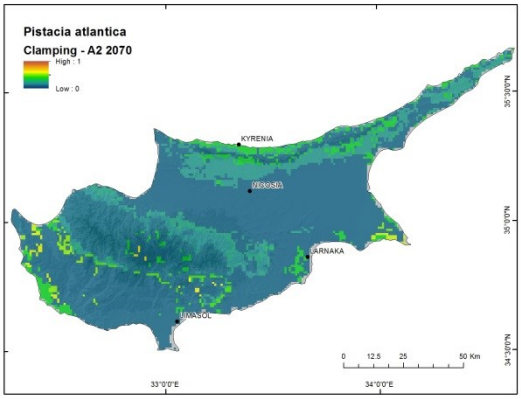

(f)

Figure 65. Clamping maps for *Pistacia atlantica* under climate scenarios A1b and A2 for 2030, 2050 and 2070. Warmer colors indicate areas where clamping, or restriction of environmental variables used to create the predictions to their values in the training data for present-day vegetation, has occurred.

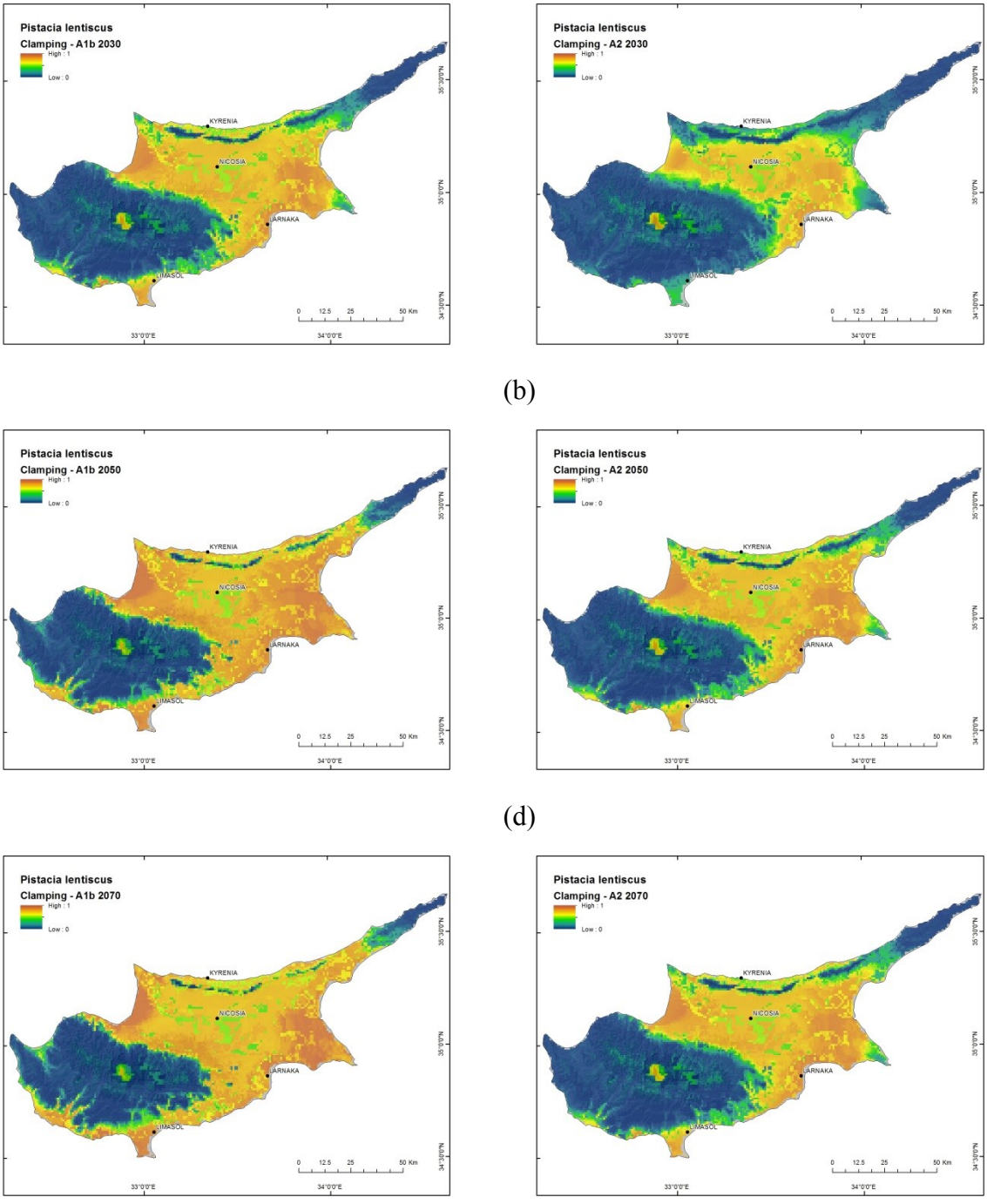

Figure 66. Clamping maps for *Pistacia lentiscus* under climate scenarios A1b and A2 for 2030, 2050 and 2070. Warmer colors indicate areas where clamping, or restriction of environmental variables used to create the predictions to their values in the training data for present-day vegetation, has occurred.

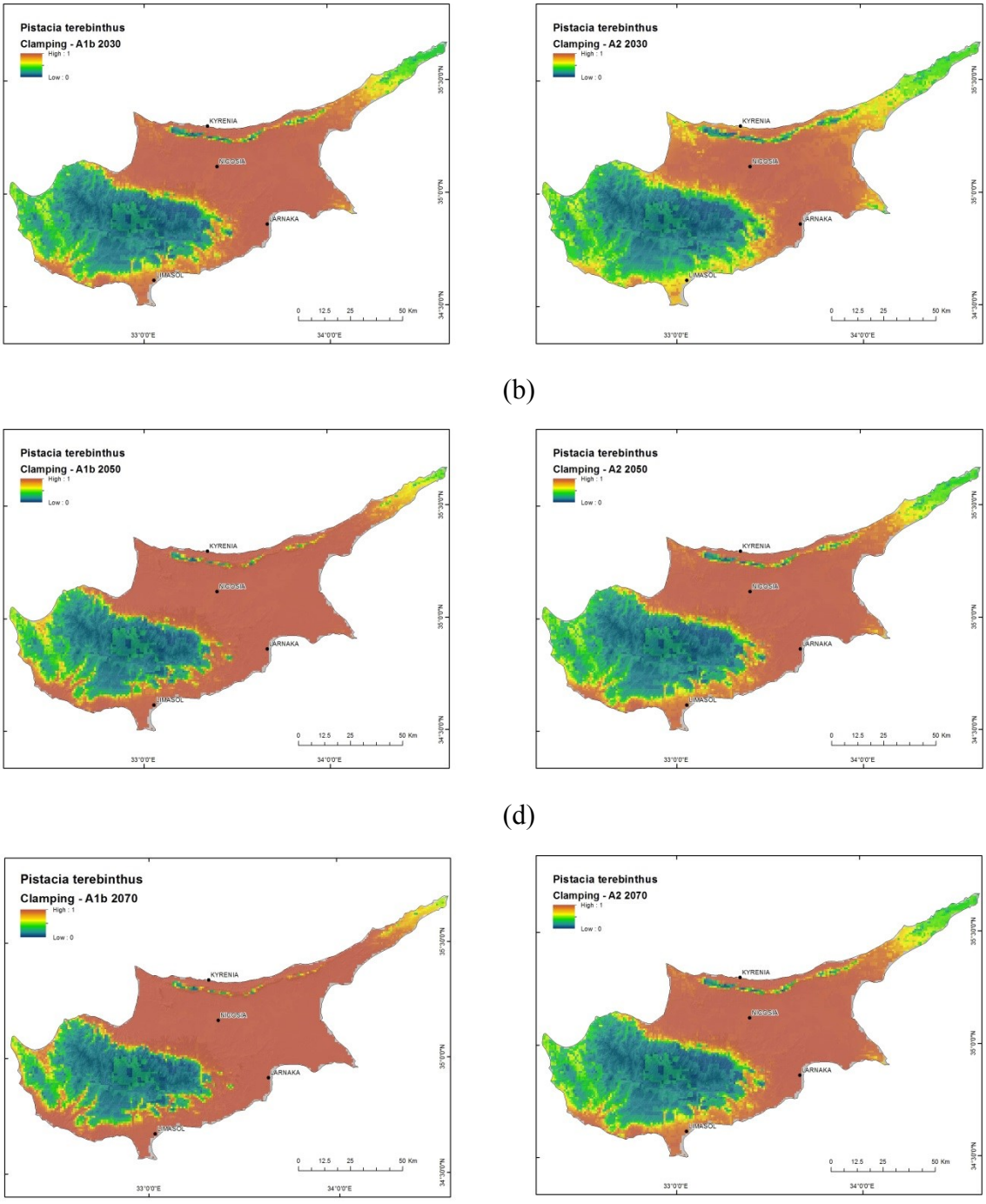

Figure 67. Clamping maps for *Pistacia terebinthus* under climate scenarios A1b and A2 for 2030, 2050 and 2070. Warmer colors indicate areas where clamping, or restriction of environmental variables used to create the predictions to their values in the training data for present-day vegetation, has occurred.

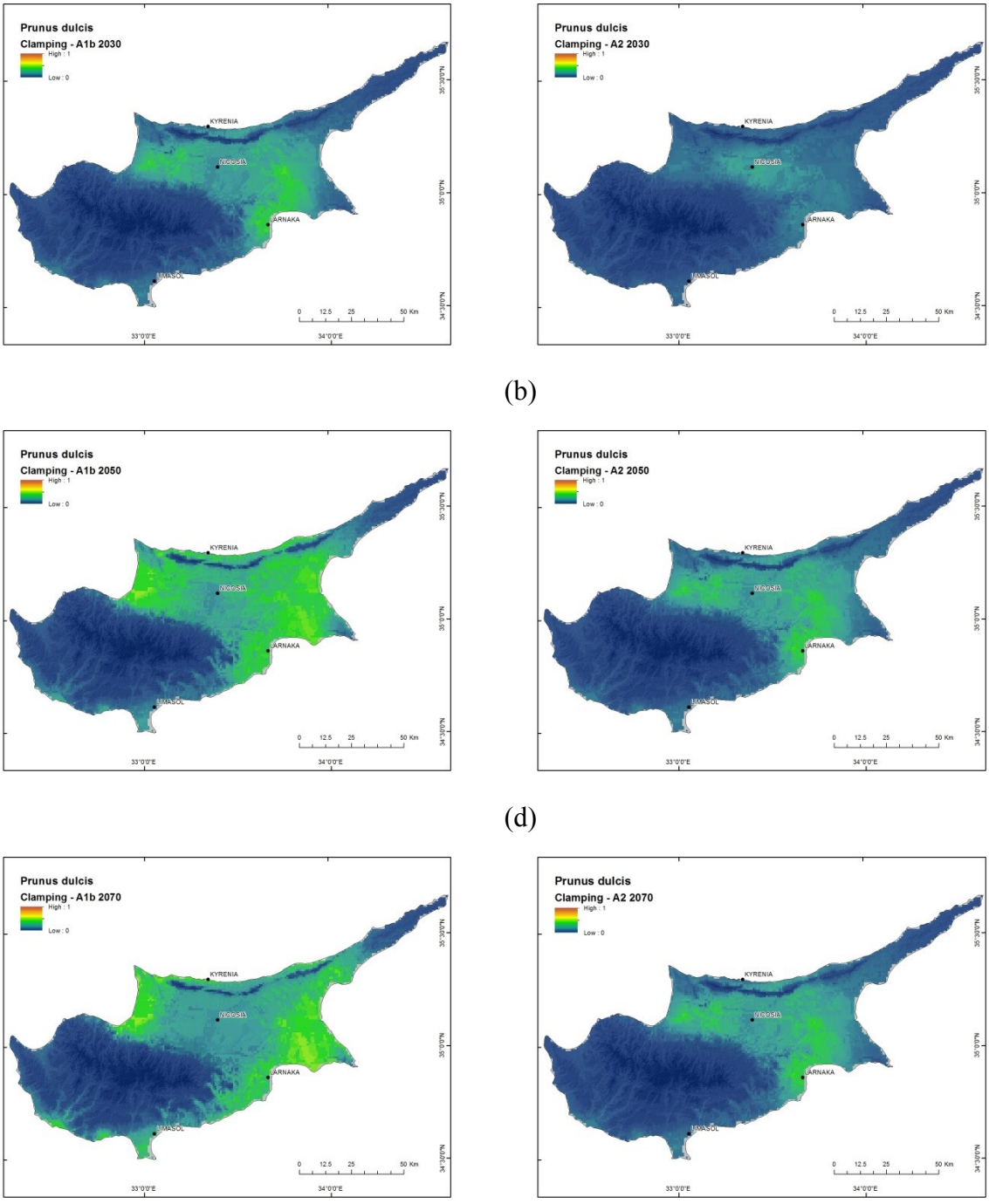

Figure 68. Clamping maps for *Prunus dulcis* under climate scenarios A1b and A2 for 2030, 2050 and 2070. Warmer colors indicate areas where clamping, or restriction of environmental variables used to create the predictions to their values in the training data for present-day vegetation, has occurred.

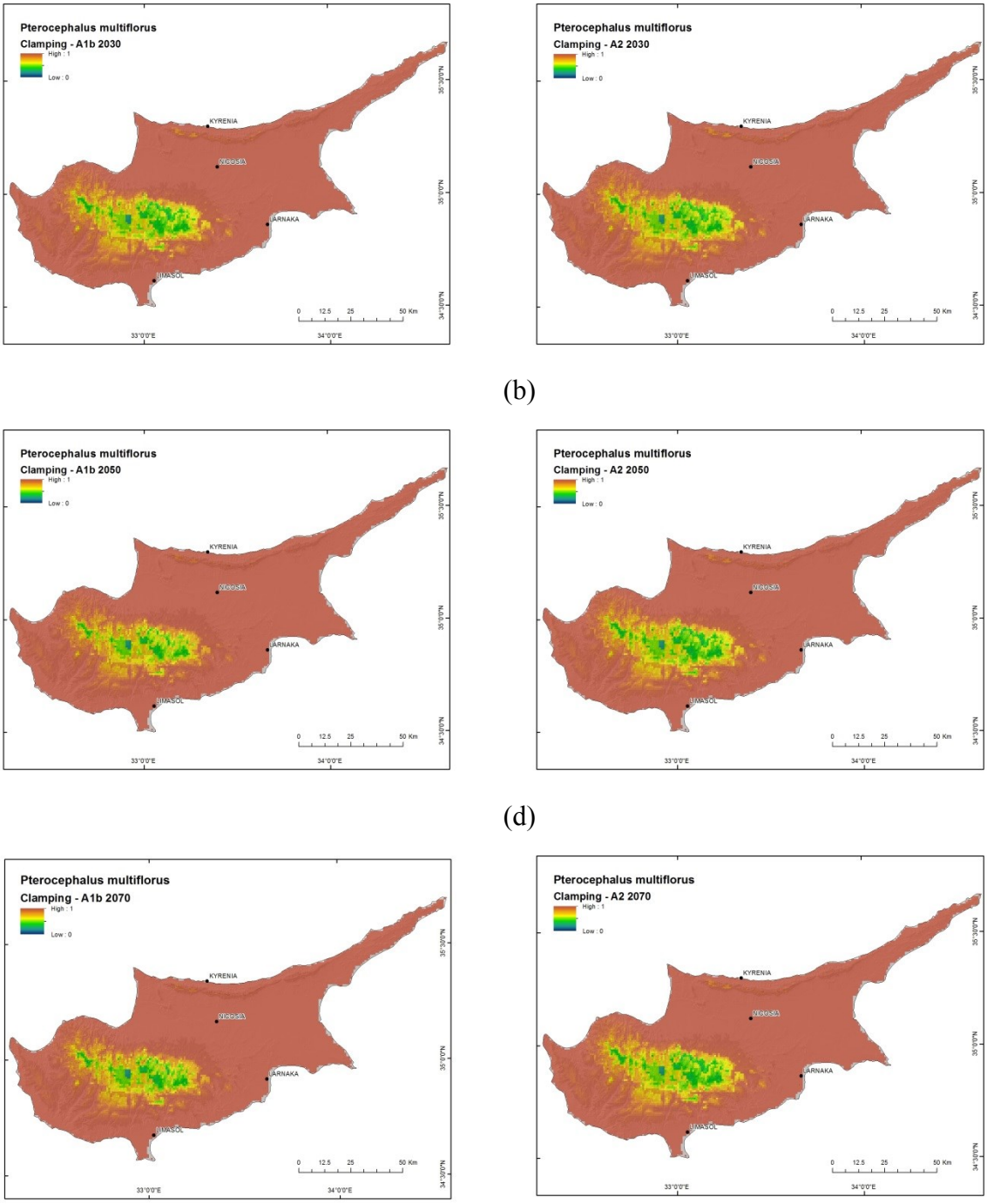

Figure 69. Clamping maps for *Pterocephalus multiflorus* under climate scenarios A1b and A2 for 2030, 2050 and 2070. Warmer colors indicate areas where clamping, or restriction of environmental variables used to create the predictions to their values in the training data for present-day vegetation, has occurred.

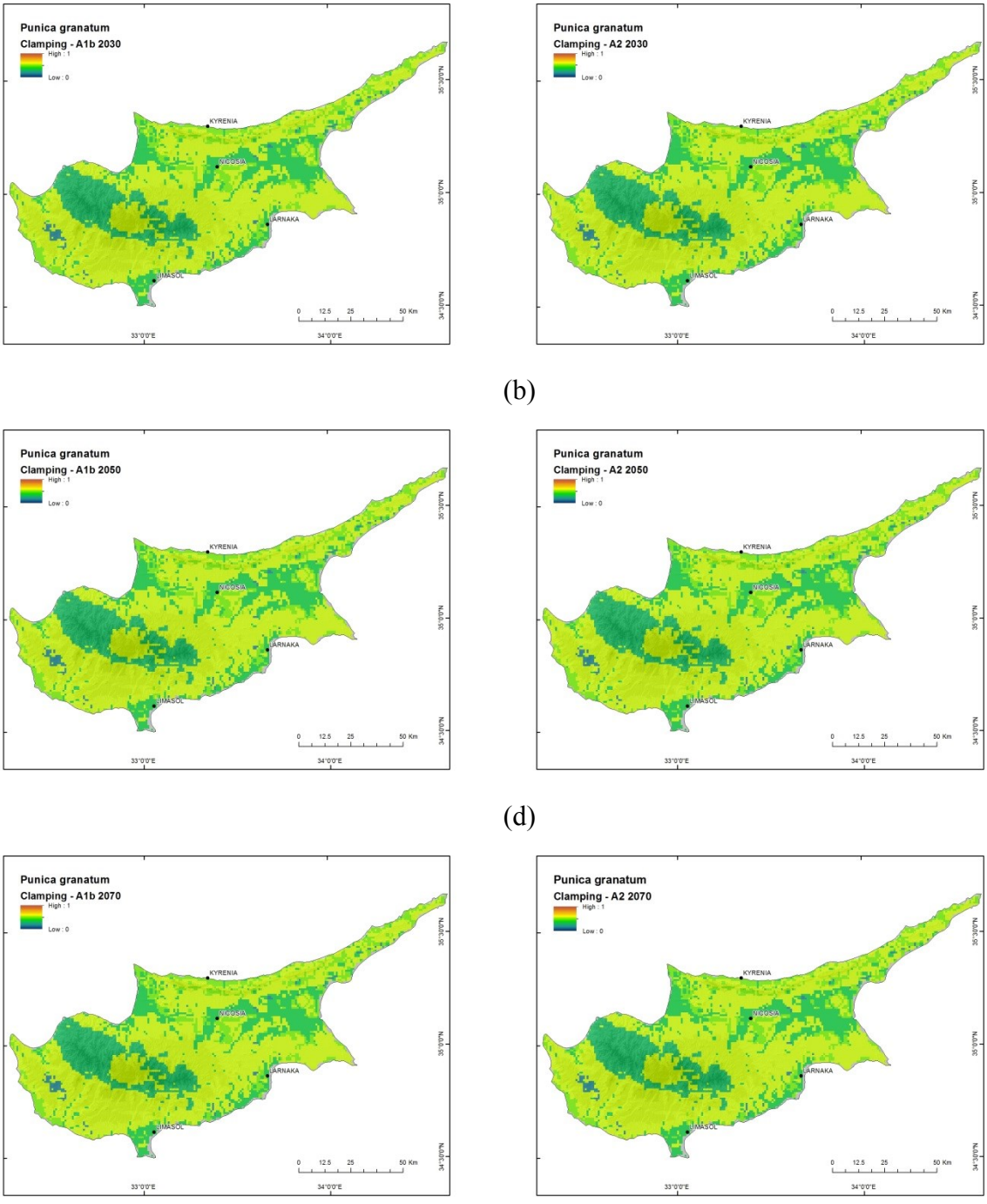

Figure 70. Clamping maps for *Punica granatum* under climate scenarios A1b and A2 for 2030, 2050 and 2070. Warmer colors indicate areas where clamping, or restriction of environmental variables used to create the predictions to their values in the training data for present-day vegetation, has occurred.

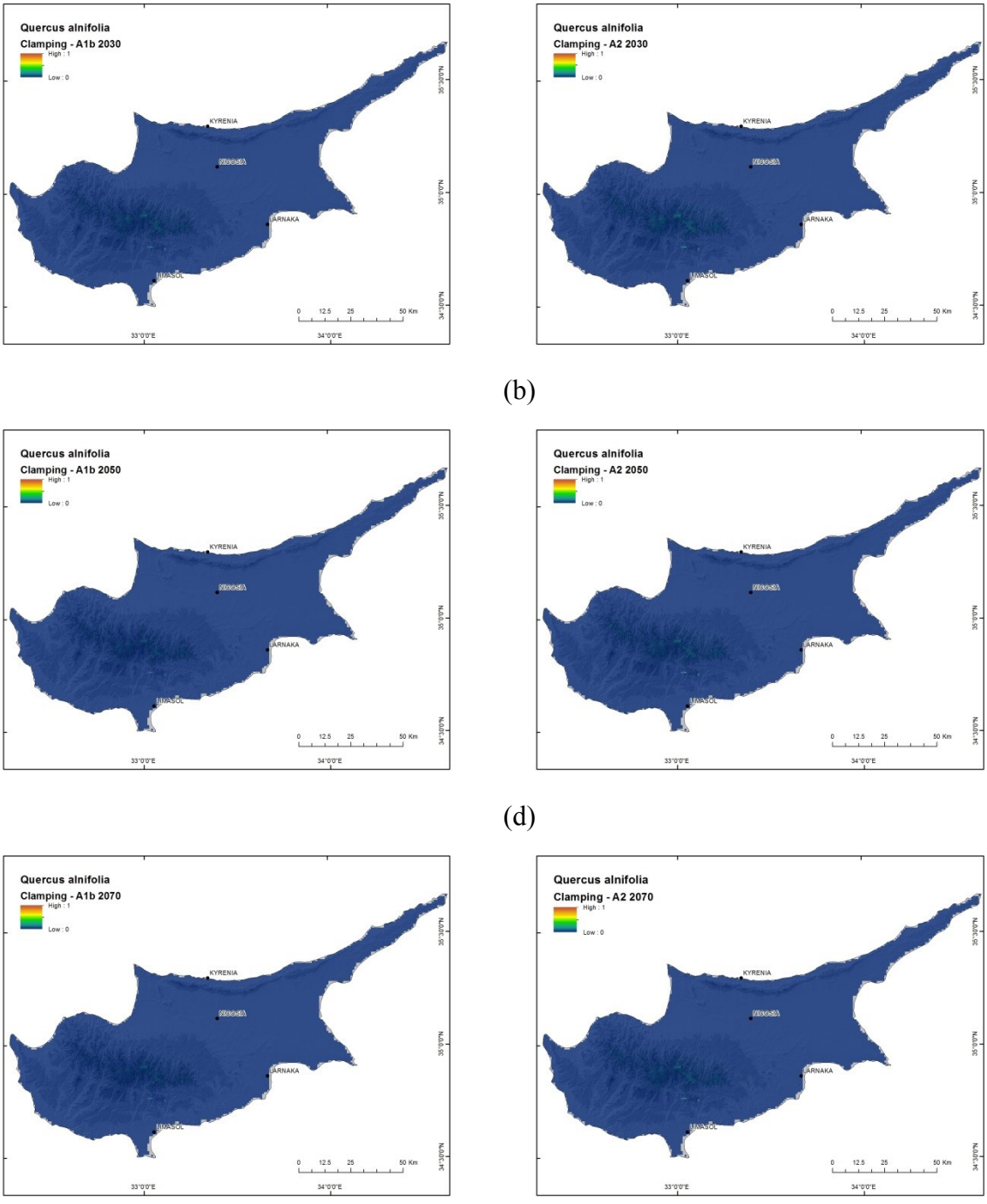

Figure 71. Clamping maps for *Quercus alnifolia* under climate scenarios A1b and A2 for 2030, 2050 and 2070. Warmer colors indicate areas where clamping, or restriction of environmental variables used to create the predictions to their values in the training data for present-day vegetation, has occurred.

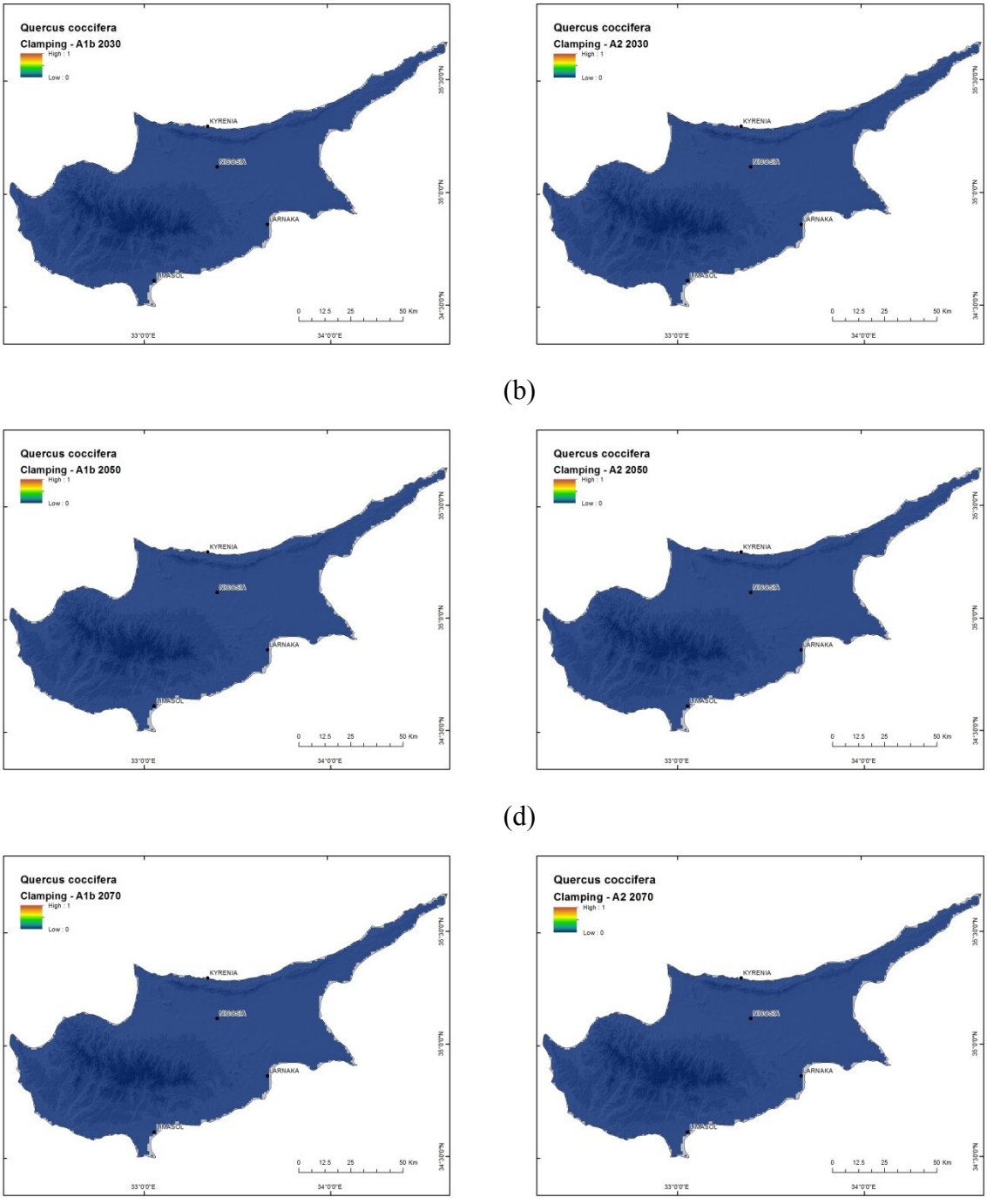

Figure 72. Clamping maps for *Quercus coccifera* under climate scenarios A1b and A2 for 2030, 2050 and 2070. Warmer colors indicate areas where clamping, or restriction of environmental variables used to create the predictions to their values in the training data for present-day vegetation, has occurred.

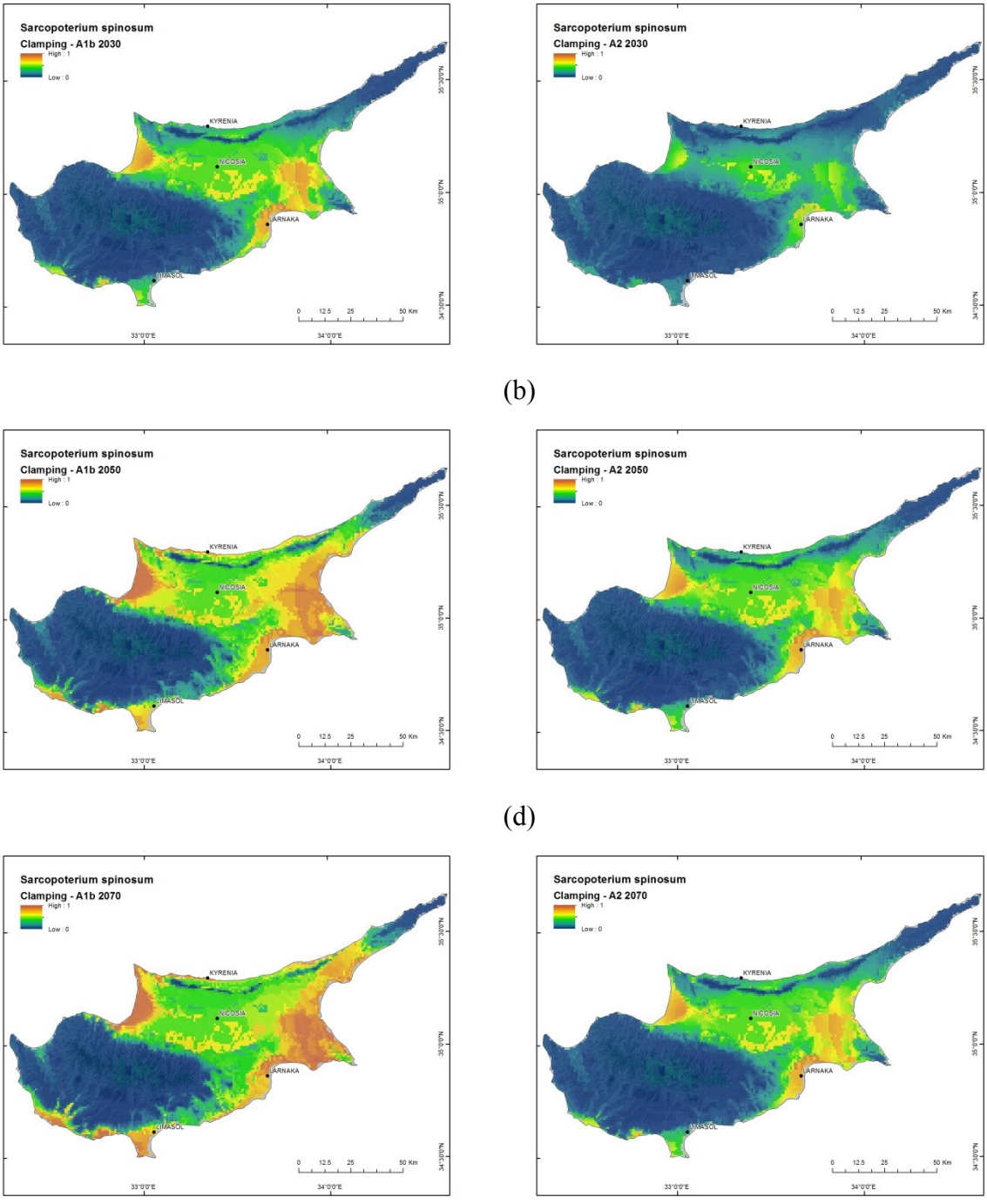

Figure 73. Clamping maps for *Sarcopoterium spinosum* under climate scenarios A1b and A2 for 2030, 2050 and 2070. Warmer colors indicate areas where clamping, or restriction of environmental variables used to create the predictions to their values in the training data for present-day vegetation, has occurred.

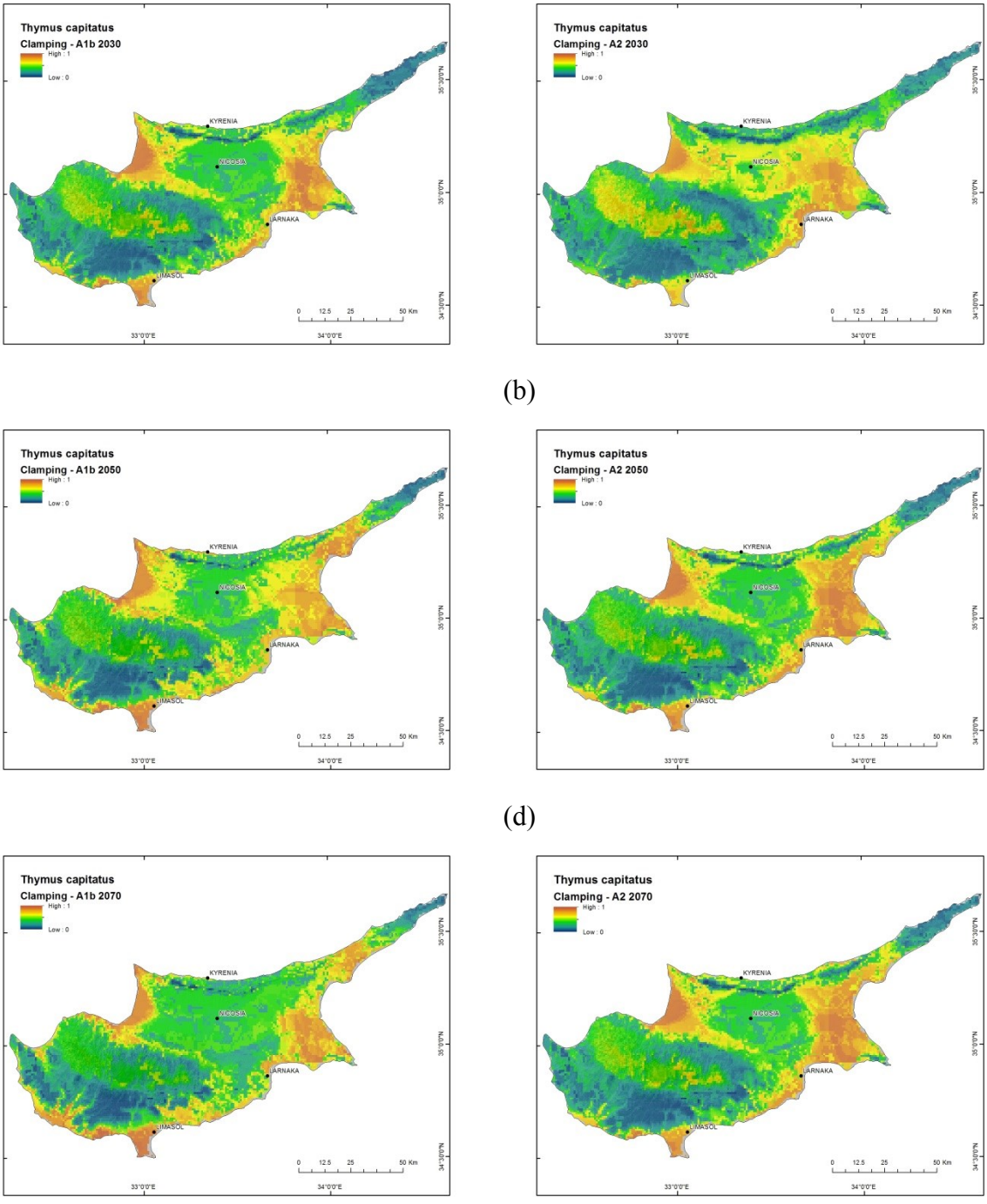

Figure 74. Clamping maps for *Thymus capitatus* under climate scenarios A1b and A2 for 2030, 2050 and 2070. Warmer colors indicate areas where clamping, or restriction of environmental variables used to create the predictions to their values in the training data for present-day vegetation, has occurred.

Multivariate environmental similarity surfaces (MESS maps)

MESS maps indicate how novel an environment is and display the differences between the training and predicted environments, with warmer colors (increasingly negative values) highlighting where the values for at least one predictor variable are outside the range of values in the training data. The number of MESS maps produced depends upon the number of times the Maxent program is parameterized, with one MESS map produced for all models for a species run under the same parameterization. Six MESS maps were produced, one for each climate scenario and time step (Figure 75) as models for each scenario/time step were run at the same time and thus have the same reference data. A similar trend is apparent across the six maps, in which the most differences in training and predicted climate covariates occur at high elevations within the Troodos and Kyrenia Ranges, as well as across the central part of the Mesaoria Plain and the Karpas Peninsula. The area and intensity of novel environments increase over time.

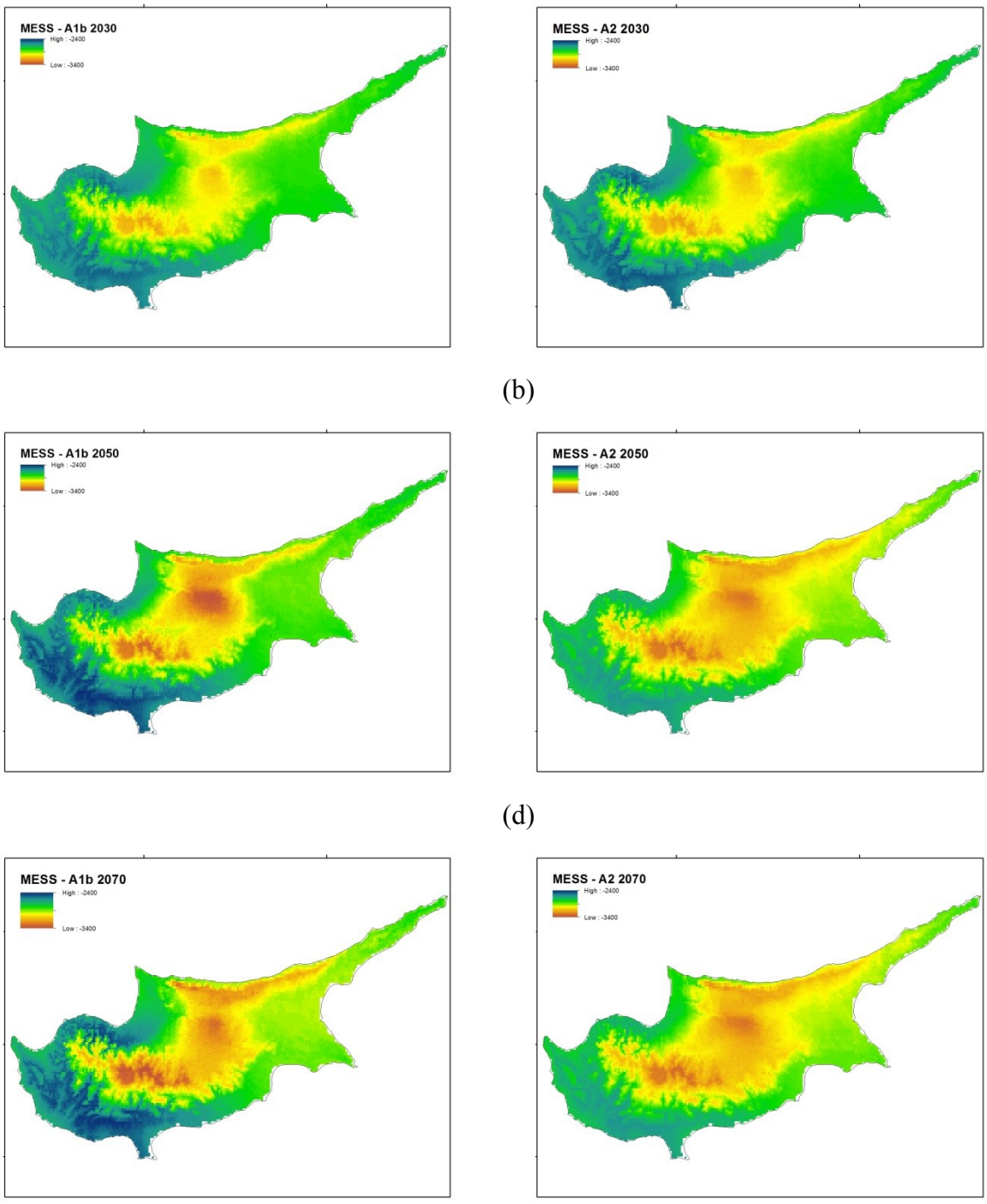

Figure 75. MESS (Multivariate environmental similarity surfaces) maps illustrate where the values of at least one future environmental variable is outside of the range of the training data for present-day environmental variables. Warmer colors indicate larger differences between the predictor covariables and the training data.

Most dissimilar variable/Limiting factor (MoD maps)

Maps that illustrate the variable most responsible for the novel environment are referred to as MoD or limiting factor maps. Six maps were produced (Figure 76), one for each climate scenario and time step. The MoD is extracted at each pixel and is the variable that has the smallest value of similarity between the training data and the projected climate covariates (Elith et al., 2010). The variable is then mapped to highlight where a particular variable is influencing the MESS and hence, the prediction. These maps show that three variables are responsible for the novel environments depicted by the MESS maps. BIO4 (temperature seasonality) primarily influences the Mesaoria Plain and Karpas Peninsula indicating that the variation in monthly temperatures in the future climate data is outside the variation in monthly temperatures for the training data. Thus BIO4 is the least similar to training conditions and is the limiting factor in the ability of the model to project over the new environmental space. BIO10 (mean temperature of the warmest quarter) influences the coastal areas for most scenario/time steps. This indicates that species may be predicted to occur here as the model is clamped to restrict predictions so as only to occur within known extremes of the training data. However, the species may not actually be suited for the increased temperatures that are predicted to occur in the climate model. BIO7 (temperature annual range) influences the Mesaoria Plain near Morfou Bay and skirts the Troodos foothills in a north to southwest fashion. The MoD maps do not indicate the variable that limits the distributions of species, but indicates the variable that is the most different from the present-day training variables, thus limiting the model's ability to predict into the new environmental space.

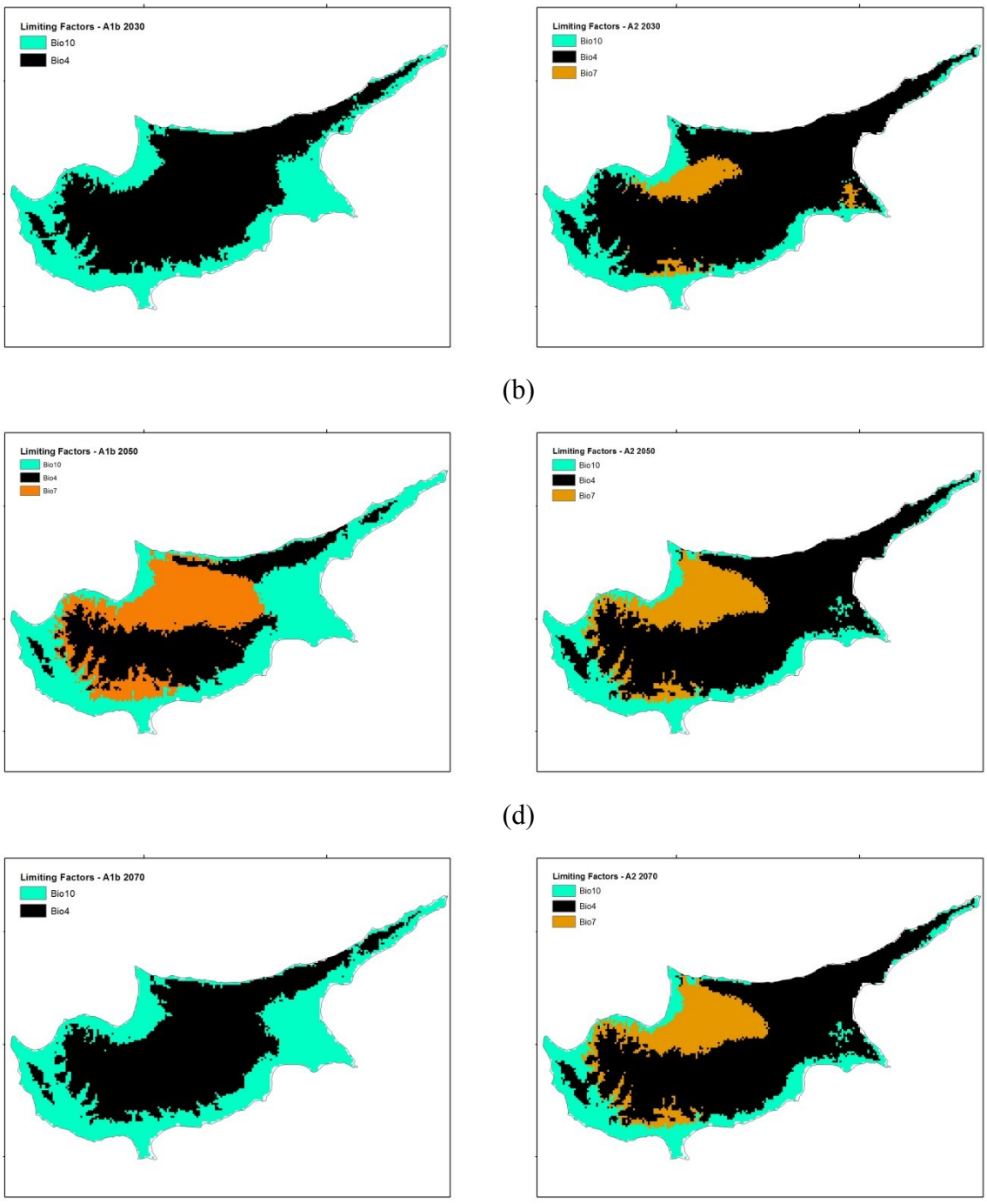

Figure 76. Limiting factor or most dissimilar variable (MoD) maps highlight the variables that are the most different in the future from the same environmental variable in the training data. BIO4, BIO7 and BIO10 area all temperature-related data, indicating the most drastic changes under future climate scenarios are in temperature.

Discussion

Endemic species and species of concern

Under both A1b and A2 climate scenarios, all four endemic species (*Cedrus brevifolia, Helianthemum obtusifolium, Pterocephalus multiflorus,* and *Quercus alnifolia*) are predicted to lose all suitable environments as soon as 2030. Modeling results for *Cedrus brevifolia* and *Q. alnifolia* represent a likely scenario as these species are currently restricted in range, only occurring at higher elevations in the Troodos Range. Although locally abundant (Meikle, 1977, 1985), *C. brevifolia* is primarily restricted to the Cedar Valley (Tripylos area of the Pafos Forest) along the western slopes of the Troodos. Many observations of this species outside of this range represent extensive planting in the forest, along roadsides, and mountain villages (Tsintides et al., 2002; personal observation). *Cedrus brevifolia* also is listed as Vulnerable under the European Red List of Vascular Plants (Bilz et al., 2011), indicating the species is considered as threatened when ranked according to the IUCN Red List Categories and Criteria, version 3.1 (IUCN, 2012). *Cedrus brevifolia* forests and scrub, and low forest vegetation containing *Q. alnifolia* are listed as priority habitat types under Annex I of the Habitats Directive (Council of European Communities, 2007), indicating a habitat type that requires the designation of special areas of conservation. The model predictions in conjunction with the current status of *C. brevifolia* and *Q. alnifolia* habitats indicate that these species are highly likely to contract in known extent due to present-day restrictions on expansion to higher elevation, as well as climate change.

Endemic forests and coastal dunes with *Juniperus* spp. are also included as priority habitats under Annex I of the Habitats Directive (Council of the European

Communities, 2007). In addition, Mediterranean arborescent matorral with *Juniperus* spp. appears in Annex I, indicating conservation of this habitat type requires designation of special areas of conservation; it is not a priority habitat type at this time, however. *Juniperus phoenicea* occurs in coastal maquis (a type of matorral), and although considered locally abundant (Meikle, 1977, 1985), is predicted to lose all suitable areas of occurrence by 2030. Although there are only 14 observations for this species, they are widely dispersed across Cyprus' coastlines. Given the restricted nature of coastal dunes and modern *J. phoenicea* ranges (*J. phoenicea* is not restricted to coastal dune habitats), the modeling results present the highly likely scenario that this species will lose all suitable environments under either climate scenario by 2030. *Juniperus foetidissima* is also highly likely to lose all suitable environments under either climate change scenario by 2030, as it is currently restricted to the higher elevations of the Troodos, often within the endemic *Pinus nigra* forests

The modeling results for *H. obtusifolium* should be interpreted with extreme caution, as sample size was low ($n = 10$) and the modern model was statistically insignificant ($p = 0.605$) and thus the null hypothesis cannot be rejected. This species has been observed across all botanical divisions of Cyprus (Hand et al., 2011; see Figure 2 for botanical divisions) and is not a current species of concern (see Table 17). Thus, the modeling results for *H. obtusifolium* are likely the product of small sample size and poor sampling distribution across its entire known range (see Figure 21h). Similar precautions apply to model results for *P. multiflorus*. This species has been observed in all botanical divisions except 4 and 8; however, observations for this study were limited to the Troodos Range (Divisions 2 and 3). Modeling results were significant ($p = 3.18 \times 10^{-8}$)

and a sample size of 38 is adequate, but with limited coverage across the known range for the species, the model's performance in terms of biological significance likely is very poor.

Although the availability of suitable habitat is predicted to decline, this represents the limited availability of habitat for the expansion or relocation of the species, in some cases as soon as 2030. However, longer-lived tree species may persist beyond this time frame particularly on the shady and/or cooler slope faces. These refuges may allow for the regeneration of species as long as the environmental conditions remain suitable and the species are not impacted by competition, disease or human-related development. The spatial resolution of the climate variables (1 km^2) influences the ability of the model to detect small regions where environmental (microclimatic) conditions remain amenable to species regeneration.

Range-expanding species

Under A1b and A2 climate scenarios, five species expanded their modern distributions (Table 21; Figures 44-52): *Ficus carica, Pistacia lentiscus, Prunus dulcis, Sarcopoterium spinosum* and *Thymus capitatus*. *Pinus brutia* also expands its range under the A2 climate scenario. Under A1b, *Ficus carica* expands across the Mesaoria Plain, along the southern coast, and into higher elevation areas of the Troodos. Under A2, this species expands across the entire island, with small areas in the Kyrenia Mountains, the Karpas Peninsula, and the Mesaoria Plain predicted as unsuitable. *Pistacia lentiscus, Sarcopoterium spinosum* and *Thymus capitatus* expand across the southwestern coast into higher elevations of the Troodos and Kyrenia ranges, and along the northeastern extent of the Karpas Peninsula under both climate scenarios. *Prunus dulcis* is predicted to increase

its suitable areas under both climate scenarios, with most of the island considered as suitable by 2070 under the A1b scenario. Under the A2 scenario, only a few places along the northern coastline, across the Mesaoria Plain and the Akamas Peninsula are predicted as unsuitable. The results for *Pistacia lentiscus* and the cultivated trees *Ficus carica* and *Prunus dulcis* and were unexpected. Although primarily restricted to cultivated areas at this time, *Ficus carica* and *Prunus dulcis* are known across the island as escapees. The models indicate that the areas suitable for their cultivation increase (assuming soil, moisture, and nutrient availability), accompanied by areas of increased environmental suitability for escapees. *Pistacia lentiscus* is commonly found on dry, rocky slopes (Meikle, 1977, 1985). It was assumed, however, that low elevation temperatures would exceed the environmental range of the modern distributions, causing the species to disperse to higher elevations, but remain within the precipitation (dryness) range of its modern distributions. It is possible that all three species are generalists and could exist in other areas on the island, but are presently restricted due to limitations on expansion or competition with other species. A common criticism of climate-based models is that species interactions, nutrient requirements, and dispersal abilities are rarely incorporated (Araujo et al., 2005; Guisan and Thuiller, 2005; Dormann, 2007; Franklin, 2010), often because appropriate data often are unavailable, particularly for rare species and species of conservation concern (Guisan and Thuiller, 2005).

Model validation

Models were evaluated using three tools built into Maxent: clamping, MESS maps, and MoD maps. Together these tools allow modelers to assess how model results are influenced when projecting potential species distributions into future climate

conditions. Some of these climate conditions are novel, since they do not occur at present across the known range of a species of interest. Additionally, it is not known how most species will react to these new climate conditions and interact with other species under new conditions (Dormann, 2007; Fitzpatrick and Hargrove, 2009; Elith et al., 2010).

Clamping

Phillips et al. (2006) address the issue of prediction into novel (or non-analogous) climatic conditions by "clamping" predictions based upon the minimum or maximum values under which the model was trained. Thus, when novel climates exceed training values in one or more of the predictor variables, the model response is not excessive (Elith et al., 2010). Although this method addresses the issue of projecting into environmental conditions under which the model was not trained, it does not accommodate the possibility of novel combinations of climatic conditions that do not exist in the training or future climate data sets (Fitzpatrick and Hargrove, 2009). Clamping was observed across a portion of the island for *Cistus salviifolius, Helianthemum obtusifolium, Juniperus phoenicea, Olea europaea, Pinus brutia, Pistacia lentiscus, Pistacia terebinthus, Pterocephalus multiflorus, Sarcopoterium spinosum,* and *Thymus capitatus*. Locations where high degrees (Figures 53-74, warmer colors) of clamping overlap with predicted distributions should be interpreted cautiously since these predictions were held to conditions within the known training data set and may not accurately represent future climatic conditions or species combinations. *Cistus salviifolius* has very weakly predicted suitable areas under future conditions, even where clamping did not occur. This species is predicted predominately in the Troodos Range and along its foothills, although it occurs today across the island and at elevations up to

1400 m. *Helianthemum obtusifolium* exhibited clamping in areas of known occurrence, indicating that climate conditions under future scenarios are very different from present conditions at sites where it is observed. This species also occurs across a larger geographical extent and elevational range than exhibited in the observation data. *Juniperus phoenicea* presently is distributed along the coastlines and up to approximately 300 (-500) m. Meikle (1977, 1985) indicates that this species occurs in localized abundances, but clustered observation points do not necessarily improve SDM predictions of suitable areas as new information is not added to the environmental conditions under which the species occurs. Clamping for *Olea* europaea, *Pinus brutia, Pistacia lentiscus, Pistacia terebinthus, Pterocephalus multiflorus, Sarcopoterium spinosum* and *Thymus capitatus* occurred primarily outside of any predicted suitable areas, thus their predicted distributions should reflect the most suitable climate conditions for these species.

Multivariate environmental similarity surfaces (MESS maps)

The MESS maps illustrate where novel climates are predicted on the basis of the reference points selected during model training (Elith et al., 2010). Increasing negative numbers (warmer colors) indicate the level of dissimilarity of at least one predictor variable that is outside of the range of environmental conditions within the reference set of points (Elith et al., 2010). In Maxent, the observation training data are used as the set of reference points (Phillips, 2010). For Cyprus the most dissimilar, or novel, predicted environments occur within the Troodos and Kyrenia Ranges across all scenario/time steps (Figure 75). Over time, environmental conditions become increasingly dissimilar over a broad geographic extent across the island, as illustrated by growing differences

between the Mesaoria Plain and Karpas Peninsula. The Mesaoria Plain has a long history of human land uses. Much of the Plain is under cultivation (current or fallow), under urban development, or falls within or near the buffer zone. As a result, many species that once occurred on the Plain are now absent. This situation skews modeling results, as approximately 35 points fall within the Plain, all of which were along roadsides. Thirteen historical points provide information predating the impacts of modern development (see Figure 5). The middle section of the Plain is sampled minimally due to the impacts of the urban outskirts of Nicosia and the inaccessibility of roadside stopping points.

Hypotheses

In response to the question "*How will the current species' distributions change with respect to IPCC AR4 A1b and A2 climate scenarios for 2030, 2050, and 2070?"* SDMs were generated to evaluate two climate scenarios over the three time steps. The following predictions were generated:

Prediction 1: Under an A1b scenario: Minimal changes are expected for most species distributions with the exceptions of high elevation or coastal species. For high-elevation species, Cyprus has only two major mountain ranges, both of which are relatively low in elevation (1952 m maximum), thus further expansion to higher elevation is not possible for some species. In addition, northward expansion entails little change in climate since Cyprus' latitude only varies by approximately 250 km. With increases in temperature and sea level, species currently restricted to the coast will likely expand their ranges inland.

Prediction 2: Under an A2 scenario: Species distributions will be limited by high temperature or low precipitation, and will expand to higher elevations. For some species

this may cause a restriction to modern distributions. Generalists will likely expand into new habitats currently unavailable to them due to resource competition or other limiting factors. High elevation species and species with modern limited distributions will be lost by the end of the 21st century.

Evaluating prediction 1

Contrary to Prediction 1, a majority (14 of 22) species are predicted to lose all suitable areas by 2070, with 11 of those eliminations occurring by 2030. *Pistacia terebinthus* and *O. europaea* will reduce their ranges by 2070 (by approximately 18% and 59%, respectively), with both species increasing their suitable areas at higher elevations, losing suitable area along the southern foothills of the Troodos, and losing small areas in the Kyrenia Mountains. *Punica granatum* will lose approximately 96% of its suitable area by 2070, leaving fragmented parcels across the lower elevations of the island. All other species will increase their ranges between the modern and 2070 predictions, an effect not expected among *F. carica, P. lentiscus,* and *P. dulcis* (see Range expanding species under Discussion).

Evaluating prediction 2

Similar trends exist under the A2 climate scenarios according to which 14 of 22 species are predicted to lose all suitable areas by 2070, with 12 of those losses occurring by 2030. The same species expand in range under the A2 scenario, with the addition of *O. europaea*, expanding its range by approximately 38%. *Pinus brutia* does not lose all of its suitable areas under this scenario, but is predicted to become more restricted in area, losing approximately 38% of its suitable area, most of this occurring along the foothills of the Troodos. Known generalists *S. spinosum* and *T. capitatus* would increase their

predicted suitable areas considerably, with expanded areas of approximately 152% and 123%, respectively.

Conclusions

This research generates models that assess how species will respond to predicted climate change on Cyprus, in particular under scenarios of global warming. Species distribution model predictions for outcomes under A1b scenarios did not meet the expectations highlighted in Prediction1 with SDMs indicating the loss of suitable habitat for many of the modeled species, including endemics and species of concern such as *C. brevifolia, P. nigra, P. multiflorus,* and *Q. alnifolia*. Under A2 scenarios, predicted SDM results are closer to expectations discussed under Prediction 2, with losses of suitable area for higher elevation species (*P. nigra, J. foetidissima*), coastline species (*J. phoenicea*), and restrictions to the ranges of other species (*P. brutia, P. terebinthus*). Under both scenarios, generalist species are predicted to gain suitable areas.

Under the selected climate model and scenarios selected, endemic and indigenous tree species such as *Quercus alnifolia* and *Cedrus brevifolia* experience a reduction to their suitable areas of occurrence as soon as 2030. The only exception to this is *Pinus brutia*, which has a 38% reduction to areas of suitability by 2070 under the A2 scenario, but no suitable areas by 2070 under A1b. Cultivated orchard species *Prunus dulcis* and *Ficus carica* are predicted to fare exceptionally well under both climate scenarios, expanding their areas of suitable occurrence. Generalist species *Sarcopoterium spinosum* and *Thymus capitatus* also increase in suitable areas of occurrence, potentially filling in areas where they are currently restricted due to competition with other species. The decline in occupied habitats will potentially leave large areas of highly reflective,

calcareous soils exposed. This may impact those species predicted to persist through the climate scenarios as albedo will increase and soil moisture content will decline in conjunction with increasing temperatures.

Species distribution models assume that the species are currently in pseudo-equilibrium with their environment as the sampling points only represent the relationship between the species and environmental variables over a limited period of time and/or space (Guisan and Thuiller, 2005). An additional assumption is that factors restricting the species' environments historically will remain limiting factors in the future (Guisan and Thuiller, 2005); however, it is unknown how species will respond to a new suite of climate conditions or to other species under these conditions and in the case of Cypriot trees, many are likely restricted in range due to historical and present-day agricultural practices. SDMs provide a method for assessing potential changes to species distributions throughout time in order to support management and conservation decisions (Guisan and Thuiller, 2005). Due to the number of indigenous species and rapid land cover transitions in Cyprus, the degree of expected climate change and sea level impacts are likely to severely reduce available habitats for many species.

Chapter 6

DISCUSSION

The species of the Mediterranean Basin have experienced changes through the modification of landscapes throughout human history. In Cyprus, the relatively recent population movements due to political instability in the late 1950s through 1974 resulted in the accelerated abandonment of agricultural systems and growth of urban areas, particularly in southern Cyprus. Although Butzer and Harris (2007) propose Cyprus biota to be resilient to human transformations of the landscape, they do not account for rapidly changing landscapes due to population migrations or the combined impact of land cover changes and climate change to species. Vegetation on Cyprus faces additional pressures under climate change due to its limited elevation and north-south extent, thus limiting the potential of species to expand their ranges. Coupled with land cover modifications to artificial surfaces, species may be left with few areas of available habitat. Given these pressures, it is important to address the combined effect of land cover changes and climate change on future distributions of vegetation in Cyprus.

Land cover was not explicitly included in the Maxent models of species for three reasons: 1) land cover, especially forests, shrub lands and grasslands, are not independent from climate data (Thuiller et al., 2004); 2) land cover is considered an indirect environmental variable that may not have the same relationships to future distributions of species (Guisan and Zimmermann, 2000; Thuiller et al., 2004); and 3) land cover transformations, their drivers and rates were not conducted as part of the land cover assessment in this dissertation. However, simple models created through the overlay of existing land cover and the binary species distribution maps can highlight areas that are

of interest for conservation or management objectives. This method will exclude areas currently classified as artificial areas and water from consideration as future suitable areas of occurrence. Bare soils were included to account for fields that might be fallow but misclassified as bare rock/ground. Using present-day land cover is a conservative estimator of the interaction between land cover and species occurrence as coastal and urban areas are still predicted to expand in the future. Additional declines in agriculture may occur, particularly in southern Cyprus, which may create the potential for suitable areas of expansion for some species and may reduce the effects predicted by the SDMs for potential areas of future occurrence. To highlight the possible interactions of climate change and land cover, only species that maintained any predicted suitable habitats under the two climate scenarios by 2070 were included in this analysis (Table 21).

Figures 77 to 85 illustrate the combined effect of present-day land cover (2011) and future species distributions. These maps are compared to the binary presence/absence maps created for each climate scenario in 2070 to determine if land cover influences the potential distributions of species (Figures 44-52). *Olea europaea, Pinus brutia, Punica granatum, Pistacia lentiscus* and *Pistacia terebinthus* do not experience reductions to predicted areas of suitability with the inclusion of land cover types. These species are primarily restricted to the forests and shrub and/or herbaceous land covers in the predictions, thus changes to artificial areas will have little impact on these species. With the exception of *Punica granatum*, these species are currently found in similar land cover types, so only the conversion from forests to shrubs or forests/shrubs to agriculture will influence the local distributions. Changes to climate conditions will most influence the potential suitable areas of occurrence. *Punica granatum* is predicted to only occur in

small patches across Cyprus by 2070 under the A1b scenario and does not have any areas predicted as suitable under A2 in 2070. *Punica granatum* currently grows as an ornamental or orchard species, although it is usually intermixed with other orchard species or planted along the boundaries of orchards or fields. It is not likely to persist outside of cultivation under future climate conditions but may exist outside of predicted areas of suitability due to care by humans.

Ficus carica and *Prunus dulcis* (Figures 77 and 80, respectively) are influenced by coastal development and are slightly restricted in potential areas of occurrence where the predictions overlap. These species may be restricted due to conversion of orchards, particularly near Limasol, to more developed areas to support coastal tourism and retirement communities. Both species are also influenced by Nicosia and the surrounding villages, which have experienced growth due to the population migrations of 1974 and increase to service-based jobs in Nicosia. Development along the coast and around Nicosia is expected to continue as fewer people live in the mountain villages and maintain their agricultural lands full time.

Generalist species *Sarcopoterium spinosum* and *Thymus capitatus* are slightly influenced by coastal development between Larnaka and Limasol (Figures 84 and 85). Potential suitable areas of occurrence are also reduced near Ayia Napa for *Sarcopoterium spinosum* and near Nicosia for *Thymus capitatus*. The reductions to potential areas of occurrence appear slight, thus changes to climate conditions will most likely influence the extent of expansion into new areas.

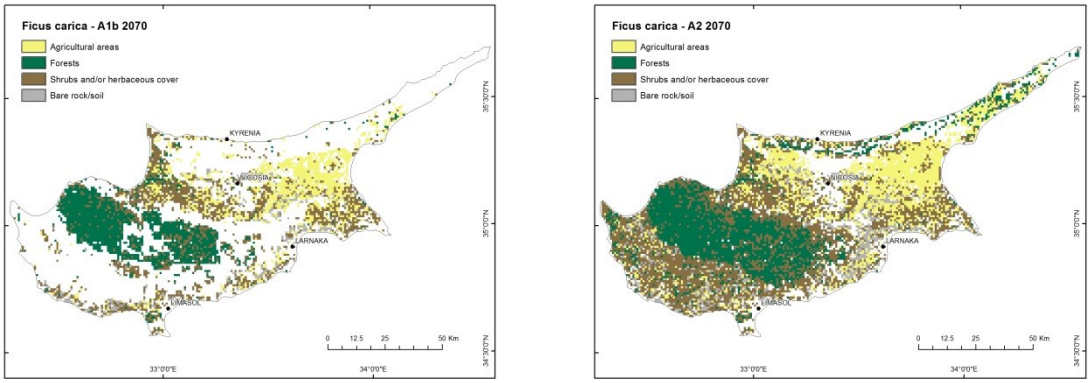

(a) (b)

Figure 77. Maps of potentially suitable areas for *Ficus carica* under A1b (a) and A2 (b) climate scenarios in 2070. The maps indicate a conservative estimate of the land cover categories where *Ficus carica* would occur by 2070, as it assumes that land cover remains static.

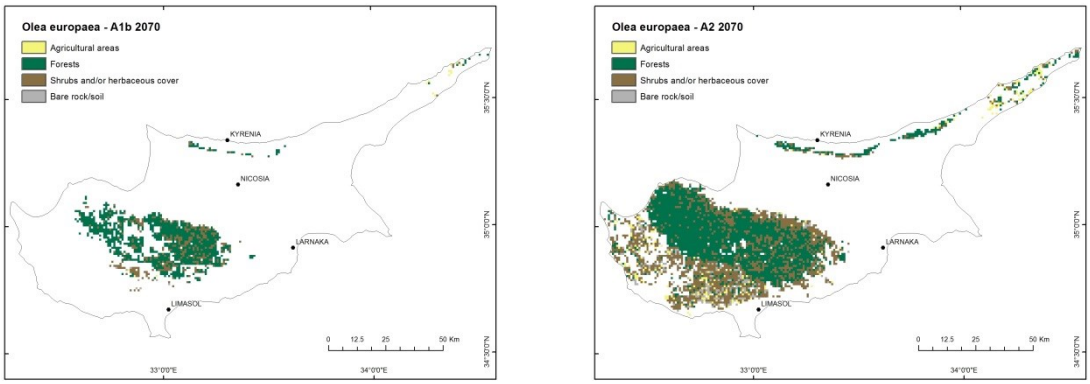

(a) (b)

Figure 78. Maps of potentially suitable areas for *Olea europaea* under A1b (a) and A2 (b) climate scenarios in 2070. The maps indicate a conservative estimate of the land cover categories where *Olea europaea* would occur by 2070, as it assumes that land cover remains static.

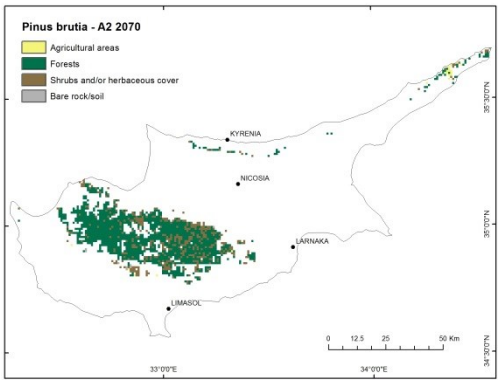

(a)

Figure 79. Map of potentially suitable areas for *Pinus brutia* A2 (a) climate scenarios in 2070. The maps indicate a conservative estimate of the land cover categories where *Pinus brutia* would occur by 2070, as it assumes that land cover remains static.

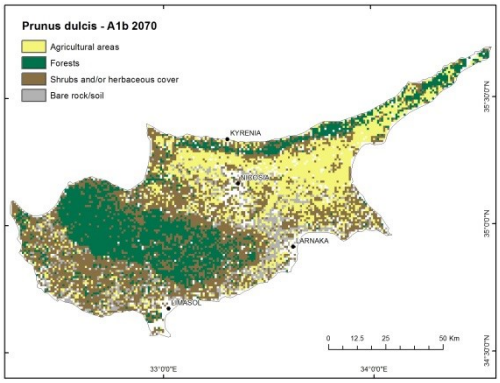

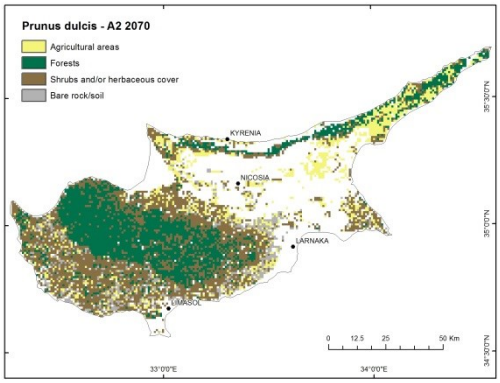

(a) (b)

Figure 80. Maps of potentially suitable areas for *Prunus dulcis* under A1b (a) and A2 (b) climate scenarios in 2070. The maps indicate a conservative estimate of the land cover categories where *Prunus dulcis* would occur by 2070, as it assumes that land cover remains static.

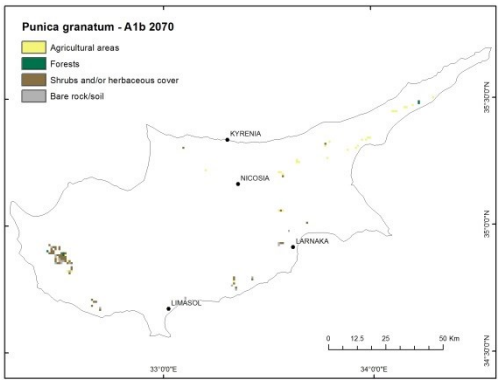

(a)

Figure 81. Maps of potentially suitable areas for *Punica granatum* under A1b (a) climate scenarios in 2070. The maps indicate a conservative estimate of the land cover categories where *Punica granatum* would occur by 2070, as it assumes that land cover remains static.

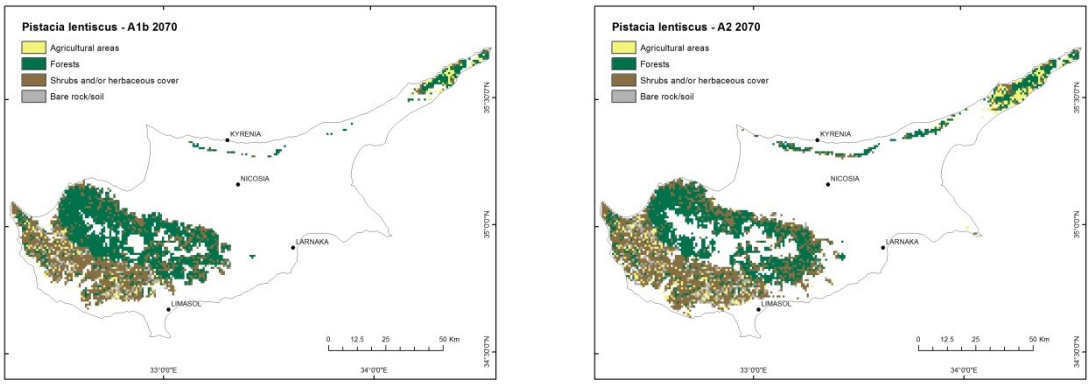

(a) (b)

Figure 82. Maps of potentially suitable areas for *Pistacia lentiscus* under A1b (a) and A2 (b) climate scenarios in 2070. The maps indicate a conservative estimate of the land cover categories where *Pistacia lentiscus* would occur by 2070, as it assumes that land cover remains static.

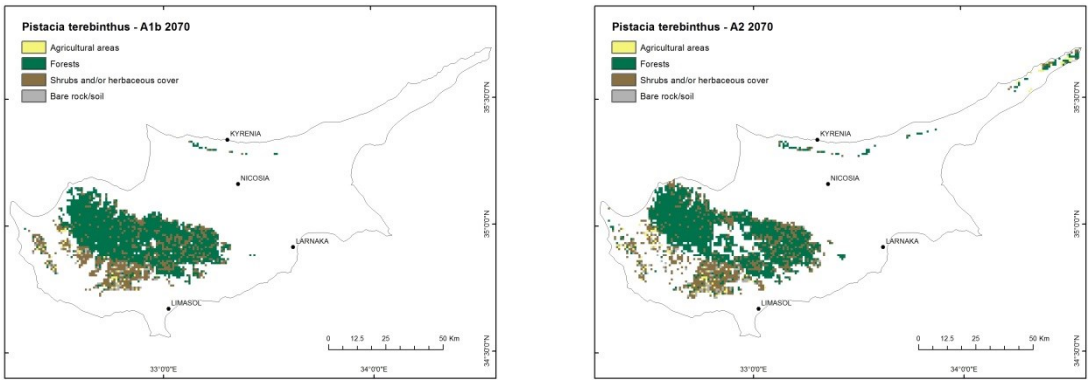

(a) (b)

Figure 83. Maps of potentially suitable areas for *Pistacia terebinthus* under A1b (a) and A2 (b) climate scenarios in 2070. The maps indicate a conservative estimate of the land cover categories where *Pistacia terebinthus* would occur by 2070, as it assumes that land cover remains static.

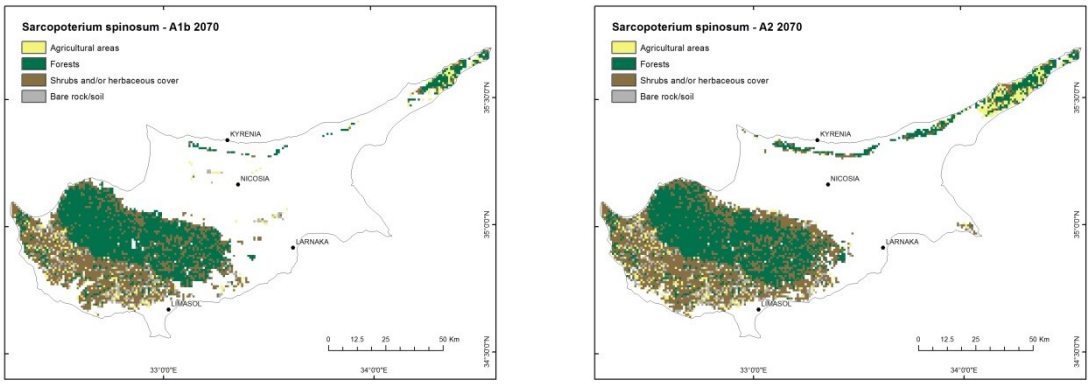

(a) (b)

Figure 84. Maps of potentially suitable areas for *Sarcopoterium spinosum* under A1b (a) and A2 (b) climate scenarios in 2070. The maps indicate a conservative estimate of the land cover categories where *Sarcopoterium spinosum* would occur by 2070, as it assumes that land cover remains static.

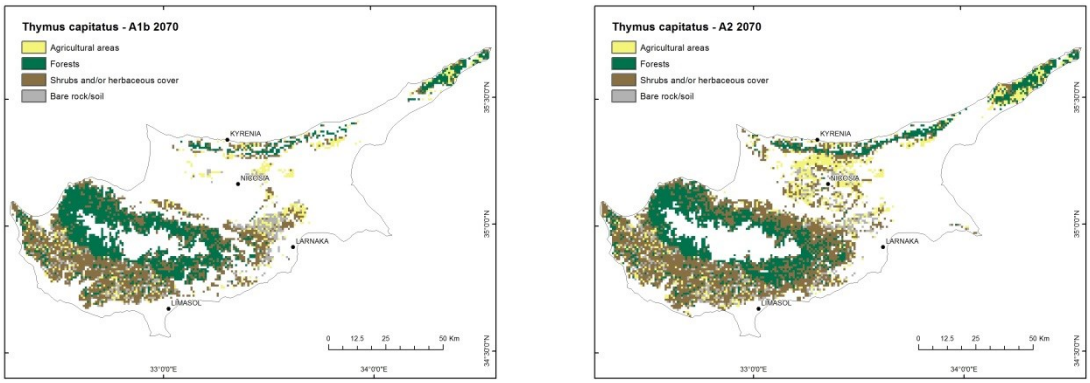

(a) (b)

Figure 85. Maps of potentially suitable areas for *Thymus capitatus* under A1b (a) and A2 (b) climate scenarios in 2070. The maps indicate a conservative estimate of the land cover categories where *Thymus capitatus* would occur by 2070, as it assumes that land cover remains static.

For the species under consideration in this simplistic model of future interactions between climate and land cover, a majority of the species have little to no impacts to potential distributions by artificial land covers. The exceptions are *Ficus carica* and *Prunus dulcis* whose extents are restricted by development along coastlines and in the urban areas. A more complex evaluation of the interactions would include a land cover transitions model in order to predict at each time step the influence of land cover change on species distributions. Additionally, this type of model would allow the restriction of expansion into areas previously predicted as transitioning to a land cover that is unsuitable for species occurrence. The simplified model illustrated here does provide a conservative approach to investigating if interactions between land cover and climate will influence species distributions. In Cyprus, it appears that many of the species modeled are highly influenced by climate alone as few species have remaining suitable areas for occurrence by 2030 (Table 21) and of species with remaining suitable habitat, only two species have substantial reductions to predicted areas of suitability. The incorporation of

land change variables such as fragmentation or interactions with other species to better model the interactions of land cover change and climate due to the correlated nature of conversions from functional habitat to urban or agricultural lands (Thuiller et al., 2004; de Chazal and Rounsevell, 2009). Loss of habitat is not of concern for many cultivated species as a majority of them are predicted to expand their ranges under climate change (see Table 21 for exceptions). However, cultivated species only sometimes occur as escapees outside of cultivation and are not presently widely distributed outside of human influenced areas.

Thuiller et al. (2004) also found that although the inclusion of land cover variables to model present-day distributions increases the predictive abilities of those models, the relationships between land cover and species distributions may not be correlated in the same manner under future climate scenarios. In comparison, Yates et al. (2010) found that land cover change influenced the prediction of future distributions in *Banksia* spp. Remnant habitat areas were calculated from a series of air photos and applied in concert with two dispersal ability scenarios to create overlays of predicted areas restricted to areas of overlap with remnant areas (no dispersal) to the ability of species to expand beyond current remnant areas into the entire predicted space (Yates et al., 2010). This approach could be very useful to examine the influences of land cover transitions in Cyprus as a more localized spatial scale; however, the spatial resolution of Landsat imagery do not allow for this type of analysis using a pixel-based classification technique. At the scale of analysis (30 meter pixels), species distributions are primarily driven by changes to climate variables over the study period.

The methodology and results presented as a result of land cover change and predictive modeling of suitable habitat provide a tool for conservation planning within non-profit and government organization in Cyprus. The Mediterranean Basin is known as a diversity hot spot and Cyprus is no exception. The high number of endemic plant species warrant protection to maintain levels of biological diversity on the island. In addition, plant communities provide the structure, nutrients and protection of other species on the island. Although change some change to environments is unpredictable and inevitable, certain types of change can be mitigated for or protected against through long-term planning by non-profit and government land managers and conservationists.

Land cover transitions, particularly from grasslands, shrublands or forests to agricultural or artificial surfaces reduce present-day habitat availability and connectivity. Land cover transitions may place a larger role than implicated in this research as the scale of analysis (30 m) may be too course to capture the loss of habitat for range restricted species or the locations of present-day refuges for plant species. However, the results presented her highlight the need for concern regarding loss of habitat along coastlines due to development. The predicted climate changes are exceptionally challenging in Cyprus, as many habitats for large trees and shrubs will disappear as soon as 2030, indicating a rapid approach to conservation of individual species and habitats is warranted. Species distribution modeling presents a tool to locate potential habitat for at least one species; however, overlapping suitable areas could be utilized in planning for protected areas. Species distribution modeling also provides a starting point for locating areas that may act as future refuges for sensitive species, particularly those of present-day conservation concern as these species are most likely the most sensitive to environmental changes.

Chapter 7

CONCLUSIONS

This dissertation examined the spatial and temporal changes to land cover and species distributions from 1973-2070. Two approaches were utilized to assess the separate influences of climate change and land cover changes to predicted areas of suitable for species occurrence. The results of the two approaches were used to evaluate the combined influences of climate change and land cover change to suitable habitat. First, Landsat data from 1973 to 2011 provide a glimpse into the major land cover transitions and their relationship to political events of 1974. Second, on-the-ground species observations collected between 2008 and 2011 were used to construct potential species distribution maps for 2011 – 2070. Future distributions were constructed under two climate change scenarios (A1b and A2) at 2030, 2050, and 2070.

The approaches were selected based on their ability to address the overarching research objectives:

1. Inference of how the landscapes of Cyprus have changed since 1974 through the use of satellite imagery and on-the-ground field observations of plant distributions;
2. Construction of modern potential vegetation models of plant species distributions based on the field observations;
3. Predict changes to the vegetation distribution under multiple climate scenarios; and,
4. Link changes of land cover and vegetation to enable detailed interpretation of changes in landscape configuration over time.

Each of these objectives was further defined by a specific research question and predictions as outlined in Chapters 3 through 5. The key findings of this research indicate that urban areas of Cyprus, particularly along the southern coast, increased in extent between 1973 and 2011 with the largest increases occurring between 1984 and 2001. Agricultural areas declined in southern Cyprus along the Troodos foothills, largely replaced by shrubs and/or herbaceous cover indicating a trend of agricultural abandonment following population relocations of the late 1950s to 1974. This trend continued as urban areas increased in size and the economic sector shifted to predominately service-based industries. At the spatial resolution of this study, agricultural areas were not consolidated in southern Cyprus into a more homogeneous landscape except along the eastern portions of the Mesaoria Plain. Increases to heterogeneity were observed over much of southern Cyprus due to continuous conversions to land cover, for example changes from agricultural lands to grassland/shrub cover to forest with each time step and at differing rates between pixels. Homogeneity may increase as agricultural lands fully transition into shrub lands or forested areas. Increases to homogeneity were observed across the northern portion of the Mesaoria Plain into the Karpas Peninsula, indicating a shift to larger agricultural plots or a more contiguous configuration of agriculture in this area.

Robust species distribution models for the present were created using field observations from 2008 to 2011, supplemented by historical accounts across areas that were not accessible for sampling (Figure 5). The models performed well using threshold-based and threshold-independent performance assessments. High AUC values for training and test data indicate that models were constructed that extrapolate well across the

present-day climate conditions. These models were then used as a baseline to construct potential distribution models under two SRES climate scenarios (IPCC, 2007) for the years 2030, 2050 and 2070. A1b scenarios assume rapid economic growth, declines of population mid-century and the introduction and quick adoption of new, efficient energy technologies. A2 scenarios assume high population growth rates, slow economic development and slow technological change. The A2 scenario is considered the extreme case out of the two. Little difference is predicted in temperature up to 2050 with diverging predictions of temperature after this time. Similar results were observed for both climate scenarios in that most of the species selected for modeling were not predicted to retain any areas of potential occurrence by 2030 (Table 21). Endemic species such as *Quercus alnifolia, Cedrus brevifolia* and *Helianthemum obtusifolium* quickly lose suitable habitat under both climate change scenarios and are absent from the landscape by 2030. Orchard species *Prunus dulcis* and *Ficus carica* are predicted to increase their potentially suitable areas under both climate scenarios. *Sarcopoterium spinosum* and *Thymus capitatus*, two indigenous and generalist species are also predicted to expand their potential areas of occurrence, possibly moving into agricultural areas as they are abandoned as well as into habitats where they are restricted possibly due to interactions with other species. The loss of species may influence species that are predicted to persist under increased temperatures. For example, as the soils are exposed the soil moisture is reduced, a process that is accelerated by higher temperature. Additionally, the loss of species may allow for the introduction or expansion of invasive species, which would put additional pressures on species that are able to respond to climate change by shifting their distribution.

Land cover changes and climate are both drivers to changes in biological diversity (e.g. Sala et al., 2000; de Chazal and Rounsevell, 2009) and although often mentioned, few studies have combined these drivers in their assessments (Thuiller et al., 2008). The problem of non-inclusion of both drivers is the possibility of over or under estimating the effects on species (de Chazal and Rounsevell, 2009). To evaluate the possible combined effects of climate change and land cover changes, a simple and conservative methodology was adopted that utilized a land cover classification for 2011 and the predicted areas of suitability for species that maintained areas of suitability through 2070 under at least one of the climate scenarios. At the scale of analysis (30 m pixels) most species distributions were the result of interactions with climatic shifts and the land cover did not further restrict the predicted areas of suitability. The two major exceptions were *Ficus carica* and *Prunus dulcis*, whose distributions are influenced by urban development, particularly along the southern coast.

The results of species distribution models indicate the necessity to include species distribution models as a tool in decision-making for conservation efforts aimed at specific plant species or vegetation communities at the national scale. Land cover changes should be included at a local scale of analysis as well as along any areas of expected urban development, particularly future coastal developments as coastal species are likely to become restricted in range due to rising sea levels, increased temperatures and pressures of urbanization.

REFERENCES

Allen, J. C. and D. F. Barnes. 1985. The causes of deforestation in developing countries. *Annuals of the Association of American Geographers* 75: 163-184.

Araujo, M. B., R. G. Pearson, W. Thuiller, and M. Erhard. 2005. Validation of species-climate impact models under climate change. *Global Change Biology* 11: 1504-1513.

Arima, E. Y., R. T. Walker, M. Sales, C. Souza Jr., and S. G. Perz. 2008. The fragmentation of space in the Amazon Basin: Emergent road networks. *Photogrammetric Engineering and Remote Sensing* 74: 699-709.

Barry, S. and J. Elith. 2006. Error and uncertainty in habitat models. *Journal of Applied Ecology* 43: 413-423.

Bauer, M. E., T. E. Burk, A. R. Ek, P. R. Coppin, S. D. Lime, T. A. Walsh, D. K. Walters, W. Befort, and D. F. Heinzen. 1994. Satellite inventory of Minnesota forest resources. *Photogrammetric Engineering and Remote Sensing* 60: 287-298.

Bergen, K. M., T. Zhao, V. Kharuk, Y. Blam, D. G. Brown, L. K. Peterson, and N. Miller. 2008. Changing regimes: Forested land-cover dynamics in central Siberia 1974 to 2001. *Photogrammetric Engineering and Remote Sensing* 74: 87-798.

Bicik, I., L. Jelecek and V. Stepanek. 2001. Land-use changes and their social driving forces in Czechia in the 19th and 20th centuries. *Land Use Policy* 18: 65-73.

Bilz, M., S. P. Kell, N. Maxted, and R. V. Lansdown. 2011. *European Red List of Vascular Plants*. Luxembourg: Publications Office of the European Union.

Birth, G. S. and G. R. McVey. 1968. Measuring the colour of growing turf with a reflectance spectrophotometer. *Agronomy Journal* 60: 640-643.

Blondel, J. 2006. The 'design' of Mediterranean landscapes: A millennial story of humans and ecological systems during the Historic Period. *Human Ecology* 34: 713-729.

Blondel, J. 2008. On humans and wildlife in Mediterranean islands. *Journal of Biogeography* 35: 509-518.

Blondel, J. and J. Aronson. 1999. *Biology and Wildlife of the Mediterranean region.* Oxford: Oxford University Press.

Bogaert, J., R. Cuelemans, and D. Salvador-Van Eysenrode. 2004. Decision tree algorithm for detection of spatial processes in landscape transformation. *Environmental Management* 33: 62-73.

Bossard, M., J. Feranec, and J. Otahel. 2000. *CORINE Land Cover Technical Guide – Addendum 2000*. Technical Report 40. Copenhagen: European Environment Agency.

Brokensha, D. and B. Riley. 1978. Forest, foraging, fences, and fuel in a marginal area of Kenya. Paper prepared for USAID Africa Bureau Firewood Workshop. Washington, D.C.

Butler, C. J., E. A. Wheeler, and L. B. Stabler. 2012. Distribution of the threatened lace hedgehog cactus (*Echinocereus reichenbachii*) under various climate change scenarios. *Journal of the Torrey Botanical Society* 139: 46-55.

Butzer, K. W. 2005. Environmental history in the Mediterranean world: Cross-disciplinary investigation of cause-and-effect for degradation and soil erosion. *Journal of Archaeological Science* 32: 1773-1800.

Butzer, K. W. and S. E. Harris. 2007. Geoarchaeological approaches to the environmental history of Cyprus: Explication and critical evaluation. *Journal of Archaeological Science* 34: 1932-1952.

Carlson, T. N. and G. A. Sanchez-Azofeifa. 1999. Satellite remote sensing of land use changes in and around San José, Costa Rica. *Remote Sensing of Environment* 70: 247-256.

Carpenter, G., A. N. Gillson, and J. Winter. 1993. DOMAIN: A flexible modeling procedure for mapping potential distributions of plants and animals. *Biodiversity and Conservation* 2: 667-680.

Chavez, P. S. 1988. An improved dark-object subtraction technique for atmospheric scattering correction of multispectral data. *Remote Sensing of Environment* 3: 459-479.

Chavez, P. S. 1996. Image-based atmospheric corrections revisited and improved. *Photogrammetric Engineering and Remote Sensing* 62: 1025-1036.

Colby, J. D. and P. L. Keating. 1998. Land cover classification using Landsat TM imagery in the tropical highlands: the influence of anisotropic reflectance. *International Journal of Remote Sensing*. 19: 1479-1500.

Congalton, R. G. 1991. A review of assessing the accuracy of classifications of remotely sensed data. *Remote Sensing of the Environment* 37: 35-46.

Council of the European Communities. 2007. Annex I – Natural habitat types of community interest whose conservation requires the designation of special areas of conservation. Council Directive 92/43/EEC. *Official Journal of the European Communities*. Consolidated version.

Cowling, R. M., P. W. Rundel, B. B. Lamont, M. Kalin Arroyo, and M. Arianoutsou. 1996. Plant diversity in Mediterranean-climate regions. *TREE* 11: 362–366.

Crist, E. P. and R. C. Cicone. 1984. A physically-based transformation of Thematic Mapper data-The TM tasseled cap. *IEEE Transactions on Geoscience and Remote Sensing* GE-22: 256-263.

Dalle, S. P., de Blois, S., J. Caballero, and T. Johns. 2006. Integrating analyses of local land-use regulations, cultural perceptions and land-use/land cover data for assessing the success of community-based conservation. *Forest Ecology and Management* 22: 370-383.

Dean, A. M. and G. M. Smith. 2003. An evaluation of per-parcel land cover mapping using maximum likelihood class probabilities. *International Journal of Remote Sensing* 14: 2905-2920.

De Chazal, J. and M. D. A. Rounsevell. 2009. Land-use and climate change within assessments of biodiversity loss: A review. *Global Environmental Change* 19: 306-315.

Di Castri, F. 1981. Mediterranean type shrublands of the world. *In* di Castri, F., D. W. Goodall, and R. L Sprecht (eds.). *Mediterranean type shrublands*. Elsevier.

Di Pasquale, G., P. di Martino and S. Mazzoleni. 2004. Forest history in the Mediterranean region. *In* S. Mazzoleni et al. (eds.). *Recent Dynamics of the Mediterranean Vegetation and Landscape*. West Sussex: John Wiley & Sons, Ltd.

Dormann, C. F. 2007. Promising the future? Global change projections of species distributions. *Basic and Applied Ecology* 8: 387-97.

Dudík, M., Phillips, S. J., and R. E. Schapire. 2007. Maximum entropy density estimation with generalized regularization and an application to species distribution modeling. *Journal of Machine Learning Research* 8: 1217-1260.

Dudík, M., R. E. Schapire, and S. J. Phillips. 2005. Correcting sample selection bias in maximum entropy density estimation. *Advances in Neural Information Processing Systems* 18: 323-330.

Eastman, J. R. 2012. *IDRISI Selva Manual*. Version 17.01. Worcester, MA: Clark Labs.

Elith, J., and C. H. Graham. 2009. Do they? How do they? WHY do they differ? On finding reasons for differing performances of species distribution models. *Ecography* 32: 66-77.

Elith, J., C. Graham, R. P. Anderson, M. Dudík, S. Ferrier, A. Guisan, R. J. Hijmans, F. Huettmann, J. Leathwick, A. Lehmann, J. Li, L. g. Lohmann, B. A. Loiselle, G. Manion, C. Moritz, M. Nakamura, Y. Nakazawa, J. M. Overton, A. T. Peterson, S. J. Phillips, K. Richardson, R. Scachetti-Pereira, R. Schapire, J. Soberon, S. E. Williams, M. S. Wisz, and N. E. Zimmermann. 2006. Novel methods improve prediction of species' distributions from occurrence data. *Ecography* 29: 129-151.

Elith, J., M. Kearney, and S. J. Phillips. 2010. The art of modelling range-shifting species. *Methods in Ecology and Evolution* 1: 330-342.

Elith, J., J. R. Leathwick. 2009. Species distribution models: Ecological explanation and prediction across space and time. *Annual Review of Ecology, Evolution, and Systematics*. 40: 677-97.

Elith, J., S. J. Phillips, T. Hastie, M. Dudík, Y. E. Chee, and C. J. Yates. 2011. A statistical explanation of MaxEnt for ecologists. *Diversity and Distributions*. 17: 43-57.

European Environment Agency (EEA). 2010. *The European environment – state and outlook 2010: synthesis*. Copenhagen: European Environment Agency.

Fall, P. L. 2012. Modern vegetation, pollen and climate relationships on the Mediterranean island of Cyprus. *Review of Paleobotany and Palynolgy* 185:79-92.

Farjon. A. 2005. A monograph of Cupressaceae and Sciadopitys.

Fitzpatrick, M. C., and W. W. Hargrove. 2009. The projection of species distribution models and the problem of non-analog climate. *Biodiversity and Conservation* 18: 2255-2261.

Forester, B. C. 1984. Derivation of atmospheric correction procedures for LANDSAT MSS with particular reference to urban data. *International Journal of Remote Sensing* 5: 799-817.

Franklin, J. 1995. Predictive vegetation mapping: Geographic modeling of biospatial patterns in relation to environmental gradients. *Progress in Physical Geography* 36: 1152-1163.

Franklin, J. 2009. *Mapping Species Distributions; Spatial Inference and Prediction.* United Kingdom: Cambridge University Press.

Franklin, J. 2010. Moving beyond static species distribution models in support of conservation biogeography. *Diversity and Distributions* 16: 321-330.

Freeman, E. A. and G. G. Moisen. 2008. A comparison of the performance of threshold criteria for binary classification in terms of predicted prevalence and kappa. *Ecological Modelling* 217: 48-58.

Friedman, J. H. 1991. Multivariate adaptive regression splines. *Annals of Statistics* 19: 1-67.

Geist, H. J. and E. F. Lambin (eds.). 2001. *What drives tropical deforestation?* LUCC Report Series No. 4. Louvain-la-Neuve: CIACO.

Geist, H. J. and E. F. Lambin. 2002. Proximate causes and underlying driving forces of tropical deforestation. *BioScience* 52: 143-150.

Gong, P., J. Wang, L. Yu, Y. Zhao, Y. Zhao, L. Liang, Z. Niu, X. Huang, H. Fu, S. Liu, C. Li, X. Li, W. Fu, C. Liu, Y. Xu, X. Wang, Q. Cheng, L. Hu, W. Yao, H. Zhang, P. Zhu, Z. Zhao, H. Zhang, Y. Zheng, P. Zhu, Z. Zhao, H. Zhang, Y. Zheng, L. Ji, Y. Zhang, H. Chen, A. Yan, J. Guo, L. Yu, L. Wang, X. Liu, T. Shi, M. Zhu, Y. Chen, G. Yang, P. Tang, B. Xu, C. Giri, N. Clinton, Z. Zhu, J. Chen, and J. Chen. 2013. Finer resolution observation and monitoring of global land cover: First mapping results with Landsat TM and ETM+ data. *International Journal of Remote Sensing* 34: 2607-2654.

Graham, C. H., R. Santiago, J. C. Ron, C. J. Santos, C. J. Schneider, and C. Moritz. 2004. Integrating phylogenetics and environmental niche models to explore speciation in dendrobatid frogs. *Evolution* 58: 1781-1793.

Grinnell, J. 1904. The origin and distribution of the Chestnut-backed Chickadee. *Auk* 21: 364-365.

Gritti, E. S., B. Smith, and M. T. Sykes. 2006. Vulnerability of Mediterranean Basin ecosystems to climate change and invasion by exotic plant species. *Journal of Biogeography* 33: 145-57.

Groombridge, B. and M. D. Jenkins (eds.). 2002 *World Atlas of Biodiversity. Earth's Living Resources in the 21st century*. University of California Press.

Grove, A. T. and O. Rackham. 1993. Threatened landscapes in the Mediterranean: examples from Crete. *Landscape and Urban Planning* 24: 279-292.

Guisan, A., and W. Thuiller. 2005. Predicting species distribution: offering more than simple habitat models. *Ecology Letters* 8: 993-1009.

Guisan, A. and N. E. Zimmerman. 2000. Predictive habitat distributional models in ecology. *Ecological Modelling* 135: 147-186.

Hall, F. G., D. E. Strebel, J. E. Nickeson, and S. J. Goetz. 1991. Radiometric rectification: Toward a common radiometric response among multidate, multisensor images. *Remote Sensing of Environment* 35: 11-27.

Hand, R. (ed.) 2004. Supplementary notes to the flora of Cyprus IV. *Willdenowia* 34: 427-456.

Hand, R., G. N. Hadjikyriakou, and C. S. Christodoulou (eds.). 2011. Flora of Cyprus – a dynamic checklist. Published at http://www.flora-of-cyprus.eu/.

Hanley, J. A. and B. J. McNeil. 1982. The meaning and use of the area under a receiver operating characteristic (ROC) curve. *Radiology* 143: 29-36.

Hastie, T. J. and R. J. Tibshirani. 1990. *Generalized Additive Models.* Chapman and Hall.

Hastie, T. and R. Tibshirani. 1996. Discriminant adaptive nearest neighbor classification. *IEEE Transactions on Pattern Analysis and Machine Intelligence*. 18: 607-616.

Heywood, V.H. and R.T. Watson (eds.). 1995. *Global Biodiversity Assessment*. Cambridge: Cambridge University Press.

Hijmans, R. J., S. E. Cameron, J. L. Parra, P. G. Jones, and A. Jarvis. 2005. Very high resolution interpolated climate surfaces for global land areas. *International Journal of Climatatology* 25: 1965-1978.

Hirzel, A. H., J. Hausser, D. Chessel, and N. Perrin. 2002. Ecological-niche factor analysis: How to compute habitat-suitability maps without absence data? *Ecology* 83: 2027-2036.

Hodgson, M. E. and B. M. Shelley. 1994. Removing the topographic effect in remotely sensed imagery. *Monitor* 6: 4-6.

Holben B. and C. Justice. 1981. An examination of spectral band ratioing to reduce the topographic effect on remotely sensed data. *International Journal of Remote Sensing* 2: 115-133.

Homer, C., J. Dewitz, J. Fry, M. Coan, N. Hossain, C. Larson, N. Herold, A. McKerrow, J. N. VanDriel, and J. Wickham. 2007. Completion of the 2001 National Land Cover Database for the conterminous United States. *Photogrammetric Engineering and Remote Sensing* 73: 337-341.

Hu, J., H. Hu, and Z. Jiang. 2010. The impacts of climate change on the wintering distribution of an endangered migratory bird. *Global Change Ecology* 164: 555-565.

Hutchinson, G. E. 1957. Concluding remarks. *Cold Spring Harbor Symposia on Quantitative Biology* 22: 415-427.

IPCC. 2000. *Summary for Policymakers: Special Report on Emissions Scenarios. A Special Report of Working Group III of the Intergovernmental Panel on Climate Change*. IPCC.

IPCC. 2007. *Climate Change: Synthesis Report*. *Contribution of Working Groups I, II and III to the Fourth Assessment Report of the Intergovernmental Panel on Climate Change* [Core Writing Team, Pachauri, R. K. and A. Reisinger (eds.)]. Geneva, Switzerland: IPCC.

Ispikoudis, I., G. Lyrintzis and S. Kyriakakis. 1993. Impact of human activities on Mediterranean landscapes in western Crete. *Landscape and Urban Planning* 24: 259-271.

IUCN. 2012. *IUCN Red List Categories and Criteria: Version 3.1*. Second edition. Gland, Switzerland and Cambridge, UK: IUCN.

Jensen, J. R. 2000. *Remote Sensing of the Environment; An earth resource perspective.* Upper Saddle River, NJ: Prentice-Hall, Inc.

Jensen, J. R., K. Rutchey, M. S. Koch, and S. Narumalani. 1995. Inland wetland change detection in the Everglades Water Conservation Area 2A using a time series of normalized remotely sensed data. *Photogrammetric Engineering and Remote Sensing* 61: 199-209.

Jones, P. G., and P. K. Thornton. 2013. Generating downscaled weather data from a suite of climate models for agricultural modeling applications. *Agricultural Systems* 114: 1-5.

Kasperson, J. X., R. E. Kasperson, and B. L. Turner. 1995. *Regions at risk: Comparisons of threatened environments*. Tokyo: United Nations University Press.

Kaufman, Y. J. 1993. Aerosol optical-thickness and atmospheric path radiance. *Journal of Geophysical Research: Atmospheres* 98: 2677-2692.

Kauth, R. J. and G. S. Thomas. 1976. The tasseled cap-A graphic description of the spectral-temporal development of agricultural crops as seen by Landsat. *Proceedings of the Symposium of Machine Processing of*

Remotely Sensed Data 4B-41-4B-50, West Lafayette, IN: Purdue University.

Kerr, J. T. and M. Ostrovsky. 2003. From space to species: Ecological applications for remote sensing. *Trends in Ecology and Evolution* 18: 299-305.

Klinge, J. 2013. *Assessment of environmental change in the Near Eastern Bronze Age*. PhD dissertation, Arizona State University. Ann Arbor: ProQuest/UMI (Publication No. pending).

Kling, J. and P. Fall. 2010. Archaeobotanical inference of Bronze Age land use and land cover in the eastern Mediterranean. *Journal of Archaeological Science* 37: 2622-2629.

Kinzig, A. P. and J. M. Grove. 2000. Urban-suburban ecology. *In* S. Levin (ed.), *The Encyclopedia of Biodiversity*. San Diego: Academic Press, Inc.

Kuemmerle, T., V.C. Radeloff, K. Perzanowski, and P. Hostert. 2006. Cross-border comparison of land cover and landscape pattern in Eastern Europe using a hybrid classification technique. *Remote Sensing of Environment* 103: 449-464.

Laba, M., R. Downs, S. Smith, S. Welsh, C. Neider, S. White, M. Richmond, W. Philpot, and P. Baveye. 2008. Mapping invasive wetland plants in the Hudson River National Estuarine Research Reserve using Quickbird satellite imagery. *Remote Sensing of Environment* 112: 286-300.

Lambin, E. F, B. L. Turner, H. J. Geist, S. B. Agbola, A. Angelsen, J. W. Bruce, O. T. Coomes, R. Dizro, G. Fischer, C. Folke, P. S. George, K. Homewood, J. Imbernon, R. Leemans, X. B. Li, E. F. Moran, M. Mortimore, P. S. Ramakrishnan, J. F. Richards, H. Skanes, W. Steffen, G. D. Stone, U. Svedin, T. Veldcamp, C. Vogel, and J. C. Xu. 2001. The causes of land-use and land-cover change: Moving beyond the myths. *Global Environmental Change Human and Policy Dimensions* 11: 261-269.

Landis, J. R. and G. G. Koch. 1977. The measurement of observer agreement for categorical data. *Biometrics* 33: 159-174.

Lark, R.M. 1995. A reappraisal of unsupervised classification: Correspondence between spectral and conceptual classes. *International Journal of Remote Sensing* 16: 1425-1443.

Lasanta-Martinez, T., S. M. Vicente-Serrano, and J. M. Cuadrat-Prats. 2005. Mountain Mediterranean landscape evolution caused by the abandonment

of traditional primary activities: A study of the Spanish Central Pyrenees. *Applied Geography* 25: 47-65.

Lawson, D. M., H. M., Regan, P. H. Zedler, and J. Franklin. 2010. Cumulative effects of land use, altered fire regime and climate change on persistence of *Ceanothus verrucosus*, a rare, fire-dependent plant species. *Global Change Biology* 16: 2518-2529.

Lillesand, T. M. and R. W. Kiefer. 2000. *Remote Sensing and Image Analysis, 4th Edition*. New York: John Wiley and Sons.

Lillesand, T. M., R. W. Kiefer, and J. W. Chipman. 2004. *Remote Sensing and Interpretation, 5th Edition*. New York: Oxford University Press.

Mahiny, A. S. and B. J. Turner. 2007. A comparison of four common atmospheric correction methods. *Photogrammetric Engineering and Remote Sensing* 73: 361-368.

Manel, S., H. Ceri Williams, and S. J. Ormerod. 2001. Evaluating presence-absence models in ecology: the need to account for prevalence. *Journal of Applied Ecology* 38: 921-31

Marsh, G. P. 1864. *Man and nature, or physical geography as modified by human action*. Cambridge, MA: Harvard University Press.

McCullagh, P. and J. A. Nelder. 1989. *Generalized Linear Models, 2nd Edition*. Chapman and Hall.

McKenney, D. W., J. H. Pedlar, K. Lawrence, K. Campbell, and M. F. Hutchinson. 2007. Potential impacts of climate change on the distribution of North American trees. *Bioscience* 57: 939-948.

McKibben, B. 1989. *The end of Nature*. New York: Random House.

Meikle, R. D. 1977. *Flora of Cyprus, Volume I*. London: Kew Royal Botanical Gardens.

Meikle, R. D. 1985. *Flora of Cyprus, Volume II*. London: Kew Royal Botanical Gardens.

Mena, C. F. 2008. Trajectories of land-use and land-cover in the northern Ecuadorian Amazon: Temporal composition, spatial configuration, and probability of change. *Photogrammetric Engineering and Remote Sensing*. 74: 737-751.

Merriam, C. H. and L. Steineger. 1890. Results of a biological survey of the San Francisco mountain region and the desert of the Little Colorado, Arizona. *North American Fauna Report 3*. Washington, D.C.: U.S. Department of Agriculture, Division of Ornithology and Mammalia.

Meteorological Service of Cyprus. 2013. Climate of Cyprus. Republic of Cyprus, Ministry of Agriculture, Meteorological Service. http://www.moa.gov.cy/moa/ms/ms.nsf/

Meyer, W. B. and B. L. Turner. 1992. Human population growth and global land-use/cover change. *Annual Review of Ecology and Systematics* 23: 39-61.

Myers, N., R. A. Mittermeier, G. A. B. da Fonseca, and J. Kent. 2000. Biodiversity hotspots for conservation priorities. *Nature* 403: 853-858.

Nagendra, H. 2001. Using remote sensing to assess biodiversity. *International Journal of Remote Sensing* 22: 2377-2400.

Nelson, G. C., E. Bennett, A. A. Berhe, K. Cassman, R. Defries, T. Deitz, A. Dobermann, A. Dobson, A. Janetos, M. Levy, D. Marco, N. Nakicenovic, B. O'Neill, R. Norgaard, G. Petschel-Held, D. Ojima, P. Pingali, R. Watson, and M. Zurek. 2006. Anthropogenic drivers of ecosystem change: an overview. *Ecology and Society* 11: 29. [online] http://www.ecologyandsociety.org/vol11/iss2/art29/

Ortega, M., R. Elena-Rosello, and J. M. Garcia del Barrio. 2003. Estimation of plant diversity at the landscape level: A methodological approach applied to three Spanish rural areas. *Environmental Monitoring and Assessment* 95: 97-116.

Pares-Ramos, I. K., W. A. Gould, and T. M. Aide. 2008. Agricultural abandonment, suburban growth, and forest expansion in Puerto Rico between 1991 and 2000. *Ecology and Society* 13(2): 1 [online] URL: http://www.ecologyandsociety.org/vol3/iss2/art1/

Parmesan, C. 2006. Ecological and evolutionary responses to recent climate change. *Annual Review of Ecology, Evolution and Systematics* 37: 637-669.

Parmesan, C. and G. Yohe. 2003. A globally coherent fingerprint of climate change impacts across natural systems. *Nature* 421: 37-42.

Pearson, R. G., C. J. Raxworthy, M. Nakamura, and A. T. Peterson. 2007. Predicting species' distributions from small numbers of occurrence records: A test case using cryptic geckos in Madagascar. *Journal of Biogeography* 34: 102-117.

Pettorelli, N., J. O. Vik, A. Mysterud, J.-M. Gaillard, C. J. Tucker, and N. C. Stenseth. 2005. Using the satellite-derived NDVI to assess ecological responses to environmental change. *Trends in Ecology and Evolution* 20: 503-510.

Phillips, S. J. 2010. MaxEnt tutorial. http://www.cs.princeton.edu/~schapire/maxent/

Phillips, S. J., R. P. Anderson, and R. E. Schapire. 2006. Maximum entropy modeling of species geographic distributions. *Ecological Modelling* 19: 231-259.

Phillips, S. J., and M. Dudík. 2008. Modeling of species distributions with Maxent: new extensions and a comprehensive evaluation. *Ecography* 31: 161-175.

Phillips, S. J., M. Dudík, J. Elith, C. H. Graham, A. Lehmann, J. Leathwick, and S. Ferrier. 2009. Sample selection bias and presence-only distribution models: implications for background and pseudo-absence data. *Ecological Applications* 19: 181-197.

Phillips, S. J., M. Dudík, and R. E. Shapire. 2004. A maximum entropy approach to species distribution modeling. *Proceedings of the Twenty-First International Conference on Machine Learning*, p. 655-662.

Pitelka, L. F. 2004. Evolution and global change. *Frontiers in Ecology and the Environment* 2: 10-10.

Pounds, J. A., M. P. I. Fogden, and J. H. Campbell. 1999. Biological responses to climate change on a tropical mountain. *Nature* 398: 611-615.

Quezél, P. and F. Medail. 2003. *Ecology and Biogeography of Mediterranean Forests.* Paris: Elsevier.

Rackham, O. 1990. *Trees and woodland in the British landscape, 2nd edition*. London: J.M. Dent and Sons Ltd.

Ramirez-Villegas, J. and A. Bueno-Cabrera. 2009. Working with climate data and niche modeling I. Creation of bioclimatic variables. Working paper. http://www.ccafs-climate.org/documentation/.

Ramirez-Villegas, J. and A. Jarvis. 2010. Downscaling Global Circulation Model Outputs: The Delta Method. *Decision and Policy Analysis Working Paper No. 1.* International Center for Tropical Agriculture, CIAT, Cali, Colombia.

Rappaport, R. 1968. *Pigs for the Ancestors: Ritual in the Ecology of a New Guinea People*. New Haven: Yale University Press.

Reddy, S. and L. M. Dávalos. 2003. Geographical sampling bias and its implications for conservation priorities in Africa. *Journal of Biogeography* 30: 1719-1727.

Root, T. L., J. T. Price, K. R. Hall, S. H. Schneider, C. Rosenzweig, and J. A. Pounds. 2003. Fingerprints of global warming on wild animals and plants. *Nature* 421: 57-60.

Rosenzweig, C., D. Karoly, M. Vicarelli, P. Neofotis, Q. Wu, G. Casassa, A. Menzel, T. L. Root, N. Estrella, B. Seguin, P. Tryjanowski, C. Liu, S. Rawlins, and A. Imeson. 2008. Attributing physical and biological impacts to climate change. *Nature* 453: 353-357.

Rudel, T. K., D. Bates, and R. Machinguiashi. 2002. A tropical forest transition? Agricultural change, out-migration, and secondary forests in the Ecuadorian Amazon. *Annals of the Association of American Geographers* 92: 87-102.

Rushton, S. P., S. J. Ormerod, and G. Kerby. 2004. New paradigms for modeling species distributions? *Journal of Applied Ecology* 41: 193-200.

Sala, O. E., F. S. Chapin, J. J. Armesto, R. Berlow, J. Bloomfield, R. Dirzo, E. Huber-Sanwald, L. F. Huenneke, R. B. Jackson, A. Kinzig, R. Leemans, D. Lodge, H. A. Mooney, M. Oesterheld, N. L. Poff, M. T. Sykes, B. H. Walker, M. Walker, and D. H. Wall. 2000. Global biodiversity scenarios for the year 2100. *Science* 287: 1770-1774.

Sanderson, E. W., M. Jaiteh, M. A. Levy, K. H. Redford, A. V. Wannebo, and G. Woolmer. 2002. The human footprint and the last of the wild. *Bioscience* 52:891-904.

Selkowitz, D. J. and S. V. Stehman. 2011. Thematic accuracy of the National Land Cover Database (NLCD) 2001 land cover for Alaska. *Remote Sensing of Environment* 115: 1401-1407.

Soberón, J. 2007. Grinnellian and Eltonian niches and geographic distributions of species. *Ecology Letters* 10: 1115-1123.

Soto-Berelov, M. 2011. *Vegetation modeling of Holocene landscapes in the southern Levant*. PhD dissertation, Arizona State University. Ann Arbor: ProQuest/UMI (Publication No. UMI 3466233).

Steel, L. 2004. *Cyprus Before History; From the Earliest Settlers to the End of the Bronze Age.* London: Gerald Duckworth & Co. Ltd.

Stockwell, D. R. B and I. R. Noble. 1992. Induction of sets of rules from animal distribution data: A robust and informative method of analysis. *Mathematics and Computers in Simulation* 33: 385-390.

Stockwell, D. R. B. and D. P. Peters. 1999. The GARP modelling system: Problems and solutions to automated spatial prediction. *International Journal of Geographical Information Systems* 13: 143-158.

Stoddart, D. R. 1965. Geography and the ecological approach: The ecosystem as a geographical principle and method. *Geographical Journal* 50: 242-251.

Sutton, P., C. Roberts, C. Eldvidge, and H. Meij. 1997. A comparison of nighttime satellite imagery and population density for the continental United States. *Photogrammetric Engineering and Remote Sensing* 63: 1303-1313.

Thomas, C. D., A. Cameron, R. E. Green, M. Bakkenes, L. J. Beaumont, Y. C. Collingham, B. F. N. Erasmus, M. F. de Siqueira, A. Grainger, L. Hannah, L. Hughes, B. Huntley, A. S. van Jaarsveld, G. F. Midgley, L. Miles, M. A. Ortega-Huerta, A. Townsend Peterson, O. L. Phillips, and S. E. Williams. 2004. Extinction risk from climate change. *Nature* 427: 145-148.

Thuiller, W., M. D. Araujo, R. G. Pearson, R. J. Whittaker, L. Brotons, and S. Lavorel. 2004. Uncertainty in predictions of extinction risk. *Nature* 430: 33.

Thuiller, W., C. Albert, M. B. Araujo, P. M. Berry, M. Cabeza, A. Guisan, T. Hickler, G. F. Midgley, J. Paterson, F. M. Schurr, M. T. Sykes, and N. E. Zimmerman. 2008. Predicting global change impacts on plant species' distributions: Future challenges. *Perspectives in Plant Ecology, Evolution and Systematics* 9: 137-152.

Thuiller, W., D. M. Richardson, P. Pysek, G. F. Midgley, G. O. Hughes, and M. Rouget. 2005. Niche-based modeling as a tool for predicting the global risk of alien plant invasions. *Global Change Biology* 11: 2234-2250.

Tsintides, T. C. 1998. *The Endemic Plants of Cyprus*. Nicosia: Bank of Cyprus.

Tsintides, T. C., G. N. Harjikyriakou, and C. S. Christodoulou. 2002. *Trees and Shrubs in Cyprus*. Lefkosia: A. G. Leventis Foundation.

Turner, B. L., W. C. Clark, R. W. Kates, J. F. Richards, J. T. Mathews, and W. B. Meyers (eds.). 1990. *The Earth as Transformed by Human Action: Global and Regional Changes in the Biosphere over the Past 300 Years*. Cambridge: Cambridge University Press.

Turner, B. L. and W. B. Meyer. 1991. Global land-use and land-cover change: An overview. *In* W. B. Meyer and B. L. Turner (eds.) *Changes in land use and land cover: A global perspective*. Cambridge, U.K.: Cambridge University Press.

Turner, M. D. 1999. Merging local and regional analyses of land-use change: The case of livestock in the Sahel. *Annals of the Association of American Geographers* 89: 191-219.

Turner, M. G., R. H. Gardner, and R. V. O'Neill. 2001. *Landscape Ecology in Theory and Practice: Pattern and Process*. New York: Springer Science and Business Media, Inc.

Turner, R. E. and M. M. Spencer. 1972. Atmospheric model for correction of spacecraft data. *Proceedings, Eighth International Symposium of Remote Sensing of the Environment* Volume II: 895-934.

Turner, W., S. Spector, N. Gardiner, M. Fladeland, E. Sterling, and M. Steininger. 2003. Remote sensing for biodiversity science and conservation. *Trends in Ecology and Evolution* 18: 306-314.

Vicente-Serrano, S. M., T. Lasanta, and A. Romo. 2004. Analysis of the spatial and temporal evolution of vegetation cover in the Spanish central Pyrenees: The role of human management. *Environmental Management* 34: 802-818.

Viney, D. E. 1994. *An Illustrated Flora of North Cyprus*. Koenigstein.

Vitousek, P. M., H. A. Mooney, J. Lubchenco, and J. M. Melillo. 1997. Human domination of Earth's ecosystems. *Science* 277: 494-499.

Vogiatzakis, I. N., A. M. Mannion, and G. H. Griffiths. 2006. Mediterranean ecosystems: problems and tools for conservation. *Progress in Physical Geography* 30: 175-200.

Von Humboldt, A. 1805/1807. Essai sur la géographie des plantes, accompangné d'un tableau physique des régions équinoxiales. Paris.

Walther, G.-R., E. Post, P. Convey, A. Menzel, C. Parmesan, T. J. C. Beebee, J.-M. Fromentin, O. Hoegh-Guldberg, and F. Bairlein. 2002. Ecological responses to recent climate change. *Nature* 416: 389-395.

Warner,T. A. and D. J. Campagna. 2009. *Remote Sensing with IDRISI Taiga: A Beginner's Guide*. Geocarto International Centre.

Warren, D. L. and S. N. Seifert. 2011. Ecological niche modeling in Maxent: The importance of model complexity and the performance of model selection criteria. *Ecological Applications* 21: 335-342.

Wilby, R. L., J. Troni, Y. Biot, L. Tedd, B. C. Hewitson, D. M. Smith, and R. T. Sutton. 2009. A review of climate risk information for adaptation and

development planning. *International Journal of Climatology* 29: 1193-1215.

Wilson, E. O. 1992. *The Diversity of Life*. Cambridge: Harvard University Press.

Wu, J. and R. Hobbs. 2002. Key issues and research priorities in landscape ecology: An idiosyncratic synthesis. *Landscape Ecology* 17: 355-365.

Wulder, M. A., S. E. Franklin, and J. C. White. 2004. Sensitivity of hyperclustering and labelling land cover classes to Landsat image acquisition date. *International Journal of Remote Sensing.* 25: 5537-5344.

Yates, C. J., J. Elith, A. M. Latimer, D. le Maitre, G. F. Midgley, F. M. Schurr, and A. G. West. 2010. Projecting climate change impacts on species distributions in megadiverse South African cape and southwest Australian floristic regions: opportunities and challenges. *Austral Ecology* 35: 374-391.

Yukimoto, S., A. Noda, A. Kitoh, M. Hosaka, H. Yoshimura, T. Uchiyama, K. Shibata, O. Arakawa, and S. Kusunoki. 2006. Present-day climate and climate sensitivity in the Meteorological Research Institute coupled GCM version 2.3. *Journal of the Meteorological Society of Japan* 84: 333-363.

Zacharides, T. 2012. Climate change in Cyprus: Impacts and adaptation policies. *Cyprus Economic Policy Review* 6: 21-37.

Zaharis, A. 1977. The forests of Crete. Ministry of Agriculture, Pub. 39. Athens.

APPENDIX A

PEARSON'S CORRELATION ANALYSIS FOR SPECIES DISTRIBUTION MODELING OF MODERN VEGETATION

	bio1proj1	bio2proj2	bio3proj1	bio4proj1	bio5proj1	bio6proj1	bio7proj1	bio8proj1	bio9proj1
bio1proj1	1								
bio2proj2	0.500419	1							
bio3proj1	0.6753	0.733175	1						
bio4proj1	-0.35837	0.076774	-0.59636	1					
bio5proj1	0.79049	0.843646	0.595612	0.133174	1				
bio6proj1	0.889604	0.21015	0.673463	-0.69826	0.471026	1			
bio7proj1	-0.01151	0.6666	-0.01159	0.77691	0.586342	-0.43839	1		
bio8proj1	0.954702	0.390361	0.748456	-0.61515	0.626193	0.972985	-0.25548	1	
bio9proj1	0.922045	0.587404	0.49318	0.025151	0.914723	0.666417	0.320023	0.771076	1
bio10proj2	0.924607	0.556082	0.47085	0.019779	0.899287	0.67305	0.298204	0.775136	0.997613
bio11proj1	0.957151	0.395835	0.749293	-0.60938	0.63143	0.971008	-0.24833	0.999795	0.775854
bio12proj	-0.88569	-0.72784	-0.69746	0.121197	-0.88084	-0.64734	-0.30302	-0.77392	-0.89536
bio13proj	-0.83613	-0.7719	-0.69172	0.071182	-0.88803	-0.57749	-0.37449	-0.71568	-0.86381
bio14proj	-0.9508	-0.4712	-0.71157	0.462497	-0.703	-0.88243	0.094066	-0.94255	-0.82531
bio15proj	-0.05378	-0.46449	0.143356	-0.77573	-0.51711	0.346066	-0.84468	0.204936	-0.37336
bio16proj	-0.86455	-0.73151	-0.6467	0.042334	-0.89517	-0.59634	-0.36446	-0.73147	-0.90433
bio17proj1	-0.93475	-0.43775	-0.7193	0.526067	-0.66113	-0.90077	0.15357	-0.95327	-0.78536
bio18proj	-0.90134	-0.57406	-0.85372	0.554165	-0.69378	-0.87638	0.097907	-0.93056	-0.74587
bio19proj	-0.91391	-0.65785	-0.68628	0.196811	-0.8545	-0.71809	-0.21121	-0.82884	-0.89742
geology3	-0.41067	-0.17709	-0.15599	0.042637	-0.35747	-0.30494	-0.08419	-0.36357	-0.41789
soils3	-0.52816	-0.26692	-0.19565	-0.00542	-0.49375	-0.36262	-0.17008	-0.44592	-0.5617

	bio10proj2	bio11proj1	bio12proj	bio13proj	bio14proj	bio15proj	bio16proj	bio17proj1	bio18proj
bio1proj1									
bio2proj2									
bio3proj1									
bio4proj1									
bio5proj1									
bio6proj1									
bio7proj1									
bio8proj1									
bio9proj1									
bio10proj2	1								
bio11proj1	0.779755	1							
bio12proj	-0.88564	-0.77964	1						
bio13proj	-0.85239	-0.72159	0.990242	1					
bio14proj	-0.82738	-0.94448	0.857321	0.805515	1				
bio15proj	-0.36563	0.197631	0.323246	0.40751	-0.05592	1			
bio16proj	-0.8956	-0.73771	0.995458	0.992163	0.827583	0.40165	1		
bio17proj1	-0.78706	-0.95435	0.82528	0.775164	0.948402	-0.12167	0.791685	1	
bio18proj	-0.73261	-0.93178	0.850076	0.808648	0.925703	-0.13626	0.80384	0.929735	1
bio19proj	-0.89164	-0.83233	0.967777	0.948592	0.890591	0.237912	0.959195	0.869436	0.870244
geology3	-0.42829	-0.36536	0.371143	0.371742	0.371008	0.160655	0.380235	0.395429	0.316926
soils3	-0.57182	-0.44864	0.510654	0.506279	0.491722	0.246466	0.525789	0.501952	0.403544

	bio19proj	geology3	soils3
bio1proj1			
bio2proj2			
bio3proj1			
bio4proj1			
bio5proj1			
bio6proj1			
bio7proj1			
bio8proj1			
bio9proj1			
bio10proj2			
bio11proj1			
bio12proj			
bio13proj			
bio14proj			
bio15proj			
bio16proj			
bio17proj1			
bio18proj			
bio19proj	1		
geology3	0.386399	1	
soils3	0.526046	0.505841	1

APPENDIX B

PEARSON'S CORRELATION ANALYSIS FOR SPECIES DISTRIBUTION MODELING OF FUTURE VEGETATION – A1B 2030 SCENARIO

	bio1a1b30	bio2a1b30	bio3a1b30	bio4a1b30	bio5a1b30	bio6a1b30	bio7a1b30	bio8a1b30	bio9a1b30
bio1a1b30	1								
bio2a1b30	0.4221828	1							
bio3a1b30	0.5667105	0.8206995	1						
bio4a1b30	-0.3071841	0.0384155	-0.5211259	1					
bio5a1b30	0.7852518	0.8080638	0.627246	0.1389364	1				
bio6a1b30	0.8770254	0.1433174	0.535223	-0.6770154	0.4509872	1			
bio7a1b30	-0.0070021	0.6781782	0.1436649	0.7500513	0.592235	-0.4520796	1		
bio8a1b30	0.9516748	0.3442856	0.6453112	-0.5796988	0.6294416	0.9685734	-0.2453642	1	
bio9a1b30	0.9141204	0.4792208	0.3897419	0.1008013	0.8935911	0.6287795	0.3253833	0.7509162	1
bio10a1b30	0.9237553	0.4481125	0.3768557	0.0760659	0.8764547	0.652356	0.286973	0.7675487	0.9979773
bio11a1b30	0.9556962	0.3524866	0.6473863	-0.5700979	0.6381023	0.9653746	-0.233821	0.9995917	0.75892
bio12a1b30	-0.8834369	-0.6479889	-0.6346307	0.0900186	-0.8717205	-0.6287057	-0.303593	-0.7724148	-0.8820565
bio13a1b30	-0.8342285	-0.6458238	-0.5760449	-0.0148351	-0.8669818	-0.5434328	-0.3758405	-0.6946173	-0.8722823
bio14a1b30	-0.9505288	-0.399406	-0.6041068	0.4210999	-0.6974208	-0.8780972	-0.0957463	-0.9423535	-0.8130054
bio15a1b30	0.1863312	-0.1229605	0.3716642	-0.8603173	-0.2090306	0.537502	-0.6941512	0.4372013	-0.1639559
bio16a1b30	-0.8626453	-0.6446832	-0.5876296	0.0113545	-0.880319	-0.5775948	-0.3583284	-0.7294935	-0.8928122
bio17a1b30	-0.9422789	-0.4052489	-0.6507524	0.5055535	-0.6724123	-0.9066865	0.1465493	-0.9669836	-0.7714103
bio18a1b30	-0.8901395	-0.5514259	-0.782958	0.5210303	-0.7070652	-0.8482737	0.0591836	-0.9221902	-0.7154913
bio19a1b30	-0.9235994	-0.569229	-0.585444	0.1282416	-0.8555682	-0.6949543	-0.2276423	-0.8256894	-0.9095079
geology	-0.3049781	-0.1304671	-0.2311103	0.2073571	-0.1898531	-0.2961508	0.0776257	-0.3215253	-0.2284787
soils	0.3622231	0.143383	0.2062699	-0.1314844	0.2843846	0.3382472	-0.0211569	0.3563759	0.3232032

	bio10a1b30	bio11a1b30	bio12a1b30	bio13a1b30	bio14a1b30	bio15a1b30	bio16a1b30	bio17a1b30	bio18a1b30
bio1a1b30									
bio2a1b30									
bio3a1b30									
bio4a1b30									
bio5a1b30									
bio6a1b30									
bio7a1b30									
bio8a1b30									
bio9a1b30									
bio10a1b30	1								
bio11a1b30	0.7749388	1							
bio12a1b30	-0.8755661	-0.7817347	1						
bio13a1b30	-0.8634056	-0.7053363	0.9902563	1					
bio14a1b30	-0.8242522	-0.9450498	0.8559842	0.7977868	1				
bio15a1b30	-0.1442204	0.4265471	0.0120471	-0.1263223	-0.3073521	1			
bio16a1b30	-0.8854901	-0.7396559	0.9957614	0.9962719	0.8267337	0.0945953	1		
bio17a1b30	-0.7855524	-0.9682876	0.8332602	0.7649416	0.9613812	-0.3917785	0.7972396	1	
bio18a1b30	-0.716065	-0.924761	0.8483839	0.7792478	0.9208778	-0.4091043	0.8036676	0.9416769	1
bio19a1b30	-0.9094014	-0.8328471	0.9728994	0.9516448	0.8932523	-0.0217247	0.9685238	0.8816358	0.8542396
geology	-0.2317216	-0.3207286	0.2983757	0.2658695	0.2979774	-0.2295484	0.275966	0.3046326	0.3236102
soils	0.3283005	0.3572929	-0.3476493	-0.334729	-0.0346772	0.0369904	-0.3403414	-0.4009807	-0.3574024

	bio19a1b30	geology	soils
bio1a1b30			
bio2a1b30			
bio3a1b30			
bio4a1b30			
bio5a1b30			
bio6a1b30			
bio7a1b30			
bio8a1b30			
bio9a1b30			
bio10a1b30			
bio11a1b30			
bio12a1b30			
bio13a1b30			
bio14a1b30			
bio15a1b30			
bio16a1b30			
bio17a1b30			
bio18a1b30			
bio19a1b30	1		
geology	0.3011464	1	
soils	-0.376375	0.0104381	1

APPENDIX C

PEARSON'S CORRELATION ANALYSIS FOR SPECIES DISTRIBUTION MODELING OF FUTURE VEGETATION – A1B 2050 SCENARIO

	bio1a1b50	bio2a1b50	bio3a1b50	bio4a1b50	bio5a1b50	bio6a1b50	bio7a1b50	bio8a1b50	bio9a1b50
bio1a1b50	1								
bio2a1b50	0.525446	1							
bio3a1b50	0.667816	0.736718	1						
bio4a1b50	-0.30935	0.096769	-0.58434	1					
bio5a1b50	0.799506	0.851033	0.588657	0.17537	1				
bio6a1b50	0.867892	0.204065	0.662083	-0.69437	0.446398	1			
bio7a1b50	0.058775	0.687962	0.023224	0.781644	0.628859	-0.41503	1		
bio8a1b50	0.950908	0.411597	0.751349	-0.58382	0.627388	0.967248	-0.20255	1	
bio9a1b50	0.912953	0.606768	0.461988	0.101993	0.921216	0.611911	0.404943	0.74683	1
bio10a1b50	0.930576	0.566844	0.460742	0.054407	0.899124	0.653526	0.346323	0.778058	0.996239
bio11a1b50	0.950908	0.411597	0.751349	-0.58382	0.627388	0.967248	-0.20255	1	0.74683
bio12a1b50	-0.88316	-0.75667	-0.70708	0.091474	-0.88624	-0.61844	-0.3637	-0.77254	-0.88346
bio13a1b50	-0.84823	-0.74121	-0.62605	-0.01515	-0.88625	-0.54376	-0.42861	-0.70657	-0.88948
bio14a1b50	-0.94545	-0.51805	-0.72167	0.410517	-0.72093	-0.85555	0.010389	-0.93282	-0.8122
bio15a1b50	0.362111	0.020953	0.56062	-0.80354	-0.02122	0.633819	-0.5723	0.568772	0.042086
bio16a1b50	-0.86177	-0.76122	-0.65703	0.011689	-0.89991	-0.56455	-0.42443	-0.7284	-0.89424
bio17a1b50	-0.94494	-0.47574	-0.74197	0.501754	-0.67763	-0.90568	0.097975	-0.9671	-0.77337
bio18a1b50	-0.89363	-0.53259	-0.84429	0.576939	-0.63717	-0.88373	0.120037	-0.94348	-0.69166
bio19a1b50	-0.86482	-0.75905	-0.65904	0.017441	-0.89976	-0.57072	-0.41892	-0.73313	-0.89513
geology	-0.30275	-0.1697	-0.27958	0.208031	-0.19203	-0.28799	0.054995	-0.32035	-0.22632
soils	0.363466	0.170851	0.240364	-0.13365	0.280974	0.337896	-0.00792	0.356645	0.319773

	bio10a1b50	bio11a1b50	bio12a1b50	bio13a1b50	bio14a1b50	bio15a1b50	bio16a1b50	bio17a1b50	bio18a1b50
bio1a1b50									
bio2a1b50									
bio3a1b50									
bio4a1b50									
bio5a1b50									
bio6a1b50									
bio7a1b50									
bio8a1b50									
bio9a1b50									
bio10a1b50	1								
bio11a1b50	0.778058	1							
bio12a1b50	-0.87539	-0.77254	1						
bio13a1b50	-0.87793	-0.70657	0.990607	1					
bio14a1b50	-0.83106	-0.93282	0.863311	0.817158	1				
bio15a1b50	0.075525	0.568772	-0.22397	-0.11264	-0.45648	1			
bio16a1b50	-0.88361	-0.7284	0.995688	0.99722	0.834152	-0.1433	1		
bio17a1b50	-0.80338	-0.9671	0.826387	0.769728	0.953305	-0.53598	0.790592	1	
bio18a1b50	-0.70921	-0.94348	0.837135	0.767134	0.927786	-0.63024	0.78825	0.942707	1
bio19a1b50	-0.88489	-0.73313	0.995191	0.996022	0.836383	-0.14686	0.999053	0.793763	0.791139
geology	-0.23104	-0.32035	0.297179	0.268317	0.29712	-0.31038	0.274973	0.292123	0.352466
soils	0.336122	0.356645	-0.34763	-0.33849	-0.34677	0.113221	-0.33961	-0.40261	-0.3481

	bio19a1b50	geology	soils
bio1a1b50			
bio2a1b50			
bio3a1b50			
bio4a1b50			
bio5a1b50			
bio6a1b50			
bio7a1b50			
bio8a1b50			
bio9a1b50			
bio10a1b50			
bio11a1b50			
bio12a1b50			
bio13a1b50			
bio14a1b50			
bio15a1b50			
bio16a1b50			
bio17a1b50			
bio18a1b50			
bio19a1b50	1		
geology	0.275498	1	
soils	-0.33962	0.010438	1

APPENDIX D

PEARSON'S CORRELATION ANALYSIS FOR SPECIES DISTRIBUTION MODELING OF FUTURE VEGETATION – A1B 2070 SCENARIO

	bio1a1b70	bio2a1b70	bio3a1b70	bio4a1b70	bio5a1b70	bio6a1b70	bio7a1b70	bio8a1b70	bio9a1b70
bio1a1b70	1								
bio2a1b70	0.4325117	1							
bio3a1b70	0.5728304	0.82615	1						
bio4a1b70	-0.27829	0.050066	-0.50304	1					
bio5a1b70	0.7867932	0.816634	0.641686	0.158107	1				
bio6a1b70	0.8711725	0.150347	0.539593	-0.66467	0.448091	1			
bio7a1b70	0.0032953	0.680449	0.156177	0.754804	0.596157	-0.45062	1		
bio8a1b70	0.9481914	0.352854	0.653108	-0.56426	0.627113	0.968062	-0.24317	1	
bio9a1b30	0.9127592	0.487766	0.395611	0.134293	0.891699	0.616842	0.33646	0.741088	1
bio10a1b70	0.9220972	0.459434	0.3841	0.110811	0.87597	0.639093	0.30077	0.757111	0.998132
bio11a1b70	0.9507943	0.356169	0.652822	-0.55813	0.631553	0.966104	-0.23698	0.999826	0.746185
bio12a1b70	-0.889939	-0.64784	-0.64285	0.078233	-0.86929	-0.63653	-0.2964	-0.77899	-0.88183
bio13a1b70	-0.844178	-0.63697	-0.56649	-0.04511	-0.86805	-0.54514	-0.37724	-0.69709	-0.88373
bio14a1b70	-0.944309	-0.41914	-0.61273	0.382119	-0.70379	-0.86235	0.071668	-0.93056	-0.81051
bio15a1b70	0.0038337	-0.38379	0.104109	-0.77947	-0.43734	0.415345	-0.80972	0.265068	-0.32067
bio16a1b70	-0.862596	-0.65821	-0.60085	-0.01154	-0.88375	-0.57149	-0.36924	-0.72572	-0.89077
bio17a1b70	-0.947582	-0.39151	-0.62845	0.466297	-0.66949	-0.90478	0.144029	-0.96585	-0.77955
bio18a1b70	-0.882623	-0.5693	-0.79237	0.490037	-0.71438	-0.83871	0.03986	-0.9132	-0.70857
bio19a1b70	-0.895114	-0.64217	-0.64233	0.091343	-0.8732	-0.65259	-0.28589	-0.79115	-0.88289
geology	-0.302954	-0.12963	-0.22725	0.204515	-0.18818	-0.29409	0.076199	-0.32217	-0.22377
soils	0.3620143	0.146917	0.209419	-0.12543	0.281938	0.335901	-0.02013	0.356362	0.318979

	bio10a1b70	bio11a1b70	bio12a1b70	bio13a1b70	bio14a1b70	bio15a1b70	bio16a1b70	bio17a1b70	bio18a1b70
bio1a1b70									
bio2a1b70									
bio3a1b70									
bio4a1b70									
bio5a1b70									
bio6a1b70									
bio7a1b70									
bio8a1b70									
bio9a1b30									
bio10a1b70	1								
bio11a1b70	0.761914	1							
bio12a1b70	-0.87649	-0.78447	1						
bio13a1b70	-0.87621	-0.7034	0.988698	1					
bio14a1b70	-0.82052	-0.9328	0.866562	0.809839	1				
bio15a1b70	-0.29968	0.25953	0.218251	0.335787	-0.1123	1			
bio16a1b70	-0.88401	-0.73176	0.99459	0.996954	0.830993	0.30898	1		
bio17a1b70	-0.7943	-0.96725	0.833505	0.765821	0.952906	-0.17834	0.791842	1	
bio18a1b70	-0.70803	-0.91479	0.859007	0.785228	0.906038	-0.15988	0.810366	0.918553	1
bio19a1b70	-0.87929	-0.79558	0.989145	0.97544	0.86922	0.226838	0.984539	0.843011	0.860106
geology	-0.22775	-0.32235	0.295726	0.264884	0.289043	-0.10966	0.273394	0.292905	0.308239
soils	0.324561	0.356755	-0.34947	-0.33668	-0.33642	-0.04017	-0.3398	-0.39804	-0.35631

	bio19a1b70	geology	soils
bio1a1b70			
bio2a1b70			
bio3a1b70			
bio4a1b70			
bio5a1b70			
bio6a1b70			
bio7a1b70			
bio8a1b70			
bio9a1b30			
bio10a1b70			
bio11a1b70			
bio12a1b70			
bio13a1b70			
bio14a1b70			
bio15a1b70			
bio16a1b70			
bio17a1b70			
bio18a1b70			
bio19a1b70	1		
geology	0.297001	1	
soils	-0.36341	0.010438	1

APPENDIX E

PEARSON'S CORRELATION ANALYSIS FOR SPECIES DISTRIBUTION MODELING OF FUTURE VEGETATION – A2 2030 SCENARIO

	bio1a230	bio2a230	bio3a230	bio4a230	bio5a230	bio6a230	bio7a230	bio8a230	bio9a230
bio1a230	1								
bio2a230	0.4221828	1							
bio3a230	0.5667105	0.8206995	1						
bio4a230	-0.3071841	0.0384155	-0.5211259	1					
bio5a230	0.7852518	0.8080638	0.627246	0.1389364	1				
bio6a230	0.8770254	0.1433174	0.535223	-0.6770154	0.4509872	1			
bio7a230	-0.0070021	0.6781782	0.1436649	0.7500513	0.592235	-0.4520796	1		
bio8a230	0.9516748	0.3442856	0.6453112	-0.5796988	0.6294416	0.9685734	-0.2453642	1	
bio9a230	0.9141204	0.4792208	0.3897419	0.1008013	0.8935911	0.6287795	0.3253833	0.7509162	1
bio10a230	0.9237553	0.4481125	0.3768557	0.0760659	0.8764547	0.652356	0.286973	0.7675487	0.9979773
bio11a230	0.9556962	0.3524866	0.6473863	-0.5700979	0.6381023	0.9653746	-0.233821	0.9995917	0.75892
bio12a230	-0.8834369	-0.6479889	-0.6346307	0.0900186	-0.8717205	-0.6287057	-0.303593	-0.7724148	-0.8820565
bio13a230	-0.8342285	-0.6458238	-0.5760449	-0.0148351	-0.8669818	-0.5434328	-0.3758405	-0.6946173	-0.8722823
bio14 230	-0.9505288	-0.399406	-0.6041068	0.4210999	-0.6974208	-0.8780972	-0.0957463	-0.9423535	-0.8130054
bio15 230	0.1863312	-0.1229605	0.3716642	-0.8603173	-0.2090306	0.537502	-0.6941512	0.4372013	-0.1639559
bio16a230	-0.8626453	-0.6446832	-0.5876296	0.0113545	-0.880319	-0.5775948	-0.3583284	-0.7294935	-0.8928122
bio17a230	-0.9422789	-0.4052489	-0.6507524	0.5055535	-0.6724123	-0.9066865	0.1465493	-0.9669836	-0.7714103
bio18a230	-0.8901395	-0.5514259	-0.782958	0.5210303	-0.7070652	-0.8482737	0.0591836	-0.9221902	-0.7154913
bio19a230	-0.9235994	-0.569229	-0.585444	0.1282416	-0.8555682	-0.6949543	-0.2276423	-0.8256894	-0.9095079
geology	-0.3049781	-0.1304671	-0.2311103	0.2073571	-0.1898531	-0.2961508	0.0776257	-0.3215253	-0.2284787
soils	0.3622231	0.143383	0.2062699	-0.1314844	0.2843846	0.3382472	-0.0211569	0.3563759	0.3232032

	bio10a230	bio11a230	bio12a230	bio13a230	bio14a230	bio15a230	bio16a230	bio17a230	bio18a230
bio1a230									
bio2a230									
bio3a230									
bio4a230									
bio5a230									
bio6a230									
bio7a230									
bio8a230									
bio9a230									
bio10a230	1								
bio11a230	0.784515	1							
bio12a230	-0.87985	-0.78287	1						
bio13a230	-0.89512	-0.7326	0.991029	1					
bio14 230	-0.83093	-0.94515	0.85806	0.824146	1				
bio15 230	0.148723	0.636107	-0.23382	-0.1523	-0.53702	1			
bio16a230	-0.88255	-0.74182	0.996644	0.996008	0.82796	-0.16096	1		
bio17a230	-0.80146	-0.96987	0.833254	0.791781	0.965926	-0.61641	0.797759	1	
bio18a230	-0.73991	-0.9449	0.853438	0.794524	0.938819	-0.64	0.811676	0.952481	1
bio19a230	-0.90114	-0.85065	0.960835	0.949102	0.90196	-0.32681	0.951345	0.89573	0.877683
geology	-0.23461	-0.32083	0.298627	0.281519	0.297977	-0.3129	0.278207	0.302987	0.350029
soils	0.333342	0.357444	-0.34808	-0.33664	-0.34677	0.142702	-0.34063	-0.39485	-0.34566

	bio19a230	geology	soils
bio1a230			
bio2a230			
bio3a230			
bio4a230			
bio5a230			
bio6a230			
bio7a230			
bio8a230			
bio9a230			
bio10a230			
bio11a230			
bio12a230			
bio13a230			
bio14 230			
bio15 230			
bio16a230			
bio17a230			
bio18a230			
bio19a230	1		
geology	0.313062	1	
soils	-0.38195	0.010438	1

APPENDIX F

PEARSON'S CORRELATION ANALYSIS FOR SPECIES DISTRIBUTION MODELING OF FUTURE VEGETATION – A2 2050 SCENARIO

	bio1a250	bio2a250	bio3a250	bio4a250	bio5a250	bio6a250	bio7a250	bio8a250	bio9a250
bio1a250	1								
bio2a250	0.51911	1							
bio3a250	0.64915	0.735704	1						
bio4a250	-0.28967	0.086971	-0.59055	1					
bio5a250	0.799907	0.842312	0.567928	0.187645	1				
bio6a250	0.867626	0.200996	0.651507	-0.68002	0.443746	1			
bio7a250	0.061873	0.681577	0.013222	0.778787	0.631743	-0.41434	1		
bio8a250	0.949566	0.409358	0.739086	-0.57043	0.625986	0.967036	-0.20075	1	
bio9a250	0.91435	0.592584	0.438084	0.118762	0.92023	0.613764	0.403663	0.746567	1
bio10a250	0.928417	0.55379	0.431432	0.080573	0.898938	0.647702	0.352683	0.771875	0.996757
bio11a250	0.949566	0.409358	0.739086	-0.57043	0.625986	0.967036	-0.20075	1	0.746567
bio12a250	-0.88447	-0.74955	-0.6885	0.074841	-0.8863	-0.61968	-0.3641	-0.77132	-0.88439
bio13a250	-0.85991	-0.71508	-0.59151	-0.03535	-0.88496	-0.55458	-0.41904	-0.71338	-0.90169
bio14 250	-0.95019	-0.48978	-0.69847	0.408786	-0.70821	-0.87258	0.035536	-0.94203	-0.81154
bio15a250	0.353143	-0.09818	0.464516	-0.82381	-0.08723	0.653937	-0.65425	0.57406	0.023343
bio16a250	-0.86194	-0.75702	-0.64996	0.008276	-0.89659	-0.5704	-0.41716	-0.73014	-0.88842
bio17a250	-0.94697	-0.45712	-0.70796	0.473705	-0.67377	-0.90147	0.095514	-0.96458	-0.78198
bio18a250	-0.88902	-0.53944	-0.83647	0.560334	-0.63977	-0.87935	0.1109	-0.93863	-0.69015
bio19a250	-0.86194	-0.75702	-0.64996	0.008276	-0.89659	-0.5704	-0.41716	-0.73014	-0.88842
geology	-0.30317	-0.16721	-0.27932	0.202315	-0.19085	-0.29162	0.058426	-0.32101	-0.2278
soils	0.362896	0.170431	0.236816	-0.12828	0.281108	0.333132	-0.00267	0.356054	0.320193

	bio10a250	bio11a250	bio12a250	bio13a250	bio14a250	bio15a250	bio16a250	bio17a250	bio18a250
bio1a250									
bio2a250									
bio3a250									
bio4a250									
bio5a250									
bio6a250									
bio7a250									
bio8a250									
bio9a250									
bio10a250	1								
bio11a250	0.771875	1							
bio12a250	-0.87511	-0.77132	1						
bio13a250	-0.89143	-0.71338	0.989672	1					
bio14 250	-0.82793	-0.94203	0.85607	0.81756	1				
bio15a250	0.060425	0.57406	-0.13781	-0.04493	-0.4652	1			
bio16a250	-0.87701	-0.73014	0.996826	0.995021	0.826005	-0.06656	1		
bio17a250	-0.80582	-0.96458	0.832156	0.787736	0.964559	-0.53689	0.797817	1	
bio18a250	-0.70032	-0.93863	0.83269	0.764594	0.929045	-0.58771	0.790122	0.938663	1
bio19a250	-0.87701	-0.73014	0.996826	0.995021	0.826005	-0.06656	1	0.797817	0.790122
geology	-0.23076	-0.32101	0.296932	0.275601	0.297977	-0.27553	0.277581	0.293257	0.352433
soils	0.333162	0.356054	-0.34806	-0.33853	-0.34677	0.105788	-0.34066	-0.40207	-0.34285

	bio19a250	geology	soils
bio1a250			
bio2a250			
bio3a250			
bio4a250			
bio5a250			
bio6a250			
bio7a250			
bio8a250			
bio9a250			
bio10a250			
bio11a250			
bio12a250			
bio13a250			
bio14 250			
bio15a250			
bio16a250			
bio17a250			
bio18a250			
bio19a250	1		
geology	0.277581	1	
soils	-0.34066	0.010438	1

APPENDIX G

PEARSON'S CORRELATION ANALYSIS FOR SPECIES DISTRIBUTION MODELING OF FUTURE VEGETATION – A2 2070 SCENARIO

	bio1a270	bio2a270	bio3a270	bio4a270	bio5a270	bio6a270	bio7a270	bio8a270	bio9a270
bio1a270	1								
bio2a270	0.51911	1							
bio3a270	0.64915	0.735704	1						
bio4a270	-0.28967	0.086971	-0.59055	1					
bio5a270	0.799907	0.842312	0.567928	0.187645	1				
bio6a270	0.867626	0.200996	0.651507	-0.68002	0.443746	1			
bio7a270	0.061873	0.681577	0.013222	0.778787	0.631743	-0.41434	1		
bio8a270	0.949566	0.409358	0.739086	-0.57043	0.625986	0.967036	-0.20075	1	
bio9a270	0.91435	0.592584	0.438084	0.118762	0.92023	0.613764	0.403663	0.746567	1
bio10a270	0.928417	0.55379	0.431432	0.080573	0.898938	0.647702	0.352683	0.771875	0.996757
bio11a270	0.949566	0.409358	0.739086	-0.57043	0.625986	0.967036	-0.20075	1	0.746567
bio12a270	-0.88447	-0.74955	-0.6885	0.074841	-0.8863	-0.61968	-0.3641	-0.77132	-0.88439
bio13a270	-0.85991	-0.71508	-0.59151	-0.03535	-0.88496	-0.55458	-0.41904	-0.71338	-0.90169
bio14a270	-0.95019	-0.48978	-0.69847	0.408786	-0.70821	-0.87258	0.035536	-0.94203	-0.81154
bio15a270	0.353143	-0.09818	0.464516	-0.82381	-0.08723	0.653937	-0.65425	0.57406	0.023343
bio16a270	-0.86194	-0.75702	-0.64996	0.008276	-0.89659	-0.5704	-0.41716	-0.73014	-0.88842
bio17a270	-0.94697	-0.45712	-0.70796	0.473705	-0.67377	-0.90147	0.095514	-0.96458	-0.78198
bio18a270	-0.88902	-0.53944	-0.83647	0.560334	-0.63977	-0.87935	0.1109	-0.93863	-0.69015
bio19a270	-0.86194	-0.75702	-0.64996	0.008276	-0.89659	-0.5704	-0.41716	-0.73014	-0.88842
geology	-0.30317	-0.16721	-0.27932	0.202315	-0.19085	-0.29162	0.058426	-0.32101	-0.2278
soils	0.362896	0.170431	0.236816	-0.12828	0.281108	0.333132	-0.00267	0.356054	0.320193

	bio10a270	bio11a270	bio12a270	bio13a270	bio14a270	bio15a270	bio16a270	bio17a270	bio18a270
bio1a270									
bio2a270									
bio3a270									
bio4a270									
bio5a270									
bio6a270									
bio7a270									
bio8a270									
bio9a270									
bio10a270	1								
bio11a270	0.771875	1							
bio12a270	-0.87511	-0.77132	1						
bio13a270	-0.89143	-0.71338	0.989672	1					
bio14a270	-0.82793	-0.94203	0.85607	0.81756	1				
bio15a270	0.060425	0.57406	-0.13781	-0.04493	-0.4652	1			
bio16a270	-0.87701	-0.73014	0.996826	0.995021	0.826005	-0.06656	1		
bio17a270	-0.80582	-0.96458	0.832156	0.787736	0.964559	-0.53689	0.797817	1	
bio18a270	-0.70032	-0.93863	0.83269	0.764594	0.929045	-0.58771	0.790122	0.938663	1
bio19a270	-0.87701	-0.73014	0.996826	0.995021	0.826005	-0.06656	1	0.797817	0.790122
geology	-0.23076	-0.32101	0.296932	0.275601	0.297977	-0.27553	0.277581	0.293257	0.352433
soils	0.333162	0.356054	-0.34806	-0.33853	-0.34677	0.105788	-0.34066	-0.40207	-0.34285

	bio19a270	geology	soils
bio1a270			
bio2a270			
bio3a270			
bio4a270			
bio5a270			
bio6a270			
bio7a270			
bio8a270			
bio9a270			
bio10a270			
bio11a270			
bio12a270			
bio13a270			
bio14a270			
bio15a270			
bio16a270			
bio17a270			
bio18a270			
bio19a270	1		
geology	0.277581	1	
soils	-0.34066	0.010438	1